Newly proposed strategies to increase the energy efficiency of water systems

Maria Cristina Morani

Supervisors: Prof. A. Carravetta
Prof. O. Fecarotta

Advisor: Prof. C. D'Ambrosio

Department of Civil, Architectural and Environmental Engineering
University of Naples Federico II

This dissertation is submitted for the degree of
Doctor of Philosophy
July 2021

To the ones who believe in me

Declaration

I hereby declare that except where specific reference is made to the work of others, the contents of this dissertation are original and have not been submitted in whole or in part for consideration for any other degree or qualification in this, or any other university. This dissertation is my own work and contains nothing which is the outcome of work done in collaboration with others, except as specified in the text.

Maria Cristina Morani
July 2021

Acknowledgements

There are so many people I would like to thank for supporting me along my PhD journey.
Firstly, I would like to thank my PhD supervisors, Armando Carravetta and Oreste Fecarotta, for their invaluable support and guidance, as well as for the precious advice, which have been crucial to develop this thesis work. Without them, most of my achievements would not be possible. I owe them much.
I would like to express my gratitude to Claudia D'ambrosio for her remarkable contribution to my work, during the six-month period spent at the Ecole Polytechnique in Paris. Thanks to her, I acquired very valuable knowledge, which have significantly enriched my area of expertise and allowed me to achieve important goals in a very challenging research field.
I am immensely grateful to Vincenzo for being always by my side. He has been my shoulder to lean on during the hardest moments, as well as the one with whom I shared every single progress and goal of mine during these three years. I cannot imagine this achievement without his immense love and support: most of this work belongs to him.
I would like to express my thankfulness to Mum, Dad and Gianfranco for being the main aid during these three years. No word of gratitude could be enough to thank them for the measureless love, as well as the enormous encouragement they have constantly given me. A special thank goes to my lovely nieces, Sveva and Ginevra, for cheering me up when I really needed it. Their love is something irreplaceable and has been my panacea in all moments of stress and dejection.
I am very grateful to the PhD for meeting a very special person, Francesco. More than a colleague, he is an invaluable support, a reliable confidant and, above all, a true friend.
I would like to thank Diana for sharing this experience with me since the first day. This PhD would not be the same without her.
Thanks to Maria Rita and Roberta for the immense encouragement. Thanks for trusting me since ever.

Contributors and Funding Sources

This thesis was part funded by the European Regional Development Fund (ERDF) through the Interreg Atlantic Area Programme 2014-2020, as part of the REDAWN project (Reducing the Energy Dependency in the Atlantic Area from Water Networks).

Abstract

One of the main challenges in the water industry consists of the reduction of environmental impacts, as well as the containment of energy use. In this research work, new solutions to achieve a sustainable management of water networks have been developed and organized in three lines of research.

The main line of research is based on the optimal location of hydraulic devices within a water distribution network in order to maximize the energy production and water savings, as well as to minimize the investment cost. Firstly, the installation of only Pumps As Turbines (PATs) has been analyzed within a literature synthetic network and a new Mixed Integer Non-Linear Programming (MINLP) model has been developed to perform the optimization. Such an optimization model has been defined by a thorough mathematical formulation in order to deal with the extremely hard technical and computational complexities affecting the optimization procedure. In this research, only deterministic solvers have been employed to search the optima, and a comparison of their performance has been also carried out. Most of the computations have been performed by a global optimization solver, which potentially finds the global optimum in both convex and non-convex problems, but is also used to find good quality local optima in very complex problems, where the achievement of the exact solution may require infinite computational time. Compared to other studies in literature on the same network, the proposed study accounts for crucial hydraulic aspects, such as the phenomenon of flow reversion during the day affecting the installation and the operation of the devices, as well as the need for installing machines generating a power above a minimum fixed value. A comparison with such previous literature works has been carried out in order to highlight the effectiveness of the newly proposed optimization procedure. Moreover, to develop a more realistic and comprehensive mathematical model, the simultaneous installation of PATs and Pressure Reducing Valves (PRVs) has been also modeled by the introduction of new variables and mathematical constraints. Indeed, in presence of large water savings but small energy recovery, a PRV might be a more viable solution than a PAT. Compared to other studies in

literature optimizing the only location of PATs within the same synthetic network, the simultaneous installation of valves and turbines, as well as the formulation of new hydraulic constraints, has significantly increased the value of the optimization model. In addition, the optimization has been extended to a real water distribution network serving the Blackstairs region (IE), with the aim of testing the robustness of the model and of the optimization procedure in more complex and larger problems. Indeed, the computational complexity affecting the optimization procedure increases according to the size of the network and the mathematical formulation proposed for the synthetic network might be not suitable for such a more complex case study. Compared to the synthetic network where the pressure reduction up to defined minimum requirements has not compromised the hydraulic operation of the system, in the analyzed real water network the exploitation of the available excess pressure to save both water and energy raises the need for employing also pumping systems to supply the most remote nodes of the network. The installation of pumping systems within the network has been therefore included within the optimization procedure and the outcome has been a new model for a Global Optimization of Hydraulic Devices Location (GOHyDeL), suitable for any water distribution network. Such a new model has been the result of progressive findings and hard attempts to deal with the enormous complexities arising during the computation. In all the performed optimization, the maximized water and energy savings and the minimized installation costs have been assessed according to a cost model used by previous authors in literature, in order to make a more straightforward comparison with such literature works. However, more recent cost models available in literature have been also employed to achieve more reasonable and realistic values of the results. According to the comparison between results obtained by using different cost models, despite the employment of more recent models leading to significantly larger investment costs and, thus, smaller values of NPV, the solutions are quite similar in terms of location of installed devices, and the achieved savings are comparable as well. However, among all the devices, the PRVs have resulted to be more affected by the choice of the cost model, due to the strong dependency of the valve costs on the pipe diameter. On the whole, beyond the large feasibility of the model within the optimal location field, a remarkable value of the proposed research also results from the new formulation of mathematical constraints and variables, which requires less computational effort and could find application also in more general optimization problems.

The second line of research defines and compares two alternative strategies to supply a real water distribution network. The first solution consists of an elevated reservoir, which is located upstream of a water distribution network and is supplied from the water source by a pumping system. In this scheme, the excess pressure is not dissipated by a traditional valve, but rather a pump as turbine is installed to contain the pressure, thus water leakage, and also recover energy. The second hydraulic scheme instead consists of a pump supplying the downstream network directly from the source. In this scheme there is not an excess pressure to convert in energy, since the elevated reservoir is bypassed and the flow is pumped to the network with lower head. Such new schemes represent two different strategies to increase the energy efficiency of a supply system, as alternatives to the use of elevated reservoir with dissipation of the excess pressure by means of pressure reducing valves. The two schemes have been properly designed in order to find the devices, in terms of diameter and rotational speed, minimizing the energy requirements, thus maximizing the energy efficiency of the whole system. Given the water network supplying a small village in Ballacolla area (IE), the direct supply of the network has resulted a more efficient strategy than the indirect supply scheme with energy recovery. Moreover, the two schemes have been compared by varying the operating conditions, thus considering different combinations of distance and elevation of the source from the water distribution network. The energy audit of the two schemes has been assessed by new energy efficiency indices and also by literature indices. The comparison has showed that the convenience of a scheme over the other significantly depends on the operating conditions. However, with equal values of pumping head in both the schemes, the indirect scheme with energy recovery is up to 5 % more convenient than the direct pumping scheme, which is instead more efficient if the pumping head could be reduced up to 6 %.

In the third line of research a new strategy to save energy in the urban water management is presented. The proposed solution consists of a mixed PAT-pump turbocharger, that is a PAT-equipped turbopump exploiting an excess pressure within the fresh water network to produce energy, which is entirely used to carry a wastewater stream towards a treatment plant. In this system, the excess pressure is converted by the PAT in a mechanical torque, which in turn supplies the pump mounted on the same shaft. Such a plant arises whenever wastewater pumping station and excess pressure point could be co-located, thus in low ground areas where high clean-water pressures occur and sewage networks are equipped with pumping systems due to the need to treat the wastewater. In this application, the water distribution network serving Ballacolla area (IE) has been assumed as case study, since it is suitable for the installation of this kind of plant. A preliminary geometric selection of the devices has been performed by a new selection method based on the maximum daily averaged values of fresh and wastewater discharge. Then, the behavior of the plant has been simulated for several wastewater hydrographs by a new mathematical model. The benefits of the plants have been assessed and compared with a conventional wastewater pumping system working in ON/OFF mode. According to the comparison, the higher Net Present Value (NPV) of the MPP plant proves the advantage of this scheme over the conventional system, at least until the useful life of the plant is reached.

List of abbreviations

AML	Algebraic modeling Language
AMPL	A Mathematical Programming Language
BB	Branch and Bound
BP	Back-Pressure
BEP	Best Efficiency Point
EDP	Energy Production Device
ER	Electrical Regulation
HR	Hydraulic Regulation
GA	Genetic Algorithm
GOHyDeL	Global Optimization of Hydraulic Devices Location
LP	Linear Programming
MEI	Minimum Efficiency Index
MILP	Mixed Integer Linear Programming
MINLP	Mixed Integer Non-Linear Programming
MP&P	Mixed PAT & Pump turbocharger
NLP	Non-Linear Programming
NPV	Net Present Value
OF	Objective Function
PAT	Pump As Turbine
PRV	Pressure Reducing Valve

P&P	PAT & Pump turbocharger
RAE	Relaxation of Affinity Equations
VOS	Variable Operating Strategy
WD	Water Distribution
WSS	Water Supply System
WT	Water Transmission

Table of contents

List of figures

List of tables

Chapter 1

Introduction

One of the main challenges in the water industry consists of the reduction of environmental impacts, as well as the containment of energy use. Water distribution networks are energy demanding systems affected by very low efficiency [14, 29] due to the high energy consumption [30, 128], as well as the large water leakage caused by high pressure [51, 116]. Such a low energy efficiency results in significant economic and environmental disadvantages. Indeed, the energy consumption represents the main part of supply operating costs, as well as contributing to increase acid rains and greenhouse emissions, such as CO_2 [102, 93, 72]. A reduction of water losses may be therefore crucial to reduce the energy consumption, as around 40 - 60 % of the consumed energy is generally lost due to leakage and flow resistances [15]. It is expected that, in the absence of any sort of intervention, the energy consumption can reach the value of 136 TWh, in 2020. Such prediction aroused the emanation of directives by European Parliament (and Council). In particular, directive 2005/32/CE introduced the integration of environmental aspects in the design of devices that use energy. In 2009, this directive was replaced with the “Energy related Products”, namely 2009/125/CE, which is still in force and has the same aim of the previous directive but with a larger application field. The sustainable growth of water systems is therefore a topic arousing large interest in the last decades, and many strategies have been proposed in literature to increase the energy efficiency of such systems.
Despite their effectiveness, rehabilitation or replacement of damaged pipes [127] are very expensive solutions to reduce the amount of water leakage. The containment of wasted water can be alternatively guaranteed by pressure control strategy [50, 47, 121]: indeed, pressure regulation valves can be installed within pipes to keep under control the pressure, ensuring significant water savings. Nevertheless, the replacement of pressure

valves with energy production devices (EPDs), such as, turbines [106], microturbines [108], Pumps as Turbines [22], may further increase the efficiency of water systems. Indeed, EPDs can be employed to reduce the pressure, thus water leakage, and also produce energy, as these devices do not waste the excess pressure, but rather convert this in energy by a generator of electricity.
Among the EPDs, the interest of the recent literature is mainly focused on Pumps As Turbines (PATs) due to the lower costs and large availability when compared to traditional turbines [8]. PATs have been deeply investigated by many authors, in terms of hydro-power potential [114, 44, 111], hydraulic behavior [92, 52, 16] and regulation [19], but very few studies investigate the optimal location of such devices within a water network due to the complexity of the optimization problem. Despite the effectiveness of this sustainable strategy, the feasibility of PAT installation strongly depends on the recoverable energy, which can be quantified by means of efficiency measures [14]. Indeed, when the producible energy is not significant, the production of energy may not cover the high purchase and installation cost, thus the employment of dissipation valves may represent a more economical solution.
Further strategies have been proposed in literature to achieve a sustainable development of water systems. Optimal pump scheduling, in terms of pump start and rotational speed, in both clear [26, 113, 60] and drainage [27, 98, 45] pumping systems has been proven to be a very efficient solution. In this regard, a recent study [45] showed that an optimal pump scheduling in a drainage system can ensure an average value of recovered energy up to 32%.
An additional innovative strategy to water pumping is represented by turbo-pumps [17], namely, systems consisting of a turbine and a pump which are directly coupled and mounted on the same shaft. Turbo-pumps ensure both the recovery of stream energy and the reduction of pumping energy consumption, increasing the whole efficiency of the hydraulic system. If a PAT is employed instead of a classic turbine in order to reduce equipment costs, the resulting system is a PAT–pump turbocharger (P&P) [17]. Such a system has been proven [17] to be suitable for completely replacing an ordinary pumping system or supplying the network in presence of high available power, and its economic value has been supported by promising energy savings.
This research aims at developing new strategies to increase the energy efficiency within water systems. The main attention will be payed to optimization techniques to find the best location of hydraulic devices within a distribution network. Minor optimizations will be also performed to develop further strategies to reduce the energy requirement

of supply systems. The aim of the research and the structure of the proposed work are deeply investigated in the next sections.

1.1 Aim of the research

The proposed research work is part of the multidisciplinary REDAWN project (Reducing Energy Dependency in Atlantic Area Water Networks). REDAWN aims to foster the adoption of hydropower technologies within the water networks of the European Atlantic Area to increase the energy efficiency and reduce the environmental impact of these systems. It is part funded by the European Regional Development Fund (ERDF) through the Interreg Atlantic Area Programme 2014-2020.
In this research study, new solutions to achieve a sustainable management of water networks are developed. The proposed work can be organized in three lines of research. The main line is based on the optimal location of hydraulic devices within a water distribution network, maximizing both water and energy savings. The optimization tools employed in this first part of the research work are the results of the knowledge acquired during the six-month period spent at the Laboratoire d'informatique de l'Ecole Polytechnique (LIX) in France. The second line of research defines and compares in terms of energy efficiency two alternative solutions of supplying a water distribution network. The third line of research is instead based on the optimal design of a new device to recover energy in a water distribution network.
The three lines of research will be better detailed in the next subsections.

1.1.1 The optimal location of hydraulic devices

The main line of research is focused on the optimization of both number and location of hydraulic devices in order to maximize the energy production and water savings, as well as minimize the investment costs. Firstly, the installation of only Pumps As Turbines will be investigated and a new mathematical model will be developed. Several modifications within the model will be proposed to deal with the strong technical complexities arising during the computation. The developed model will be firstly applied to a literature synthetic network and, then, a real water distribution network will be also assumed as case study. Moreover, the optimization will be extended to the pressure reducing valves as well, as the installation of turbines may not represent always a viable solution. Indeed, whenever the reduction of pressure leads to large water savings but small energy recovery, a valve can be more convenient than a turbine. Finally, the installation of pumping systems will be also considered within the optimization procedure. Such a choice basically derives from the need to develop a more realistic and comprehensive mathematical model to optimize the location of hydraulic devices, suitable for any case study network.

The optimal location of a head-loss (i.e. a turbine or a valve) within a water network is a challenging topic affected by strong computational and technical complexities. First, the insertion of any device within a branch of the network strongly affects the hydraulic behavior of the network, and the operation of the installed devices in turn depends on the hydraulic behavior of the network itself [107, 119]. Furthermore, since the studied network will be not solved by any external hydraulic solvers, it will be modeled within the optimization procedure by means of the mass continuity equation in the nodes, and the momentum balance equation along the pipes. The discharges flowing through the pipes and the pressures within the nodes will be therefore variables of the optimization as well. As a result, the mathematical model will consist of both linear and non-linear inequalities constraining the optimization problem, as well as non-linear equations modeling the hydraulic resolution of the network. The total variables of the problem will be both binary (i.e. the installation of a device within a branch) and continuous (i.e., pressure in the nodes and the discharges within the pipes). The resulting model will be mixed-integer non-linear programming (MINLP), which represent the most challenging class of optimization problems. Moreover, when the optimization problem is applied to a hydraulic network, the number of variables increases along with the size of the network and also the complexity of the optimization increases accordingly. Finally, in this kind of optimization problems, it is worth highlighting that the number of variables is also significantly affected by the kind of hydraulic simulation (i.e. unsteady, steady, quasi-steady) [61], thus modelling the network according to the variable operating conditions further increases the computational effort of the optimization.

Due to the strong technical complexities affecting the mathematical problem, many efforts will be attempted to succeed in the simultaneous optimization of devices location. In particular, new formulations of the mathematical model will be proposed, and several relaxation techniques will be experimented to tackle the complexity of the optimization problem.

Despite the promising results achieved by heuristic methods in literature, in this research only deterministic solvers will be employed to perform the optimization, and a comparison of their performance will be also carried out. Most of the computations will be performed by a global optimization solver, which theoretically finds the global optimum of the optimization problem. The result will be a Global Optimization of Hydraulic Devices Location (GOHyDeL) model, suitable for any water distribution network.

1.1.2 Newly proposed supply solutions

Strategies based on the increase of the energy efficiency could be an important added value in the definition of new water supply chains with lower environmental impact. The second line of research is focused on the definition of two efficient solutions to supply a real water distribution network, as an alternative to the use of elevated water tanks or reservoirs with fixed pressure level.

A first hydraulic scheme will be investigated, consisting of a pump carrying the water up to a reservoir, which supplies a downstream water network. The available excess pressure will be not dissipated by a traditional valve, but rather a pump as turbine will be there installed to control leakage and also produce energy. The second scheme consists of a pump supplying the same downstream network directly from the water source, bypassing the upstream reservoir. Both the schemes will be designed in order to minimize the energy requirement, thus, maximize the energy efficiency of the whole system. In particular, such an optimal design will be intended to select the devices employed in the two schemes, in terms of both diameter and rotational speed.

1.1.3 A newly proposed device to save energy in urban water management

The third line of research regards the development of a new plant to increase the energy efficiency of a water distribution network, where the dissipation node is located close to a wastewater pumping station. The proposed plant consists of a PAT and a pump directly coupled and mounted on the same shaft: the PAT exploits the excess pressure within the fresh water network, and converts such a hydraulic energy in a mechanical torque. The torque supplies in turn the pump, which carries the wastewater of the sewage system into a treatment plant. In this last study, the optimization work will be not intended for its proper mathematical meaning, thus no solver will be applied to any mathematical model and no objective function will be actually optimized. Nevertheless, the proposed plant will be designed by a new selection strategy: several combinations of pumps and PATs will be therefore evaluated to select the most advantageous couple for the plant, namely, the combination better suiting the operating conditions. Then, the designed plant will need to be verified and simulated for different boundary conditions, and an economic comparison with a conventional wastewater pumping system working in ON/OFF mode will be also carried out.

1.2 Thesis structure

A general introduction of the research topic, as well as a presentation of the aim of the proposed work have been given so far. Henceforward, the document will be organized in nine further chapters.

- Chapter 2 investigates the hydropower potential of water supply systems. The problem of water leakage and the need of exploiting the excess pressures are also addressed in this chapter. Then, the main aspects of the hydropower plants and the involved technologies in both transmission and distribution networks are investigated. Among the energy production devices, main attention will be payed to pumps as turbines and their operation.

- Chapter 3 gives an overview of the main optimization tools used in the research work. In particular, this chapter presents in detail the solvers employed to perform the optimization procedures in the proposed research study, investigating the algorithms and techniques on which the selected solvers are based.

- Chapter 4 addresses the problem of the optimal location of only Pumps As Turbines within a water distribution network. After an investigation of the main works in literature dealing with the optimal PATs location, the new proposed mathematical model is presented and applied to a literature synthetic network, in both daily average and variable end-user demand conditions. Then, the results of the optimization are presented and compared with the solutions achieved by other authors in literature on the same water network. Finally, the limits of the solver employed to perform the optimization are also investigated.

- In Chapter 5, a global optimization solver is proposed to further tackle the problem. Since the mathematical model needs to be properly modified in order to be suitable for such a global optimization solver, a new formulation of objective function and mathematical constraints is therefore given, and a literature optimization method is adopted to deal with the computational complexity of the problem, when a daily variable end-user demand is assumed. Then, the results achieved by the new proposed optimization solver are presented and compared with the solution previously shown in chapter 4. Limits of optimal PATs location problem are finally investigated.

- In chapter 6, the simultaneous optimization of PATs and Pressure Reducing Valves (PRVs) is analyzed. Firstly, an overview of literature works dealing with the optimization of valves location within water networks is presented and classified depending on the optimization approach these studies are based on (i.e. heuristic or deterministic). Then, the mathematical model for optimal PATs location is integrated with new variables and constraints accounting for the installation of PRVs within the network. A new procedure to tackle the computational complexity of the optimization procedure is developed in order to achieve good results in acceptable time. Then, the results are presented for both daily average and variable demand conditions and compared with other studies in literature.

- In chapter 7, a real water distribution network is assessed as case study. Due to the increased complexity of the problem, pressure valves are initially not taken into account. Nevertheless, the reduction of excess pressure by PATs results in the inability for the flow to achieve the most remote nodes of the network, unless pumping systems are installed. Thus, the simultaneous installation of both turbines and pumps is investigated in the first part of chapter, and the mathematical model is properly modified with new variables and constraints. Then, the installation of PRVs will be also investigated and a new formulation of the mathematical model will be necessary to deal with the extremely hard computational complexity of the problem.

- Chapter 8 investigates the energy audit of a real water supply system. Two different solutions to supply a water network are developed and compared in terms of energy efficiency. New energy indices are introduced to assess the energy requirement of the proposed schemes, for different boundary conditions.

- In chapter 9 a new plant to increase the energy efficiency of a case study network is presented. This plant consists of a pump and PAT mounted on the same shaft, and operating with sewage and fresh water, respectively. The resulting plant is therefore called mixed PAT-pump turbocharger. The plant is designed by a preliminary selection strategy and simulated for different boundary condition. A comparison with a traditional pumping system operating in ON/OFF mode is also carried out and the limits of the plant will be finally presented.

- In chapter 10 a summary of the three lines of research is given and the expected developments of future research are also presented.

Chapter 2

Pressure management and hydropower energy recovery

2.1 Energy potential of Water Supply Systems

Water sources have an energy value as the water flow, Q, is related to an hydraulic power according to the following relation:

$$P = \gamma \ H \ Q \tag{2.1}$$

where γ is the specific weight of the water, and H is the total head, which is strictly related to the water pressure as follows:

$$H = z + \frac{p}{\gamma} + \frac{V^2}{2g} \tag{2.2}$$

with z geodetic elevation, $\frac{p}{\gamma}$ pressure head, $\frac{V^2}{2g}$ kinetic head of the water current, and V the mean flow velocity, related to the flow rate Q [126]. As a result, the water source presents a proper energy value, based on the entity of the flow rate (Q), the geodetic elevation (z) and the pressure (p).

The water transportation from the source to the end-user is designated to water supply systems (WSS), which include drinking water transmission (WT) and distribution systems (WD) [117]. A sketch of WSS is showed in Figure 2.1.

With reference to Figure 2.1, in the WT part of the system the water is transferred from the spring to several storage tanks located upstream of inhabited centres. Being

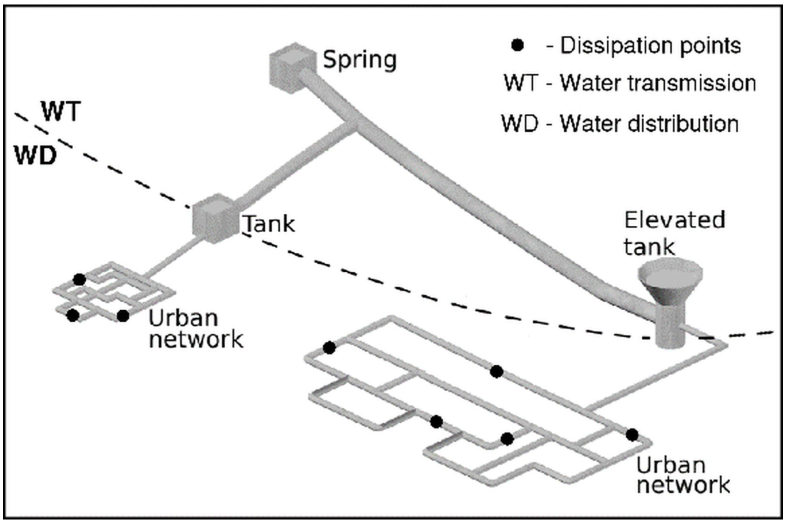

Fig. 2.1 Sketch of a water supply system (WSS) including water transmission (WT) and water distribution (WD) [20].

far from the end-users, WT networks present flow rate and pressure rather constant. In such systems, pumping or hydro power stations are generally introduced in order to address the differences between the spring and demand characteristics. With reference to WD part of the system, the network transfers water from the storage tank directly to the end-users by a complex system of pipelines. Unlike WTs, WD networks are characterized by variable flow rate and variable pressure, due to the fluctuation of the water demand [25]. Furthermore, WDs are generally divided into different water districts, characterized by homogeneous elevation levels. Moreover, within a same district, the pressure head could vary by several meters due to the flow resistance and the variation of both ground elevation and buildings height. An excess pressure could therefore occur and this represents an unfavorable condition since water leakage (q_l) increases accordingly:

$$q_l = f \ (\frac{p}{\gamma})^{\beta} \tag{2.3}$$

with f and β leakage coefficient and leakage exponent, respectively [3].

Nowadays reducing water leakage within distribution networks represents an important challenge for the water utilities [51]. Figure 2.2 shows the results of statistics referred to European countries in the time period 2012-2015. According to Figure 2.2, the amount of water loss significantly varies among the countries and its mean value is 23 %. Around half of the energy consumed to transport water is lost by resistance and leakage, thus reducing the amount of leaked water can be crucial to decrease the total energy consumption within water supply systems.

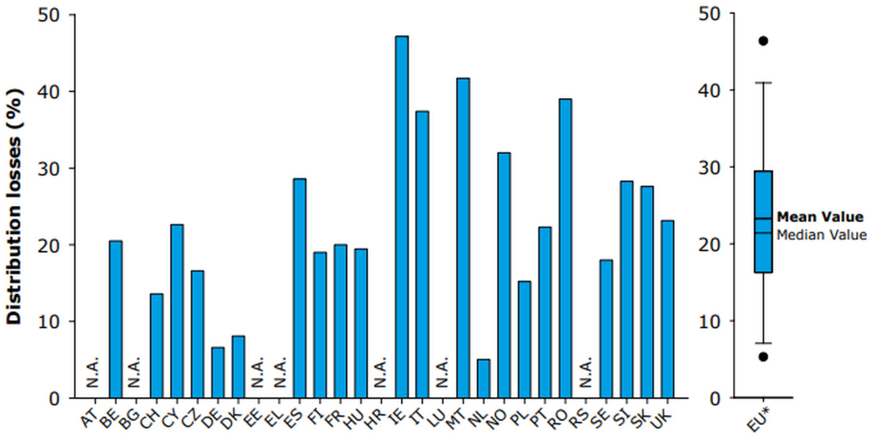

Fig. 2.2 Water distribution losses in EC countries in the 2012-2015 period (https://www.eureau.org/resources/publications/1460-eureau-data-report-2017-1/file).

Pressure reducing strategy commonly relies on the use of pressure reducing valves (PRVs), which dissipate the excess pressure that is not needed for the distribution, ensuring a pressure head closer to the optimal one [61].

Fig. 2.3 Pressure Reducing Valve (https://www.raci.it).

Nevertheless, the dissipation of the excess pressure within a pressure reducing valve is merely a loss of the energy embedded in the water stream. To save such an available amount of energy, EPD can be employed in place of PRVs in order to both reduce pressure, thus leakage, and produce energy (Figure 2.4)

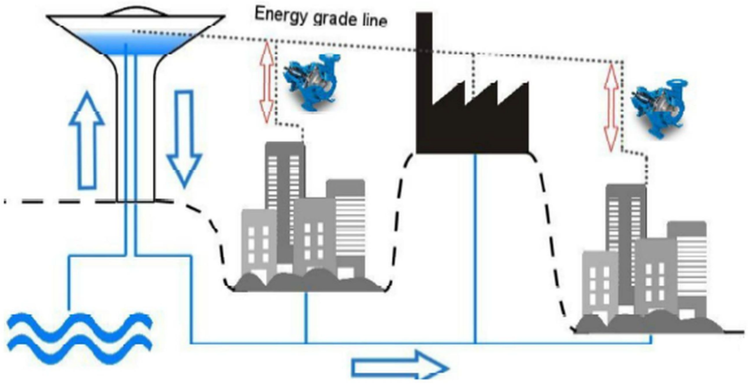

Fig. 2.4 Sketch of a water distribution network where the available excess pressure could be converted in energy by EPDs [97].

2.2 Hydropower plants in WT systems

Hydropower stations are widely diffused in water transmission systems, where the variability of flow rate and pressure drop are limited and the available power is frequently larger than 20-30 kW. In these plants, the only problem is represented by the complexity of the connection to the electric grid and by the absence of energy users nearby. Nevertheless, the additional costs for a grid connection do not affect significantly the payback period of the plant investment.
Due to the stability of the flow rate and head drop, traditional hydraulic machines, such as Francis (Figure 2.5(a)), Pelton (Figure 2.5(b)) or Banki (Figure 2.5(c)) turbines, are suitable for these plants.

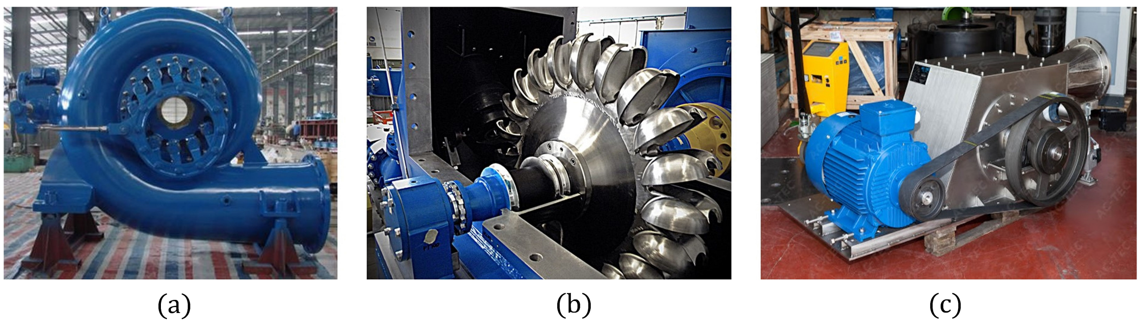

Fig. 2.5 Francis (https://www.energy-xprt.com) (a), Pelton (https://www.zeco.it) (b) and Banki (https://www.AC-TEC.it) (c) turbines installed in WT systems.

Francis turbine is used for power plant located along a transmission pipeline, in presence of backpressure. The smaller limit for Francis turbines employment is around 40-50 kW. The turbine is generally equipped with complex control system, allowing for the automatic opening of a bypass pipeline in case of any anomalies of the turbine or of the electric grid. Conversely, Pelton and Banki turbines are frequently installed at the end of a transmission pipeline, in absence of backpressure. The first turbine is suitable for medium to high head drops, while the second for small to medium head drops.

2.3 Energy production in WDs: Pumps As Turbines

Conversely to water transmission systems, in water distribution networks the production of energy is affected by several problems and limitations. First of all, the power available in WDs is often less than 10 kW and, due to the high cost per kW, a traditional turbine is not suitable for such a low power [97]. Moreover, the strong fluctuation of the flow rate and head drop, due to the demand variability, significantly decreases the efficiency of a traditional turbine [24]. It should be also considered that any additional cost dramatically increases the payback period [18], and the total income may be very small, so that it could be not appealing for the WSS management [92]. Finally, the installation of turbines and control equipment may be limited by limitation of space issues [91]. It is also worth highlighting that in the water distribution management the energy production is not the only aim of the EPDs employment, but rather there are further aspects that should be taken into consideration, such as the reduction of pressure within the network, the minimization of power plant cost and the maximization of power plant reliability. Due to the above mentioned reasons, traditional turbines are not viable for the energy production within water distribution networks. Therefore, new strategies have been developed for micro and pico hydropower generation in pressurized systems in order to overcome the aforementioned limitations. These strategies properly rely on regulation systems to address the daily fluctuations of flow rate and head drop [21], as well as new installation techniques or accurate choices of the dissipation points to contain additional costs [1]. Moreover, new energy policies have been developed in the last years, making the incomes more attractive for the WSS management [55].
Among the EPDs suitable for water distribution networks (e.g, Pumps as Turbine, Saint Gobain PAM microturbine, pressurized Banki-Mitchell, tubular propeller, pico-centrifugal turbine, energy booster, etc.), Pumps as Turbines (PATs) (Figure 2.6) are the most diffuse ones for high power production. PATs are traditional pumps used in inverse mode, thus in turbine mode, as shown in Figure 2.6.

Fig. 2.6 Pumps as Turbines (https://www.ksb.com).

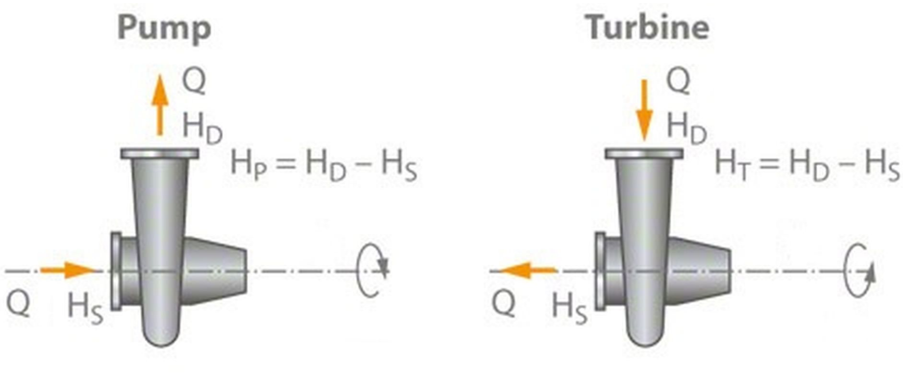

Fig. 2.7 Reverse mode operation of a pump.

Such devices are characterized by a motor working as generator of current. As for asynchronous motors, also for such generators the rotational speed only depends on frequency and number of poles and it is independent of supplied mechanical power and generated electric power. Thus, performance curves of this kind of machine are characterized by a fixed rotational speed that is imposed by the frequency of electrical network. In black out condition, such machine is not able to transform the mechanical power in electric power due to lack of current, thus it increases the rotational speed until dissipating the power.

2.3.1 Advantages and disadvantages of PAT installation

PATs present several functional and economic advantages. With reference to the functional aspects, such devices are characterized by a more compact dimension compared to most of the conventional solutions, as well as a very high reliability. In addition, mass manufacturing of pumps makes them easily available in a large number of standard sizes and characteristics. On the other hand, best efficiency point (BEP) of PAT is around 0.6–0.7, thus it is a bit lower than the maximum efficiency achieved by traditional turbines [23]. From an econonomic point of view, the main advantage is the low cost of PATs compared with microturbines. Indeed, the latter have an average installation cost approximately equal to 1800 €/kW [99], while PATs present installation costs reaching 350 €/kW and payback period less than 1 year [19]. Further advantages of PATs are: short delivery time, easy installation, operation and maintenance, large availability of spare parts.
Despite the above mentioned positive aspects, it is worth mentioning some drawbacks. Indeed, due to the rigid geometric configuration of volute case and impeller, centrifugal pumps do not offer possibility for flow rate regulation. Moreover, the operation of pumps in inverse mode requires some modifications which manufacturers do not always do, such as locking the impeller due to the thread direction. Furthermore, PAT manufacturers do not usually provide customers with PAT turbine characteristic charts, thus analytical methods need to be applied to estimate them. In particular, such scarceness of data can be overcome by applying the affinity laws to the performance curves of a prototype PAT. The affinity laws allow for the prediction of performance curves of devices by relating the performance of the prototype to the performance of a similar machine (having different diameter and rotational speed). Nevertheless, the prediction of performances curve by affinity laws is affected by an error, resulting from the assumption that the efficiency of similar devices is constant, although rotational

speed varies. Such assumption disagrees with the real behavior of turbomachines [110] which shows that the efficiency of a machine is significantly dependent on the rotational speed, and the maximum efficiency is achieved only at a given speed value. The error affecting the prediction by affinity laws increases as the rotational speed of the prototype and the simulated device diverge, thus the validity of affinity laws concerns an established range of rotational speed. Nevertheless, Fecarotta et al. (2016) [46] developed a model, that is, relaxation of affinity equations (RAE) predicting the variation of the efficiency with the runner speed. However, this model presents some limits since it can be considered valid only for an precise category of machines with a specific range of speeds.

2.3.2 PAT regulation and operation

A considerable problem in water distribution networks is represented by the need of dealing with variable operating conditions. Indeed, centrifugal pumps do not offer possibility for flow rate regulation due to the rigid geometric configuration of volute case and impeller. To guarantee a required head despite the variable conditions, modulation plants are required [94], such as a hydraulic regulation (HR mode) or an electrical regulation (ER mode) [20, 24].

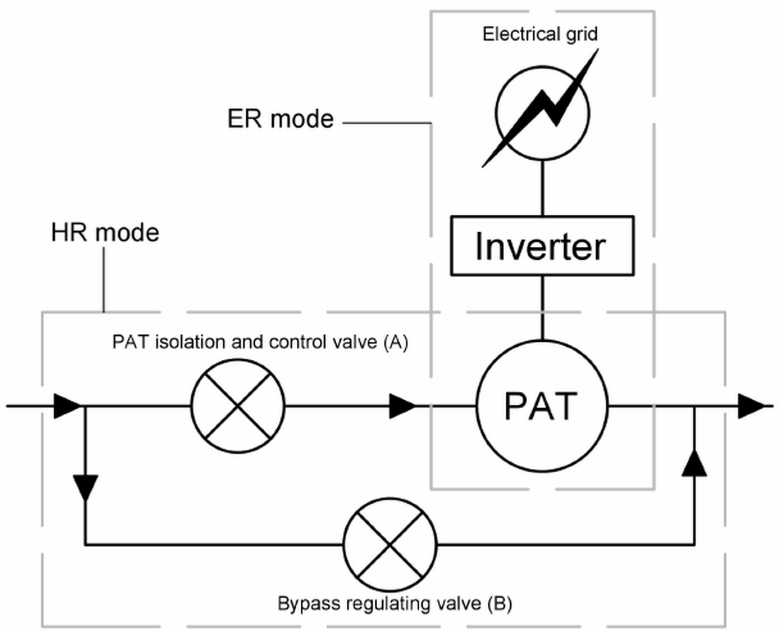

Fig. 2.8 Hydraulic regulation (HR) and Electrical regulation (ER) mode of a Pump as Turbine [19].

With reference to Figure 2.8, the hydraulic mode (HR) allows for the regulation of flow rate and head drop within the PAT, by means of a series-parallel hydraulic circuit. According to HR operation, when the head is higher than the head-drop deliverable by the machine, the excess pressure is dissipated by a valve (PRV); instead, when the discharge is larger, a bypass is opened to reduce the discharge flowing through the PAT, which otherwise would produce a head-drop higher than the available head, as shown in Figure 2.9.

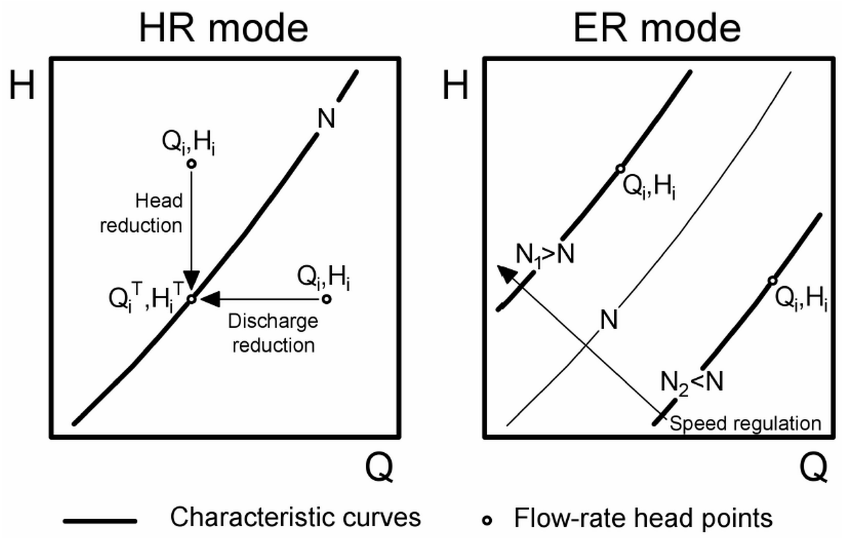

Fig. 2.9 Operating conditions of a PAT in HR mode (left) and ER mode (right) [19].

On the contrary, in ER mode, the regulation is performed by the use of an inverter, which modifies the frequency, thus the rotational speed, of the device itself to match the operating conditions determined by the instant flow discharge and head drop values. Compared to HR, ER mode presents lower efficiency [19] when the working conditions are different from the design values. Moreover, in ER mode the cost of equipment are higher than HR mode and the operating condition lie in a narrow band.

Chapter 3

Deterministic approach and optimization tools

Optimization methods can be classified as heuristic and deterministic approaches. Heuristic approaches rely on a computational procedure that searches for an optimal solution by iteratively attempting to improve a candidate solution according to a given measure of quality. Heuristics implement some forms of stochastic search optimization, such as evolution programming, evolution strategy, genetic algorithms, genetic programming, and differential evolution. Many works in literature based on heuristic approaches will be mentioned in section 6.2.1.
Deterministic approaches instead rely on the analytical properties of the problem to generate a sequence of points converging to a global optimum or an approximately global optimum [81]. Figure 3.1 gives an overview of existing problem types related to deterministic approach. With reference to Figure 3.1, at the base of any classification is the distinction between convex and non-convex optimization problems. The definition of convexity and its properties will be provided in detail in the next section. Given a convex optimization problem, if both the objective function and constraints are linear, it yields a Linear Programming (LP), whereas in presence of any non-linearities in the objective function and/or constraints it yields a convex Non-Linear Programming (NLP). Instead, non-convex problems are classified depending on the type of variables. In presence of integer variables (i.e. variables that must take integer values), the problem will be Mixed Integer Linear Programming (MILP), characterized by linear objective function and constraints. If the problem instead consists of any non-linearities in the objective function and/or in the constraints, the resulting problem will be non-

convex Mixed Integer Non-Linear Programming (MINLP) and convex Mixed Integer Non-Linear Programming (MINLP), depending on the continuous relaxation, that is, the problem obtained by relaxing the integrality requirement of the integer variables. Indeed, if the continuous relaxation yields a non-convex NLP problem, the resulting MINLP will be non-convex as well, and vice versa if the continuous relaxation is convex. Finally, non-convex optimization problems with continuous variables (i.e. variables that can take any value within a given range) yield non-convex Non-Linear Programming (NLP).

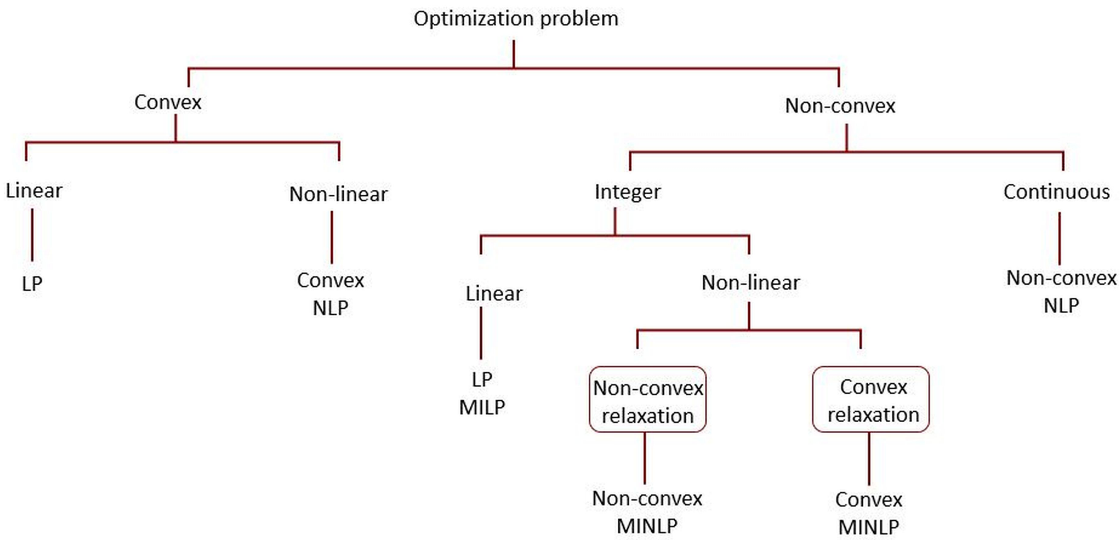

Fig. 3.1 Overview of problem types related to the deterministic approach [81].

In the following sections, the main tools employed in the proposed research for solving the optimization procedures are presented.

3.1 Mixed integer non-linear programming: generalities

Mixed-integer non-linear programming (MINLP) combines the modeling capabilities of mixed-integer linear programming (MILP) and non-linear programming (NLP) into a versatile modeling framework [76]. Mixed-integer non-linear programming addresses a general class of optimization problems with non-linearities in the objective and/or constraints, as well as both integer and continuous variables. A general MINLP problem can be expressed as:

$$\begin{aligned}
\min_{x,y} \quad & f(x,y) \\
& g(x,y) \leq 0 \\
& x \in X \cap \mathbb{Z}^q \\
& y \in Y
\end{aligned} \tag{3.1}$$

where $f : \mathbb{R}^{qxp} \to \mathbb{R}$, $g : \mathbb{R}^{qxp} \to \mathbb{R}^m$, with f and g both twice continuously differentiable, X and Y are two polyhedra of appropriate dimension (including bounds on the variables).

A MINLP is convex when its continuous relaxation - i.e. the problem obtained by relaxing the integrality requirement on the x variable - results in a convex NLP problem [76].

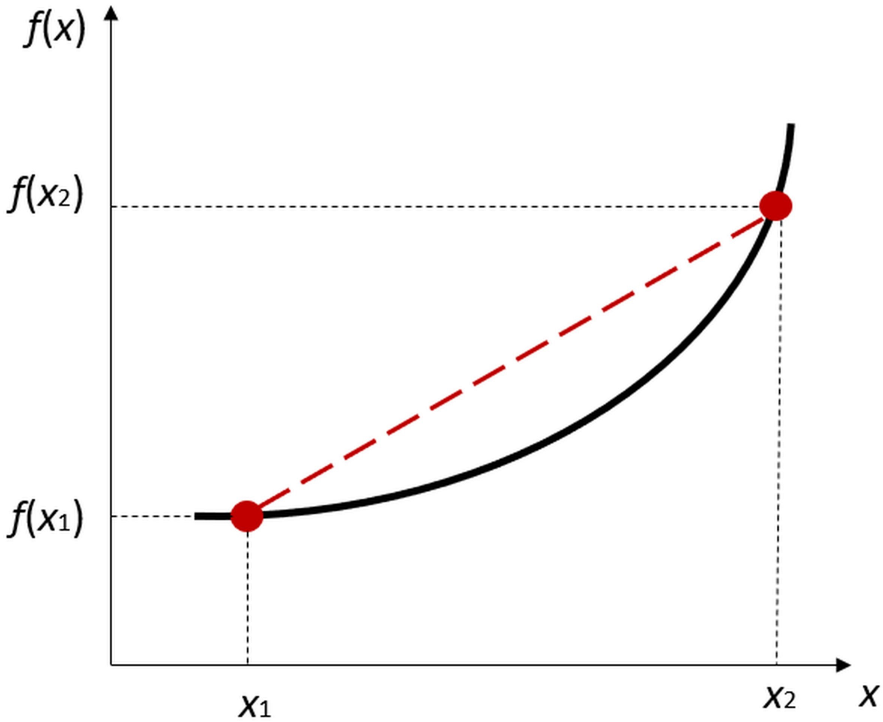

Fig. 3.2 General convex function.

In general, a convex optimization problem is a problem consisting of all the constraints being convex functions, and the objective being a convex function if minimizing, or a concave function if maximizing. With reference to Figure 3.2, a function defined on an n-dimensional interval is called convex if the line segment between any point $(x_1, f(x))$

to another point $(x_2, f(y))$, that is, the chord from x_1 to x_2 lies on or above the graph between the two points. In general, a twice-differentiable function of a single variable is convex if and only if its second derivative is non-negative on its entire domain.
The convexity represents a very crucial aspect in MINLPs. Indeed, in non-convex MINLPs, solutions that are optimal within a restricted part of the feasible region (i.e. local optima) may not be optimal with respect to the entire feasible region, thus, may not be global optima. This does not happen in convex MINLPs, which present the peculiarity of local optima being also global optima.

3.2 Optimization solvers

In the proposed research work, both NLP and MINLP solvers have been employed to perform the optimization.
With reference to MINLPs, most of the solvers dealing with this kind of problems are not based on a single algorithm, but rather combine several decomposition techniques. Such techniques simplify the general MINLP in Non-Linear Programming (NLP) and Mixed Integer Linear Programming (MILP) sub-problem, in whose fields there have been very promising developments in the recent years [76]. In particular, NLP sub-problems play a crucial role in the solution of MINLPs, and different types of solvers are available, both commercial and open-source. However, it should bear in mind that standard NLP solvers only guarantee local optima. In non-convex problems, indeed, the NLP solver may find different local optima when started from different starting points [39]. Thus, MINLP solvers relying on these standard NLP sub-solvers are exact only for convex MINLPs (local optima being also grobal optima) but only heuristic for non-convex MINLPs. As it will explained later on, only global optimization solvers guarantee the global optimality also in non-convex problems.

3.2.1 BONMIN

BONMIN (Basic Open-source Nonlinear Mixed INteger programming) is an open-source solver for MINLP problems [10]. The default solvers in BONMIN for MILP and NLP sub-problems are Interior Point OPTimizer (IPOPT) [123] and the Coin-or branch and cut (Cbc), respectively. Several algorithmic options are available within BONMIN, including Branch and-Bound-based (B-BB) and outer-approximation-based (B-OA) methods, which are exact only for convex MINLPs. To solve heuristically a problem with non-convex constraints, Branch-and-Bound- based algorithm (B-BB) should be only used [39], and several options are available for BONMIN to deal with non-convex problems.

Branch and bound

The Branch and Bound is an algorithm partitioning the solution space into disjointed subsets, which can be schematized as nodes of the branching tree (Figure 3.3). The

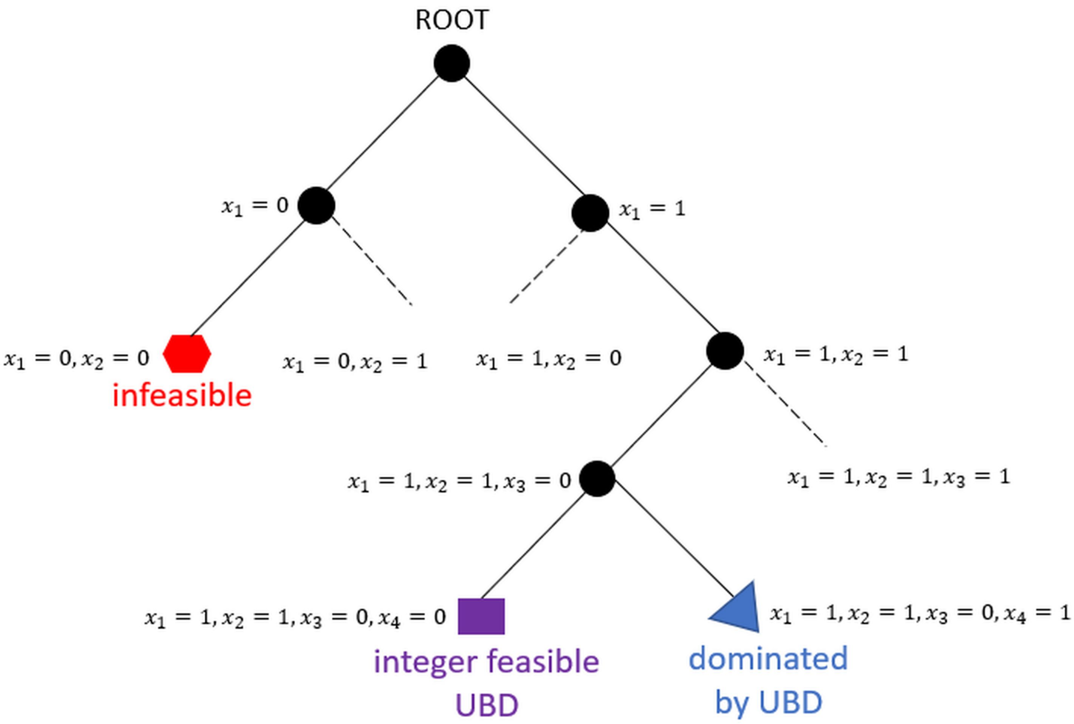

Fig. 3.3 Tree structure of Branch and Bound algorithm [6].

algorithm starts by solving the continuous relaxation of the MINLP, i.e. NLP^0, which represents the so called root node. As above mentioned, continuous relaxation consists of relaxing all the integrality requirements and treating the integer variables as continuous. If such continuous relaxation is infeasible (i.e. NLP^0 is infeasible), then MINLP is also infeasible. If the solution of the relaxation is totally integer, then it also solves the MINLP. Otherwise, branch-and-bound searches a tree whose nodes correspond to NLP sub-problems, and whose edges represent branching decisions [6]. Indeed, if the solution of the continuous relaxation (x^*,y^*) is not totally integer, the algorithm branches on any fractional variable $x_i = x^*_f$, which becomes the branch variable. Branching on a variable x_i means defining two new sub-problems by the introduction of two new constraints (one for each sub-problem), that is, $x_i \leq \lfloor x^* \rfloor$ and $x_i \geq \lceil x_f^* \rceil$, $\lfloor x_f^* \rfloor$ and $\lceil x_f^* \rceil$ being the lower and upper rounded integer values of x_f^*. Each sub-problem is a child node of the BB tree and in each node the branch variable x_i is subject to new bounds, according to the new additional constraints. During the branch operation, several pruning rules are observed:

1. If the solution of the continuous relaxation of the sub-problem (x^*,y^*) is integer and feasible, then this is a new incumbent solution only if the value of the objective function $f(x^*,y^*) \leq U$, where U represents the upper bound of the problem, set equal to infinite at the beginning. A new incumbent solution represents the best feasible solution encountered so far and the upper bound of the problem is updated as $U = f(x^*, y^*)$. Otherwise, the node is pruned because the optimal value of the NLP sub-problem (i.e. the lower bound associated to the sub-problem) is dominated by the upper bound and, in a convex problem, there cannot be any better integer solution in the sub-tree rooted at this node.

2. If the solution of the continuous relaxation of the sub-problem (x^*,y^*) is infeasible, then any problem in the sub-tree rooted at this node is also infeasible and it can be pruned.

With reference to Figure 3.3, the label "infeasible" refers to a node that has been pruned due to the infeasibility of the NLP sub-problem at that node. Then, label "dominated by UBD" is representative of a NLP sub-problem whose solution is larger than the upper, whereas the best feasible solution is labeled as "integer feasible UBD". Finally, the dashed lines represent opened nodes of the BB tree which have been not solved yet. The algorithm terminates when there are not any node left to explore, and it returns the incumbent solution, that is, the best feasible solution found so far. Although the attention here is focused on MINLPs, it is quite straightforward that Branch and Bound can be performed on both MILPs and MINLPs, with the difference that in the former problems, at each nodes the sub-problem is LP, whereas in the latter it is a NLP.
Several decisions are crucial components of BB algorithm. One among these is definitely the selection of the branching variables. Branching variables are good when maximize the increase in the lower bound at a node, in order to ideally reduce the size of the BB tree. A further strategic decision may regard which node should be solved next, in order to quickly find a good feasible solution proving the optimality of the current incumbent solution. It is worth underlining that the above mentioned decisions are significantly crucial in non-convex MINLPs, where these affect the quality of the found

local optimum (i.e. the solution at which the algorithm stops). All these decisions are deeply investigated in [6] and [68].
It exists a variation of Branch and Bound, namely, the Branch-and-Cut algorithm [7], which extends the branch-and-bound algorithm by an additional step, generating and adding to a node one or more cutting planes in order to cut off a fractional optimal solution. A node is branched on only if the relaxed optimal solution of the NLP sub-problem remains fractional even after a certain number of cuts or if no suitable cuts could be further generated. A cut basically consists of an inequality cutting off the fractional variable x_f^* from the feasible set of the NLP sub-problems. Cutting planes are added with the aim of determining a significant reduction of the tree size, cutting on fractional variables instead of branching on these. The branching on the variable x_i is performed only in case of no possible cuts to add.
With reference to BONMIN, if Branch-and-Bound- based algorithm (B-BB) is selected among all the available algorithmic options, a simple Branch-and-Bound is performed and no cuts are generated.

3.2.2 SCIP

SCIP (Solving Constraint Integer Programs) is a solver developed by the Optimization Department at the Zuse Institute of Berlin. SCIP was first developed as an MILP solver and then evolved into a global optimization solver allowing for the search of global optima in both convex and non-convex MINLPs. SCIP implements a Spatial Branch-and-Bound algorithm which is based on a sequence of solving sub-problems obtained by partitioning the whole original domain. Several heuristics are employed throughout the solving process to achieve feasible solutions early [122]. SCIP includes SoPlex for solving the LP sub-problems, but CLP, CPLEX, Gurobi, Mosek or XPress can be also used by the solver if available. Furthermore, SCIP uses IPOPT to solve NLP sub-problems.

Spatial Branch and Bound in SCIP

Unlike the traditional Branch and Bound algorithms, spatial Branch and Bound (sBB) are exact algorithms allowing for the achievement of global optima also in non-convex problems. The term "spatial" results from the partition of the Euclidean space into smaller regions (i.e. sub-problems) where the problem is solved progressively by generating converging sequences of upper and lower bounds to the objective function value [79]. Each of these sub-problems is associated with a node in a spatial branch-and-bound tree, where the original MINLP problem is allocated in the "root node". At each iteration of the algorithm, a lower and an upper bound of the objective function can be defined for each sub-region. Then, if the bounds are very close together, a global optimum of that region has been found. The whole process performed by the algorithm is iterative and consists of several steps [79, 112]. The process starts with an initialization, so that the convergence tolerance is set as $\epsilon \geq 0$, the best current objective function value as $U = \infty$ and the solution point as $x^* = (\infty, \ldots, \infty)$. Each iteration consists of the following steps:

1. (Choice of Region) A list of all possible regions to explore is available and progressively updated. If the list of regions is empty (i.e. there are not any left region to explore), the process stops providing the solution x^*. Otherwise, region R within the list is chosen by the algorithm according to some rules (the region with lowest lower bound is generally chosen). Then, the region R is deleted from the list.

2. (Evaluation of Lower Bound) A convex relaxation is solved in the region R to obtain an underestimation Λ of the objective function (i.e. a lower bound). Such a convex relaxation is obtained by dropping the integrality requirements and relaxing non-convex non-linear constraints (more detailed information will be presented later on). If the convex relaxation is infeasible (i.e. the resulting LP is infeasible), then the region R is deleted from the list. If either $\Lambda \geq U$ or the relaxed problem is infeasible, the algorithm goes back to step 1. Regardless, bounding is an useful tool to decide whether improving solutions can be found in a sub-region, as it is explained in the next steps.

3. (Evaluation of Upper Bound) The original MINLP problem is solved in the selected region R by a local minimization algorithm in order to obtain a locally optimal solution x' with objective function value υ. Several schemes to perform this step have been proposed in literature, such as, local MINLP optimization, NLP optimization with added ‘discreteness’ constraints, local NLP optimization with fixed discrete variables (see [112]). With reference to SCIP, it searches for a local optimum of the NLP obtained from the MINLP by fixing all integer variables to the values of the integer-feasible solution of the previous LP relaxation. Each feasible solution of this NLP is also a feasible solution of the MINLP.

4. (Pruning) If $U \geq \upsilon$, the solution x^* and the upper bound U are updated as x' and υ, respectively. Then, all regions in the list having lower bounds bigger than U are deleted as they cannot contain the global minimum.
5. (Check Region) If $\upsilon - \Lambda \leq \epsilon$, υ can be considered a global minimum for this region and the algorithm goes back to step 1, otherwise, the next step is followed.
6. (Branching) The current region R is split into two further sub-regions by applying some branching rules. The list of region is updated according to the new additional sub-regions (whose initial lower bound is Λ. Then, the algorithm returns to step 1.

The convex relaxation mentioned in step 2 is crucial to determine the lower bound of the problem in case of non-convex constraints and objective function. The aim of such relaxation is to reformulate the original MINLP (3.1) into a simpler form such that complex non-convex functions can be expressed as "basic" functions at the cost of additional variables and constraints. Then, such simpler non-linearities are relaxed using envelopes/underestimators [122, 84, 40] yielding an LP. With reference to Equation (3.1), the constraint $g(x,y)$ can be expressed as following:

$$g(x,y) = \sum_{i=1}^{m} g_i(x,y) \tag{3.2}$$

Actually, SCIP first performs a convexity detection, thus it may know that some constraints $g_i(x,y)$ are convex or concave. If $g_i(x,y)$ is convex, a linear underestimator is obtained by linearization of $g_i(x,y)$ at a known point (x^*,y^*), as shown in Equation (3.3).

$$g(x,y) \geq g(x^{*k},y^{*k}) + \nabla g(x^{*k},y^{*k})^T \begin{pmatrix} x - x^{*k} \\ y - y^{*k} \end{pmatrix}, \tag{3.3}$$

The first-order Taylor series approximation determines a set of supporting hyperplanes and any collection of such hyperplanes forms a polyhedral relaxation of these convex constraints, yielding an LP. An illustration of a linear polyhedral relaxation by hyperplanes is shown in Figure 3.4.

With reference to SCIP, if $g_i(x,y)$ is neither convex nor concave, but continuously differentiable, then SCIP can compute a linear underestimator of $g_i(x,y)$ by using interval arithmetic on the gradient of $g_i(x,y)$. Nevertheless, SCIP is able to handle

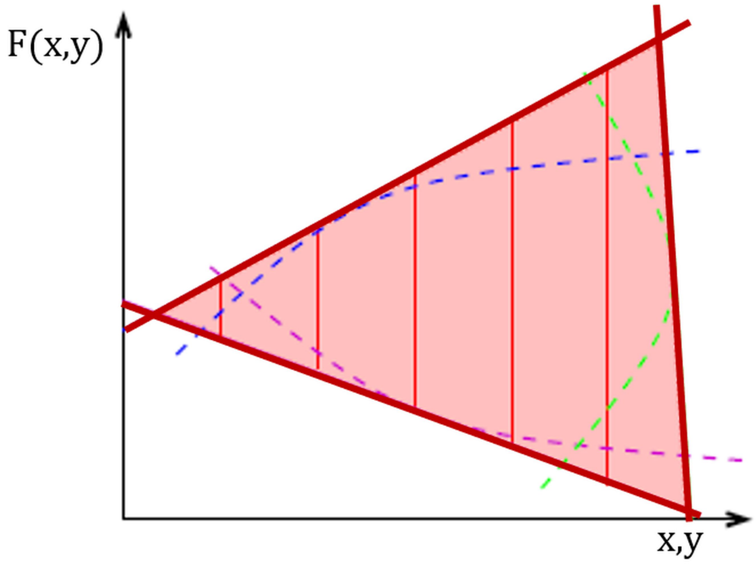

Fig. 3.4 Illustration of a linear relaxation by hyperplanes [6].

also more complex non-convex functions, such as, odd and signed power function, non-convex quadratic functions (by the McCormick underestimators [84]), second-order cones, factorable quadratic functions, and so forth.
For the sake of illustration, let g be a factorable function that can be rewritten as:

$$g = \sum_{\mu} \prod_{\nu} g_{\mu\nu}(x,y) \tag{3.4}$$

According to Equation (3.4), a complex function g can be reformulated and decomposed into simpler non-linear functions $g_{\mu\nu}(x,y)$, by auxiliary variables and constraints:

$$s_{\mu\nu} = g_{\mu\nu}(x,y) \tag{3.5}$$

$$s'_{\mu} = \prod_{\nu} s_{\mu\nu} \tag{3.6}$$

$$s''_{\nu} = \sum_{\mu} s'_{\mu} \tag{3.7}$$

This reformulation allows to obtain predetermined operators for which linear underestimators are readily available for the solver.

Main MINLP solving loop of SCIP

The main solving loop implemented by SCIP can be represented by the flow chart in Figure 3.5.

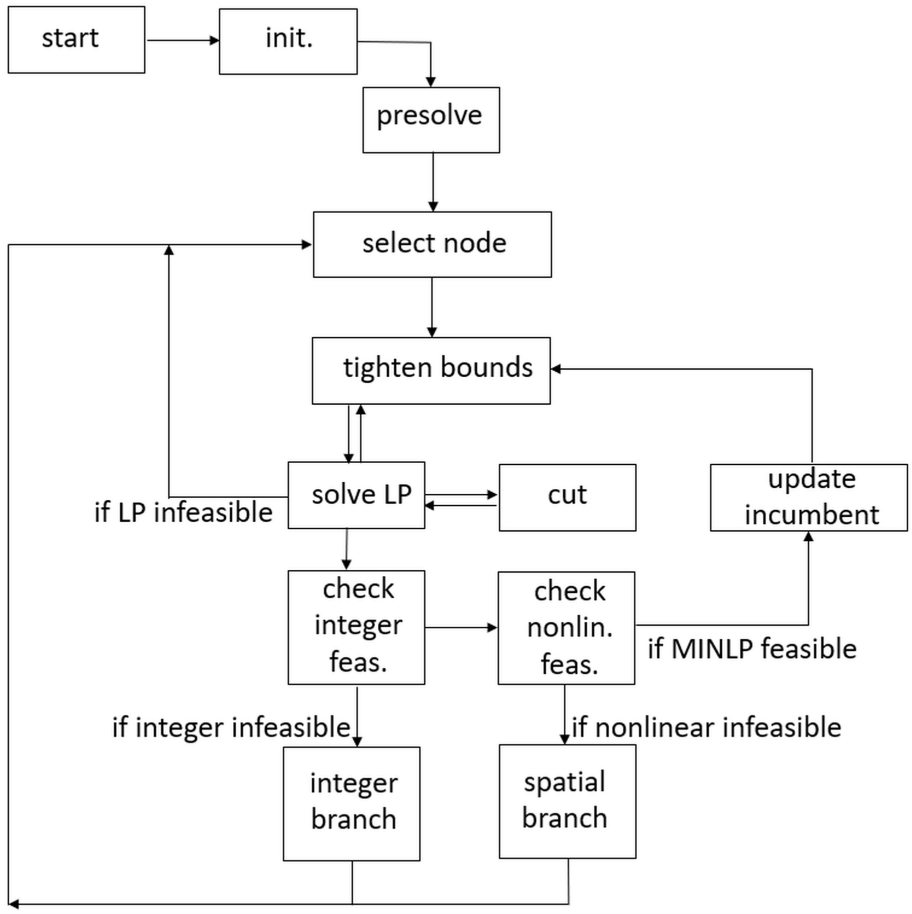

Fig. 3.5 Flow chart of the main solving loop of SCIP.

With reference to Figure 3.5, after the initialization, SCIP performs a presolving phase in order to reformulate complex factorable non-linear constraints into basic non-linearities by the aid of auxiliary variables, as previously mentioned. The difficulty lies in the fact that some reformulations are not known a-priori, but rather only become valid during the solving process, and, in addition, reformulated constraints may lead to further problem reductions. Thus, presolving phase is organized in iterated rounds, and for each round SCIP calls several methods to reformulate and reduce the constraints by preprocessings and convexity detection [122]. With regard to the tightening bound in Figure 3.5, this is a crucial procedure performed by the majority of MINLP solvers to obtain good quality solution in a reasonable time. In particular, bound tightening

refers to a class of algorithms aimed at reducing the bound intervals on the variables [6] in order to detect better lower bound on the objective. Once the tightening bound is performed, SCIP then applies the convex relaxation with linear cuts and solves the resulting LP (without both non-linearity and integrality requirements), as shown in Figure 3.5. If LP is infeasible, then SCIP prunes the sub-problem investigated at the current node, otherwise, it checks the integrality of the found solution. Thus, if the solution of LP consists of any fractional values of integer variables, then SCIP branches on that variable and comes back to selection of a different node (i.e. sub-problem), otherwise SCIP checks whether the solution of LP satisfies the non-linear constraints of the original MINLP problem. Then, in case of non-linear infeasibility (i.e. the solution of LP does not satisfy the non-linear constraints of the original MINLP problem), SCIP branches on the continuous variable violating non-linear constraints. It is worth noting that, unlike traditional branch and bound, spatial branch and bound can branch on both integer (integer branching) and continuous (spatial branching) variables. However, in case of feasibility of non-linear constraints (i.e. the solution of LP satisfies the non-linear constraints of the original MINLP problem), the integer variables are fixed according to the found LP solution and the resulting NLP sub-problem of the original MINLP is solved to local optimality. Indeed, due to the non-convexity of the original problem, feasible solution achieved by any NLP solver will be likely a local optimum. Finally, if the NLP is feasible, the original MINLP is feasible as well, thus the found solution is updated as new upper bound (i.e. new incumbent solution). Moreover, primal heuristics are applied at various points in order to attempt to find high-quality solutions early during the process.
The process will be iterated until the difference between upper and lower bound of the problem is less than the fixed convergence tolerance ϵ, as well as there are not any sub-regions left to explore. In other words, branching is performed as long as the relaxations are tight enough to provide solutions that are ϵ-feasible for the original problem [40]. The resulting solution will be a global optimum.

3.2.3 FMINCON

FMINCON (Find minimum of constrained nonlinear multivariable function) is an NLP solver available in MATLAB Optimization Toolbox [83]. FMINCON uses Interior-point as default optimization algorithm, but many algorithms can be selected by the solver, such as trust region reflective, active set, and sequential quadratic programming (sqp).

Interior point in FMINCON

Let assume a general NLP problem is given:

$$\begin{aligned} \min_{x} \quad & f(x) \\ & g(x) \leq 0 \\ & h(x) = 0 \end{aligned} \tag{3.8}$$

where $f : \mathbb{R}^n \to \mathbb{R}$, $h : \mathbb{R}^n \to \mathbb{R}^t$ and $g : \mathbb{R}^n \to \mathbb{R}^m$ are smooth functions, that is, have continuous derivatives up to some desired order over their domain.
For each $\kappa \geq 0$, the NLP general problem in Equation (3.8) can be written as:

$$\begin{aligned} \min_{x,\sigma} \quad & f(x) - \kappa \sum_i \ln(\sigma_i) \\ & g(x) + \sigma = 0 \\ & h(x) = 0 \end{aligned} \tag{3.9}$$

where $\sigma_i (i = 1 \ldots m)$ is a slack variable, which is restricted to be positive to keep the natural logarithm bounded, whereas the logarithmic term is called "barrier function". The new approximate objective function presented in Equation (3.9) is $f_\kappa(x, \sigma)$. The much κ decreases to zero, the more $f_\kappa(x, \sigma)$ tends to the original function (i.e. $f(x)$ in Equation (3.8)). To solve the approximate problem, the algorithm uses one of two main types of steps at each iteration. The first is the Direct step, also known as Newton step, whereas the second is the Conjugate Gradient step. By default, the algorithm first attempts to take the Direct step and, if it cannot, it attempts the Conjugate Gradient step. In the Newton step, the auxiliary Lagrangian function is first computed, as following:

$$L(x, \lambda) = f(x) + \sum_i \lambda_{g,i} g_i(x) + \sum_j \lambda_{h,j} h_j(x) \tag{3.10}$$

$\lambda_{g,i}$ and $\lambda_{h,j}$ being the Lagrange multipliers. Then, based on the calculation of $L(x, \lambda)$, the following quantities are also computed:

- H, that is, the Hessian of the Lagrangian $L(x, \lambda)$:

$$H = \nabla^2 f(x) + \sum_i \lambda_{g,i} \nabla^2 g_i(x) + \sum_j \lambda_{h,j} \nabla^2 h_j(x) \tag{3.11}$$

- J_g , which is the Jacobian of the constraint function g.
- J_h , which is the Jacobian of the constraint function h.
- Σ and χ as diagonal matrices of σ and λ, respectively.
- λ_h representing the Lagrange multiplier vector associated with h.
- e denote the vector of ones having the same size as g.

The search direction $(\Delta x, \Delta\sigma, \Delta\lambda_h, \Delta\lambda_g)$ can be computed by Equation (3.12).

$$\begin{bmatrix} H & 0 & J_h^T & J_g^T \\ 0 & \Sigma\,\chi & 0 & -\Sigma \\ J_h & 0 & I & 0 \\ J_g & -\Sigma & 0 & I \end{bmatrix} \begin{bmatrix} \Delta x \\ \Delta\sigma \\ -\Delta\lambda_h \\ -\Delta\lambda_g \end{bmatrix} = - \begin{bmatrix} \nabla f - J_h^T\, y - J_g^T\, \chi \\ \Sigma\lambda - \kappa e \\ h \\ g + \sigma \\ \end{bmatrix} \tag{3.12}$$

Major details about system (3.12) can be found in Byrd et al. (1999) [13]. However, before updating x, σ and Lagrangian multipliers according to the found search direction $(\Delta x, \Delta\sigma, \Delta\lambda_h, \Delta\lambda_g)$ (i.e. summing the search direction to the values of x, σ and Lagrangian multipliers at the previous iteration), the algorithm evaluates a "merit function" at each iteration, as following:

$$f_\kappa(x,\sigma) + \nu \parallel h(x), g(x) + \sigma \parallel \tag{3.13}$$

where $\nu \geq 0$ is a penalty parameter, which may increase with iteration number in order to force the solution towards feasibility. In literature many authors proposed different rules [124] of ν. However, if at a given iteration, the merit function is decreased enough [83], the algorithm updates x, σ and Lagrangian multipliers by summing the new search direction step $(\Delta x, \Delta\sigma, \Delta\lambda_h, \Delta\lambda_g)$ and goes back to Equation (3.10). Otherwise, the algorithm rejects the current search step and attempts a different shorter step, calculating a new value of the merit function.
Major details are available within the manual of MATLAB Global Optimization Toolbox [83].

3.3 Comparing BONMIN and SCIP

In this research study, the optimization of hydraulic devices location will be performed by both BONMIN and SCIP, whereas minor optimizations (presented in chapter 8 and 9.) will be performed by FMINCON.
As previously mentioned, BONMIN implements Branch and Bound algorithm, and calls the sub-solver CBC to perform all the MILP operations, such as tree search, whereas calls IPOPT as a sub-solver for NLP sub-problems. Relying on NLP solvers, BONMIN is an exact method only for convex problems. Indeed, during the resolution of each NLP sub-problem, the NLP solver provides a valid bound of the problem (i.e. the global optimum of the NLP sub-problem) only if the NLP is convex (i.e. any local optima found are also global optima). On the contrary, if the NLP sub-problem is non-convex, the optimum found by the NLP solver is likely to be local and the found solution does not represent a valid lower bound of the general MINLP problem. It may therefore happen that a node of the tree containing solutions better than the incumbent is inappropriately pruned as the associated lower bound (which is not a valid bound in non-convex problem) is larger than the upper bound.
Unlike BONMIN, SCIP allows to achieve global optima, no matter if the problem is convex or non-convex. Indeed, SCIP implements a global optimization method, that is the Spatial Branch and Bound, building a sequence of decreasing upper bounds and increasing lower bounds to the global optimum of the problem. Nevertheless, the computational time required by SCIP to achieve such a global optimum may be infinite. For this reason, in optimization problems affected by hard complexities, SCIP is used even to find sub-optimal solutions. Despite this, the enormous power of a global optimization solver as SCIP lies in the possibility for the user to evaluate the effectiveness of the found local optimum, providing the solver the gap between the incumbent solution and the effective bound of the problem.

3.4 Algebraic modeling Languages

An important tool in the framework of optimization methods is the language used to model the problem, namely, the modeling language.
Modeling languages convert a mathematical model to a form readable by the optimization solver and in turn translate the solution provided by the solver in a form readable by the user. Algebraic modeling languages (AML) represent the most used modeling

languages due to their intuitive syntax which is very similar to the mathematical notation. In addition, in non-linear programming (NLP), AML provides the solver with the first and second derivatives at a given point, as well as the proper value of a function, which is generally required by NLP solves and may be not straightforward for a non-expert user [39]. It is worth mentioning that AMLs cannot use external solvers, as well as do not perform any computation as solvers do, but at the most can perform a presolve phase, attempting to simplify a problem instance before it is sent to a solver and also detecting any trivial infeasibilities. The most used algebraic modeling languages in MINLP are GAMS [11] and AMPL [53]. AMPL is particularly notable for its general syntax, and for its variety of set and indexing expressions. AMPL presents a decoupled structure keeping distinct the file containing the mathematical model from the data file. This allows to separate the logical structure of the model from the proper values of the numerical data, or to change the data without the need of modifying the model, thus avoiding to introduce errors.
In this research study, all MINLPs will be modeled by the language AMPL.

Chapter 4

Optimal location of Pumps as Turbines

4.1 Introduction

In this chapter, the optimal location of PATs within a water distribution network is investigated in order to maximize both water and energy savings and minimize the investment costs. The installed devices will not be designed as real machines, but rather will be simulated as head losses within the pipes. New mathematical constraints will be defined in order to develop a new more comprehensive optimization model, compared with other models in literature. The resulting mathematical model will be applied to a literature synthetic network [73] and both daily average and variable end-user demand will be considered.

In this study [87], instead of using external programs to solve the hydraulic network, the evaluation of the flow rate within the pipes and the pressure at the nodes will be accomplished within the same mathematical model by means of proper hydraulic constraints. The optimization procedure will be performed by a deterministic optimization solver and the results will be compared with the solution achieved by other authors in literature on the same hydraulic network, in order to highlight the obtained improvements.

Before presenting the optimization problem, the state of the art of the optimal location of PATs within water distribution networks will be firstly investigated in the next section.

4.2 PATs optimal location: state of the art

In the optimization of turbines location, the energy saving due to the production of energy should be taken into account together with the reduction of water leakage. The complexity of the optimization further increases if real turbines are simulated by applying the affinity laws to a wide set of characteristic curves.

Giugni et al. [61] used a genetic algorithm to investigate the optimal location of a fixed number of PATs in a water distribution network. The authors did not manage to optimize simultaneously both water and energy savings, but rather performed two different optimizations to maximize the production of energy and the reduction of water leakage separately, with consequent different results. Corcoran et al. [31] used a mixed-integer non-linear solver to optimize the location of a fixed number of turbines in order to maximize the only production of energy. The authors performed a two-step optimization: in the first step the optimal location of devices under steady flow conditions was investigated, then a second optimization was performed to find the optimal value of the head losses according to the daily pattern, once the location was known. Jafari et al. (2015) [71] proposed two steps to control pressure and recover energy. In the first step, a genetic algorithm was used to investigate the optimal location and setting of PRVs, in order to minimize the pressure within the network. In the second step, PRVs determining high head-loss were replaced by PATs. This study shows that the replacement of PRVs with PATs can ensure significant water and energy savings, as well as the investment is payed back in a very short time. An important novelty in literature has been introduced by Fecarotta and McNabola (2017) [48], who investigated the optimal location of PATs within a water network by a single objective function accounting for both water and energy savings. In the study [48] the optimization solver BONMIN [6] has been employed to solve a mixed inter non-linear programming model. The number of turbines has been not set a-priori, but rather it is a variable of the optimization procedure as well. According to the comparison with the works investigating the same hydraulic network [61, 31], the results achieved by Fecarotta and McNabola [48] resulted improved in terms of both energy production and water leakage. Despite this, the phenomenon of flow reversion as well as the definition of a minimum power producible by the PATs have not been included in the mathematical model.

A very interesting study has been carried out by Lima et al. [80], who applied the optimization to three fictitious water networks and optimized both energy and water savings. The authors set a-priori the number of PATs and performed the optimization

of the location, as well as the selection of machines, by using a bio-inspired algorithm, thus a meta-heuristic technique based on the behavior of bird groups, namely, PSO. A set of complete characteristic curves of pumps was used and the rotational speeds of PATs were obtained according to the nearest available curve. Given a fixed number of devices, the optimization found the best location within the network, as well as, the BEP of the machines. The installed PATs were selected to operate at the higher consumption period, whereas, when the flow decreased, there was no energy production. The authors [80] made a comparison with the results achieved by replacing such turbines with PRVs, observing a more significant water saving during low consumption periods, as PATs cannot maintain adequate outlet pressure, yielding high leakage rates.
Further improvements have been achieved by Tricarico et al. (2017) [119] performing a multi-objective optimization by a genetic algorithm, in order to minimize both the surplus pressures and pumping operational costs, as well as maximize the energy recovery. The optimization was applied to real water networks and real machines have been considered by the selection of a wide set of PAT characteristic curves. Fixed a maximum number of installed devices, the aim of the study [119] was to develop a methodology for the optimal management of water systems, decision variables being locations and types of PATs to be installed, as well as, the related pump schedules and initial tank levels. As water demand varies along the day, the characteristic curves have been also studied away from the BEP. The results achieved by the authors show that significant energy recovery may result from the installation of PATs in network with high differences in pressure level. The convenience of such strategy therefore strongly depends on the characteristic of the hydraulic network.
Tahani et al. (2019) [118] performed an optimization methodology aiming at maximizing the produced power in a real water distribution network and minimize the upsurge ratio (in order to minimize network risks and increase the safety of the network). As variables of the problem, the pipe number, as well as, the position along the selected pipe, have been assumed. Different inspired optimization algorithms have been attempted to perform the optimization.
Garcia et al. (2019) [57] used different multi-objective approaches to optimize both the location and settings of either PRVs or PATs in a water distribution network. The optimization of PRVs aimed at minimizing the unperceived profits due to water leakage, as well as minimize the capital costs due to the PRVs installation. This approach has shown an effective performance in the reduction of water leakage by using a small number of valves in the network. The second approach consisted in finding the optimal location and setting of PATs in order to minimize the unreceived profits due to water

losses, as well as maximizing the potential energy savings. Several characteristic curves were considered in order to evaluate different machines, but the capital costs of the PAT are not considered. As a result, this approach installed a PAT at each pipe of the system, which is not feasible due to the high investment cost.
Nguyen et al. (2020) [95] devoloped a MINLP model to optimize the location of PATs, modelled as head-loss within the water network. The authors did not take into account the simultaneous maximization of water and energy savings, but rather optimized the only power produced by the turbines. The MINLP model also consists of constraints fixing a minimum value of produced power, as well as preventing the installation of PATs in the branches where the flow reverts. The comparison with the results achieved by Giugni et al. [61] on the same network [73] shows an improvement in leakage reduction. The authors [95] also applied the model to a real network. After the optimal location of PATs was found, the non-linear optimization problem (i.e. with the fixed locations of the PATs) was solved for the 24 demand patterns to evaluate the benefit of placing PATs by reducing the excess pressure.

4.3 Case study and literature results

In this research work, a literature synthetic network [115] has been assumed as case study. The layout of the network is shown in Figure 4.1 whereas the characteristics of the pipes and nodes are presented in Appendix. The network in question consists of 37 links and 23 nodes and is fed by gravity by three reservoirs, whose level has been assumed as constant. The daily pattern of the demand coefficient δ representative of the operating condition of the network is presented in Figure 4.2. Several abovementioned studies in literature applied the optimization problem of PATs location to the same case study network.
Giugni et al. [61] optimized the location of a fixed number of devices within the synthetic water network [73]. A genetic algorithm was used to find the branches where installing the turbines under steady conditions, while an external solver was employed to model the hydraulic behaviour of the network. The authors performed two optimization procedures using two different objective functions: the first (i.e. OF1) aims at minimizing water leakage by minimizing excess pressure, the second (i.e. OF2) at maximizing energy production. In the latter case, the author introduced a penalty term within the objective function to avoid a node pressure lower than the target value.

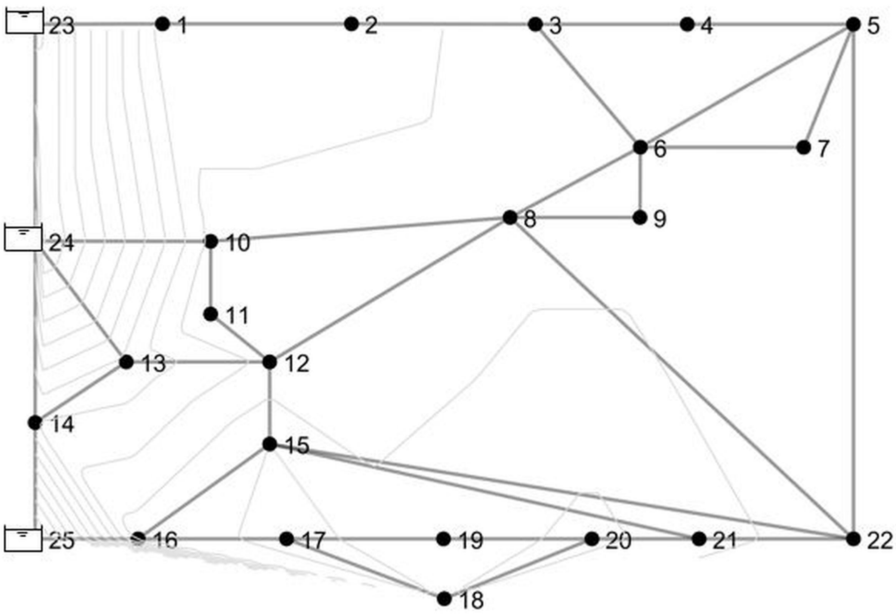

Fig. 4.1 Benchmark network layout [73].

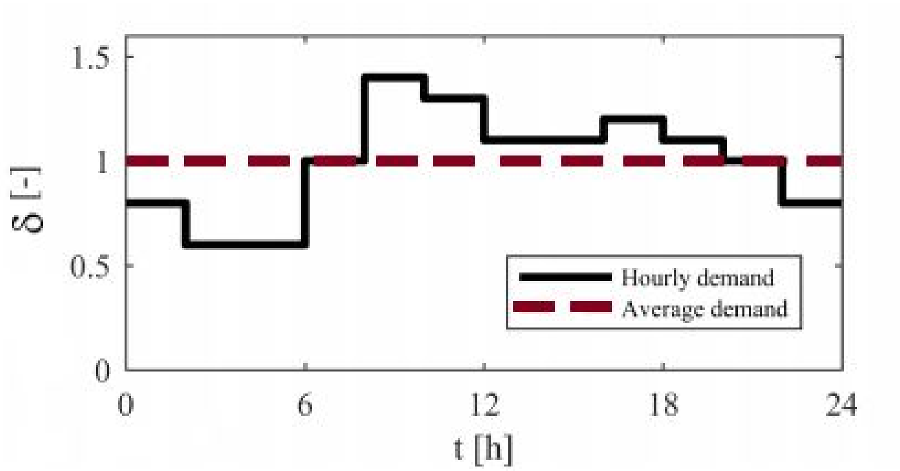

Fig. 4.2 Daily pattern of end-user demand coefficient [48].

According to the results presented in Figure 4.3, minimizing the excess pressure (see OF1) determines significant leakage reduction and may also determine the production of energy, while maximizing the energy production (see OF2) ensures higher energy production and only a slightly decreased leakage volume reduction. Both water and energy savings have been evaluated by varying the number of devices (i.e. nv) between one and three.

Corcoran et al. [31] used a mathematical programming to optimize the location of a fixed number of turbines. As objective function, the only maximization of the energy

OF	*nv*	1	2	3
(1)	Leakage volume reduction (m^3)	568.8	689.8	732.5
(2)		529.1	604.1	709.5
(1)	Potentially recoverable energy (kWh)	123.5	198.6	206.9
(2)		129.3	275.3	327.0

Fig. 4.3 Daily water and energy savings according to the solution obtained by Giugni et al. (2014) [61].

production was considered by the authors. The optimization was divided into two steps: in the first step a MINLP was performed under steady flow condition and fixing the number of devices to install; then a second optimization was performed to find the turbine operation according to the daily pattern, once the location was fixed according to the previous step. Fixing the number of turbines as three, the authors varied the constraints on the head drop, obtaining different values of total power generation, as shown in Figure 4.4.

Three turbine combination	Total power generation (kW)	Solution time (s)
Links 5, 11, 24	14.02	8.28
Links 1, 5, 11	16.43	10.87
Links 11, 5, 8	14.96	14.26
Links 11, 24, 25	10.12	7.01

Fig. 4.4 Total power generation assuming machine efficiency equal to 100% and computational time [31].

Significant improvements have been achieved by Fecarotta and McNabola (2017). The authors investigated the optimal location of PATs in the network [73] accounting for both water and energy savings within one single objective function, i.e. the Net Present Value (NPV) of the investment. Unlike the aforementioned authors, the number of turbines was not set a-priori, but rather was a variable of the oprimization problem. A MINLP model was developed and then solved by BONMIN [6] solver. The optimization was undertaken investigating both daily average and variable flow conditions and, for each demand condition, three scenarios were considered (Figure 4.5). In the first scenario, the water leakages were not taken into consideration, while in the second and in the third scenarios were included into the simulation. Only the third scenario accounted for the economic value of the water. Despite the promising results achieved

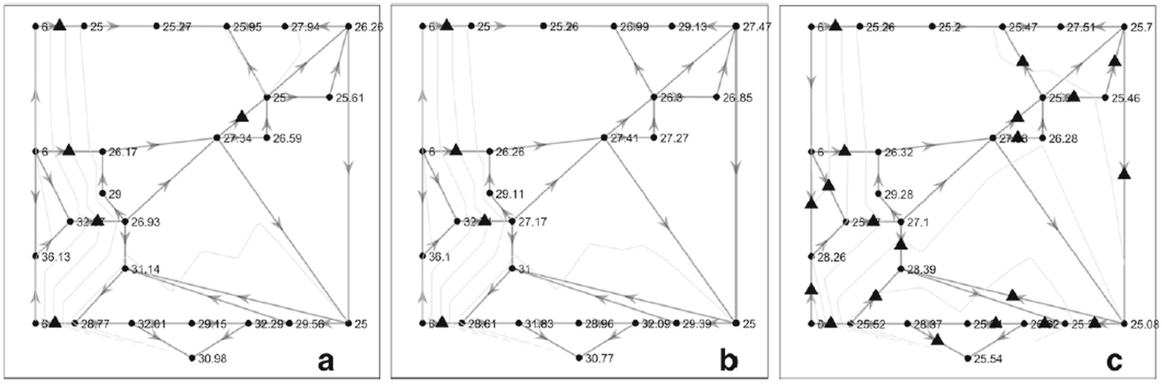

Fig. 4.5 Optimal location of turbines and pressure values at nodes according to the solution achieved by Fecarotta and McNabola (2017) [48] in daily pattern simulation for scenario 1 (a), 2 (b) and 3 (c), respectively.

by Fecarotta and McNabola (2017) [48] in terms of both energy and water savings, the study presented several weaknesses. Indeed, in the third scenario simulation, most of the installed turbines produced very low power (i.e. less than 500 W), since the high increase of the NPV due to water savings pushed the algorithm to install a high number of devices, no matter if several turbines produced low power. However, since installing low power devices does not represent a viable solution, the authors tried to include within the model a constraint fixing a minimum value of producible power, but the resulting optimization did not terminate successfully. For this reason, the authors replaced a-posteriori low power turbines with PRVs. Another weakness is represented by the fact that the authors did not take into account the phenomenon of flow reversion that may occur during the day, indeed they verified a-posteriori whether the flow reverted within the pipes where turbines had been installed by the solver. Fortunately, this happened only in the branches where at the most low power devices had been installed, so the flow reversion did not seem to affect the found solution. However, the authors did not provide any information about the kind of installed valves, as well as the way such devices could operate in case of flow reversion.
Nguyen et al. (2020) [95] optimized both number and location of PATs, modeled as head losses within the pipes. The authors maximized the only power production, thus the minimization of water leakage was not included within the objective function. A MINLP model was developed, including the phenomenon of flow reversion during the day and also a constraint fixing a minimum value of producible power. The optimization was performed by considering different values of minimum power produced by the turbines (i.e. 0.25 kW, 0.75 kW and 1.5 kW), and also considering both constant and variable water levels within the reservoirs (Figure 4.6).

Scenarios P_{min}	PAT Locations	Computation Time (s)
0.25 kW	25–16; 24–10;23–1;13–12	3542.20
0.75 kW	24–10; 23–1; 13–12	1537.86
1.0 kW	24–10; 13–12	2185.59
1.2 kW	24–10; 13–12	26.38
1.5 kW	24–10; 13–12	1224.92

Fig. 4.6 Optimal location of turbines for different values of minimum producible power [95].

4.4 Optimization variables

In this newly proposed study, given a network of l links and n nodes, the optimization procedure aims at finding the best number and location of PATs in order to maximize both energy and water savings. The network has been modeled as a directed graph, so that each branch k has a direction. The presence of a turbine within a branch k of the network is modeled by a binary variable (I_k^T), which is equal to one if the turbine is located in that branch, zero otherwise. In the branches where the turbines are located, the optimization procedure also aims at determining the head-loss within the turbines, that is, H_k^T. As the installation of turbines affects the hydraulic behavior of the network, the discharge flowing through the k-th link (Q_k) and the pressure head in the i-th node (H_i) are additional variables of the problem. The discharge (Q_k) will be positive if it flows according to the direction of the branch k, and negative otherwise. With regard the head $H_i(t)$, it has been constrained as following:

$$\frac{p_{min}}{\gamma} \leq H_i(t) - z_i \leq \frac{p_{max}}{\gamma} \tag{4.1}$$

p_{min} and p_{max} being the minimum and maximum pressure values allowable at each node, z_i the elevation of the i-th node, and γ the specific weight of water. If the node is a reservoir, the corresponding head $H_i(t)$ is a boundary condition and the variable is the discharge flowing into or out of such reservoir, that is q_r.
The end-user demand has been concentrated in the nodes of the network and, with reference to the node $i(i = 1..n)$ and time $t(t = 1..24h)$, such demand $q_i^d(t)$ can be expressed as:

$$q_i^d(t) = \delta(t)\ \overline{(q_i^d)} \tag{4.2}$$

where $\overline{(q_i^d)}$ is the daily average demand of the node i, and $\delta(t)$ the demand coefficient at time t whose daily pattern has been previously shown in Figure 4.2.
According to Figure 4.2, as the demand coefficient $\delta(t)$, thus the demand end-user demand $q_i^d(t)$, has the same value in different time intervals, the variables of the problem need to be computed only once for each value of $\delta(t)$. As in the study [48], the simulation can be therefore divided into n_d ranges of demand coefficients δ, each one presenting a duration Δt_d. To summarize, the number of independent variables can be therefore accounted according to Table 4.1:

Table 4.1 Summary of the binary (B) and continuous (C) independent variables of the optimal PAT location problem.

Variable	I_k^T	$H_k^T(\theta)$	$Q_k(\theta)$	$H_i(\theta)$	$q_r(\theta)$
Number	l	$l \cdot n_d$	$l \cdot n_d$	$(n-\varsigma)\cdot n_d$	$\varsigma \cdot n_d$
Type	B	C	C	C	C

with $(\theta = 1 \ldots n_d)$ and ς being the number of reservoirs.

4.5 Non-linear constraints

The non-linear constraints consist of the hydraulic equations modelling the resolution of the network, such as the momentum balance equations along the pipes and the mass continuity equations within the nodes. Given a node i $(i = 1..n)$ and a demand step θ $(\theta = \ldots n_d)$ the mass continuity equation for an incompressible fluid can be written as following:

$$\sum_{k=1}^{K_i} Q_k^{in} - \sum_{k=1}^{K_i} Q_k^{out} - f_i \, p_i^{\beta} - q_i^d = 0 \tag{4.3}$$

Q_k being the total discharge in the k-th link belonging to the set K_i of links approaching the node i, and the superscripts *in* and *out* refer to a discharge flowing into and out of the i-th node, respectively. With regard to $f_i \, p_i^{\beta}$, it represents the leakage term and will be detailed in section 4.7.1. For the sake of notation simplicity, in Equation (4.3) the dependence on the demand step θ $(\theta = 1 \ldots n_d)$ has been omitted. The constraint (4.3) has been written for each node i $(i = 1 \ldots n)$ and for each demand step θ $(\theta = 1 \ldots n_d)$, thus the total number of mass continuity equations can be accounted as $(n \cdot n_d)$. Given a link k ($k = 1 \ldots l$) and a demand step θ ($\theta = 1 \ldots n_d$), the momentum balance equation is:

$$H_i - H_j - r_k L_k - H_k^T \frac{Q_k}{|Q_k|} = 0 \tag{4.4}$$

H_i and H_j being the head pressure in the initial (i-th) and final (j-th) node of the k-th link, and $r_k L_k$ is the head-loss along the k-th pipe (with length L_k) due to the resistance. The unit head-loss r_k has been calculated by Hazen-Williams formula:

$$r_k = \frac{10.67\ Q_k^{1.852}}{C_k^{1.852}\ D_k^{4.8704}} \tag{4.5}$$

where C_k and D_k are the roughness coefficient and the diameter of the k-th pipe, respectively. The momentum balance equation can be written for each link k ($k = 1 \ldots l$) and for each demand step θ ($\theta = 1 \ldots n_d$), thus the total number of such equations can be accounted as ($l \cdot n_d$). As in constraint (4.3), the dependence on the demand step has been also omitted in constraint (4.4) for the sake of brevity notation. Further non-linear constraints have been introduced in order to handle the phenomenon of flow reversion during the day. This aspect is very crucial, as a turbine cannot produce energy in both the directions of the flow, unless it is inserted in a very complex hydraulic circuit. Any effort made by Fecarotta and McNabola (2017) [48] to account for these constraints failed, thus the authors verified a-posteriori whether the flow reverted in the pipes where turbines were inserted. In this study a first formulation of flow reversion constraints has been proposed, as follows:

$$I_k^T \leq 2 + \frac{Q_k(\theta)}{|Q_k(\theta)|} - \frac{Q_k(\theta-1)}{|Q_k(\theta-1)|} \tag{4.6}$$

$$I_k^T \leq 2 - \frac{Q_k(\theta)}{|Q_k(\theta)|} + \frac{Q_k(\theta-1)}{|Q_k(\theta-1)|} \tag{4.7}$$

Constraints (4.6) and (4.7) force the binary variable I_k^T to be equal to 0 if the sign of Q_k changes at least once between two consecutive demand steps, that is, the flow reverts. Such constraints can be written for each link k ($k = 1 \ldots l$) and for each demand step θ ($\theta = 1 \ldots n_d$), thus the total number of such equations can be accounted as ($2 \cdot l \cdot n_d$). Unfortunately, the formulation of constraints according to Equation (4.6)-(4.7) made the problem infeasible, thus a new formulation has been proposed with the aim of enhancing the convergence of the problem:

$$I_k^T \leq 2 + \frac{Q_k(\theta_1)}{|Q_k(\theta_1)|} - \frac{Q_k(\theta_2)}{|Q_k(\theta_2)|} \tag{4.8}$$

$$I_k^T \leq 2 - \frac{Q_k(\theta_1)}{|Q_k(\theta_1)|} + \frac{Q_k(\theta_2)}{|Q_k(\theta_2)|} \tag{4.9}$$

$Q_k(\theta_1)$ and $Q_k(\theta_2)$ being the discharges corresponding to the demand coefficient θ_1 ($\theta_1 = 1 \ldots n_d$) and θ_2 ($\theta_2 = 1 \ldots n_d$), respectively, with $\theta_1 \leq \theta_2$. Constraints (4.8)-(4.9) are written for each possible combination of demand step (θ_1, θ_2) with ($\theta_1 < \theta_2$), thus the number of flow reversion constraints has been significantly increased, being now proportional to $(2 \cdot l \cdot n_d^2)$. Such increase of constraints reduces the feasible region of the continuous relaxation to be explored, thus enhances the convergence of the optimization.

4.6 Linear constraints

A new set of linear constraints has been introduced in order to avoid the selection of low power turbines:

$$\overline{P_k}\ \eta^T \geq \overline{P_{min}}\ I_k^T \tag{4.10}$$

where $\overline{P_k}$ is the time average of the hydraulic power, which represents a dependent variable, being dependent on H_k^T and Q_k according to Equation (4.11).

$$P_k^T = \gamma\ H_k^T(\theta)\ Q_k(\theta) \tag{4.11}$$

It is worth underlining that, being the devices modeled as head losses in this study, the power produced by the PATs does not take into account that a part of the discharge should be bypassed according to HR mode. As a result, the power computed by the optimization is an overestimation of the power output, since its effective value should be determined according to the characteristic curves of the installed machines.
With reference to the set of constraints (4.10), $\overline{P_{min}}$ represent a minimum allowable power producible by the turbines, if I_k^T is equal to 1. If I_k^T is instead equal to 0, the

inequality (4.10) collapses to an identity. Such constraints (4.10) can be written for each link k $(k = 1 \dots l)$ of the network, thus the total number amounts to l.
A further set of variables can be written for each link k $(k = 1 \dots l)$ of the network, in order to set a maximum value of the variable head-loss within the turbine (H_k^T), whether it is installed (i.e. I_k^T is equal to 1):

$$H_k^T(\theta) \leq H_{k_{max}} \ I_k^T \tag{4.12}$$

where $H_{k_{max}}$ represents the difference between the maximum and minimum allowable head within the network. The set of constraints (4.12) are intended to reduce the research space in order to enhance the convergence of the problem.

4.7 The objective function

The objective function of the optimization has been assumed as the Net Present Value (NPV) of the investment:

$$NPV = \sum_{y=0}^{Y} \frac{(C_y^{in} - C_y^{out})}{(1+r)^y} \tag{4.13}$$

Y being the number of y years (i.e. 10 years), C_y^{in} and C_y^{out} the cash inflow and outflow, respectively, at the y-th year, and r the discount rate (set equal to 5%). The NPV can be further specified as following:

$$NPV = \sum_{k=1}^{l} -c_k^T \ I_k^T + \sum_{y=1}^{Y} \frac{(E_y^p + W_y^s)}{(1+r)^y} \tag{4.14}$$

With reference to Equation (4.14), c_k^T is the cost due to the installation of PATs and it occurs only at the begin of the investment (i.e. $y = 0$), whereas E_y^p and W_y^s are the annual inflow cash due to energy and water savings, respectively.

4.7.1 Cost model

The computation of both outflow and inflow cash results from the selection of a cost model. With regard to the inflow cash due to the installation of devices, in literature many studies are available proposing model to compute turbines costs. In addition,

the evaluation of the annual income due to energy and water savings strongly depends on the definition of a unit cost of selling price for both energy and water. As a result, the selection of a cost model to compute both outcome and income of the investment is very crucial, since it totally affects the objective function (NPV), thus, the results of the optimization.
In this study, the cost model employed by Fecarotta and McNabola (2017) [48] has been mainly employed in order to make a reasonable comparison with the results achieved by the authors in literature. Furthermore, also more recent cost models will be used to evaluate how much the choice of the cost model affects the found solutions. According to Fecarotta and McNabola (2017) [48], the cash outflow can be calculated as the sum of the total cost of installed turbines (c_k^T):

$$c_k^T = c_P \; P_{max}^T + c_z + c_{inst} \tag{4.15}$$

With reference to Equation (4.15), c_P is the cost of the generator (fixed as 220 €/kWh), c_z is a specific coefficient cost of PATs (fixed equal to 450 €), P_{max}^T is the maximum power produced by the PAT in the k-th pipe (expressed in kW) and c_{inst} is the installation cost set as 2500 €. With reference to Equation (4.14), the annual energy income E_y^p can be expressed as:

$$E_y^p = c_e \sum_{k=1}^{l} 365 \sum_{\theta=1}^{n_d} P_k^T(\theta) \; \eta^T \; \Delta t_d(\theta) \tag{4.16}$$

c_e being the energy unit selling price, set equal to 0.1 €/kWh; η^T the efficiency of the PAT, assumed as a constant and equal to 0.65 and Δt_d the duration of the θ-th ($\theta = 1 \dots n_d$) demand step.
The annual income due to water saving (W_y^s), can be instead calculated as following:

$$W_y^s = c_w \left(\sum_{\theta=1}^{n_d} Q_l^0(\theta) \; \Delta t_d(\theta) - \sum_{\theta=1}^{n_d} Q_l^S(\theta) \; \Delta t_d(\theta) \right) \tag{4.17}$$

With reference to Equation (4.17), the annual water saving has been calculated as difference between the total leaked volume without turbines installation and the total volume leaked once the pressure control strategy is performed. Such a water saving has been multiplied by the water unit cost c_w, which has been fixed as 0.3 €/m^3 [48].

According to the formulation proposed by Araujo et al. [4], the total leaked discharge Q_l can be evaluated as the sum of the discharges leaked in all nodes of the network:

$$Q_l(\theta) = \sum_{i=1}^{n} q_i^l(\theta) = \sum_{i=1}^{n} f_i \ (H_i(\theta) - z_i)^{\beta} \tag{4.18}$$

β being an exponent depending on the material, as well as the shape of the orifice [64], and set equal to 1.18, according to Araujo et al. [4, 48]. With regard to f_i, it is a leakage coefficient that can be expressed as following:

$$f_i = c \sum_{j=1}^{K_i} 0.5 \ L_{i,j} \tag{4.19}$$

c being a coefficient equal to 0.00001 l/(s m$^{(1+\beta)}$) [4, 48] and K_i is the number of pipes approaching the j-th node and linking nodes i and j with a length $L_{i,j}$.

4.8 Tolerances

Due to the high number of variables, as well as the strong non-linearity of the hydraulic constraints, in this study the optimization procedure is affected by strong computational and technical complexities. To push the solver to find a solution in a reasonable time, the non-linear equations (4.3) and (4.4) have been replaced with inequalities, thus two tolerances tol_i^Q and tol_k^H have been introduced. Solvers generally have a tolerance, but in this study, instead of modifying it, such a tolerance has been increased for only a few set of constraints, as in the study made by Fecarotta and McNabola [48]. As a result of this choice, the non-linear constraints (4.3) and (4.4) have been modified as following:

$$- \leq tol_i^Q \leq \sum_{k=1}^{K_i} Q_k^{in} - \sum_{k=1}^{K_i} Q_k^{out} - f_i \ p_i^{\beta} - q_i^d \leq tol_i^Q \tag{4.20}$$

$$-tol_k^H \leq H_i - H_j - r_k L_k - H_k^T \frac{Q_k}{|Q_k|} \leq tol_k^H \tag{4.21}$$

If such tolerances are small enough, the introduced error may be negligible. Nevertheless, it is worth underlining that the model is already affected by uncertainties due to the evaluation of end-user demand, as well in the employment of the Hazen-Williams

formula.
In this study, the tolerances have been set according to the formulation proposed by Fecarotta and McNabola (2017) [48]:

$$tol_i^Q(\theta) = \epsilon_Q \left(q_i^d(\theta) + \sum_{j \in J_i} q_j^d(\theta) \right) \tag{4.22}$$

$$tol_k^H = \epsilon_H \ H_{k_{max}} \tag{4.23}$$

with ϵ_Q and ϵ_H equal to 0.01, and J_i the set of the j $(j = 1 \ldots n)$ nodes connected to the i-th node (with $i = 1 \ldots n$) by a single pipe.

4.9 The Mathematical Model

As a result of all constraints and variables detailed in the previous sections, a mathematical model has been developed:

$$\begin{cases} \underset{\substack{I_k^T, H_k^T \\ Q_k, H_i, q_r}}{\text{maximize}} & NPV = \sum_{k=1}^{l} -c_k^T \ I_k^T + \sum_{y=1}^{Y} \frac{(E_y^p + W_y^s)}{(1+r)^y} \\ & -tol_i^Q \leq \sum_{k=1}^{K_i} Q_k^{in} - \sum_{k=1}^{K_i} Q_k^{out} - f_i \ p_i^\beta - q_i^d \leq tol_i^Q \\ & -tol_k^H \leq H_i - H_j - r_k L_k - H_k^T \frac{Q_k}{|Q_k|} \leq tol_k^H \\ & \overline{P_k^T} \ \eta^T \geq \overline{P_{min}} I_k^T \\ & P_k^T = \gamma \ H_k^T(\theta) \ Q_k(\theta) \\ & I_k^T \leq 2 + \frac{Q_k(\theta_1)}{|Q_k(\theta_1)|} - \frac{Q_k(\theta_2)}{|Q_k(\theta_2)|} \\ \text{subject to} & I_k^T \leq 2 - \frac{Q_k(\theta_1)}{|Q_k(\theta_1)|} + \frac{Q_k(\theta_2)}{|Q_k(\theta_2)|} \\ & \frac{p_{min}}{\gamma} \leq H_i(t) - z_i \leq \frac{p_{max}}{\gamma} \\ & H_k^T \geq 0 \\ & H_k^T(\theta) \leq H_{k_{max}} \ I_k^T \\ & 0 \leq I_k^T \leq 1 \\ & I_k^T \in \mathbb{Z}, \ H_k^T \in \mathbb{R}, \ Q_k \in \mathbb{R}, \ H_i \in \mathbb{R}, \ P_k^T \in \mathbb{R} \\ & \forall i,j = 1 \ldots n, \qquad \forall k = 1 \ldots l, \qquad \forall \theta = 1 \ldots n_d, \\ & \forall \theta_1, \theta_2 = 1 \ldots n_d : \theta_1 < \theta_2 \end{cases} \tag{4.24}$$

In this study, the pressure $(H_i - z_i)$ within the nodes have been bounded between p_{min}/γ set equal to 25 m and $p_{max}\gamma$ set as 100 m. The maximum value of head-loss within the turbines $H_{k_{max}}$ has been fixed as the difference between the maximum and minimum allowable head within the network. Finally, the minimum allowable power produced by the PATs (i.e. $\overline{P_{min}}$) has been set equal to 500 W. The code has been written by A Mathematical Programming Language (AMPL) [65], being an algebraic modeling language supporting many solvers, both open source and commercial software, as well as suitable to solve high-complexity problems for large-scale mathematical computing. The optimization has been then performed on an Intel @ Xeon(R) CPU E5-2620 v4 @ 2.10 GHz x 16 with 64 GB RAM. As solver of the optimization, (BONMIN) [6] has been selected. As explained several times, this algorithm guarantees a global optimum only in convex problems, whereas it achieves heuristic solutions in case of non-convex problems. Due to the high complexity of the problem, in this study the convexity cannot be easily proven, thus the solution may be a local optimum. Nevertheless, several options for the resolution of non-convex problems have been selected in order to improve the quality of the heuristic solution.

4.10 Optimization for a constant end-user demand

In average demand condition the optimization consists of 235 variables and 210 constraints. Having assumed the demand as constant in all nodes of the network, the constraints modeling the flow reversion within the pipes can be neglected. The optimal solution was found by the solver in 23 seconds and the main results of the proposed optimization are shown in Figure 4.7. With reference to Figure 4.7 (a), the installation of turbines within the network determines a significant pressure reduction. Figure 4.7 (b) and (c) show, respectively, the power production, as well as the head turbined by the installed PATs.

In Table 4.2 the main figures of the proposed optimization are shown and compared with the results achieved by Fecarotta and McNabola (2017) [48] and Corcoran et al. (2015) [31]. According to Table 4.2, the proposed optimization ensures a NPV equal to 778495 €, as well as selects 9 turbines producing a total average power of 12.04 kW. The optimization performed by Fecarotta and McNabola [48] instead selects a larger number of turbines (i.e. 16), but 10 among these produced a very low power (less than 500 W), thus this solution is definitely not very viable. Nevertheless, since the authors [48] did not succeed in including a mathematical constraint fixing a minimum value of produced power, they replaced a-posteriori all low power turbines with PRVs.

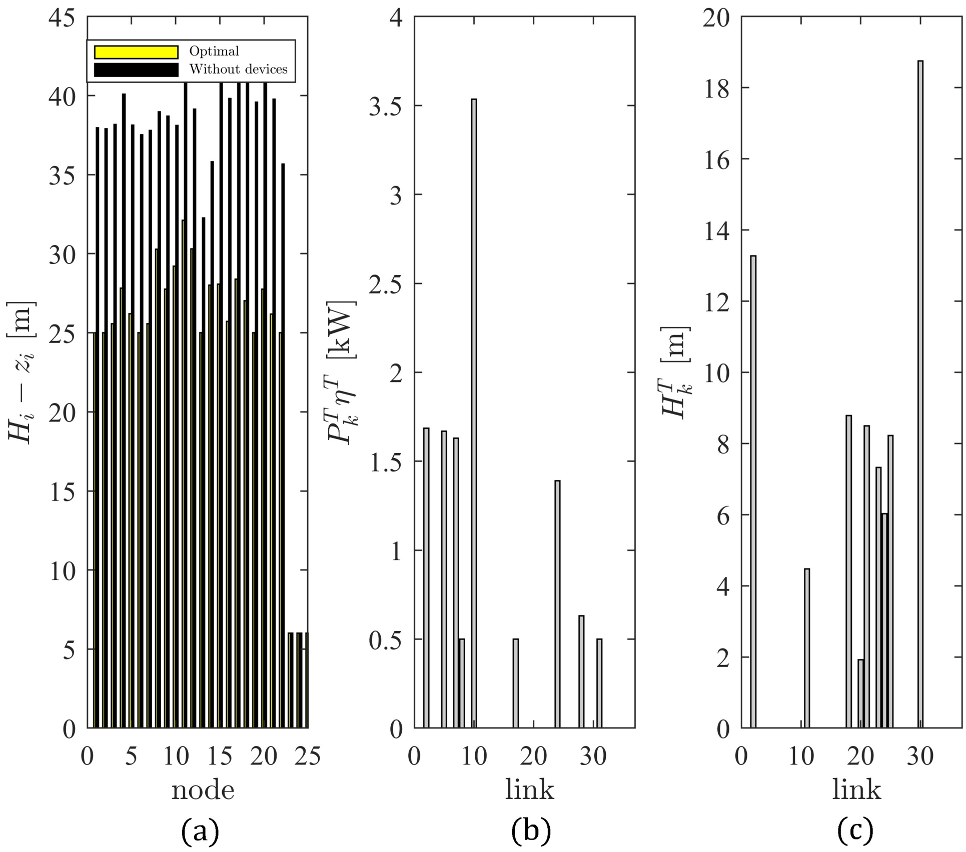

Fig. 4.7 Main results of the optimization by solver BONMIN in average condition, in terms of pressure head (a), power production (b) and head-loss (c).

Table 4.2 Main figures of the proposed optimization for constant end-user demand.

	NPV [€]	N of PATs [−]	Average Power [kW]	Investment cost [€]	Water saving [m^3/day]	DPP$_e$ [years]
Proposed optimization	778495	9	12.04	29199	859	3
Fecarotta McNabola (2017)	833740/ 830679	16/6	14.53/14.06	50396// 50293	929	4.7
Corcoran et al. (2015)	64915	3	10.68	11200	–	–

As a result, the final number of installed PATs accounts to 6, as well as the average produced power slightly decreases from 14.53 kW to 14.06 kW. Due to the high number of dissipation points (i.e. 6 turbines and 10 valves), the large water saving compensates for the reduction of energy income due to the replacement of low power turbines, thus the NPV decreases very slightly (i.e. from 833740 € to 830679 €). However, the lack of any constraints fixing a minimum value of produced power is definitely a weakness of the study [48], which in this work has been overcome by the minimum power constraint in Equation (4.10). On the other hand, the proposed optimization is penalized if compared with the procedure performed by Fecarotta and McNabola [48]. Indeed, the minimum power constraint significantly reduces the number of possible dissipation points, thus the water saving, as shown in Table 4.2. Despite this, the convenience of the proposed optimization results from the achievement of high values of NPV with low investment cost (29199 € against 50293 €), as well as, DPP_e, that is, the discounted payback period when only the energy income is considered. In the evaluation of the DPP_e, water savings are not taken into account. Indeed, such savings in the study [48] are distorted by the a-posteriori installation of valves, thus these may be not meaningful. With reference to the study made by Corcoran et al. (2015) [31], only the production of energy was optimized and the number of installed turbines was fixed as three. According to Table 4.2, the authors achieved less promising results, consisting of a value of NPV as 64915 €, as well as a produced power equal to 10.68 kW.

4.11 Optimization for a variable end-user demand

If the whole daily pattern is assumed, the mathematical problem is affected by a much higher computational complexity, since the number of variables and constraints increases to 757 and 1248, respectively. In daily pattern condition, the solution has been found by the solver in 84081 seconds and it is presented in Table 4.3.

Table 4.3 Main figures of the proposed optimization for variable end-user demand.

	NPV [€]	N of PATs [-]	Average Power [kW]	Investment cost [€]	Water saving [m^3/day]	DPP_e [years]
Proposed optimization	727817	6	10	20647	797	2.3
Fecarotta McNabola (2017)	790320/ 783992	20/6	13.43/12.63	62556/ 62256	901	6.8
Giugni et al. (2014) - OF1	–	0/3	8.62	–	732.5	–
Giugni et al. (2014) - OF2	–	3	13.62	–	709.5	–
Nguyen et al. (2020)	–	4	9.22	–	703	–

As shown in Table 4.3, the new optimization ensures a value of NPV equal to 727817 € and selects 6 turbines producing an average power of 10 kW. The trend of turbines characteristics during the day is shown in Figure 4.8. According to the patterns in Figure 4.8, even though H_k^T and Q_k, thus P_k, assume very small values at certain time intervals, the averaged value of the P_k η is guaranteed to be greater than 500 W.

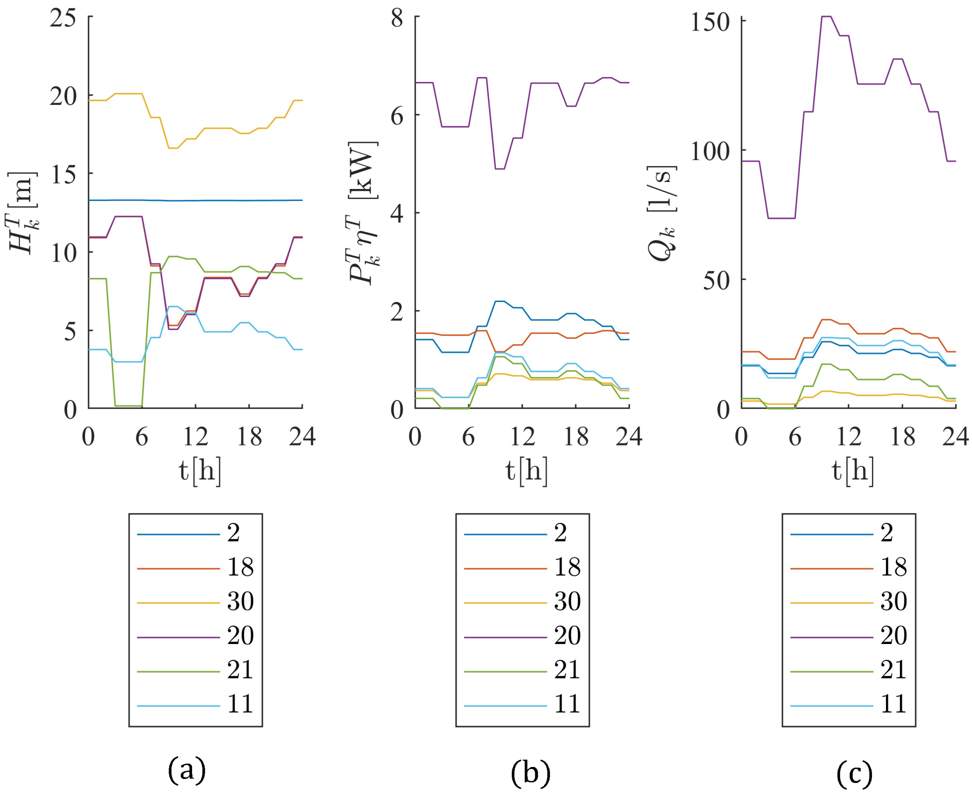

Fig. 4.8 Main results of the optimal PATs location by solver BONMIN in daily pattern condition, in terms of head-loss (a), produced power (b) and flow through the pipes where PATs are installed (c).

Fecarotta and McNabola [48] found a solution consisting of a NPV equal to 790320 €, as well as selected 20 turbines producing an average power of 13.43 kW. In [48] the power produced by 14 turbines was less than 500 W, thus the authors replaced such low power turbines with valves. As a result, the average power amounted to 12.63 kW, as well as, the NPV decreased from 790320 € up to 783992 €. As already highlighted, the study made by Fecarotta and McNabola (2017) [48] is affected by several weaknesses. A minimum low power constraint is not included in the model, thus turbines producing less than 500 W were replaced a-posteriori with valves. In addition, the model in [48] does not account for the phenomenon of flow reversion. The authors therefore verified a-posteriori whether the flow reverted in the branches where turbines were installed by the optimization. This study overcomes the weaknesses of the optimization procedure performed by Fecarotta and McNabola [48] by the introduction of new mathematical constraints. The new solution can be considered a promising result, as the discounted payback period (when only the income due to energy saving is accounted for) is equal to 2.3 years, whereas in the previous study, it is almost 7 years. Furthermore, in Fecarotta and McNabola [48], the large number of installed devices (i.e. 6 turbines and 14 valves) implicates a high investment cost (62256 € that is about three times the cost achieved by the new optimization), as well as it increases the need for repair and maintenance works.

Giugni et al. (2014) [61] fixed the number of devices and performed two optimizations with two different objective functions (i.e. OF1 and OF2 in Table 4.3). When only water leakages are optimized (see OF1), the water saving resulting from the installation of 3 valves amounts to 732.5 m^3 per day. As the production of energy is not taken into account in the objective function OF1, the optimized dissipation points are basically valves ensuring only water saving. If such valves are replaced with turbines, the producible power can be accounted as 8.62 kW. On the other hand, maximizing the only production of energy (see OF2), the water saving decreases to 709.5 m^3 per day, while the average power increases to 13.62 kW.

Nguyen et al. (2020) [95] used BONMIN [6] solver to perform the optimization considering different values of minimum producible power (i.e. 1.5 kW, 0.75 kW and 0.25 kW). The highest energy and water savings are ensured when a minimum producible power of 0.25 kW is set, as more turbines are selected by the optimization. Table 4.3 shows the results achieved by the authors [95] when such a minimum power of 0.25 kW is fixed as lower bound of the variable power. According to Table 4.3, the optimization performed by Nguyen et al. (2020) [95] selects 4 PATs producing an average power equal to 9.22 kW and ensuring a water saving of 703 m^3/day. Despite the fact that both the investment cost and the discounted payback period cannot be evaluated in [95] due to the lack of data, these quantities should be quite small as only 4 turbines have been selected. According to Table 4.3, the results achieved by Nguyen et al. (2020) [95] are less promising than the solutions found by Fecarotta et al. (2017) [48] and by the proposed optimization. This is maybe due to the maximization of the only produced power in the objective function considered in [95], whereas a simultaneous optimization of water and energy savings may ensure better results.

In all the abovementioned literature works, as well as in the proposed research work, the correct operation of HR is not captured, being the devices modeled as head losses within pipes. All the power values presented and compared are therefore an overestimation of the real power output, which should be assessed according to the performance curves of the installed machines.

4.12 Options and limits of BONMIN solver

As previously mentioned, in case of non-convex problems, the solver can retrieve heuristic solution and several options can be implemented to improve the quality of such solution. Owing to the strong complexity of the problem, the convexity has not been proven and several options specifically designed for non-convex problems have been selected.
For both the optimization procedures in daily average and daily pattern condition, the following options have been set:

- *num resolve at infeasibles*: number of attempts to resolve an infeasible node of the branch and bound tree with different starting points. This option has been set equal to 10, thus the solver has solved all the infeasible nodes with 10 different random starting points and stored the best local optimum found. Such option could be set to any value between 0 and +inf and the default value is 0.
- *num resolve at nodes*: number of attempts to resolve a node of the branch and bound tree with different starting points. This option has been set equal to 10, thus the solver has solved all the nodes with 10 different random starting points and kept the best local optimum found. Such option could be set to any integer value between 0 and +inf and the default value is 0.
- *num resolve at root*: number of attempts to resolve a root node of the branch and bound tree with different starting points. This option has been set equal to 10, thus the solver has solved all the nodes with 10 different random starting points and kept the best local optimum found. Such option could be set to any integer value between 0 and +inf and the default value is 0.

In daily pattern condition, additional options have been set due to the complexity of the problem:

- *max consecutive infeasible*: number of consecutive infeasible sub-problems before declaring the problem as infeasible. This option has been set equal to 1000, thus the solver has continued exploring a branch of the tree until 1000 consecutive problems are considered locally infeasible by the NLP sub-solver. The option could be set to any integer value between 0 and +inf and the default value is 0.

- *constr viol tol*: desired threshold for the constraint violation. This option has been set equal to 10, thus a successful termination occurs when the max-norm of the constraint violation is less than 10. This option could assume any real value between 0 and +inf and its default value is 0.0001.
- *acceptable constr viol tol*: acceptable threshold for the constraint violation. As *constr viol tol*, this option has been set equal to 10, thus an acceptable termination occurs when the max-norm of the constraint violation is less than 10. This option could assume any real value between 0 and +inf and its default value is 0.01.
- *dual inf tol*: desired threshold for the dual infeasibility. This option has been set equal to 10, which means that a successful termination occurs whether the max-norm of the dual infeasibility is less than 10. This option could assume any real value between 0 and +inf and its default value is 1.
- *acceptable dual inf tol*: acceptable threshold for the dual infeasibility. As *dual inf tol*, this option has been set equal to 10, which means that an acceptable termination occurs whether the max-norm of the dual infeasibility is less than 10. This option could assume any real value between 0 and +inf and its default value is $1 \cdot 10^{10}$.
- *compl inf tol*: desired threshold for the complementarity conditions. This option has been fixed equal to 10, thus a successful termination requires that the max-norm of the complementarity is less than 10. Such option may assume any real value between 0 and +inf and its default value is 0.0001.
- *acceptable compl inf tol*: acceptable threshold for the complementarity conditions. Having fixed this option equal to 10, an acceptable termination requires that the max-norm of the complementarity is less than 10. Such option may assume any real value between 0 and +inf and its default value is 0.01.
- *acceptable tol*: acceptable convergence tolerance. Having set this option equal to 10 means that the acceptable overall optimality error is 10. Such option may assume any real value between 0 and +inf and its default value is $1 \cdot 10^{-6}$.
- *acceptable obj change tol*: acceptance stopping criterion based on the change of the objective function. Having fixed this option as 10, the criterion is satisfied

whether the relative change of the objective function is less than 10. This option may assume any real value between 0 and +inf and its default value is $1 \cdot 10^{20}$

- *dynamic def cutoff decr*: if enabled by the string "yes", it allows to define the parameter *cutoff decr* automatically. The *cutoff decr* represents the amount by which the parameter *cutoff* is decremented below a new best upper-bound, *cutoff* being the value of a feasible solution so that the algorithm will only seek solutions better than such value. The default value of *cutoff* is $1 \cdot 10^{100}$.

In the above list of options, some optimaly conditions have been mentioned. These conditions are also known as Karush–Kuhn–Tucker (KKT) [13] and consist of dual/primal feasibility conditions, as well as complementarity conditions (see [70] for an extensive investigation). The satisfaction of these conditions is necessary for a found solution to be a local optimum.
According to the above list of options, two possible levels of termination criteria can be defined. If the ”desired” tolerances (see *constr viol tol*, *dual inf tol*, *compl inf tol*) are satisfied, the algorithm immediately terminates the process with a success message. On the other hand, if the algorithm meets *acceptable iter* at many iterations, it will stop the process before the desired convergence tolerance is met. This can be helpful where the algorithm might not be able to achieve the ”desired” level of accuracy. The option *acceptable iter* is the number of ”acceptable” iterates before terminating the process and it has been left equal to its own default value, that is, 15.
In addition, several MINLP heuristics have been selected, such as, RINS heuristic, Dive MIP Fractional heuristic, Dive MIP VectorLength heuristic, Dive Fractional heuristic, Dive VectorLength heuristic, heuristic feasibility pump, heuristic feasibility pump for MINLP.
All the options above mentioned are needed to improve the quality of the heuristic solution, as well as increase the convergence of the solver. Without the aid of such options, the optimization resulted to terminate with a failure message. Despite the introduction of small values of tolerances, it is worth underlining that the desired threshold for the constraints violation has been set as 10 (see *constr viol tol*). Nevertheless, the results have been validated a-posteriori and the constraints violation has been verified to be below the tolerance thresholds (tol_i^Q, tol_k^H) in all links and nodes of the network, except for link 21. In such link the momentum balance equation resulted to be violated by 7 metres in the first demand step and this definitely represents a weakness of the presented optimization.

In the next section, the performance of the Solving Constraint Integer Programs (SCIP) [122] will be investigated and a comparison with the solver BONMIN will be presented.

List of Symbols

β	Exponent in the relation between leakage and pressure
γ	Specific weight of water
$\delta(t)$	Demand coefficient
Δt_d	Duration of the time steps with the same demand coefficient
ϵ_H	Coefficient in the evaluation of tol_k^H
ϵ_Q	Coefficient in the evaluation of tol_i^Q
η^T	Efficiency of turbine
θ	Index for demand step
ς	Number of reservoirs
c	Coefficient for the evaluation of f_i
c_e	Energy unit selling price
c_{inst}	Installation cost of turbine
c_k^T	Total cost of turbine
c_P,c_Z	Coefficients for the evaluation of the turbine total cost
c_w	Cost of water
C_k	Roughness coefficient of the k-th pipe
C_y^{in}	Cash inflow at the y-th year
C_y^{out}	Cash outflow at the y-th year
D_k	Diameter of the k-th pipe
E_y^p	Energy production during the y-th year

f_i	Leakage coefficient
H_i	Head at the i-th node
H_i^0	Head at the i-th node without pressure control
H_k^T	Head-loss within the turbine in the k-th pipe
H_{kmax}	Upper bound of the head-loss within the turbine
i, j	Indices for nodes
I_k^T	Binary variable representing the presence of a turbine within the k-th pipe
k	Index for pipes
K_i	Number of pipes approaching the i-th node
l	Number of pipes of the network
$L_{i,j}$	Length of pipe connecting the i-th and j-th nodes
n	Number of nodes of the network
n_d	Number of ranges in the daily pattern of demand coefficients
NPV	Net present value
p_{max}	Maximum allowable pressure
p_{min}	Minimum allowable pressure
P_k^T	Hydraulic power of the turbine in the k-th pipe
$\overline{P_k^T}$	Daily average hydraulic power produced by the turbine in the k-th pipe
$q_i^d(t)$	End-user demand at the i-th node
$\overline{q_i^d}$	Average end-user demand at the i-th node
q_r	Discharge flowing into or out of the reservoir
Q_k	Total discharge flowing through the k-th pipe
Q_k^{in}	Total discharge flowing through the k-th pipe into the i-th node
Q_k^{out}	Total discharge flowing through the k-th pipe out of the i-th node
Q_l^0	Total leaked discharge without pressure control
Q_l^S	Total leaked discharge with pressure control strategy

r	Discount rate
r_k	Resistance term of the k-th pipe calculated by Hazen-Williams formula
t	Time
tol_i^Q	Feasibility tolerance within continuity equation
tol_k^H	Feasibility tolerance within momentum balance equation
y	Index for years
Y	Number of years
W_y^s	Water saving during the y-th year
z_i	Elevation of the i-th node

Chapter 5

A comparison between optimization solvers

5.1 Introduction

The optimization procedure presented in chapter 4 has been also performed by the solver SCIP [122]. As deeply detailed in chapter 3, SCIP implements a spatial branch-and-bound algorithm with linear relaxation, various heuristics, and bound-tightening procedures. Despite the fact that SCIP is a global optimization solver suitable for both convex and non-convex mixed integer non-linear problems, this solver requires the mathematical model to be lacking of any non-differentiable functions (such as, absolute values, if/sign function, etc.). In a hydraulic problem, the employment of non-differentiable functions may derive from the need of modeling the constraints according to the versus of the flow in pipes [48]. As it will be explained in the next section, accessory variables are therefore needed in order to properly model the hydraulic constraints according to the versus of the flow, avoiding constraints with any non-differentiable functions. The result will be a model consisting of only continuous and differentiable equations, which is therefore suitable for SCIP. Despite the power of such solver, the achievement of the global optimum can be dramatically time demanding, thus SCIP can be also adopted with the aim of searching good quality local optima. Nevertheless, in this hydraulic problem, the achievement of any solution (also local optima) is significantly hard and time demanding, especially in daily pattern condition due to the increased number of variables and constraints. The optimization in daily pattern condition will be therefore performed by the subgradient method [5], which will be presented in detail in section 5.4.1.

5.2 New formulation of variables

A different formulation of the variables has been proposed in order to develop a new version of the mathematical model, consisting of only continuous and differentiable functions.
According to the formulation proposed by Belotti et. al. (2013) [6], the discharge $Q_k(t)$ has been split into its positive and negative parts by adding binary variables $\zeta_k \in \{0,1\}$ as follows:

$$Q_{min}\ \zeta_k(\theta) \leq q_k^+(\theta) \leq Q_{max}\ \zeta_k(\theta) \tag{5.1}$$

$$Q_{min}\ (1-\zeta_k(\theta)) \leq q_k^-(\theta) \leq Q_{max}\ (1-\zeta_k(\theta)) \tag{5.2}$$

q_k^+ and q_k^- being the positive and negative part, respectively, of the discharge flowing through the k-th branch, whereas Q_{max} and Q_{min} the upper and lower bound of such variables, respectively. The total discharge $Q_k(\theta)$ at the demand step θ $(\theta = 1 \dots n_d)$ can be therefore replaced as:

$$Q_k(\theta) = q_k^+(\theta) - q_k^-(\theta) \tag{5.3}$$

According to the previous equations, when ζ_k is equal to 1, $Q_k(\theta)$ consists of the only positive part, thus it is positive as well and it flows according to the direction of k-th pipe, vice versa when ζ_k is equal to 0. This formulation allows to express the absolute value as a linear, thus differentiable, function $(q_k^+(\theta) + q_k^-(\theta))$.
As the discharge, the head-loss within the turbine (i.e. $H_k^T(\theta)$) has been split into its positive and negative part:

$$0 \leq H_k^{T+}(\theta) \leq H_{k_{max}}\ \zeta_k(\theta) \tag{5.4}$$

$$0 \leq H_k^{T-}(\theta) \leq H_{k_{max}}\ (1-\zeta_k(\theta)) \tag{5.5}$$

The total head-loss within the turbine is therefore a dependent variable:

$$H_k^T(\theta) = H_k^{T+}(\theta) + H_k^{T-}(\theta) \tag{5.6}$$

Finally, the power produced by the turbine is a dependent variable as well, expressed as:

$$P_k^T = \gamma \; (H_k^{T+}(\theta) + H_k^{T-}(\theta)) \; (q_k^+(\theta) + q_k^-(\theta)) \tag{5.7}$$

where $(q_k^+(\theta) + q_k^-(\theta))$ is the absolute value (being this term always positive) of the discharge flowing through the k-th link at the θ-th demand step.
Table 5.1 summarizes the independent variables according to the new formulation of the optimization problem.

Table 5.1 Summary of the binary (B) and continuous (C) independent variables of the new optimal PAT location problem.

Variable	I_k^T	$\zeta_k(\theta)$	$H_k^{T+}(\theta)$	$H_k^{T-}(\theta)$
Number	l	$l \cdot n_d$	$l \cdot n_d$	$l \cdot n_d$
Type	B	B	C	C

Variable	$H_i(\theta)$	$q_k^+(\theta)$	$q_k^-(\theta)$	$q_r(\theta)$
Number	$(n-\varsigma) \cdot n_d$	$l \cdot n_d$	$l \cdot n_d$	$\varsigma \cdot n_d$
Type	C	C	C	C

5.3 New formulation of constraints

Given a node i $(i = 1..n)$ and a demand step θ $(\theta = 1 \ldots n_d)$, the mass continuity equation can be written according to the new formulation of the variables:

$$\sum_{k=1}^{K_i} (q_k^+ - q_k^-)^{in} - \sum_{k=1}^{K_i} (q_k^+ - q_k^-)^{out} - f_i \; p_i^\beta = q_i^d \tag{5.8}$$

Given a link k $(k = 1 \ldots l)$ and a demand step θ $(\theta = 1 \ldots n_d)$, the new formulation of momentum balance equation is instead presented in (5.9).

$$H_i - H_j - r_k L_k - (H_k^{T+} - H_k^{T-}) = 0 \tag{5.9}$$

where r_k can be expressed as:

$$r_k = \frac{10.67\ [(q_k^+)^{1.852} - (q_k^-)^{1.852}]}{C_k^1.852\ D_k^{4.8704}} \tag{5.10}$$

It is worth underlining that in Equations (5.8)- (5.10) the dependence on the demand step θ $(\theta = 1 \dots n_d)$ has been omitted for the sake of brevity notation.
The introduction of a new binary variable ζ_k is crucial for a new continuous and differentiable formulation of flow reversion constraints:

$$I_k^T \leq 1 + \zeta_k(\theta_1) - \zeta_k(\theta_2) \tag{5.11}$$

$$I_k^T \leq 1 - \zeta_k(\theta_1) + \zeta_k(\theta_2) \tag{5.12}$$

$\zeta_k(\theta_1)$ $(\theta_1 = 1 \dots n_d)$ and $\zeta_k(\theta_2)$ $(\theta_2 = 1 \dots n_d)$ being the binary variable ζ_k evaluated at two different demand coefficients, with $\theta_1 < \theta_2$. Such constraints reduce the research space of the binary variables to the only branches where the flow does not reverse, that is, when the binary variable ζ_k representing the direction of the flow does not vary for each different demand step along the day.

5.4 Tolerances

As in section 4.8, some tolerances have been introduced in order to enhance the convergence of the problem. Nevertheless, the introduction of a new binary variable ζ_k for each link k $(k = 1 \dots l)$ and demand step θ $(\theta = 1 \dots n_d)$, as well as the split of both discharge Q_k and head-loss H_k^T into their positive and negative parts, significantly increase the number of variables, thus the computational complexity of the problem. For this reason, in daily pattern condition the optimization has been performed by the subgradient optimization method, explained in detail in the next subsection. With regard to the daily average flow simulation, owing to the reduced number of variables, the optimization has been directly performed without any auxiliary method and the tolerances have been fixed according to Equations (4.22)-(4.23).

5.4.1 The subgradient optimization method

The subgradient optimization method is an effective strategy to perform the optimization procedure in problems affected by severe computational and technical complexities. As the general problem with small values of tolerances is not easily solvable by the optimization solver, the subgradient method is here performed with the aim of finding good solutions for values of tolerances as small as possible. The tolerances therefore become new variables of the problem and need to be minimized. Further constraints for each demand step θ ($\theta = 1 \dots n_d$) have been introduced in the mathematical model:

$$tol_i^Q(\theta) \leq \epsilon_Q \left(q_i^d(\theta) + \sum_{j \in J_i} q_j^d(\theta) \right) \tag{5.13}$$

$$tol_k^H \leq \epsilon_H \; H_{k_{max}} \tag{5.14}$$

The mathematical model results to be further complicated by the addition of new variables (tol_i^Q and tol_k^H) and constraints (5.13-5.14). Nevertheless, according to the subgradient optimization method, a new sub-problem (i.e. the Lagrangian problem $P_L(\lambda)$) can be defined, in which constraints (5.13) and (5.14) are relaxed and taken into account into a new objective function, as follows:

$$maximize \left(NPV - \sum_{i=1}^{n} \sum_{\theta=1}^{n_d} \lambda_i^1(\theta) \; L_i(\theta) - \sum_{k=1}^{l} \sum_{\theta=1}^{n_d} \lambda_k^2(\theta) \; N_k(\theta) \right) \tag{5.15}$$

λ_i^1 and λ_k^2 being the Lagrangian multipliers. With regard to L_i and N_k, these are the so called subgradients, basically representing the deviation of the i-th relaxed constraint (5.13) and the k-th relaxed constraint (5.14) respectively, as shown following:

$$L_i(\theta) = tol_i^Q(\theta) - \epsilon_Q \left(q_i^d(\theta) + \sum_{j \in J_i} q_j^d(\theta) \right) \tag{5.16}$$

$$N_k(\theta) = tol_k^H - \epsilon_H \; H_{k_{max}} \tag{5.17}$$

According to Equation (5.15), given a solution x: (i) if $L_i(\theta) > 0$ (and/or $N_k(\theta) > 0$) the i-th constraint (5.13) (and/or the k-th constraint (5.14)) is violated, thus the term $\lambda_i^1(\theta) \; L_i(\theta)$ (and/or $\lambda_k^2(\theta) \; N_k(\theta)$) penalizes the objective function by decreasing its

value; (ii) if $L_i(\theta) \leq 0$ (and/or $N_k(\theta) \leq 0$) the i-th constraint (5.13) (and/or the k-th constraint (5.14)) is respected, thus the term $\lambda_i^1(\theta)\ L_i(\theta)$ (and/or $\lambda_k^2(\theta)\ N_k(\theta)$) rewards the objective function by increasing its value.
The subgradient method is an iterative procedure starting by values of λ_i^1 and λ_k^2 fixed equal to zero, for each link k ($k = \ldots l$) and node i ($i = 1 \ldots n$), respectively, as well as for each θ ($\theta = 1 \ldots n_d$). If a fixed convergence condition is achieved, then the iteration stops, otherwise the Lagrangian multipliers are modified as following:

$$\textbf{for } i = 1 \ldots n \textbf{ do } \lambda_i^1(\theta) = \max(0, \lambda_i^1(\theta) + t_L\ L_i(\theta)) \tag{5.18}$$

$$\textbf{for } k = 1 \ldots l \textbf{ do } \lambda_k^2(\theta) = \max(0, \lambda_k^2(\theta) + t_N\ N_k(\theta)) \tag{5.19}$$

t_L and t_N being fixed steps, $\lambda_i^1(\theta)$ and $\lambda_k^2(\theta)$ positive quantities. For each iteration there are three different possible cases:

1. if $L_i(\theta) > 0$ (and/or $N_k(\theta) > 0$) the i-th constraint (5.13) (and/or the k-th constraint (5.14)) is violated, thus the Lagrangian multiplier $\lambda_i^1(\theta)$ (and/or $\lambda_k^2(\theta)$) is so much small that it does not sufficiently penalize the objective function and it therefore needs to be increased;

2. if $L_i(\theta) < 0$ (and/or $N_k(\theta) < 0$) the i-th constraint (5.13) (and/or the k-th constraint (5.14)) is satisfied, thus the Lagrangian multiplier $\lambda_i^1(\theta)$ (and/or $\lambda_k^2(\theta)$) rewards the objective function so much that it needs to be decreased;

3. if $L_i(\theta) = 0$ (and/or $N_k(\theta) = 0$) the i-th constraint (5.13) (and/or the k-th constraint (5.14)) is respected and it is not loose, thus the Lagrangian multiplier $\lambda_i^1(\theta)$ (and/or $\lambda_k^2(\theta)$) does not need to be varied.

With regard to the evaluation of the steps t_L and t_N, the following expressions [82] have been used:

$$t_L = \omega\ \frac{(UB - \Psi(\lambda))}{\sum_{i=1}^{n} \sum_{\theta=1}^{n_d} (L_i(\theta))^2} \tag{5.20}$$

$$t_N = \omega\ \frac{(UB - \Psi(\lambda))}{\sum_{k=1}^{l} \sum_{\theta=1}^{n_d} (N_k(\theta))^2} \tag{5.21}$$

Ψ being the value of the best feasible solution of the Lagrangian problem until then; ω is a parameter which decreases as the number of iterations increases. At the first iteration, ω is usually set equal to 1 (or 2), and then halved once a certain number of iterations is achieved. With regard to UB in Equations (5.20)-(5.21), it is the upper bound of the problem. It is strongly recommended to use a good quality value of the upper bound, in order to enhance the convergence of the method. An efficient way to assign UB a reasonable value may be fixing some variables according to the solution $\Psi(\lambda)$ of the Lagrangian problem $P_L(\lambda)$ and, then, solving the original optimization problem. Fixing some variables may help the optimization solver to quickly find a sub-optimal solution of the original problem, which can be used as a reasonable upper bound of the Lagrangian problem. The iterative procedure terminates when either the convergence condition is achieved (see next section) or after a certain number of iterations. In this study, a maximum number of 20 iterations have been fixed.

5.4.2 Convergence condition of subgradient method

As explained in the previous section, the subgradient method is based on a Lagrangian relaxation, according to which some constraints are relaxed and taken into account in the objective function by means of some multipliers (see Equation (5.15)). An important feature of Lagrangian relaxation is that the optimal solution of the Lagrangian subproblem is not guaranteed to be also optimal for the original problem, owing to such a modification of the objective function. Indeed, once an optimal solution of the Lagrangian subproblem $P_L(\lambda)$ is found, three different situations may occur:

- The optimal solution of $P_L(\lambda)$ is not feasible for the original problem, as in Figure 5.1 (a);
- The optimal solution of $P_L(\lambda)$ is feasible for the original problem, but it is not optimal, as in Figure 5.1 (b);
- The optimal solution of $P_L(\lambda)$ is also optimum of the original problem, as in Figure 5.1 (c). This case only occurs if the following conditions are simultaneously satisfied:

$$\sum_{i=1}^{n} \sum_{\theta=1}^{n_d} \lambda_i^1(\theta)\ L_i(\theta) = 0 \tag{5.22}$$

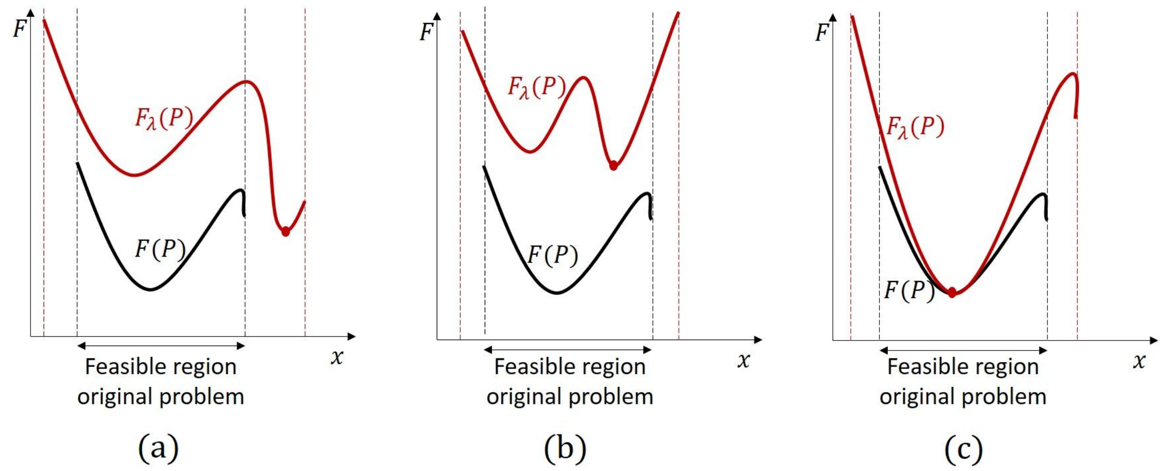

Fig. 5.1 Optimal solution of $P_L(\lambda)$ not feasible for the original problem (a); optimal solution of $P_L(\lambda)$ feasible for the original problem but not optimal (b); optimal solution of $P_L(\lambda)$ feasible and also optimal for the original problem (c). $F_\lambda(P)$ is the objective function of Lagrangian sub-problem; $F(P)$ is the objective function of the original optimization problem.

$$\sum_{k=1}^{l} \sum_{\theta=1}^{n_d} \lambda_k^2(\theta)\ N_k(\theta) = 0 \tag{5.23}$$

According to Equations (5.22)-(5.23), the convergence is reached whether the solution of the method presents either null multipliers for each constraint greater than zero, or constraints satisfied with equality for each non-null multiplier.
Note that the performed subgradient method does not rely on any rounding scheme to deal with integrality requirements of the binaries. The resulting solution will be therefore integer feasible, i.e. the integer variables will not take a fractional value.
Having fixed in this study as termination condition a maximum number of iterations, this method is heuristic.

5.5 New formulation of the mathematical model

Hereafter the new mathematical model resulting from the new formulation of variables and constraints is presented:

$$
\begin{cases}
\underset{\substack{I_k^T,\zeta_k,q_r,q_k^+,q_k^- \\ H_i,H_k^{T+},H_k^{T-}}}{\text{maximize}} & NPV = \sum_{k=1}^{l} -c_k^T \; I_k^T + \sum_{y=1}^{Y} \frac{(E_y^p + W_y^s)}{(1+r)^y} \\
 & -tol_i^Q \leq \sum_{k=1}^{K_i} (q_k^+ - q_k^-)^{in} - \sum_{k=1}^{K_i} (q_k^+ - q_k^-)^{out} - f_i \; p_i^\beta + \\
 & -q_i^d \leq tol_i^Q \\
 & -tol_k^H \leq H_i - H_j - r_k L_k - (H_k^{T+} - H_k^{T-}) \leq tol_k^H \\
 & \overline{P_k^T} \; \eta^T \geq \overline{P_{min}} \; I_k^T \\
 & P_k^T = \gamma \; (H_k^{T+}(\theta) + H_k^{T-}(\theta)) \; (q_k^+(\theta) + q_k^-(\theta)) \\
 & I_k^T \leq 1 + \zeta_k(\theta_1) - \zeta_k(\theta_2) \\
 & I_k^T \leq 1 - \zeta_k(\theta_1) + \zeta_k(\theta_2) \\
 & \frac{p_{min}}{\gamma} \leq H_i(t) - z_i \leq \frac{p_{max}}{\gamma} \\
 & 0 \leq H_k^{T+}(\theta) \leq H_{k_{max}} \; \zeta_k(\theta) \\
\text{subject to} & 0 \leq H_k^{T-}(\theta) \leq H_{k_{max}} \; (1 - \zeta_k(\theta)) \\
 & H_k^T(\theta) \leq H_{k_{max}} \; I_k^T \\
 & H_k^T(\theta) = H_k^{T+}(\theta) + H_k^{T-}(\theta) \\
 & Q_{min} \; \zeta_k(\theta) \leq q_k^+(\theta) \leq Q_{max} \; \zeta_k(\theta) \\
 & Q_{min} \; (1 - \zeta_k(\theta)) \leq q_k^-(\theta) \leq Q_{max} \; (1 - \zeta_k(\theta)) \\
 & 0 \leq I_k^T \leq 1 \\
 & 0 \leq \zeta_k \leq 1 \\
 & (I_k^T, \zeta_k) \in \mathbb{Z}, \quad (H_k^{T+}, H_k^{T-}, H_k^T) \in \mathbb{R} \\
 & (q_k^-, q_k^-) \in \mathbb{R}, \quad H_i \in \mathbb{R}, \quad P_k^T \in \mathbb{R} \\
 & \forall i,j = 1 \dots n, \quad \forall k = 1 \dots l, \quad \forall \theta = 1 \dots n_d, \\
 & \forall \theta_1, \theta_2 = 1 \dots n_d : \theta_1 < \theta_2
\end{cases}
\tag{5.24}
$$

The mathematical model (5.24) is completely lacking of any non-differentiable functions, being therefore suitable for the solver SCIP.

5.6 Comparison in daily pattern condition

With reference to Equations (5.13)-(5.14), the values of ϵ_Q and ϵ_H should be both set equal to around 0.01, in order to make a comparison with the results previously achieved by the solver BONMIN. Performing the optimization of such a complex MINLP problem by the solver SCIP is highly challenging and any effort made to achieve a solution failed. Despite its effectiveness, even the optimization by the subgradient method may be not successful whether too small values of tolerances are set, due to the high computational time. The smallest values of ϵ_Q and ϵ_H allowing for a fast and successful optimization by the subgradient method resulted 0.015 and 0.03, respectively, but such values of coefficients are not meaningful to make a comparison with the results achieved by BONMIN (with ϵ_Q and ϵ_H both equal to 0.01). However, it has been noticed that providing the solver with a feasible starting solution may significantly help it to find good solution in a reasonable time, even though small values of tolerances are considered. The difficulty lies in finding such a feasible solution to employ as starting point of the optimization 5.24. To overcome this problem, a tailored heuristic has been defined, consisting of a sequence of optimization steps:

1. The subgradient method is performed to achieve a first heuristic solution. As previously mentioned, the smallest values of tolerances allowing for a solution in a reasonable time by this method result from ϵ_Q and ϵ_H equal to 0.015 and 0.03, respectively.

2. The tolerances are fixed to the desired values, that is, ϵ_Q and ϵ_H are decreased to around 0.01. Then, the general optimization procedure is performed with binary variables fixed according to the solution found by the subgradient method in step 1. Fixing some binary variables allows to solve a less complex optimization sub-problem, thus may be crucial to enhance the convergence of the optimization and speed up the procedure. The solution of the optimization sub-problem is certainly a feasible solution of the general problem.

3. The general optimization problem is solved by using the solution found in step 2 as starting point. Providing the solver with such a feasible solution allows to reach a good optimum in a reasonable time.

Hereafter the results achieved by SCIP solver are presented and compared with the results of the optimization performed by BONMIN. As previously presented in section

Table 5.2 Comparison of results achieved by different optimization solvers in daily pattern condition.

	NPV [€]	N of PATs [−]	Average Power [kW]	Investment cost [€]	Water saving [m^3/day]	DPP_e [years]
BONMIN	727817	6	10	20647	797	2.3
SCIP	734998	4	12.6	15076	786	1.4

4.11, BONMIN solver selects 6 turbines producing an average power of 10 kW and determining a water saving of 797 m^3 per day.

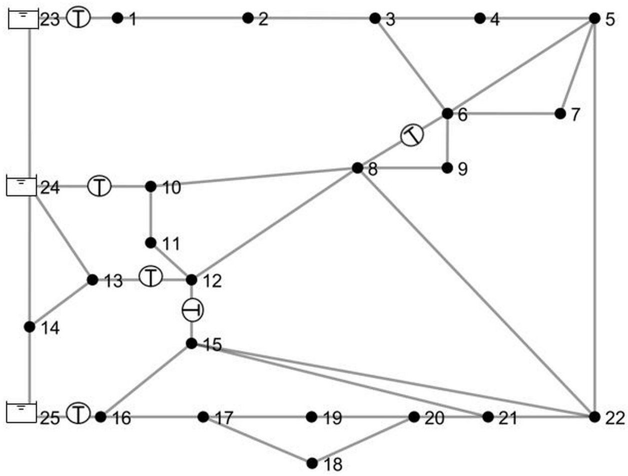

Fig. 5.2 PATs location according to the solution found by BONMIN.

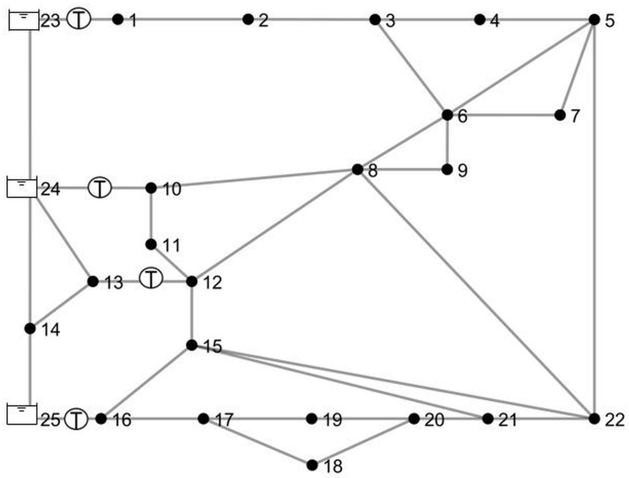

Fig. 5.3 PATs location according to the solution found by SCIP.

According to the Table 5.2, SCIP solver achieves a slightly improved NPV equal to 734998 €. The solution found by SCIP consists of 4 turbines producing an average power of 12.6 kW and the consequent water saving amounts to 786 m^3 per day.
The installation of turbines within the network selected by the two solvers is presented in Figures 5.2 and 5.3. According to Figures 5.2 and 5.3, most of the links selected by the solvers for PATs installation are the same.
With reference to the comparison in Table 5.2, SCIP selects less turbines producing an higher average power, whereas the reduction of water leakage is nearly the same. Due to the small number of selected devices, the solution achieved by SCIP consists of small investment costs (i.e. 15076 €) and discounted payed-back period (i.e. 1.4 years).
With regard to the performance of the implemented solvers, BONMIN achieves the global optimum only in convex problems, whereas it retrieves heuristic solution in non-convex problems. It is worth mentioning that in this application BONMIN has been implemented by selecting several options for the resolution of non-convex problems, as the convexity of the mathematical problem cannot be easily proved. On the contrary, being a global optimization solver, SCIP could find global optima also in non-convex problems. Nevertheless, the above presented solution found by SCIP is a local optimum, since in such a complex application the search of global optima could require an infinite time. However, as previously mentioned, the strength of using a global optimization solver to find local optima lies in the possibility of evaluating the effectiveness of the found solution, compared to heuristic methods which do not give even a general idea about the goodness of the solutions. Indeed, according to Figure 5.4, SCIP provides the user with the relative gap between the found solution and the upper bound (or lower bound if minimizing) of the problem, i.e. the maximum value (or the lower value if minimizing) that could be assumed by the objective function. During the computation performed by SCIP, the solver reduces the upper bound (or increases the lower bound if minimizing) and improves the solution, thus the relative gap is progressively reduced. When a global optimum is found, the upper bound and the solution value are the same, that is, the relative gap is zero. Nevertheless, the solver struggles more to decrease the upper bound of the problem (or increase the lower bound if it is a minimization problem) than to improve the solution. As a result, even when a very good solution is found, the gap could be large. For the sake of example, despite the found solution being a promising result, the gap amounts to 350 %. Despite this, it is worth considering that leaving the solver computing the optimization for a very long period (i.e. several days), it is likely that the solution will be not improved but the bound will be decreased, thus the resulting gap could decrease accordingly. Unfortunately, such a kind of attempt has

been not made for memory issues and it has not been possible to use any technique of cloud computing or memory virtualization, being not suitable for the employed solver.

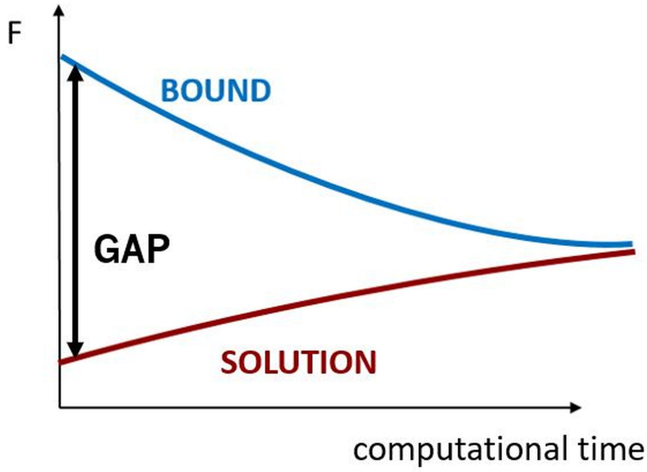

Fig. 5.4 Relative gap between the upper bound of the problem (blue line) and the found solution (red line).

With regard to the computational time, BONMIN took around 23 hours to find the solution. The computational time required by SCIP to achieve any local or global optima may be significantly long, unless a feasible starting solution is provided. In this application, once the feasible solution is provided, SCIP finds the solution after 4300 seconds and 1484 solved nodes.

5.7 Comparison between cost models

In this study, the choice of the cost model (see section 4.7.1) has been made to compare the new proposed optimization with other literature works based on the same cost model. Nevertheless, it is worth considering that more comprehensive cost models have been recently proposed in literature, which could allow to obtain more realistic results. For this reason, the results obtained so far have been compared with the results achieved by using the cost model proposed by Novara et al. (2019) [97]. According to this model, the cost of a centrifugal PAT with a connected four-pole asynchronous motor used as a generator can be evaluated as following:

$$C_{GEN+MOT} = 12717.29\ Q_{BEP}\ \sqrt{H_{BEP}} + 1038.44 \tag{5.25}$$

where Q_{BEP} and H_{BEP} are the flow and the turbined head, respectively, at the Best Efficiency Point (BEP). In this study, such flow and turbined head have been assumed as the maximum value $((q_k^+ + q_k^-)\ \sqrt{H_k^T})$ occurring during the day. Moreover, according to Garcia et al. (2019) [57], since the purchase of a PAT and its generator can be accounted as 26% of the total cost of the installation on average, the cost in Equation (5.25) has been divided by 0.26 in order to achieve a quite real estimation of the total cost related to the device installation.

Due to the introduction of further non-linearities (see Equation (5.25)) within the objective function, the optimization is more challenging, so that BONMIN does not manage to find any solution. Table 5.3 compares the results obtained by only SCIP solver using the two different cost models (i.e. the cost model (1) presented in section 4.7.1 and the cost model (2) according to Novara et al. (2019) [97]).

Table 5.3 Comparison of solutions according to the cost model in section 4.7.1 [48] (cost model (1)) and Novara et al. (2019) [97] (cost model (2)).

	NPV [€]	N of PATs [–]	Average Power [kW]	Investment cost [€]	Water saving [m^3/day]	DPP_e [years]
Cost model (1)	734998	4	12.6	15076	786	1.4
Cost model (2) [97]	711663	5	12.2	39684	791	4.2

With reference to Table 5.3, the most difference clearly lies in the value of the investment costs: according to the cost model proposed by Novara et al. (2019), the investment cost of 5 turbines is more than twice the investment of 4 turbines resulting from the cost model in section 4.7.1. As a result, the discounted payed-back period (if only the income represented by the energy recovery is considered) increases to 4.2 years, which is more reasonable than 1.4 years of the previous cost model. Nevertheless, despite the fact that the cost model in section 4.7.1 does not give a realistic estimation of the installation cost and of the time to pay it back, the two solutions are quite similar in terms of average power, water saving and also device location (see Figure 5.5).

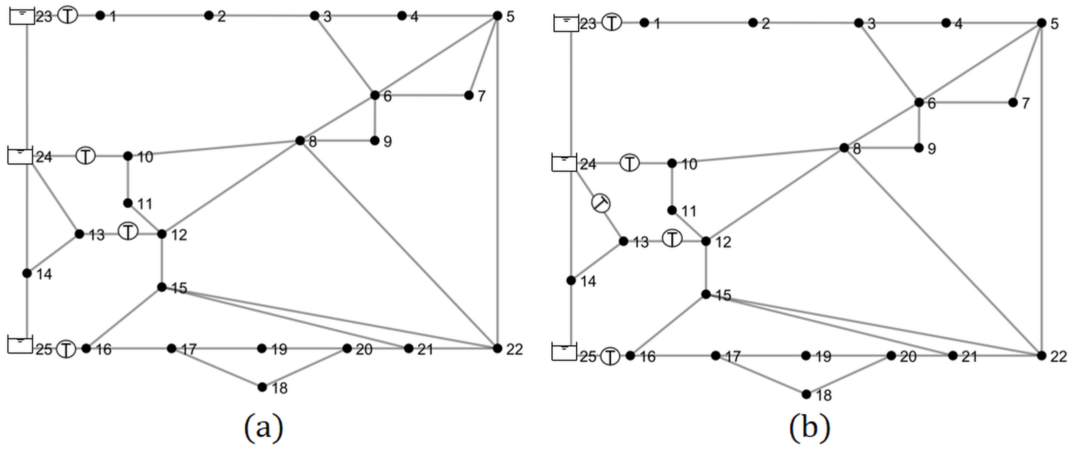

Fig. 5.5 Location of the devices according to the cost model in section 4.7.1 (a) and Novara et al. (2019) [97] (b).

On the whole, the cost model presented in section 4.7.1 can be preferred over more recent and comprehensive literature models as it allows to make a more straightforward comparison with literature results and to highlight the improvements obtained, without compromising the quality of the found optimal solution.

5.8 Final remarks

In this chapter, a comparison between the optimization solvers BONMIN and SCIP has been proposed. When provided with a feasible starting point, the solver SCIP ensures a fast computation, achieving a slightly improved solution in a significantly reduced time.

Regardless of the kind of solver employed to perform the optimization, the effectiveness of the newly proposed optimization lies in the development of a more comprehensive mathematical model for the optimal location of PATs within a water distribution network, accounting for the flow reversion along the day, as well as setting a minimum allowable power producible by the turbines. The convenience of the found solution also results from the selection of a small number of devices, thus, low investment costs and reduced need for repair and maintenance works. Moreover, according to the values of DPP_e, the investment cost results to be paid back by the energy income after a very short time. Nevertheless, the set of a minimum producible power strongly reduces the number of possible dissipation points, which results in reduced water savings. As the installation of valves in not considered in any way, in the proposed optimization the NPV is penalized. Indeed, when the energy recoverable is not significant, the installation of pressure reducing valves may be a more viable solution. A more realistic optimization procedure should therefore account for the simultaneous installation of turbines and valves. All the efforts made to accomplish this goal will be deeply explained in the next chapter.

To achieve more realistic and reasonable value of the investment costs, in this chapter the optimization has been also performed by using more recent literature cost models [97, 57]. The comparison has shown that, despite the significantly higher costs required for installing the machines resulting in lower NPV and higher payback periods, the amount of both water and energy savings is approximately equal to the values achieved by using the previous cost model presented in section 4.7.1.

Finally, it is worth mentioning that a realistic optimization should also involve the installation of real turbines and the design on the installed machines should be integrated within the mathematical model, in order to better represent the behavior of the installed turbines and simulate the operation of the HR effectively. Indeed, a proper simulation of HR mode would allow to better assess the produced power, which has been overestimated so far, since the portion of the flow that is by-passed in HR mode according to the characteristic curve of the machines has not been taken into consideration in this study.

List of Symbols

β	Exponent in the relation between leakage and pressure
γ	Specific weight of water
$\delta(t)$	Demand coefficient
Δt_d	Duration of the time steps with the same demand coefficient
ϵ_H	Coefficient in the evaluation of tol_k^H
ϵ_Q	Coefficient in the evaluation of tol_i^Q
ζ_k	Binary variable modeling the versus of the flow within the k-th pipe
η^T	Efficiency of turbine
θ	Index for demand step
λ_i^1, λ_k^2	Lagrangian multipliers
ψ	Best feasible solution of Lagrangian sub-problem
ς	Number of reservoirs
ω	Parameter for the evaluation of the step in the subgradient method
c	Coefficient for the evaluation of f_i
c_e	Energy unit selling price
c_{inst}	Installation cost of turbine
c_k^T	Total cost of turbine
c_P,c_Z	Coefficients for the evaluation of the turbine total cost
c_w	Cost of water
C_k	Roughness coefficient of the k-th pipe

C_y^{in}	Cash inflow at the y-th year
C_y^{out}	Cash outflow at the y-th year
D_k	Diameter of the k-th pipe
E_y^p	Energy production during the y-th year
E_y^p	Energy consumption during the y-th year
f_i	Leakage coefficient
H_i	Head at the i-th node
H_i^0	Head at the i-th node without pressure control
H_k^T	Head-loss within the turbine in the k-th pipe
H_k^{T+}	Positive component of the head-loss within the turbine in the k-th pipe
H_k^{T-}	Negative component of the head-loss within the turbine in the k-th pipe
H_{kmax}	Upper bound of the head-loss within the turbine
i, j	Indices for nodes
I_k^T	Binary variable representing the presence of a turbine within the k-th pipe
k	Index for pipes
K_i	Number of pipes approaching the i-th node
l	Number of pipes of the network
K	Positive integer parameter
$L_{i,j}$	Length of pipe connecting the i-th and j-th nodes
L_i, N_k	Deviation of the i-th and k-th relaxed constraint in the subgradient method
n	Number of nodes of the network
n_d	Number of ranges in the daily pattern of demand coefficients
NPV	Net present value
p_{max}	Maximum allowable pressure
p_{min}	Minimum allowable pressure
P_k^T	Hydraulic power of the turbine in the k-th pipe

$\overline{P_k^T}$	Daily average hydraulic power produced by the turbine in the k-th pipe
q_k^+	Positive component of the discharge flowing in the k-th pipe
q_k^-	Negative component of the discharge flowing in the k-th pipe
$(q_k^+ + q_k^-)^{in}$	Total discharge flowing through the k-th pipe into the node
$(q_k^+ + q_k^-)^{out}$	Total discharge flowing through the k-th pipe out of the node
$q_i^d(t)$	End-user demand at the i-th node
$\overline{q_i^d}$	Average end-user demand at the i-th node
q_r	Discharge flowing into or out of the reservoir
Q_{max}	Upper bound of total discharge Q_k
Q_l^0	Total leaked discharge without pressure control
Q_l^S	Total leaked discharge with pressure control strategy
r	Discount rate
r_k	Resistance term of the k-th pipe calculated by Hazen-Williams formula
t	Time
t_L, t_N	Steps within the iterative procedure implemented by the subgradient method
tol_i^Q	Feasibility tolerance within continuity equation
tol_k^H	Feasibility tolerance within momentum balance equation
y	Index for years
Y	Number of years
UB	Upper bound
W_y^s	Water saving during the y-th year
z_i	Elevation of the i-th node

Chapter 6

Optimal location of PATs and PRVs within a water distribution network

6.1 Introduction

The employment of PATs within a water network is a very efficient strategy to increase the sustainability of the water management in WDs. Nevertheless, the feasibility of such devices strongly depends on the amount of energy that is recoverable. Indeed, when the recoverable energy is small (i.e. the head drop and/or the flow rate are small), the production of energy may not cover the high purchase and installation costs, thus the employment of dissipation valves may represent a more viable and economical solution to reduce the excess pressure and save water.
In this chapter, the simultaneous installation of PATs and PRVs within the literature synthetic network [73] will be investigated in both daily average and variable demand condition [88]. The mathematical model (previously presented in Equation (5.24)) will be accordingly modified by the introduction of new variables and constraints. The results will be compared with other literature studies investigating the location of only turbines on the same synthetic network, in order to highlight the improvements obtained by the simultaneous installation of turbines and valves.

6.2 Optimal location and setting of PRVs: state of the art

The use of optimization for controlling the water pressure in water networks has been significantly investigated in the past and in recent times. The optimal location, as well as the opening adjustment of these valves, is crucial for an effective reduction of water leakage, thus for a financial saving in annual operational costs.
Two main lines of research can be defined in this context: the former regards the optimal location and control of valves, while the latter concerns the real time regulation of these devices. In this thesis, the attention is mainly payed to the former line of research, whose evolution in the literature research is going to be investigated in this section.
The pioneers of this topic were Sterling and Bargiela (1984) [115] and Germanopoulos and Jowitt (1989) [58]. The former optimized the control of a given number of valves, located in a given position within a water distribution network, in order to minimize the discrepancies between a current and an optimal head profile, thus reducing water leakages. The non-linearities of the problem have been tackled by a method of iterative linearization based on the Newton-Raphson process. The proposed approach has been tested on several different sized networks and the results showed a potential reduction of the volume of leakages around 20%. Germanopoulos and Jowitt (1989) [58] also optimized the only control of valves within a network to minimize the waste of water, including leakage explicitly in a hydraulic network formulation. These authors proposed a methodology for the determination of optimal control valve settings to minimize excess pressures, which are strictly related to water leakage. The proposed excess pressure minimization problem consisted of a linear objective function and a non-linear set of constraints. The non-linear constraints were linearized by the linear theory method [125], so that the resulting problem was linear programming (LP). The resolution of the linear program allowed to determine a solution point which was again used to linearize the problem. The procedure was iterated until a specific termination criterion was achieved. Jowitt and Xu (1990) [73] extended the work reported by Germanopoulos and Jowitt (1989) [58], defining the total losses as the objective function to be minimized directly. A novel approach in optimization of valve control was proposed by Vairamoorthy and Lumbers (1998) [120] who developed a technique involving a sequence of quadratic programming (SQP) subproblems, as an approximation of the original problem, to obtain at each iteration a search direction useful to update the solution vector. The quadratical convergence of the SQP-based method proposed by

Vairamoorthy and Lumbers (1998) [120] is enhanced when compared with the linearly convergence of previous methods [115, 73].
The successive studies in literature are presented in the next sections and classified according to the kind of optimization approach these are based on.

6.2.1 Metaheuristic optimization

The term metaheuristic refers to heuristic algorithms combining several heuristic processes to achieve the optimization objectives. Heuristic algorithms allow to find acceptable solutions by "trail-and-error" in a reasonable time [75]. What can be considered as "acceptable" and "reasonable" is clearly subjective and depends on the kind of the addressed optimization problem. Heuristic methods generally do not find the best or global optimum, but a good solution may be a rapidly determined local optima situated close to the global optimum.
Scatter search (SS) is a population-based metaheuristic which guarantees high-quality outcomes for hard combinatorial optimization problems. It uses strategies for combining solution vectors, making limited use of randomization. Such kind of algorithm was used by Liberatore and Sechi (2009) [78] proposing a combined procedure for optimal location and calibration of valves. Such procedure consists of a first phase restricting the location of valves to candidate sets of pipes defined by hydraulic analysis. Then, the meta-heuristic Scatter Search routines are performed to determine the best location and calibration of valves. As objective function of the model, a weighted multi-objective function was defined, considering the cost of inserting valves and the penalty when the pressures at nodes do not meet the pressure requirements. Such a combined procedure allows for a rapid optimization controlling network pressure with a limited number of valves.
Harmony search (HS) algorithms apply the principles employed by musicians and composers when struggling to achieve the best combination of musical notes to improve an existing musical score and produce a harmonious outcome [41]. According to these algorithms, the scores are improved as a result of three different processes: (I) playing parts of the original scores; (II) playing some parts of the scores in a slightly different combination of notes; (III) creating new sections of the score by a random substitution of notes [75]. The improved scores are stored in a matrix known as harmony memory (HM) which is used to converge to the optimum solution [77]. These algorithms have been used by De Paola et al. (2017) [41] who proposed a new methodology to optimize the location and setting of an assigned number of PRVs. The performed procedure

integrates the Harmony Search (HS) approach with the hydraulic network solver EPANET. Also in this study, the objective function minimizes the excess pressure at network nodes in order to reduce water leakages and a penalty coefficient is introduced to guarantee pressure requirements. According to the comparison with previous works on the same network [73], this approach determines similar locations of PRVs, whereas the settings were found to be more effective in reducing water leakage.
Genetic Algorithms (GAs) seek the optimal solution by applying the principles of evolution found in nature. These algorithms involve an evolutionary process, typically starting with a random set of feasible solutions, followed by steps of evolution. Each step is an iteration aiming at improving the objective function by modifying some genetic operators and employing mechanisms inspired to the biological evolutionary processes. There are many advantages of GAs over traditional optimization algorithms. Firstly, GAs allow to deal with complex problems, as well as various types of optimizations, whether the objective (i.e. fitness) function is stationary or changes with time, linear or non-linear, continuous or discontinuous. In addition, GAs allow to explore the research space in many different directions simultaneously, as well as different groups of encoded strings can be manipulated at the same time. However, genetic algorithms present some disadvantages. Any inappropriate choice of the optimization parameters will make it difficult for the algorithm to converge or it will simply produce meaningless results. The formulation of a fitness function, the use of population size and the selection criteria are also crucial to obtain meaningful results, thus should be established carefully. Nevertheless, genetic algorithms remain the most widely used optimization algorithms in modern nonlinear optimization. Savic and Walters (1996) [109] minimized the excess pressure by setting isolating valves operating in complete opened or closed position. The authors assumed that each pipe in the network contained at least one valve: disconnecting one or more pipes from a node (i.e. closing one or more of these valves) affects the distribution of flows and pressures in the network. The authors optimized the valve settings (i.e. closed or open) to attain the best possible pressure distribution without compromising the hydraulic performance of the network. The combinatorial problem was solved by the integration of a simulation program with a GA based approach. Reis et al. (1997) [103] reported an application of a simple genetic algorithm (GA) to the problem of optimal location and setting of valves within a water network. In this study, leakage was first minimized to obtain the valve settings for given valve locations by the linear theory method [125], and then leakage reduction was maximized by a genetic algorithm to determine the optimal location of these valves. Linear programming (LP) was indeed embedded in the genetic algorithm to

search for the optimal valve settings for each location of valves proposed as a solution by GA. It is worth underlining that the solution achieved by GA strongly depends on the choice of parameters, such as population size, probabilities of crossover and mutation. Araujo et al. (2006) [4] proposed a methodology based on EPANET model for the hydraulic simulation and two operational models based on a Genetic Algorithm technique were developed for pressure control optimization. Such methodology consists of two steps: in the first step, both number and location of valves was optimized by a single objective function, then a second step is performed for the adjustment of valves opening degree. In both optimization levels, the objective function was to minimize the pressure variation from the minimum requirement. Giustolisi and Savic [62] tackled the design of an isolation valve system as a two-objective problem by the use of GAs. A first objective function was defined to minimize the number of valves in the isolation system, and a second to minimize the maximum undelivered demand, i.e. the demand that is not fulfilled during the repair operations. Gupta et al. (2018) [67] improved the reference pressure algorithm proposed by [78] by using a new algorithm. In particular, multiobjective genetic algorithm (NSGA-II) was used for finding out the optimized operational control setting of valves for leakage minimization. According to the results, the modified reference pressure algorithm led to better leakage reduction of 20.81% with a reduced number of pressure reducing valves. In addition, the modified reference pressure algorithm was computationally simpler and very efficient, when compared to GA [4] or MINLP [37]. In a study developed by Ali (2015) [2], the non linear leakage minimization problem was solved using a real coded GA to determine the optimal valve location and setting for a specific number of valves. In this study, the search space was reduced by selecting the potential sites for the control valves. The candidate pipes selection exploited the knowledge about the hydraulic performance of water distribution networks. As a result of the pipe selection, the shrunk research space enhanced the robustness and efficiency of the GA, as well as ensured a very good solution with a leakage reduction of about 16%. Fontana et al. (2012) [51] also used GA to optimize the location of a given number of PRVs in a real water distribution network for reducing water losses. In a following phase, some PRVs were replaced by PATs for hydropower generation. The potential revenues and the water loss reduction were estimated for the case study, showing that a promising energy recovery could be achieved together with a significant reduction in water loss, as well as profits and capital payback period may be attractive. Jafari et al. (2015) [71] used GAs to search for both the optimal placement and setting of PRVs in a real water distribution system. Then PRVs with an adequate amount of head and flows were replaced by

PATs and their hydropower potential was evaluated. According to the results, both the potential generation electric power and water leakage reduction were remarkable, and the investment was demonstrated to be payed back in a very short time. Covelli et al. (2016) [32] also performed the optimization of locations and settings of PRVs by means of a GA, once the number of devices was fixed. Each pipe in the network was considered eligible for PRVs positioning. Once the optimal locations and settings of PRVs have been determined, the optimal number of valves to install within the network is evaluated by a Cost-Benefit analysis.

Many studies in literature propose multi-objective approaches, in order to obtain a Pareto front of optimal solutions representing a compromise between number of installed valves and water savings. Nicolini and Zovatto (2009) [96] implemented a real-coded multiobjective genetic algorithm with a new mutation operator enhancing the performance of the algorithm. For small systems, like the synthetic network [73], the Pareto front is affected by a small degree of variability. On the other hand, if the optimization is applied to real larger networks, the computational time significantly increases, as well as, the set of optimal solutions presents a larger variability, especially in the region of many-valve solutions, where there is a negligible contribution to leakage reduction. Creaco et al. (2010) [34] proposed a modified version of the NSGA II multi-objective genetic algorithm to find the optimal locations of the isolation valves within the water distribution network in Ferrara (Italy). The results of the calculation showed that the most appropriate objective functions for solving such an optimal location were the total cost of the valves and the weighted average demand shortfall based on the likelihood of failures occurring within the pipes. Creaco and Pezzinga (2015)[36] performed a multiobjective algorithm for the simultaneous optimization of pipe replacement and control valves in order to reduce leakage. The authors implemented an hybrid algorithm, consisting of a GA to search for the pipe replacements, control valve installations and isolation valve closures, and the linear programming (LP) to instead search for the optimal settings of the installed control valves. Creaco and Pezzinga (2015) [35] also developed a multi-objective low level hybrid algorithm (LLHA) for the optimization of control valves. The hybridization is due to the embedding of an iterated LP algorithm in the multiobjective genetic algorithm. Such hybridization was accomplished by dividing the search space of decisional variables into two sub-spaces: the sub-space made of the discontinuous integer variables representing the valve positions was assigned to the GA whereas the other sub-space of the continuous real variables (relative to the valve settings) was assigned to the iterated linear programming (LP) optimizing the control valve settings for each solution proposed by the GA. This study proved that

LLHA has a good computational efficiency, since the GA is generally not so much efficient in handling continuous variables. Creaco et al. (2016) [33] optimized design and operation of a water network by GAs, searching for trade-off solutions between: 1) installation cost; 2) operational cost; 3) cost of the installed pressure reducing valves. To tackle the three objective functions, the authors split the process into subsequent 2D optimizations, where the trade-off between installation cost and operational cost was first explored, followed by that between cost of pressure reducing valves and operational cost. The final solution was selected after an approximated 3D Pareto surface was obtained, by applying a criterion based on the minimum total cost, obtained as the sum of installation, operational, and valve costs. Gupta et al. (2020) [66] proposed a nodal matrix analysis for the localization of pressure-reducing valves in larger-scale water distribution networks after applying the modified reference pressure algorithm mentioned above [67], which generally fails selecting a dramatically high number of devices. A multi-objective GA was also used in order to search for the optimized pressure control value across PRVs, when operating in active mode. With reference to a real water network, the effectiveness of such approach was proved by a reduction of water leakage of 20 % by installing only 4 PRVs. The authors also verified that the installation of further devices was not a cost-effective solution.

6.2.2 Deterministic optimization

Compared to the studies based on metaheuristic approaches, a few works dealing with deterministic optimization exist in literature.

Dai and Li (2014) [37] reformulated the MINLP problem for PRVs location as a mathematical program with complementarity constraints (MPCC), which was solved in a sequence of NLPs by the solver IPOPT [123] with an increasing penalty parameter. Furthermore, the relaxed solution of NLP was rounded to binary values by a novel scheme in order to ensure the feasibility of the original MINLP problem. This ensured smaller computational time and increased the robustness of the method, as well as guaranteed higher reduction of water leakage as compared with those given in the literature for the same synthetic network [73]. The approach was also applied to a real large-scale water network to prove its effectiveness. Dai and Li (2016) [38] dealt with the optimal setting problem of PRVs, once their location was determined in the previous study [37]. The non-smoothness of the model was smoothed by an interior-point approximation approach, so that the original problem resulted in a NLP. The comparison between optimal results achieved by the authors and existing PRV models proved the robustness of the model in terms of both quality and solution accuracy for many demand scenarios. Pecci et al. (2019) [101] combined network model reduction techniques in order to tackle the computational complexities affecting MINLPs in complex large scale networks. The authors implemented the Outer Approximation with Equality-Relaxation (OA/ER), which consists of an alternating sequence of master mixed integer linear programs (MILPs) and primal nonlinear programs (NLPs), until a termination criteria was met. Master MILPs were defined by linearizations of the nonlinear equality constraints and the solution achieved consists of a set of candidate valve locations. On the other hand, the primal NLP corresponded to the problem of optimizing valves control settings, while their locations were fixed according to the solution of MILP. The solver IPOPT [123] was used to perform the NLP optimization, whereas the MILP problem was optimized by the solver GUROBI [69]. The application of the optimization procedure on a reduced network model did not result in an equivalent MINLP and its solution might be severely sub-optimal. To deal with this, the authors introduced an arbitrary parameter of the reduction algorithm in order to regulate the trade-off between model size reduction and sub-optimality of the found solutions. A further valuable contribution has been made by Pecci et al. (2018) [100] in the field of global optimization in water distribution networks. The authors tailored a branch and bound algorithm, relying on a MILP relaxation of the original non-convex MINLP, as well as a tailored domain reduction procedure to tighten the MILP relaxations and also improve the convergence properties of the algorithm. The tailored branch and bound algorithm was proved to outperform some state-of-the-art global optimization solvers (i.e. SCIP [122] and BARON [105]) for solving the problem of optimal placement and operation of control valves. Despite not properly related to optimal location problem, another interesting work is worth mentioning has been presented by Ghaddar et al. (2017) [59] proposing polynomial optimization techniques to solve the valve setting problem to global optimality. The optimization problem consisted of a linear objective, polynomial constraints, and continuous variables. The global solver Couenne [7] and the local solver IPOPT [74] were employed to perform the optimization, both benefiting from the quadratic formulation, in terms of solution quality (e.g., better bounds) and the computational time. The study proved that the proposed quadratic formulation resulted in improved quality of global optimal solution and shorter computational time.

6.3 The integrated optimization procedure

Given a water distribution network, the aim of the optimization is to find the best location, as well as number, of both PATs and PRVs, in order to reduce pressure, thus water leakage, and also produce energy. The solver SCIP [122] will be used to perform the optimization and the mathematical model presented in Equation (5.24) will be assumed as reference model, having a particular formulation to be suitable for the solver SCIP. In the next sections, a new more comprehensive mathematical model will result from the introduction of new variables and constraints accounting for the simultaneous installation of turbines and valves within the network.

6.3.1 Additional variables

Given a network of l links and n nodes, the presence of a valve within a branch k of the network is modeled through the binary variable I_k^V, which is equal to 1 if the device is installed, 0 otherwise. As the head-loss within turbines, the head dissipated by valves (i.e. H_k^V) can be split according to the formulation proposed by Belotti et al. (2013) [6]:

$$0 \leq H_k^{V+}(\theta) \leq H_{k_{max}}\ \zeta_k(\theta) \tag{6.1}$$

$$0 \leq H_k^{V-}(\theta) \leq H_{k_{max}}\ (1-\zeta_k(\theta)) \tag{6.2}$$

The total head-loss within the valve can be therefore expressed as:

$$H_k^V(\theta) = H_k^{V+}(\theta) + H_k^{V-}(\theta) \tag{6.3}$$

According to the previous formulation, given a k-th pipe where a valve is installed (i.e. $I_k^V = 1$), if at the θ-th demand step the discharge flows according to the direction of the pipe (i.e. $\zeta_k(\theta) = 1$ with reference to Equation (5.1)), the head-loss within the valve consists of the only positive term (H_k^{V+}), vice versa if the discharge flows in the opposite direction.

Table 6.1 summarizes the total number of independent variables of the optimization procedure. According to Table 6.1, $H_i(\theta)$ ($\theta = 1 \ldots n_d$) is a variable in all nodes of the network, excluding the reservoirs where the head is constant. When the node is a reservoir r $(r = 1..\varsigma)$, the variable is rather the discharge $q_r(\theta)$ flowing into or out of the reservoir itself.

Table 6.1 Summary of the binary (B) and continuous (C) independent variables of the optimal PATs and PRVs location problem.

Variable	I_k^T	I_k^V	$\zeta_k(\theta)$	$q_k^+(\theta)$	$q_k^-(\theta)$	$q_r(\theta)$
Number	l	l	$l \cdot n_d$	$l \cdot n_d$	$l \cdot n_d$	$\varsigma \cdot n_d$
Type	B	B	B	C	C	C

Variable	$H_k^{T+}(\theta)$	$H_k^{T-}(\theta)$	$H_k^{V+}(\theta)$	$H_k^{v-}(\theta)$	$H_i(\theta)$
Number	$l \cdot n_d$	$l \cdot n_d$	$l \cdot n_d$	$l \cdot n_d$	$(n-\varsigma) \cdot n_d$
Type	C	C	C	C	C

6.3.2 New formulation of the mathematical model

An integration of the mathematical model (5.24) is needed to account for the installation of valves.

With regard to the objective function, the NPV has been reformulated as following:

$$NPV = \sum_{k=1}^{l} (-c_k^T \; I_k^T - c_k^V \; I_k^V) + \sum_{y=1}^{Y} \frac{(E_y^p + W_y^s)}{(1+r)^y} \tag{6.4}$$

c_k^V being the cost related to the installation of valves, which has been assumed as the sum of c_z and c_{inst} (see also Equation (4.7)):

$$c_k^V = c_z + c_{inst} \tag{6.5}$$

Regarding the momentum balance equation (5.9) modeling the resolution of the network, it has been reformulated to account for the installation of valves as well.

Given a link k $(k = 1..l)$ and a demand step θ $(\theta = 1 \dots n_d)$, the momentum balance equation can be formulated as following:

$$H_i - H_j - r_k L_k - (H_k^{T+} - H_k^{T-}) - (H_k^{V+} - H_k^{V-}) = 0 \tag{6.6}$$

For the sake of notation simplicity, in Equation (6.6) the dependence on the demand step θ $(\theta = 1 \dots n_d)$ has been omitted.

In this study hydro-valves operating in only one direction of the flow have been considered. To avoid the installation of any device in the pipes where the flow reverses, constraints (5.11)-(5.12) have been therefore reformulated:

$$I_k^T + I_k^V \leq 1 + \zeta_k(\theta_1) - \zeta_k(\theta_2) \tag{6.7}$$

$$I_k^T + I_k^V \leq 1 - \zeta_k(\theta_1) + \zeta_k(\theta_2) \tag{6.8}$$

$\zeta_k(\theta_1)$ $(\theta_1 = 1 \ldots n_d)$ and $\zeta_k(\theta_2)$ $(\theta_2 = 1 \ldots n_d)$ being the binary variable ζ_k evaluated at two different demand coefficients, with $\theta_1 < \theta_2$.
To avoid the installation of both turbine and valve within a same pipe, a new constraint has been introduced:

$$I_k^T + I_k^V \leq 1 \tag{6.9}$$

Constraint (6.9) has been written for each link k $(k = 1 \ldots l)$ of the network, thus the number of these constraints can be accounted as l. According to such constraints, the binary variables cannot be simultaneously equal to 1, thus, given a k-th pipe, either one device is installed or no pressure control strategy is performed. Apparently, constraint (6.9) is redundant, as constraints (6.7)-(6.8) may already avoid the simultaneous installation of a valve and a turbine within the same pipe. Despite this, the addition of constraint (6.9) is crucial to achieve good solutions in reasonable time, as it further shrinks the feasible region of the continuous relaxation.
As the head-loss within turbines, the head dissipated by the valve has been linearly constrained, as follows:

$$\overline{H_k^V} \geq \overline{H_{kmin}}\ I_k^V \tag{6.10}$$

$$H_k^V(\theta) \leq H_{k_{max}}\ I_k^V \tag{6.11}$$

Constraint (6.10) has been used in order to set a minimum average value of the variable head-loss within the valve (H_k^V), whether it is installed in the k-th branch (i.e. I_k^V is equal to 1). Such constraint has been written for each pipe k $(k = 1 \ldots l)$ of the network. As a result of both constraints (6.10)-(6.11), if I_k^V is equal to 0 (i.e. the device is not located in the k-th pipe), the corresponding head-loss is forced to be equal to 0 as well.

$$\left\{\begin{array}{ll}
\underset{\substack{I_k^T, I_k^V, \zeta_k, q_r \\ q_k^+, q_k^-, H_i, H_k^{T+} \\ H_k^{T-}, H_k^{V+}, H_k^{V-}}}{\text{maximize}} & NPV = \sum_{k=1}^{l}(-c_k^T\ I_k^T - c_k^V\ I_k^V) + \sum_{y=1}^{Y} \frac{(E_y^p + W_y^s)}{(1+r)^y} \\
& -tol_i^Q \leq \sum_{k=1}^{K_i}(q_k^+ - q_k^-)^{in} - \sum_{k=1}^{K_i}(q_k^+ - q_k^-)^{out} + \\
& -f_i\ p_i^{\beta} - q_i^d \leq tol_i^Q \\
& -tol_k^H \leq H_i - H_j - r_k L_k - (H_k^{T+} - H_k^{T-}) + \\
& -(H_k^{V+} - H_k^{V-}) \leq tol_k^H \\
& \overline{P_k^T}\ \eta^T \geq \overline{P_{min}}\ I_k^T \\
& P_k^T = \gamma\ (H_k^{T+}(\theta) + H_k^{T-}(\theta))\ (q_k^+(\theta) + q_k^-(\theta)) \\
& I_k^T + I_k^V \leq 1 + \zeta_k(\theta_1) - \zeta_k(\theta_2) \\
& I_k^T + I_k^V \leq 1 - \zeta_k(\theta_1) + \zeta_k(\theta_2) \\
& \frac{p_{min}}{\gamma} \leq H_i(t) - z_i \leq \frac{p_{max}}{\gamma} \\
\text{subject to} & 0 \leq H_k^{T+}(\theta) \leq H_{k_{max}}\ \zeta_k(\theta) \\
& 0 \leq H_k^{T-}(\theta) \leq H_{k_{max}}\ (1 - \zeta_k(\theta)) \\
& 0 \leq H_k^{V+}(\theta) \leq H_{k_{max}}\ \zeta_k(\theta) \\
& 0 \leq H_k^{V-}(\theta) \leq H_{k_{max}}\ (1 - \zeta_k(\theta)) \\
& H_k^T(\theta) = H_k^{T+}(\theta) + H_k^{T-}(\theta) \\
& H_k^T(\theta) \leq H_{k_{max}}\ I_k^T \\
& H_k^V(\theta) = H_k^{V+}(\theta) + H_k^{V-}(\theta) \\
& \overline{H_k^V} \geq \overline{H_{kmin}}\ I_k^V \\
& H_k^V(\theta) \leq H_{k_{max}}\ I_k^V \\
& Q_{min}\ \zeta_k(\theta) \leq q_k^+(\theta) \leq Q_{max}\ \zeta_k(\theta) \\
& Q_{min}\ (1 - \zeta_k(\theta)) \leq q_k^-(\theta) \leq Q_{max}\ (1 - \zeta_k(\theta)) \\
& 0 \leq I_k^T \leq 1 \\
& 0 \leq I_k^V \leq 1 \\
& 0 \leq \zeta_k \leq 1 \\
& (I_k^T, I_k^V, \zeta_k) \in \mathbb{Z}, \quad P_k^T \in \mathbb{R} \\
& (H_k^{T+}, H_k^{T-}, H_k^T, H_k^{V+}, H_k^{V-}, H_k^V) \in \mathbb{R} \\
& (q_k^-, q_k^-) \in \mathbb{R}, \quad H_i \in \mathbb{R} \\
& \forall i, j = 1 \ldots n, \quad \forall k = 1 \ldots l, \quad \forall \theta = 1 \ldots n_d, \\
& \forall \theta_1, \theta_2 = 1 \ldots n_d : \theta_1 < \theta_2
\end{array}\right. \tag{6.12}$$

The number of constraints (6.10) can be accounted as l, whereas the number of constraints (6.11) amounts to $l \cdot n_d$. Finally, it is worth underlining that such linear constraints are not intended for their proper hydraulic meaning, but rather have been opted for reducing the research space and enhance the convergence of the problem.
The reformulated constraints presented in this section have been integrated in Equation (5.24), resulting in a new more comprehensive mathematical model accounting for both turbines and valves installation.
With reference to the model (6.12), all parameters have been fixed as in section 5.5. Regarding the minimum average value of head-loss $\overline{H_{kmin}}$, it has been fixed as 0.5 m. The optimization will be performed to the synthetic network [73] by SCIP, in order to make a comparison with the results achieved by the optimization of only turbines location on the same hydraulic network.

6.4 Optimization in average condition

In average demand condition the optimization consists of 358 variables and 605 constraints. The optimization solver selected 6 turbines and 3 valves, whose location within the network is presented in Figure 6.1. Such solution has been found in 3500 seconds, after solving 537240 nodes. After 7200 seconds and 849000 nodes, the relative gap from the bound of the problem can be accounted as 37%, proving the achievement of a very promising solution. In Table 6.2 the main figures of the proposed optimization are shown and compared with literature results [48, 31].

Table 6.2 Main figures of PATs and PRVs optimization procedure for daily average end-user demand.

	NPV [€]	N of PATs [−]	N of PRVs [−]	Average Power [kW]	Investment cost [€]	Water saving [m^3/day]
Proposed optimization	851960	6	3	14.60	29761	926
Fecarotta McNabola (2017)	833740/ 830679	16/6	0/10	14.53/14.06	50396/ 50293	929
Corcoran et al. (2015)	64915	3	−	10.68	11200	−

According to Table 6.2, the proposed optimization ensures a value of NPV equal to 851960 €, and the investment cost amounts to 29761 €. The average power produced

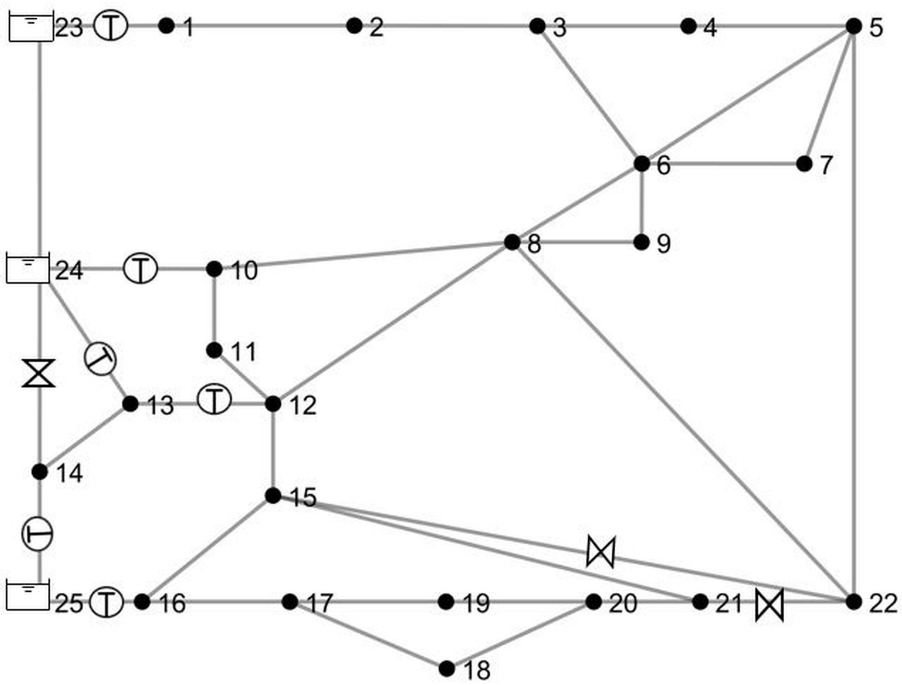

Fig. 6.1 Optimal installation of PATs and PRVs within the network in average condition.

by the turbines is equal to 14.60 kW and the water saving due to the devices installation amounts to 926 m^3 per day. This investment is paid back by water and energy savings after only 3 months. If the only energy production is considered as income, the discounted payed-back period amounts to 2 years and 6 months.

Figure 6.2 shows the main results of the optimization model, in terms of node pressure, produced power and pressure reduction. With reference to Figure 6.2 (a), the installation of valves and turbines determines a significant pressure reduction. Figure 6.2 (b) and (c) show, respectively, the produced power, as well as the head-loss within the devices. A contour plot of the pressure at the nodes of the network is shown in Figure 6.3, which presents the pressure distribution within the network when no devices are installed (top plot) and in presence of leakage control (bottom plot). According to the bottom plot in Figure 6.3, the leakage control significantly reduces the amount of wasted water whithin the network, keeping the pressure at the nodes around the minimum allowable value, that is, 25 m.

With reference again to Table 6.2, the optimization performed by Fecarotta McNabola (2017) [48] ensures a NPV equal to 833740 €, that is slightly lower than the value achieved by the proposed optimization, as well as selects a larger number of turbines (i.e. 16). Nevertheless, in the study [48] the investment cost is very high (i.e. 50293 €) due to the high number of installed devices. With regard to the water saving, in

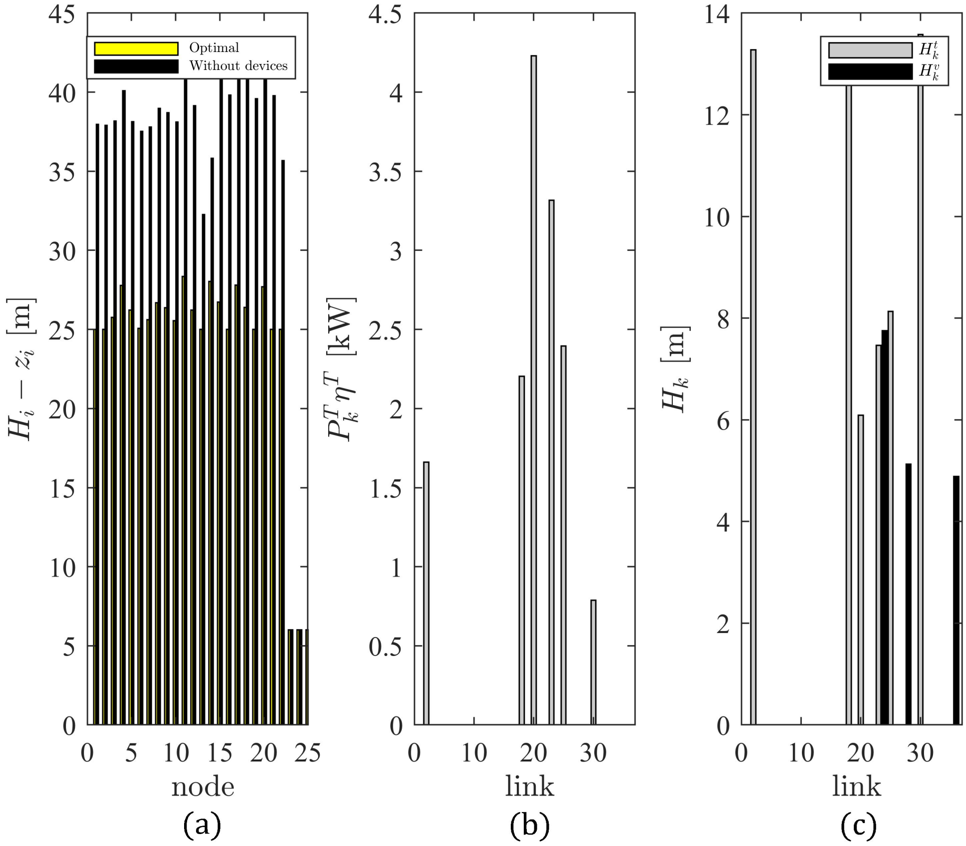

Fig. 6.2 Main results of the optimization procedure in average demand condition.

both the optimizations it has been accounted as about 927 m^3/day, thus the reduction of water leakage has been resulted the same. Owing to the large water savings, the discounted payed-back period is accounted as 5 months. If the only energy production is considered, the investment is paid back after around 4.5 years. Nevertheless, the large number of installed devices (i.e. 6 turbines and 10 valves) implicates the need for repair and maintenance works. In the study made by Corcoran et al. (2015) [31], only the production of energy was optimized and the number of installed turbines was a fixed parameter. With reference to Table 6.2, with a fixed number of devices equal to 3, the authors achieved less promising results, consisting of a value of NPV as 64915 €, as well as a produced power equal to 10.68 kW.

The model has been also tested with zero tolerances in order to investigate the influence of the feasibility tolerances on the found solution. The location of valves and PATs has been fixed, according to the solution found by the proposed optimization. Then, the algorithm has been used to find the optimal settings that satisfies the continuity and

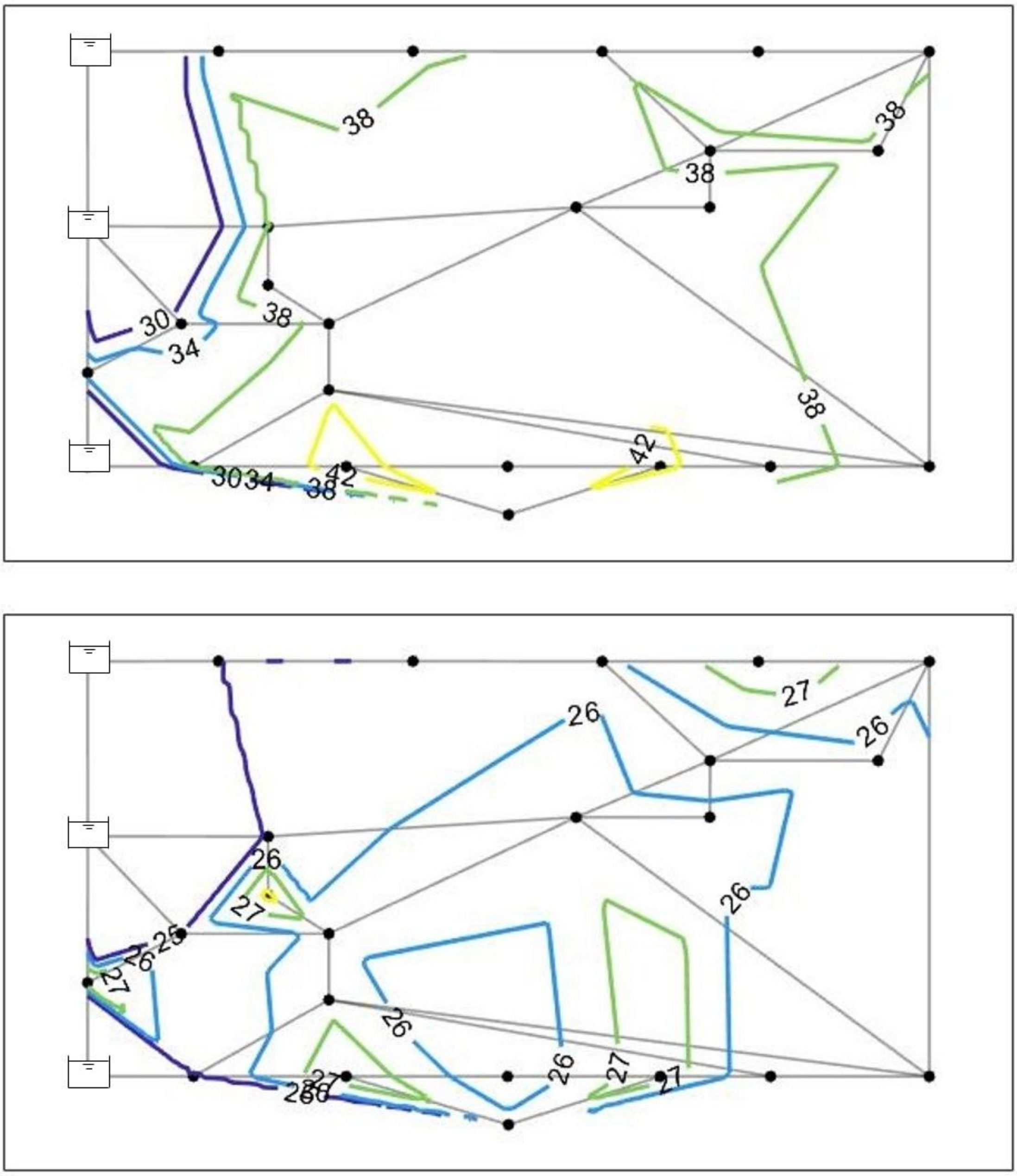

Fig. 6.3 Pressure distribution within the network in daily average demand condition, before (top plot) and after (bottom plot) performing the pressure control strategy.

the momentum balance equations without tolerances. The results, in terms of pressure and flow, are rather different, since the studied network (which is not real) presents very small values of roughness coefficients in some pipes, and also very short distance between some consecutive nodes (see Table A.1 in Appendix). As a result, very small variations of tolerances determine significant variations of flow and pressure within the network. Nevertheless, the produced energy and leaked volume in zero tolerance simulation result to be very similar to the amounts in Table 6.2.

6.5 Optimization in daily pattern condition

In daily pattern condition, the number of variables increases to 2062 and the constraints amount to 5641. The optimization has been carried out by the subgradient method [5, 82] (see section 5.4.1), which has found a solution in 16500 seconds. It is worth underlining that the minimum values of ϵ_Q and ϵ_H allowing for a fast and successful ptimization by the subgradient method are 0.025 and 0.02, respectively.
The solution obtained by the subgradient method is following summarized in Table 6.3.

Table 6.3 Main figures of turbines and valves optimization by subgradient method in daily pattern condition.

	NPV [€]	N of PATs [−]	N of PRVs [−]	Average Power [kW]	Investment cost [€]	Water saving [m^3/day]
Subgradient method	793401	7	1	18.29	27624	847

According to Table 6.3 the proposed optimization ensures a value of NPV as 793401 €. The total number of installed devices amounts to 8 (i.e. 7 turbines and 1 valve) and the resulting investment cost has been accounted as 27624 €. Such solution ensures an average power equal to 18.29 kW, as well as a water saving of 847 m^3 per day. In Figure 6.4 the daily pattern of valves and turbines characteristics are presented in terms of head-loss (H_k^T, H_k^V), produced power (P_k) and flowing discharge (Q_k, that is, $q_k^+ + q_k^-$). Despite the promising results, the tolerances of the optimization procedure can be further improved. It is worth highlighting that on the one hand increased values of ϵ_Q and ϵ_H, thus of tolerances, result in reduced computational time, but on the other the error in the hydraulic modelling of the network increases with such feasibility tolerances. In order to decrease the tolerances tol_i^Q and tol_k^H to more reasonable values, the coefficients ϵ_Q and ϵ_H have been both reduced to 0.015. As a result, the reduction of the feasibility tolerances determines such an increased computational complexity that both the subgradient method and MINLP heuristics within SCIP resulted to fail. Nevertheless, providing the solver with a feasible solution as guess point of the

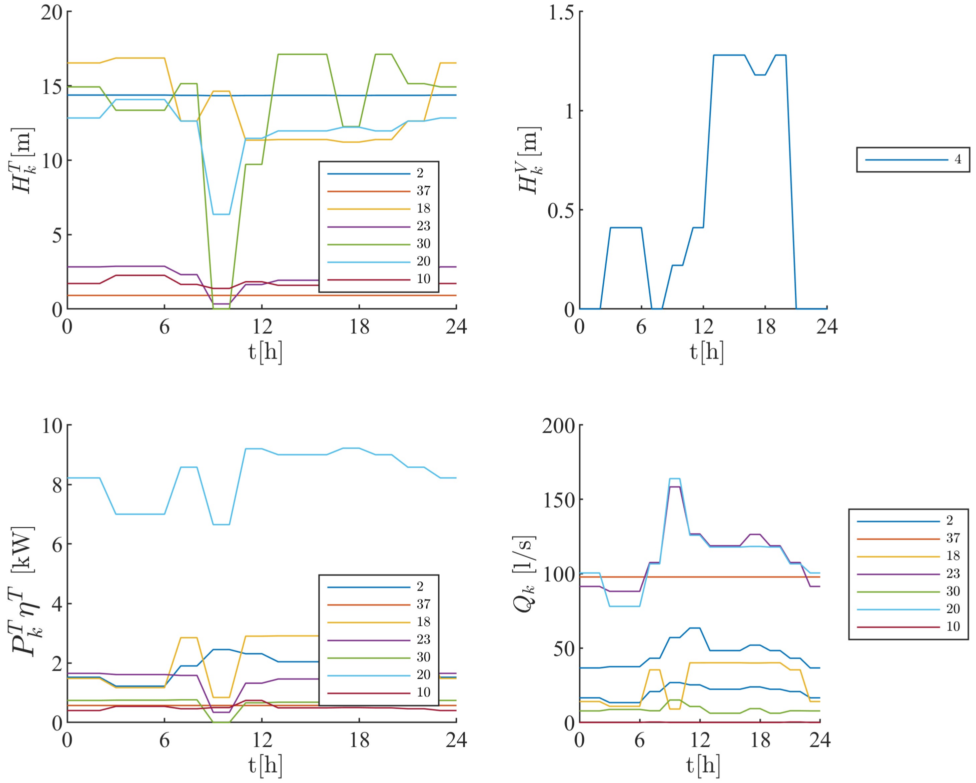

Fig. 6.4 Main results of subgradient optimization procedure in daily pattern condition.

optimization may significantly improve the performance of the solver itself. Note that the solution of the subradient method (presented in Table 6.3) is not feasible for the general problem (in Equation 6.12) with reduced values of tolerances. A tailored heuristic has been therefore developed in order to seek a feasible solution to provide to the solver as starting point of the general optimization problem. Such procedure consists of fixing the binary variables I_k^T and I_k^V according to the solution found by the subgradient method and then solving the general optimization model (Equation 6.12) with reduced values of feasibility tolerances. The solver significantly benefited from the fixed binaries and managed to find a solution in less than two hours. The process was interrupted once a first solution was found – no matter how accurate it was – since it was computed with the only aim of generating a feasible solution of the general problem. Since it is not a meaningful result, this solution is not presented here. However, when such a feasible solution was provided as starting point, the practical convergence of the optimization was significantly enhanced and the solver menaged to achieve in a very short time (i.e. 2500 seconds) the solution presented in Table 6.4.

According to Table 6.4, the found solution consists of a NPV as 778806 €. The total number of installed devices is 6 and the resulting investment cost has been accounted as 21276 €. This investment is paid back after around 3 months by both energy and water savings, and after two years by the only energy income. The localization of the devices within the network is shown in Figure 6.6. The average power produced by the turbines amounts to 12 kW and the resulting water saving amounts to 849 m^3 per day. Compared to the solution in Table 6.3, the new solution results to be slightly less promising in terms of objective function, but it is definitely more meaningful due to the reduced values of tolerances.
The final daily pattern of head-loss within devices, the discharge within the pipes and the power produced by turbines are following presented in Figure 6.5.

Table 6.4 Main figures of PATs and PRVs optimization in daily pattern condition.

	NPV [€]	N of PATs [−]	N of PRVs [−]	Average Power [kW]	Investment cost [€]	Water saving [m^3/day]
Proposed optimization	778806	5	1	12	21276	849
Fecarotta McNabola (2017)	790320/ 783992	20/6	0/14	13.43/12.63	62556/ 62256	901
Giugni et al. (2014) - OF1	−	0/3	3/0	8.62	−	732.5
Giugni et al. (2014) - OF2	−	3	−	13.62	−	709.5
Nguyen et al. (2020)	−	4	−	9.22	−	703

The optimization performed by Fecarotta and McNabola (2017) [48] selected 20 PATs, ensuring an average power of 13.43 kW and a water saving as 901 m^3 per day. Machines producing less than 500 W were a-posteriori replaced with valves, thus the initial number of 20 installed turbines decreased to 6. As a result, the NPV slightly decreased from 790320 € to 783992 €, as well as the produced power amounted to 12.63 kW. Although the investment was paid back after only 7 months, the large number of installed devices increased the need of repair and maintenance works. If the only production of energy is taken into account, the investment is paid back after around 7 years. Due to the lack of any constraints handling the flow reversion during the day, the authors [48] performed an a-posteriori approach in order to verify whether the solution was affected by the flow reversion. Although the authors [48] verified that flow reversion occurred where turbines were replaced by valves, any information about the kind of installed valves, as well as the way such devices can operate in case of flow reversion, has been provided.

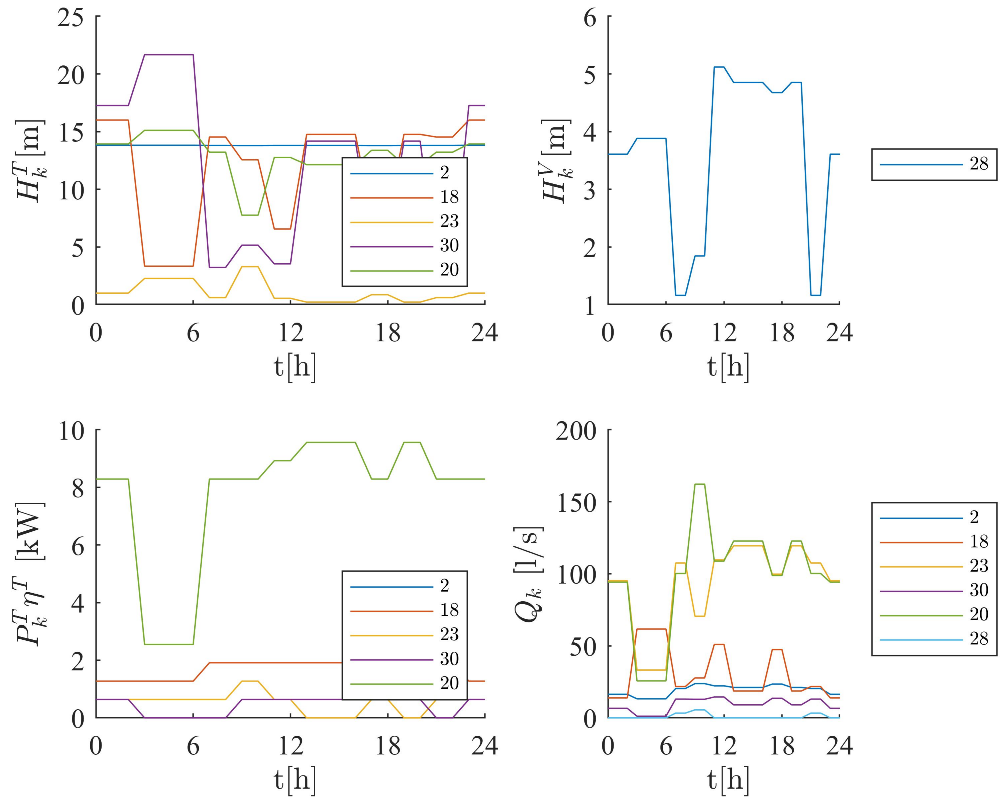

Fig. 6.5 Main results of final optimization procedure in daily pattern condition.

As previously highlighted, in the study made by Giugni et al. (2014) [61], when only water leakages are optimized (i.e. the objective function is OF1), the optimal solution corresponding to 3 fixed devices ensures a water saving equal to 732.5 m^3 per day and the recoverable power is equal to 8.62 kW. On the other hand, when only the production of energy is maximized (i.e. the objective function is OF2), the optimal location of 3 turbines ensures a smaller water saving equal to 709.5 m^3 per day, as well as an increased average power equal to 13.62 kW.

The results obtained Nguyen et al. (2020) [95] are less promising than the solutions found by Fecarotta et al. (2017) [48] and the proposed optimization. This is maybe due to the maximization of the only produced power in the objective function considered in [95], whereas a simultaneous optimization of water and energy savings might ensure better results.

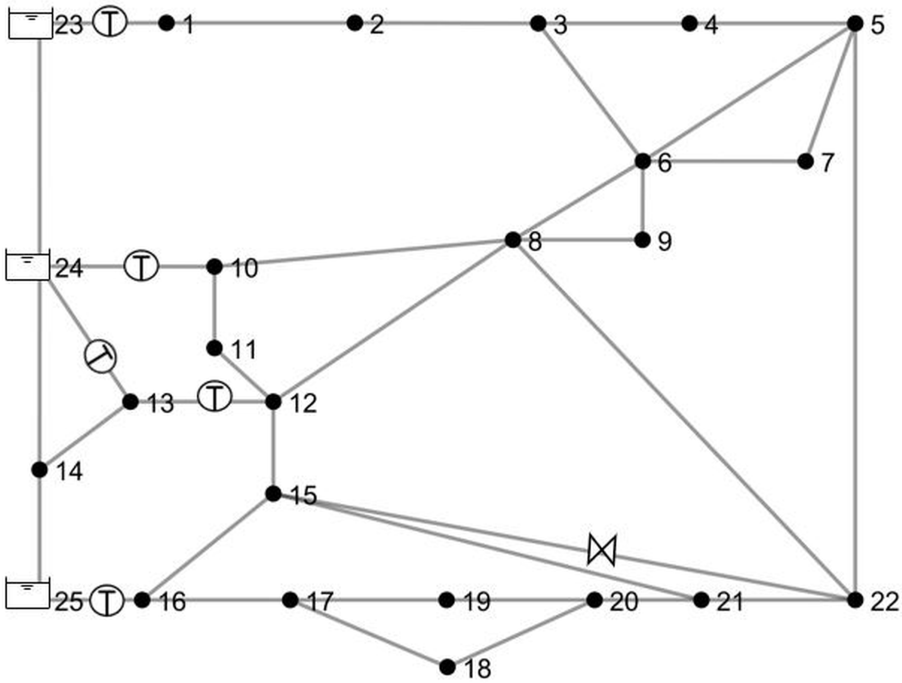

Fig. 6.6 Optimal installation of PATs and PRVs within the network in daily pattern condition.

6.6 Comparison between cost models

As already clarified in section 5.7, the cost model employed so far has been chosen to directly compare the results of the proposed optimization with literature works and to better highlight the improvements achieved. To obtain a more realistic value of the investment, in this study the optimization has been also performed employing more recent cost models. As in section 5.7, the costs of PATs have been assessed according to the model developed by Novara et al. (2019) [97], while the total cost of PRVs has been evaluated according to the study made by Garcia et al. (2019) [57].

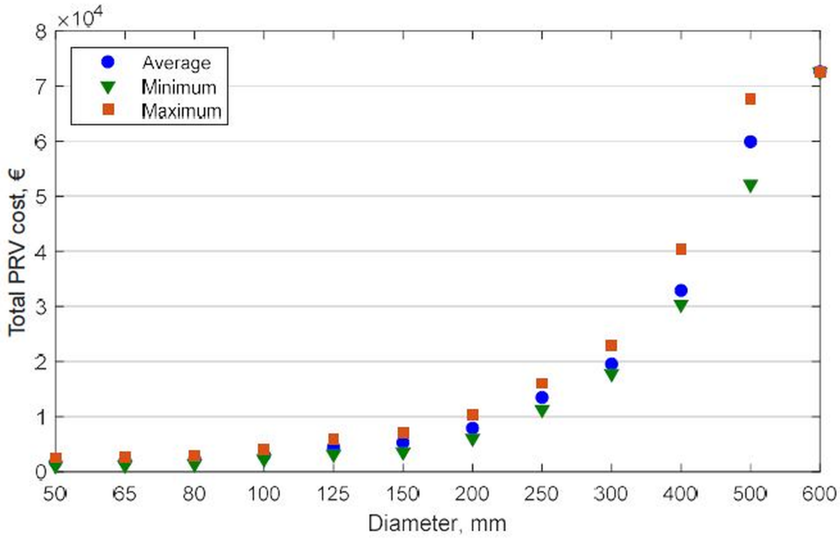

Fig. 6.7 Total PRV cost depending on pipe diameter [57].

With reference to Figure 6.7, the total cost of PRVs is significantly dependent on the pipe diameter according to Garcia et al. (2019) [57]. Among all cost values in Figure 6.7, in this study the total cost has been assessed for each pipe diameter with reference to the only average values (i.e. blue dots).
Table 6.5 compares the solution obtained by using the abovementioned new cost models [97, 57] (i.e. cost model 2) with the solution previously presented in Table 6.2 (i.e. cost model 1), for the daily average demand.

Table 6.5 Comparison of the cost model presented in section 4.7.1 [48] and Equation (6.5) (cost model (1)) with more recent cost models [97, 57] (cost model (2)) in daily average condition.

	NPV [€]	N of PATs [−]	N of PRVs [−]	Average Power [kW]	Investment cost [€]	Water saving [m^3/day]
cost model 1	851960	6	3	14.60	29761	926
cost model 2	796275	7	2	14.2	84551	928

According to Table 6.5, the new cost model (see cost model 2) results in far larger investment cost and, thus, in a smaller NPV. Nevertheless, the two solutions are quite similar in terms of water savings, produced power and total number of installed devices. As shown in Figure 6.8, the location of the installed devices within the network is the same for the two cost models, except for only one turbine which has been located in place of a valve in the link 24-14 according to the new cost model.

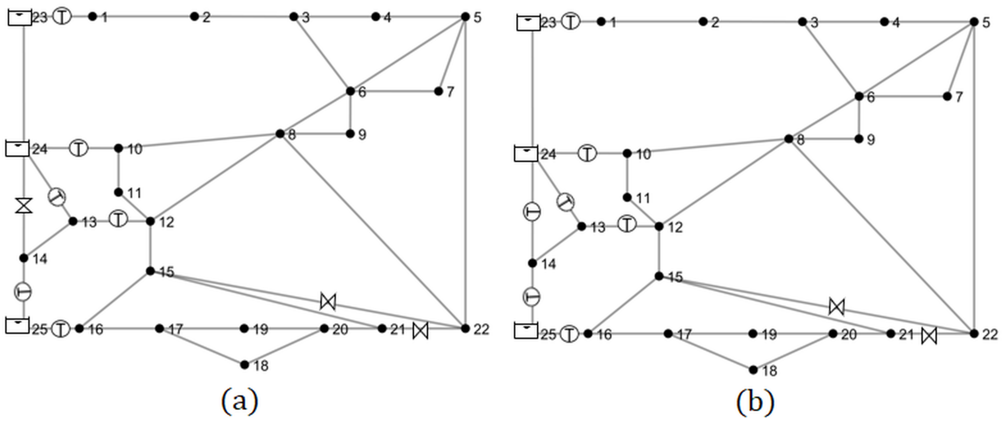

Fig. 6.8 Location of the devices according to the previous cost model (a) and to the new cost model [97, 57] (b) in daily average condition.

Table 6.6 Comparison of the cost model presented in section 4.7.1 [48] and Equation (6.5) (cost model (1)) with more recent cost models [97, 57] (cost model (2)) for the whole daily pattern.

	NPV [€]	N of PATs [−]	N of PRVs [−]	Average Power [kW]	Investment cost [€]	Water saving [m^3/day]
cost model 1	778806	5	1	12	21276	849
cost model 2	692082	6	2	13.3	74080	800

According to Table 6.6, the solution obtained by the new cost model (see cost model 2) consists of 6 PATs and 2 PRVs, that is, two devices more than the number selected by the previous cost model (see cost model 1). According to Figure 6.9, the turbines have been located in the same positions for both the cost models while the valves have been placed in different locations. Indeed, the new total cost pushes the solver to place the valves where an excess pressure is available and the pipe diameters are small at the same time, in order to maximize water savings and contain the installation cost. However, according to the solution obtained by the new cost model, the location of an extra PAT has ensured a slightly larger average power (i.e. 13.3 kW against 12 kW), whereas the water saving is a little smaller (i.e. 800 m^3 per day against 849 m^3 per day).

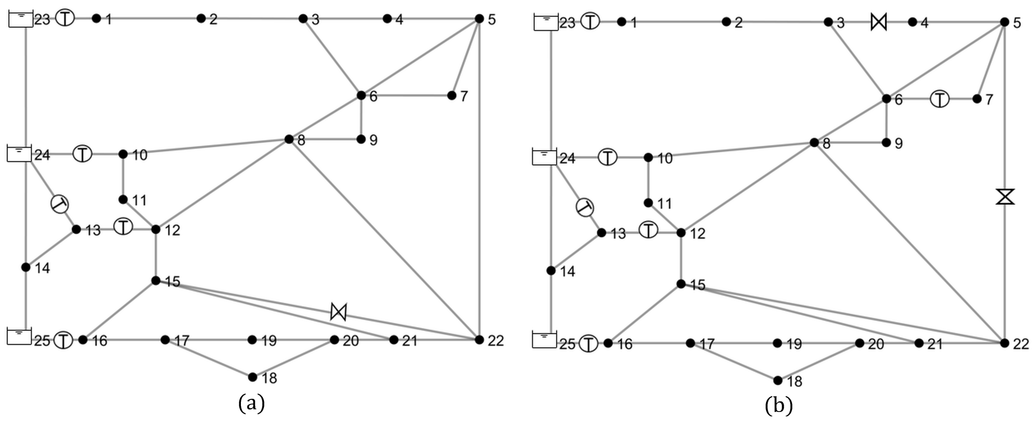

Fig. 6.9 Location of the devices according to the previous cost model (a) and to the new cost model [97, 57] (b) in daily pattern condition.

6.7 Final remarks and next developments

In this chapter, a global optimization solver has been used to perform the optimization. In average condition, the solver has found a solution consisting of 3 valves and 6 turbines producing a total power of 14.60 kW, and the NPV has been accounted as 851960 €. If the whole daily pattern is considered, the NPV decreases to 778806 € and the total number of devices amounts to 6, that is, 1 valve and 5 turbines producing an average power of 12 kW. According to the comparison with the solution achieved by Giugni et al. (2014) [61] and Nguyen et al. (2020) [95] on the same network, the proposed optimization ensures better results in terms of both energy production and water savings. Compared to the study carried out by Fecarotta and McNabola (2017) [48], the achieved results are quite comparable in terms of both water and energy savings. Nevertheless, the proposed optimization ensures the installation of a number of devices significantly smaller, which means smaller investment costs, as well as reduced need of repair and maintenance works.

A comparison between results achieved by different cost models has been also proposed. With reference to the daily average condition, the solutions result to coincide in terms of both location and savings, whereas in daily pattern condition there is a slight difference in terms of savings. In particular, the choice of the cost model seems to affect more valve than turbine location.

A comparison between the optimal location of PATs and the optimal location of PATs and PRVs according to the proposed optimization performed by the solver SCIP is following presented: According to Table 6.7, the simultaneous optimization of PATs and PRVs location ensures a better NPV due to the increased water saving (i.e. 849

Table 6.7 A comparison between the optimal location of PATs and the optimal location of PATs and PRVs according to the proposed optimization .

	NPV [€]	N of PATs [−]	N of PRVs [−]	Average Power [kW]	Investment cost [€]	Water saving [m^3/day]
Optimal location PATs+PRVs	778806	5	1	12	21276	849
Optimal location PATs	734998	4	–	12.6	15076	786

m^3 per day against 786 m^3 per day), whereas the average produced power is basically the same.

Beyond the enhanced results, the effectiveness of the proposed optimization results from the development of a new more realistic mathematical model, accounting for the phenomenon of flow reversion during the day, as well as selecting only viable turbines producing high power. Moreover, the proposed model allows for the simultaneous optimization of both turbines and valves within the water network.

In the next chapter, the optimization procedure will be extended to a real water distribution network.

List of Symbols

β	Exponent in the relation between leakage and pressure
γ	Specific weight of water
$\delta(t)$	Demand coefficient
Δt_d	Duration of the time steps with the same demand coefficient
ϵ_H	Coefficient in the evaluation of tol_k^H
ϵ_Q	Coefficient in the evaluation of tol_i^Q
ξ	Positive integer parameter in local branching
ζ_k	Binary variable modeling the versus of the flow within the k-th pipe
η^T	Efficiency of turbine
θ	Index for demand step
ς	Number of reservoirs
τ_k	Parameter accounting for the diameter, the roughness coefficient and the length of the k-th p
c	Coefficient for the evaluation of f_i
c_e	Energy unit selling price
c_{inst}	Installation cost of turbine
c_k^T	Total cost of turbine
c_k^V	Total cost of valve
c_P,c_Z	Coefficients for the evaluation of the turbine and valve total cost
c_w	Cost of water
C_k	Roughness coefficient of the k-th pipe

C_y^{in}	Cash inflow at the y-th year
C_y^{out}	Cash outflow at the y-th year
D_k	Diameter of the k-th pipe
$E_y^{p,T}$	Energy production during the y-th year
$E_y^{s,P}$	Energy consumption during the y-th year
f_i	Leakage coefficient
H_i	Head at the i-th node
H_i^0	Head at the i-th node without pressure control
$\overline{H_{kmin}}$	Minimum average head loss within the device in the k-th pipe
H_k^T	Head-loss within the turbine in the k-th pipe
H_k^{T+}	Positive component of the head-loss within the turbine in the k-th pipe
H_k^{T-}	Negative component of the head-loss within the turbine in the k-th pipe
H_k^V	Head-loss within the valve in the k-th pipe
H_k^{V+}	Positive component of the head-loss within the valve in the k-th pipe
H_k^{V-}	Negative component of the head-loss within the valve in the k-th pipe
H_{kmax}	Upper bound of H_k^T and H_k^V
i, j	Indices for nodes
I_k^T	Binary variable representing the presence of a turbine within the k-th pipe
I_k^V	Binary variable representing the presence of a valve within the k-th pipe
k	Index for pipes
K_i	Number of pipes approaching the i-th node
l	Number of pipes of the network
$L_{i,j}$	Length of pipe connecting the i-th and j-th nodes
n	Number of nodes of the network
n_d	Number of ranges in the daily pattern of demand coefficients
NPV	Net present value

p_{max}	Maximum allowable pressure
p_{min}	Minimum allowable pressure
P_k^T	Hydraulic power of the turbine in the k-th pipe
$\overline{P_k^T}$	Daily average hydraulic power produced by the turbine in the k-th pipe
$\overline{P_{min}}$	Minimum allowable power producible by the turbine
q_k^+	Positive component of the discharge flowing in the k-th pipe
q_k^-	Negative component of the discharge flowing in the k-th pipe
$(q_k^+ + q_k^-)^{in}$	Total discharge flowing through the k-th pipe into the node
$(q_k^+ + q_k^-)^{out}$	Total discharge flowing through the k-th pipe out of the node
$q_i^d(t)$	End-user demand out of the the node
$\overline{q_i^d}$	Average end-user demand at the i-th node
q_r	Discharge flowing into or out of the reservoir
Q_{min}	Lower bound of total discharge Q_k
Q_{max}	Upper bound of total discharge Q_k
Q_l^0	Total leaked discharge without pressure control
Q_l^S	Total leaked discharge with pressure control strategy
r	Discount rate
r_k	Resistance term of the k-th pipe calculated by Hazen-Williams formula
t	Time
tol_i^Q	Feasibility tolerance within continuity equation
tol_k^H	Feasibility tolerance within momentum balance equation
y	Index for years
Y	Number of years
W_y^s	Water saving during the y-th year
x^*	Feasible reference solution
z_i	Elevation of the i-th node

Chapter 7

Optimal location of hydraulic devices in a real water distribution network: the GOHyDeL model

7.1 Introduction

In this chapter, a real water distribution network is assumed as case study in order to test the behavior of the optimization solver, as well as the robustness of the newly proposed mathematical model, when networks with increased size are considered. Indeed, compared to the previous chapters involving a synthetic water network, the complexity affecting the optimization procedure significantly increases if a real, larger network is assumed as case study, and the mathematical formulation of the model developed so far may be not suitable to deal with such an increased computational complexity.

Given a real water network, the installation of dissipation points (i.e. turbines and/or valves) in respect of minimum pressure requirements may determine such a reduction of the overall pressure within the system, that the remaining head at the nodes may be not enough to supply the most disadvantaged parts of the network, unless pumping systems are installed. This situation does not arise in the literature synthetic network previously investigated, since the reduction of the pressure up to the minimum requirements (see Figure 6.3) did not require the aid of pumps to supply some parts of the network. However, in real networks characterized by strong variability in ground elevation, locating turbines and valves where the water and energy savings are significant to

maximize water and energy savings, and pumps where the energy requirements are contained may be an efficient strategy for a sustainable management of WDs.
In this chapter, the mathematical model developed in chapter 6 (see Equation (6.12)) is extended to a real water network. In such a new studied network, due to the large topographical variability, the placement of valves and turbines requires the simultaneous location of pumping systems to deal with the reduction of the overall pressure and, thus, to supply the most remote nodes of network. As a result, the addition of new variables and constraints to also model the installation of pumps, together with the increased size of the case studied network, make the optimization dramatically challenging. To gradually deal with such hard complexities, the model (6.12) will be firstly employed with reference to the installation of only turbines and pumps, in order to test its robustness when switching from a synthetic to a larger real water network. Note that considering pumps instead of valves does not affect the complexity of the optimization procedure, since the size of the problem - in terms of number of independent variables and constraints - will be left unchanged with respect to the problem in Equation (6.12). Then, the installation of valves will be also integrated within the optimization and the model (6.12) will be progressively modified in order to tackle the additional complexities arising during the computation. The final result will be a Global Optimization of Hydraulic Devices Location (GOHyDeL) model, suitable for any water distribution network. Finally, a strong reduction of feasibility tolerances will be attempted in order to set the tolerances as more reasonable values, increasing the accuracy of the optimization results and reducing the error in the hydraulic modelling of the network.

7.2 Study Area

The case study concerns a water distribution network in Ireland, located in the region Blackstairs. Figure 7.2 presents the map of the case study area, where the blue multi-line marks the skeleton of the hydraulic network. With reference to Figure 7.2, several water tanks are present along the pipelines in order to control the head. Such tanks represent hydraulic disconnections determining a sort of districtualization of the network, but detailed information about the hydraulic operation of such tanks are not available. Nevertheless, the knowledge of the current hydraulic configuration of the network is not required by this study, which rather investigates the best localization and setting of devices in order to both control the pressure and recover energy.
In this study the presence of water tanks is not taken into account, but rather the available excess pressure is exploited to produce energy. It is worth underlining that

Fig. 7.1 Geographic localization of Blackstairs Mountains.

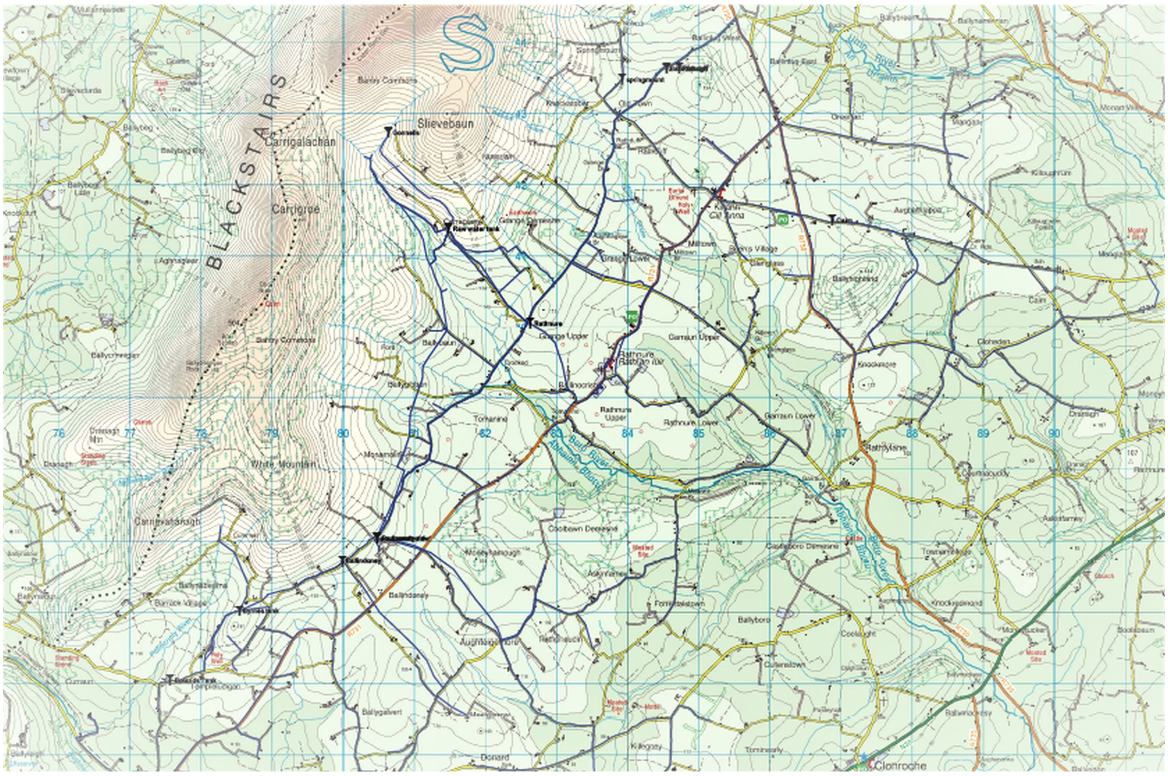

Fig. 7.2 Map of the case study area.

reducing the overall pressure to save water and produce energy means to renounce to supply the most remote nodes of the network, unless pumping systems are installed

within the network.
In this chapter, a comprehensive optimization procedure has been carried out to search the optimal location of turbines, valves and pumps, in order to exploit the excess pressure where the potential water and energy savings are large (i.e. where the available head drop and/or the flow rate are large), instead installing pumps where the consumable power is small (i.e. where the flow rate is small too).
The network layout is presented in Figure 7.3 and the geometric and hydraulic characteristics are presented in detail in Appendix. The network in question consists of

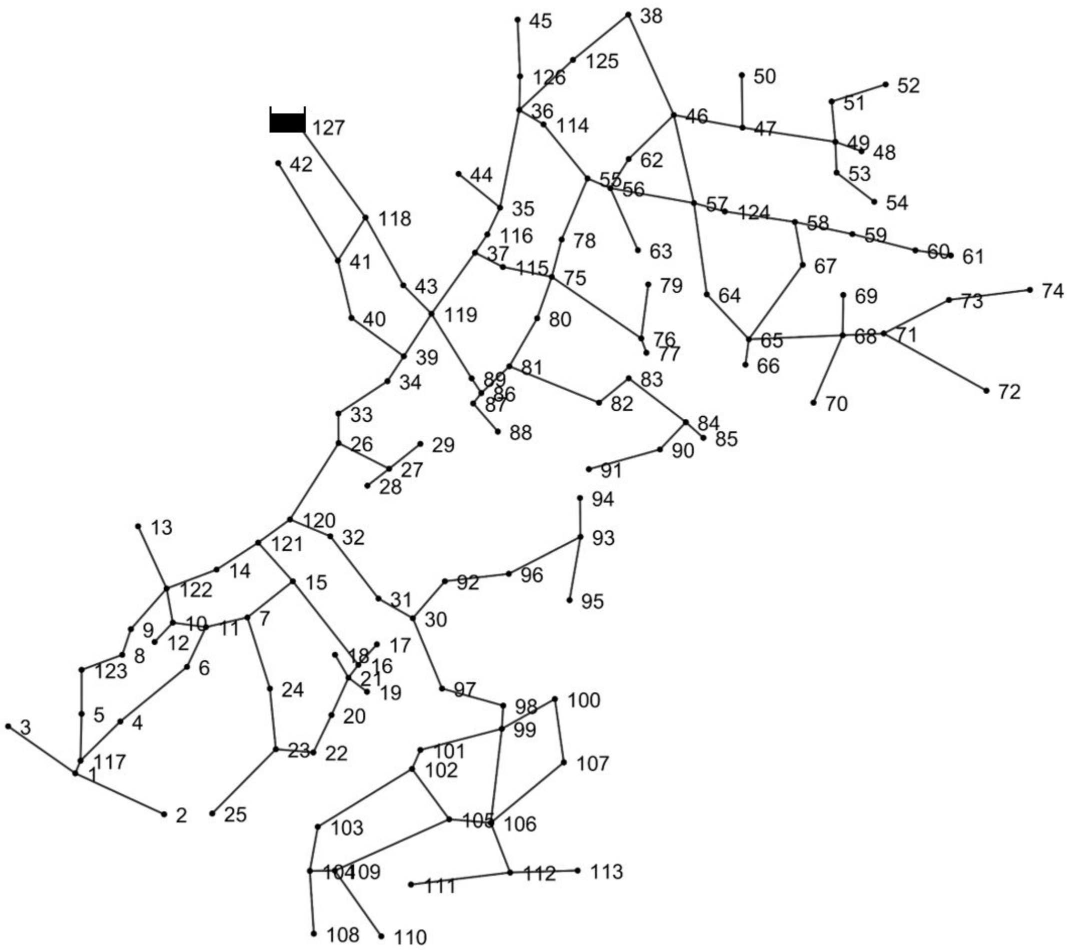

Fig. 7.3 Layout of the case study network.

127 nodes and 138 links (both looped and non-looped) and it is supplied by one single

reservoir, whose level has been assumed as constant. The based demand at the nodes of the network is significantly small (i.e. 0.12 l/s), and in some nodes is even null.
For the sake of simplicity, in this application the real water leakage affecting the network has not been properly assessed, but rather has been simulated according to the formulation proposed by Araujo at al. (2006) [4]. With reference to Equation (4.18)-(4.19), the exponent β and the coefficient c should be fixed in order to guarantee a quite realistic simulation of water leakage within the network. Such parameters have been therefore fixed so that the daily leaked volume of the whole network could be accounted as around 20/30 % of the total daily volume supplied by the reservoir. As a result, the exponent β has been fixed as 0.7 and the coefficient c as 0.000001 l/(s $\mathrm{m}^{(1+\beta)}$).
With regard to the water demand, the daily pattern is presented in Figure 7.4. The

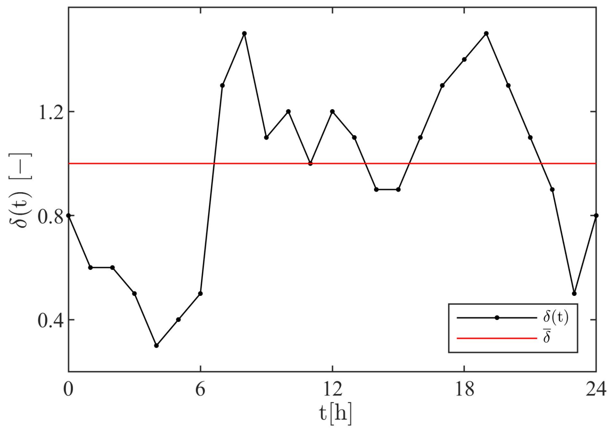

Fig. 7.4 Daily pattern of end-user demand coefficient for the case study network.

demand coefficients have been gathered in a few intervals and an average value ($\hat{\delta}$) of such coefficients has been defined as presented in Table 7.1.

The resulting daily pattern is then shown in Figure 7.5.

Table 7.1 Intervals of demand coefficients.

Demand interval	$\hat{\delta}$	Duration [h]
$[0.3-0.5]$	0.4	5
$]0.5-0.7]$	0.6	2
$]0.7-0.9]$	0.8	1
$]0.9-1.1]$	1	8
$]1.1-1.3]$	1.2	2
$]1.3-1.5]$	1.4	6

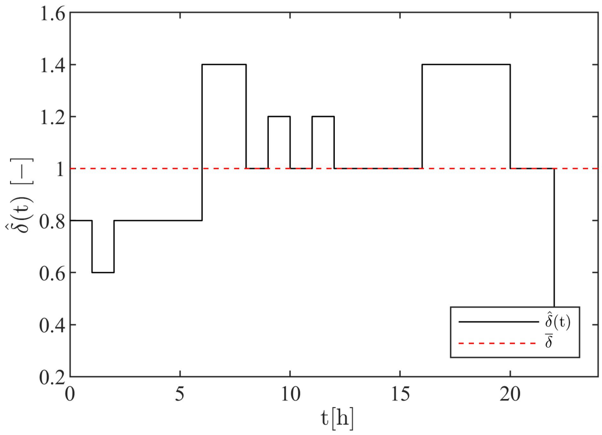

Fig. 7.5 Simplified daily pattern of end-user demand coefficient for the case study network.

Due to the increase in network size, a first optimization of only turbines and pumps is going to be presented. As in the literature synthetic network, the optimization procedure will be performed in both daily average (i.e. $\delta = 1$) and daily pattern conditions. The insertion of pressure reducing valves will be attempted later on, provided that the optimization of only turbines and pumps within the new larger network will be successfully performed.

7.3 Optimal location of turbines and pumps within the case study network

To define the optimization model representative of the new case study, additional variables have been introduced.
Given a network of l links and n nodes, the presence of a pump within a branch k ($k = 1 \ldots l$) of the network is represented by a further binary variable, i.e, I_k^P. As for turbines and valves in the previous chapters, also for the pump installation the head can be split according to Belotti et al. (2013) [6], as following:

$$0 \leq H_k^{P+}(\theta) \leq H_{k_{max}}^P \; \zeta_k(\theta) \tag{7.1}$$

$$0 \leq H_k^{P-}(\theta) \leq H_{k_{max}}^P \; (1 - \zeta_k(\theta)) \tag{7.2}$$

The total pumping head within the pump can be therefore expressed as:

$$H_k^P(\theta) = H_k^{P+}(\theta) + H_k^{P-}(\theta) \tag{7.3}$$

According to the previous formulation, given a pipe with an installed pump (i.e. $I_k^P = 1$), the pumping head at the demand step θ ($\theta = 1 \ldots n_d$) consists of the only positive part (H_k^{P+}) if $\zeta_k(\theta) = 1$ (i.e. the discharge flows according to the direction of the k-th pipe), whereas it consists of the only negative part (H_k^{P-}) whether $\zeta_k(\theta) = 0$. A table summarizing the total number of independent variables is presented in Table 7.5.

Table 7.2 Summary of the binary (B) and continuous (C) variables of the optimal PAT and pump location problem.

Variable	I_k^T	I_k^P	$\zeta_k(\theta)$	$q_k^+(\theta)$	$q_k^-(\theta)$	$q_r(\theta)$
Number	l	l	$l \cdot n_d$	$l \cdot n_d$	$l \cdot n_d$	$\varsigma \cdot n_d$
Type	B	B	B	C	C	C

Variable	$H_k^{T+}(\theta)$	$H_k^{T-}(\theta)$	$H_k^{P+}(\theta)$	$H_k^{P-}(\theta)$	$H_i(\theta)$
Number	$l \cdot n_d$	$l \cdot n_d$	$l \cdot n_d$	$l \cdot n_d$	$(n-\varsigma) \cdot n_d$
Type	C	C	C	C	C

Given a link k ($k = 1..l$) and a demand step θ ($\theta = 1 \ldots n_d$), the momentum balance equation can be formulated as follows:

$$H_i - H_j - r_k L_k - (H_k^{T+} - H_k^{T-}) + (H_k^{P+} - H_k^{P-}) = 0 \tag{7.4}$$

For the sake of notation simplicity, in Equation (7.4) the dependence on the demand step θ $(\theta = 1 \dots n_d)$ has been omitted.
To avoid the installation of any device in the pipes where the flow reverses, constraints (7.5)-(7.6) have been defined:

$$I_k^T + I_k^P \leq 1 + \zeta_k(\theta_1) - \zeta_k(\theta_2) \tag{7.5}$$

$$I_k^T + I_k^P \leq 1 - \zeta_k(\theta_1) + \zeta_k(\theta_2) \tag{7.6}$$

$\zeta_k(\theta_1)$ $(\theta_1 = 1 \dots n_d)$ and $\zeta_k(\theta_2)$ $(\theta_2 = 1 \dots n_d)$ being the binary variable ζ_k evaluated at two different demand coefficients, with $\theta_1 < \theta_2$. The number of both constraints (7.5)-(7.6) amounts to $(l \cdot n_d)$.
To avoid the installation of hydraulic devices within a same link, the binary variables cannot be simultaneously equal to 1, as follows:

$$I_k^T + I_k^P \leq 1 \tag{7.7}$$

Constraint (7.7) has been written for each link k $(k = 1 \dots l)$ of the network. The number of constraints (7.7) can be therefore accounted as l. As the head-loss within turbines and valves, the pumping head within the pump has been linearly constrained, as follows:

$$\overline{H_k^P} \geq \overline{H_k^P}_{k\ min}\ I_k^P \tag{7.8}$$

$$H_k^P(\theta) \leq H_{k_{max}}^P\ I_k^P \tag{7.9}$$

Constraint (7.8) is intended to set a minimum average value of the variable pumping head (H_k^P), whether the pump is installed in the k-th branch (i.e. I_k^V is equal to 1). Such constraint has been written for each pipe k $(k = 1 \dots l)$ of the network. Equation (7.9) sets a maximum value that the variable (H_k^P) can assume whether I_k^P is equal to 1. As a result of both constraints (7.8)-(7.9), the pumping head in the k-th link is

forced to be equal to 0 if the pump is not installed. The number of constraints (7.8) can be accounted as l, whereas the number of constraints (7.9) amounts to $(l \cdot n_d)$.
In order to reduce the number of variables, the dependent variables H_k^P and H_k^T have been cut out, by replacing their formulation (presented in Equations (7.3) and (5.6), respectively) within constraints (7.8), (7.9) and (4.12), as follows:

$$\overline{(H_k^{P+} + H_k^{P-})} \geq \overline{H_k^P}_{min} \ I_k^P \tag{7.10}$$

$$H_k^{P+}(\theta) + H_k^{P-}(\theta) \leq H_{k_{max}}^P \ I_k^P \tag{7.11}$$

$$H_k^{T+}(\theta) + H_k^{T-}(\theta) \leq H_{k_{max}} \ I_k^T \tag{7.12}$$

With regard to the objective function that is still the NPV of the investment, it can be expressed now as:

$$NPV = \sum_{k=1}^{l}(-c_k^T \ I_k^T \ - c_k^P \ I_k^V) + \sum_{y=1}^{Y} \frac{(E_y^{p,T} - E_y^{s,P} + W_y^s)}{(1+r)^y} \tag{7.13}$$

where c_k^P is the total cost of the installed pumps, expressed as following:

$$c_k^P = c_P \ P_{max}^P + c_z + c_{inst} \tag{7.14}$$

With reference to Equation (7.14), c_P, c_z and c_{inst} have been assumed according to the cost model in section 4.7.1, whereas P_{max}^P is the maximum power consumed by the pump in the k-th pipe (expressed in kW).
With reference to Equation (7.13), $E_y^{p,T}$ is the annual energy income, whereas the annual energy outcome is $E_y^{s,P}$ and can be expressed as:

$$E_y^{s,P} = c_e \sum_{k=1}^{l} 365 \sum_{\theta=1}^{n_d} \frac{P_k^P(\theta)}{\eta^P} \ \Delta t_d(\theta) \tag{7.15}$$

c_e being the energy unit selling price, set equal to 0.1 €/kWh; η^P the efficiency of the pump, assumed as a constant and equal to 0.65 and Δt_d the duration of the θ-th

($\theta = 1 \dots n_d$) demand step. Finally, $P_k^P(\theta)$ is the hydraulic power of the pump, defined as:

$$P_k^P(\theta) = \gamma\ (H_k^{P+}(\theta) + H_k^{P-}(\theta))\ (q_k^+(\theta) + q_k^-(\theta)) \tag{7.16}$$

The hydraulic power of the pump should be written for each pipe k ($k = 1 \dots l$) of the network.
The resulting mathematical model is herein presented in Equation (7.17).
In model (7.17) the parameters have been set as in chapter 4. With regard to the minimum average and the maximum value of pumping head within the valve ($\overline{H_k^P}_{min}$ and $H_{k_{max}}^P$), these have been fixed as 0.5 m and 200 m, respectively, whereas the minimum discharge flowing through the pipes (i.e. Q_{min}) has been set as 0.01 l/s.

$$
\left\{
\begin{array}{ll}
\underset{\substack{I_k^T, I_k^P, \zeta_k, q_r \\ q_k^+, q_k^-, H_i, H_k^{T+} \\ H_k^{T-}, H_k^{P+}, H_k^{P-}}}{\text{maximize}} & NPV = \sum_{k=1}^{l} (-c_k^T \ I_k^P - c_k^P \ I_k^V) + \sum_{y=1}^{Y} \frac{(E_y^{p,T} - E_y^{s,P} + W_y^s)}{(1+r)^y} \\
& -tol_i^Q \leq \sum_{k=1}^{K_i} (q_k^+ - q_k^-)^{in} - \sum_{k=1}^{K_i} (q_k^+ - q_k^-)^{out} + \\
& - f_i \ p_i^{\beta} - q_i^d \leq tol_i^Q \\
& -tol_k^H \leq H_i - H_j - r_k L_k - (H_k^{T+} - H_k^{T-}) + \\
& + (H_k^{P+} - H_k^{P-}) \leq tol_k^H \\
& \overline{P_k^T} \ \eta^T \geq \overline{P_{min}} I_k^T \\
& P_k^T = \gamma \ (H_k^{T+}(\theta) + H_k^{T-}(\theta)) \ (q_k^+(\theta) + q_k^-(\theta)) \\
& I_k^T + I_k^P \leq 1 + \zeta_k(\theta_1) - \zeta_k(\theta_2) \\
& I_k^T + I_k^P \leq 1 - \zeta_k(\theta_1) + \zeta_k(\theta_2) \\
& I_k^T + I_k^P \leq 1 \\
& \frac{p_{min}}{\gamma} \leq H_i(t) - z_i \leq \frac{p_{max}}{\gamma} \\
\text{subject to} & 0 \leq H_k^{T+}(\theta) \leq H_{k_{max}} \ \zeta_k(\theta) \\
& 0 \leq H_k^{T-}(\theta) \leq H_{k_{max}} \ (1 - \zeta_k(\theta)) \\
& 0 \leq H_k^{P+}(\theta) \leq H_{k_{max}}^P \ \zeta_k(\theta) \\
& 0 \leq H_k^{P-}(\theta) \leq H_{k_{max}}^P \ (1 - \zeta_k(\theta)) \\
& (H_k^{T+}(\theta) + H_k^{T-}(\theta)) \leq H_{k_{max}} \ I_k^T \\
& (H_k^{P+}(\theta) + H_k^{P-}(\theta)) \leq H_{k_{max}}^P \ I_k^P \\
& \overline{(H_k^{P+} + H_k^{P-})} \geq \overline{H_k^P}_{min} \ I_k^P \\
& Q_{min} \ \zeta_k(\theta) \leq q_k^+(\theta) \leq Q_{max} \ \zeta_k(\theta) \\
& Q_{min} \ (1 - \zeta_k(\theta)) \leq q_k^-(\theta) \leq Q_{max} \ (1 - \zeta_k(\theta)) \\
& 0 \leq I_k^T \leq 1 \\
& 0 \leq I_k^P \leq 1 \\
& 0 \leq \zeta_k \leq 1 \\
& (I_k^T, I_k^P, \zeta_k) \in \mathbb{Z}, \quad P_k \in \mathbb{R} \\
& (H_k^{T+}, H_k^{T-}, H_k^T, H_k^{P+}, H_k^{P-}, H_k^P) \in \mathbb{R} \\
& (q_k^-, q_k^-) \in \mathbb{R}, \quad H_i \in \mathbb{R} \\
& \forall i, j = 1 \dots n, \quad \forall k = 1 \dots l, \quad \forall \theta = 1 \dots n_d, \\
& \forall \theta_1, \theta_2 = 1 \dots n_d : \theta_1 < \theta_2
\end{array}
\right.
\tag{7.17}
$$

7.3.1 Optimization procedure in average condition

As already highlighted in the previous sections, the increased size of the network further increased the computational complexity of the optimization problem. Indeed, in average condition the number of variables amounts to 1369 whereas the number of constraints is equal to 2175. Nevertheless, providing the optimization solver with a feasible starting solution may be an effective strategy, pushing the solver to achieve a solution in a reasonable time. To seek such a feasible solution, a tailored heuristic has been performed by the solver SCIP, as follows:

1. A first optimization is performed on a simpler problem, where the binary variables are represented by only I_k^T and ζ_k, whereas the binary variables indicating the presence of pumps (I_k^P) are fixed equal to zero in the whole network. To solve the hydraulic problem without the aid of pumping systems, the pressure in the nodes has been allowed to be up to 150 m;
2. In the second step of the heuristic procedure, the binary variables ζ_k are fixed according to the solution obtained in the first step. In such step the binary variables I_k^P are not fixed and the maximum allowable pressure within the nodes is restored to 100 m. Fixing the direction of the flow within the pipes (ζ_k) pushes the solver to install a pump where the discharge cannot flow by gravity.

The solution obtained by step 2 represents a feasible solution of the general problem and can be crucial to solve it whether provided to the solver as a starting point of the optimization procedure.
The results of the final optimization are shown hereafter.

Table 7.3 Main figures of turbines (PATs) and pumps (Ps) optimization in average demand condition.

	NPV [€]	N of PATs [−]	N of Ps [−]	Av. produced/spent power [kW]	Investment cost [€]	Water saving [m^3/day]
Proposed optimization	139404	8	8	10.33/2.38	49996	160

According to Table 7.3, the performed optimization found a solution consisting of a NPV equal to 139404 €. The solver selected 8 turbines and 8 pumps and the resulting investment cost has been accounted as 49996 €. The location of the installed devices within the case studied network is presented in Figure 7.6. The water saving has been accounted as 160 m^3/day, whereas the amount of power produced by turbines and

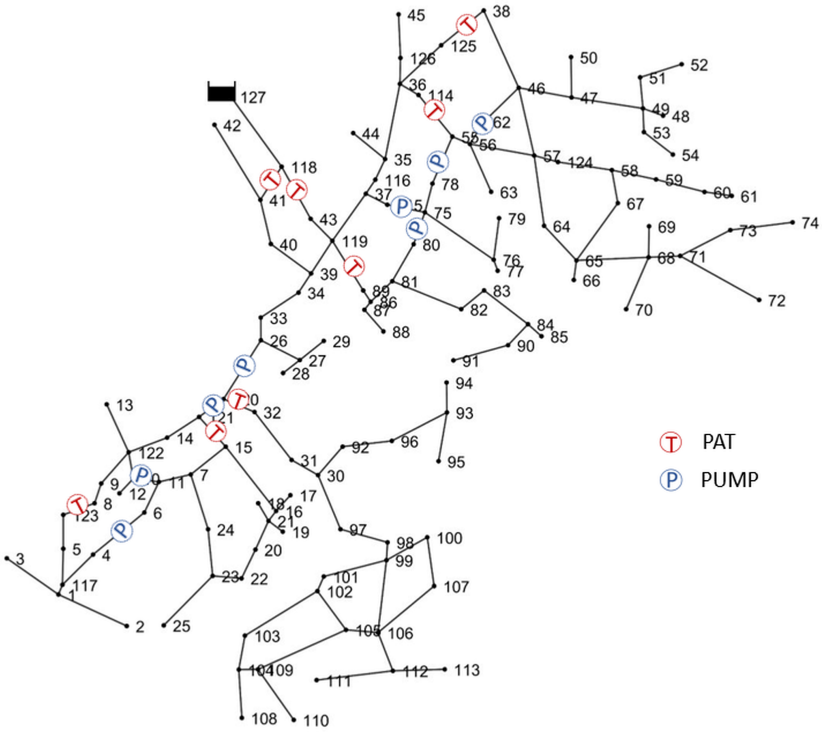

Fig. 7.6 Location of the installed turbines and pumps within the network in daily average demand condition.

consumed by pumps amounts to 10.33 kW and 2.38 kW, respectively, with a resulting net power (i.e. difference between produced and consumed power) equal to 7.95 kW. The values of power and head-loss within the installed devices are shown in Figure 7.7. Note that the power absorbed by the pump is a significant percentage of the power produced by the PATs. Figure 7.8 instead shows the pressure contour plot before the installation of pumps and PATs within the network. Note that pressure values are significantly high in the whole network and a pressure control strategy is necessary to reduce the amount of leaked water. The distribution of pressure at nodes, once turbines and pumps are installed within the network, is presented in Figure 7.9.

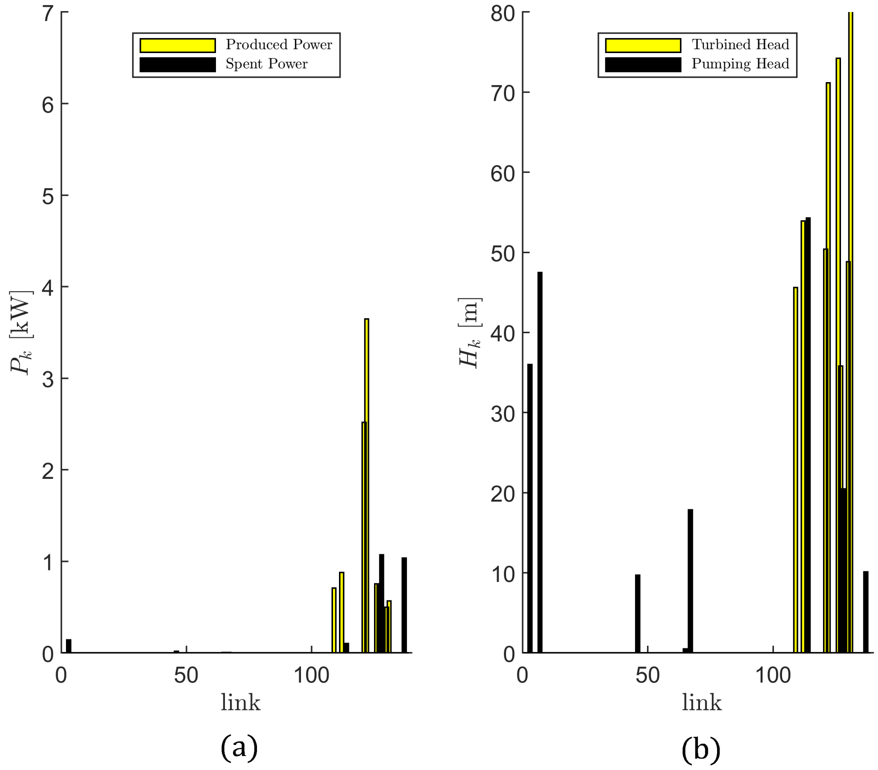

Fig. 7.7 Main results of the optimization of turbines and pumps for the real case study in average condition.

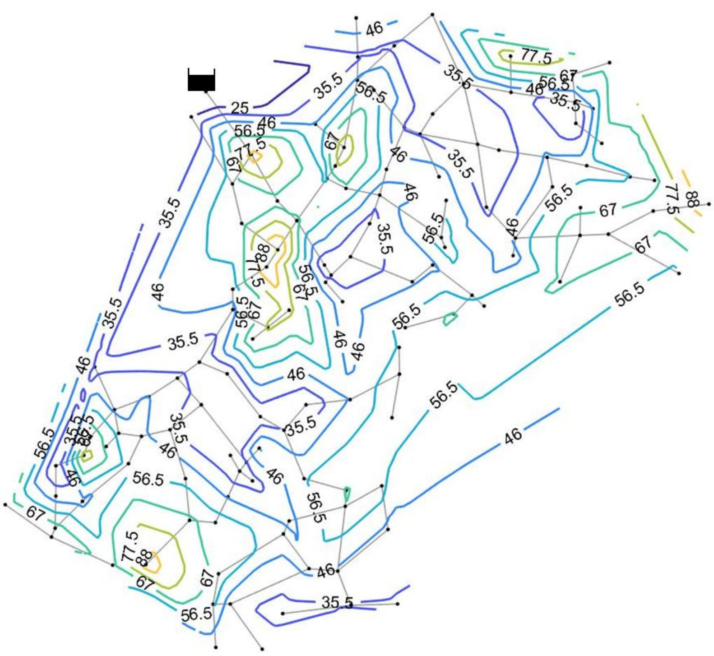

Fig. 7.9 Pressure contour plot in average demand condition, in presence of pressure control and energy production strategy.

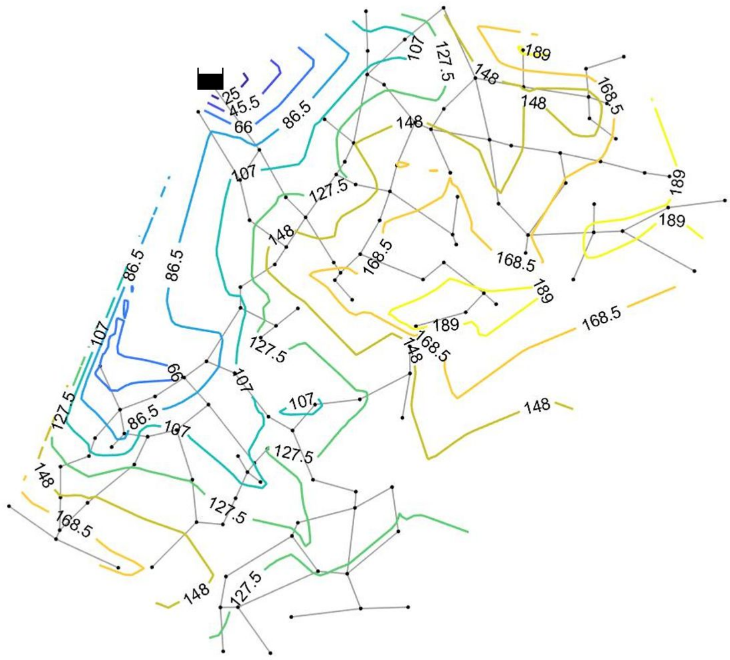

Fig. 7.8 Pressure contour plot in average demand condition before the installation of the devices within the network.

7.3.2 Optimization procedure in daily pattern condition

In daily pattern condition, the complexity of the problem dramatically increases, since the number of variables amounts to 6834 whereas the number of constraints increases to 12636.

In order to provide the optimization solver with a feasible starting solution, a further tailored heuristic has been defined, consisting of a sequence of sub-problems performed by the solver SCIP itself. It is worth underlining that the optimization performed in each step will terminate as soon as a first solution will be achieved by the solver. Indeed, the aim of such procedure is not to find the best solution, but rather to achieve a good quality feasible solution, which will be an aid for the solver to tackle the general optimization problem. Compared with the procedure developed for the average demand condition (see subsection 7.3.1), the optimization in daily pattern condition requires some additional steps, due to the complexity of the problem.

For the sake of illustration, the steps in which the tailored heuristic has been organized are following presented:

1. The subgradient optimization method is performed on a simpler sub-problem, where the binary variables are represented by only I_k^T and ζ_k, fixing the binary variables I_k^P equal to zero in the whole network. The pressure in the nodes has been allowed to be up to 150 m, in order to supply the network without the aid of pumping systems. To speed up the subgradient method, the water leakages are not taken into account in this first step (i.e. $f_i = 0$), as well as, high values of tolerances have been set (i.e. ϵ_Q and ϵ_H both equal to 0.02). As a result, the procedure is very fast and a solution is found by SCIP in a few seconds.

2. In the second step, the binary variables ζ_k are fixed according to the solution obtained in the step 1. The only binary variables of the optimization problem are I_k^P and I_k^T and the maximum allowable pressure within the nodes is restored to 100 m. Fixing the direction of the flow within the pipe (ζ_k) significantly reduces the research space and pushes the solver to install pumps where nodes cannot be supplied by gravity. The tolerances are kept the same as in the step 1 and the water leakage are not taken into account yet. As a result, the optimization is very fast and the solver SCIP achieves a first solution in a few seconds.

3. In this step, the binary variables ζ_k and I_k^T are fixed according to the solution found in step 2. The water leakages are introduced in the optimization, whereas the tolerances are still kept high (i.e. ϵ_Q and ϵ_H both equal to 0.02). The computational time required by the solver to achieve a first solution has been accounted as 860 seconds, after a number of explored nodes equal to 104.

4. The binary variables ζ_k and I_k^T have been fixed according to the latter step and the tolerances are reduced, so that ϵ_Q and ϵ_H have been properly set equal to 0.01 and 0.005, respectively. A solution has been quickly computed by the solver in 760 seconds at the first explored node.

The solution obtained by step 4 is a solution of the general problem and it is provided to the solver SCIP as a starting point of the optimization procedure. The results of the final optimization are presented in Table 7.4.

Table 7.4 Main figures of the optimal location of turbines (PATs) and pumps (Ps) on the case study network in daily pattern condition.

	NPV [€]	N of PATs [−]	N of Ps [−]	Av. produced/spent power [kW]	Investment cost [€]	Water saving [m^3/day]
Proposed optimization	115075	6	12	9.46/3.82	57335	159

With reference to Table 7.4, the proposed optimization found a solution with a NPV equal to 115075 € and an investment cost of 57335 €. The number of installed turbines amounts to 6 and the resulting energy and water savings result as 9.46 kW and 159 m^3 per day, respectively. The total number of installed pumps has been accounted as 12, whereas the consumption of power due to the pumping installation amounts to 3.82 kW. The net power therefore amounts to 5.64 kW. The high number of selected pumps is due to the installation of only PAT as dissipation points, which are located by the solver where the available producible power is above the minimum fixed value of 500 W. As a result, the dissipation points determine such a reduction of the pressure, that require the installation of a large number of pumping systems to supply the most remote parts of the network, which otherwise could not be supplied by gravity. The location of the installed devices within the network is shown in Figure 7.10.

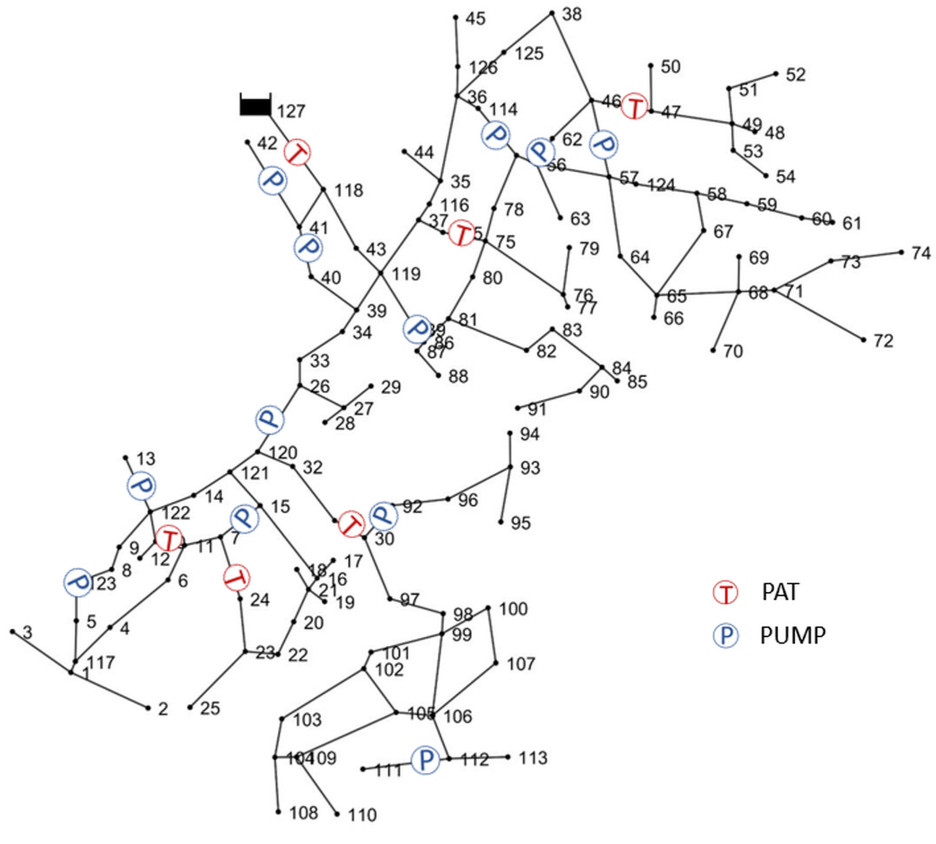

Fig. 7.10 Location of the installed turbines and pumps within the case studied network.

The daily pattern of the head-loss within the devices (H_k^T, H_k^P), of the power produced by the PATs ($P_k^T \eta^T$) and of the discharge through the pipes (Q_k) are presented in Figure 7.11.

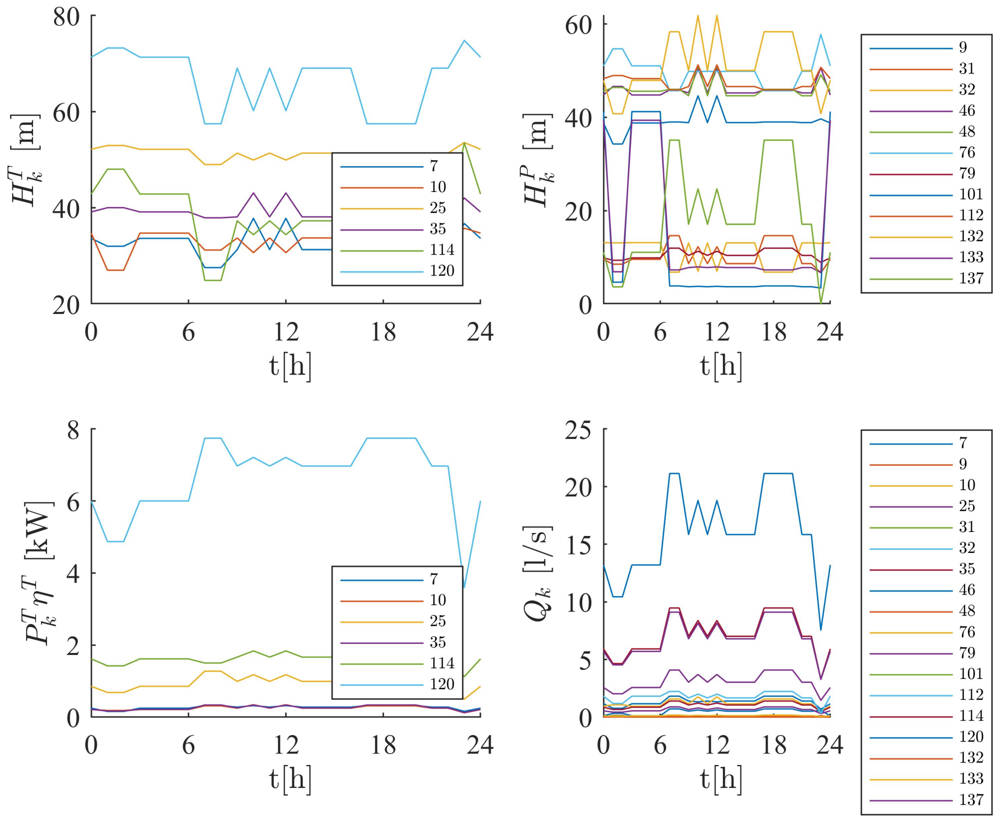

Fig. 7.11 Main results of the optimization of turbines and pumps for the real case study in daily pattern condition.

7.4 Optimal location of turbines, valves and pumps

The next step of the research work is an attempt of introducing also pressure reducing valves within the new case study network.

As already mentioned in section 6, the insertion of the valve within a branch k of the network is represented by the binary variable I_k^V. The head-loss within the valve has been already presented in Equations (6.1)-(6.3). The total number of variables is instead presented in Table 7.5.

With reference to constraints (7.5)-(7.7), these can be now expressed as:

$$I_k^T + I_k^V + I_k^P \leq 1 + \zeta_k(\theta_1) - \zeta_k(\theta_2) \tag{7.18}$$

$$I_k^T + I_k^V + I_k^P \leq 1 - \zeta_k(\theta_1) + \zeta_k(\theta_2) \tag{7.19}$$

$$I_k^T + I_k^V + I_k^P \leq 1 \tag{7.20}$$

Table 7.5 Summary of the binary (B) and continuous (C) independent variables of optimal location of PATs, PRVs and pumps.

Variable	I_k^T	I_k^V	I_k^P	$\zeta_k(\theta)$	$q_k^+(\theta)$	$q_k^-(\theta)$	$q_r(\theta)$	$H_k^{T+}(\theta)$
Number	l	l	l	$l \cdot n_d$	$l \cdot n_d$	$l \cdot n_d$	$\varsigma \cdot n_d$	$l \cdot n_d$
Type	B	B	B	B	C	C	C	C

Variable	$\mathrm{H}_k^{T-}(\theta)$	$H_k^{V+}(\theta)$	$H_k^{V-}(\theta)$	$H_k^{P+}(\theta)$	$H_k^{P-}(\theta)$	$H_i(\theta)$
Number	$l \cdot n_d$	$l \cdot n_d$	$l \cdot n_d$	$l \cdot n_d$	$l \cdot n_d$	$(n-\varsigma) \cdot n_d$
Type	C	C	C	C	C	C

With regard to the momentum balance equation, it can be rewritten accounting for the head-loss within the valve:

$$H_i - H_j - r_k L_k - (H_k^{T+} - H_k^{T-}) - (H_k^{V+} - H_k^{V-}) + (H_k^{P+} - H_k^{P-}) = 0 \tag{7.21}$$

Finally, the objective function can expressed as presented in Equation (7.22).

$$NPV = \sum_{k=1}^{l} (-c_k^T \ I_k^T \ - c_k^V \ I_k^V \ - c_k^P \ I_k^P) + \sum_{y=1}^{Y} \frac{(E_y^{p,T} - E_y^{s,P} + W_y^s)}{(1+r)^y} \tag{7.22}$$

Compared with the problem presented without valve location, the introduction of further binary variables and mathematical constraints significantly increases the computational complexity of the optimization problem, so that even the subgradient method and MINLP heuristics within the solver SCIP resulted to fail. Moreover, the definition of a feasible starting point neither helped the solver to find a good solution in a reasonable time.

To deal with the strong complexity of the problem, several mathematical expedients have been attempted to enhance the practical convergence of the optimization. Among these, a very effective modification consisted in reformulating the objective function, reducing as many non-linearities as possible and introducing new dependent variables. Indeed, with reference to Equation (7.22), the terms $c_k^T\ I_k^T$ and $c_k^P\ I_k^P$ are strongly non-linear as the binary variables I_k^T and I_k^P are multiplied by c_k^T and c_k^P, which are in turn function of the maximum power produced (P_{max}^T) and absorbed (P_{max}^P), respectively, by the turbines and pumps, according to Equations (4.15) and (7.14). By definition, the maximum powers (P_{max}^T) and (P_{max}^P) are mathematically expressed by the maximum argument of the non-linear variables P_k^T and P_k^P. Such a maximum argument together with the above mentioned non-linearities is definitely not easily handled by the optimization solver. A first attempt has been therefore made with the aim of removing the use of the operator maximum argument by new constraints:

$$P_{max}^T \geq P_k^T(\theta) \tag{7.23}$$

$$P_{max}^P \geq P_k^P(\theta) \tag{7.24}$$

Constraints (7.23)-(7.24) force P_{max}^T and P_{max}^P to be greater than P_k^T and P_k^P, respectively, for each value of θ ($\theta = 1 \ldots n_d$). Nevertheless, since the solver tends to minimize P_{max}^T and P_{max}^P (which in turn determine the installation cost of the devices according to Equations (4.15) and (7.14)), P_{max}^T and P_{max}^P will be automatically set by the solver as the minimum value being greater than P_k^T and P_k^P, respectively, for each value of θ ($\theta = 1 \ldots n_d$), that is, the maximum argument of P_k^T and P_k^P among θ. In addition, P_{max}^T and P_{max}^P have been bounded as:

$$P_{max}^T <= (\gamma\ H_{k_{max}}\ Q_{max}\ \eta^T)\ I_k^T \tag{7.25}$$

$$P_{max}^P <= (\frac{\gamma\ H_{k_{max}}^P\ Q_{max}}{\eta^P})\ I_k^P \tag{7.26}$$

According to constraints (7.25)-(7.26), P_{max}^T and P_{max}^P are forced to be equal to 0 whether I_k^T is zero in the branch k ($k = 1 \ldots l$), since these cannot assume negative values. Note that such constraints are not intended for their proper hydraulic meaning, but rather have been opted for reducing the research space and enhance the convergence of the problem.

Since bounding the optimization problem is crucial to shrink the research space, the minimum producible power constraint has been extended to P_{max}^T as well:

$$P^T_{max} >= \overline{P_{min}}\ I^T_k \tag{7.27}$$

Moreover, the upper bound defined within constraints (7.25)-(7.26) have been also extended to the hydraulic powers (P^T_k and P^P_k), which will be therefore bounded as follows:

$$P^T_k\ (\theta) <= (\gamma\ H_{k_{max}}\ Q_{max})\ I^T_k \tag{7.28}$$

$$P^P_k\ (\theta) <= (\gamma\ H^P_{k_{max}}\ Q_{max})\ I^P_k \tag{7.29}$$

A further crucial modification regards the objective function, which has been linearly reformulated by the introduction of new dependent variables (i.e. C^T_k, C^V_k and C^P_k), as presented in Equation (7.30).

$$NPV = \sum_{k=1}^{l}(-C^T_k\ - C^V_k\ - C^P_k) + \sum_{y=1}^{Y}\frac{(E^{p,T}_y - E^{s,P}_y + W^s_y)}{(1+r)^y} \tag{7.30}$$

With reference to the previous formulation of the objective function (see Equation (7.22)), the terms c^T_k, c^V_k and c^P_k were not variables, but rather were expressed within the objective function according to Equations (4.15),(6.5) and (7.14). Moreover, such terms were multiplied by the binary variables (i.e. $-c^T_k\ I^T_k - c^V_k\ I^V_k - c^P_k\ I^P_k$), making the objective function strongly non-linear. The introduction of the new dependent variables C^T_k, C^V_k and C^P_k may be therefore crucial to reduce the complexity of the optimization problem if properly constrained. As constraints, the following inequalities (7.31)-(7.33) have been therefore used:

$$C^T_k \geq c_P\ P^T_{max}\ + (c_z + c_{inst})\ I^T_k \tag{7.31}$$

$$C^V_k \geq (c_z + c_{inst})\ I^V_k \tag{7.32}$$

$$C^P_k \geq c_P\ P^P_{max} + (c_z + c_{inst})\ I^P_k \tag{7.33}$$

It may seem more reasonable to opt for equality constraints to define the new dependent variables, as following:

$$C_k^T = c_P \; P_{max}^T \; + (c_z + c_{inst}) \; I_k^T \tag{7.34}$$

$$C_k^V = (c_z + c_{inst}) \; I_k^V \tag{7.35}$$

$$C_k^P = c_P \; P_{max}^P + (c_z + c_{inst}) \; I_k^P \tag{7.36}$$

On the other hand, equality constraints could be not easily handled by the optimization solver, thus may increase the computational complexity of the problem itself. Indeed, inequality constraints are generally preferred over equalities as they enhance the convergence of the problem and reduce the computational effort of the optimization. However, it is worth noting that the use of the inequalities (7.31)-(7.33) does not affect the values of C_k^T, C_k^V and C_k^P, as the optimization solver tends to minimize the outflow cash within the objective function (i.e. maximize the outflow cash with the minus sign). As a result, the solver automatically sets such variables as the minimum values allowable by the constraints (7.31)-(7.33), and the inequality constaints collapse to the equalities presented in Equations (7.34)-(7.36). In addition, C_k^T and C_k^P have been also bounded by upper values to further shrink the research space, as follows:

$$C_k^T \leq ((c_P \; \gamma \; H_{k_{max}} \; Q_{max} \; \eta^T) \; + c_z + c_{inst}) \; I_k^T \tag{7.37}$$

$$C_k^P \leq ((c_P \; \frac{\gamma \; H_{k_{max}}^P \; Q_{max}}{\eta^P}) + c_z + c_{inst}) \; I_k^P \tag{7.38}$$

With reference to the new formulation of the objective function in Equation (7.30), the terms representative of the energy income, energy outcome and water saving (i.e, $E_y^{p,T}$, $E_y^{s,P}$ and W_y^s), which were previously expressed within the objective function according to Equations (4.16), (7.15) and (4.17) respectively, also become new dependent variables, constrained by the following inequalities:

$$E_y^{p,T} \leq c_e \sum_{k=1}^{l} 365 \sum_{\theta=1}^{n_d} P_k(\theta) \; \eta^T \; \Delta t_d(\theta) \tag{7.39}$$

$$E_y^{s,P} \geq c_e \sum_{k=1}^{l} 365 \sum_{\theta=1}^{n_d} \frac{P_k^P(\theta)}{\eta^P} \; \Delta t_d(\theta) \tag{7.40}$$

$$W_y^s \leq c_w \left(\sum_{\theta=1}^{n_d} Q_l^0(\theta)\ \Delta t_d(\theta) - \sum_{\theta=1}^{n_d} Q_l^S(\theta)\ \Delta t_d(\theta) \right) \tag{7.41}$$

With reference to the new constraints (7.39), (7.40) and (7.41), as the solver tends to maximize $E_y^{p,T}$ and W_y^s, and minimize $E_y^{s,P}$, the former will be automatically set equal to their upper bound whereas $E_y^{s,P}$ will be set as its lower bound. This means that the inequality constraints (7.39), (7.40) and (7.41) collapse to equalities and the hydraulic meaning of $E_y^{p,T}$, W_y^s and $E_y^{s,P}$ is totally preserved. Finally, for $E_y^{p,T}$ and $E_y^{s,P}$, the following upper bounds have been defined:

$$E_y^{p,T} \leq c_e \sum_{k=1}^{l} 365 \sum_{\theta=1}^{n_d} (\gamma\ H_{k_{max}}\ Q_{max}\ \eta^T)\ I_k^T\ \Delta t_d(\theta) \tag{7.42}$$

$$E_y^{s,P} \leq c_e \sum_{k=1}^{l} 365 \sum_{\theta=1}^{n_d} (\frac{\gamma\ H_{k_{max}}^P\ Q_{max}}{\eta^P})\ I_k^P\ \Delta t_d(\theta) \tag{7.43}$$

The new mathematical model (GOHyDeL) resulting from the introduced modifications is presented in Equation (7.45).
As previously explained, the optimization solvers significantly benefits from the use of a feasible solution provided as starting point of the general optimization. However, given a hydraulic network, there does not exist a unique tailored procedure to generate a feasible solution, but any succession of smaller sub-problems (obtained by fixing some variables alternately) can represent an heuristic procedure providing a feasible solution. In sections 7.3.1 and 7.3.2, examples of heuristic procedures tailored for the case study network have been presented. However, despite the use of a starting feasible point, the solver may still struggle to find better solutions. To push the solver to change the incumbent solution, in this application the heuristic local branching [49] has been performed. According to this heuristic, given a feasible reference solution x^*, a neighborhood of the solution x^* is defined as the set of the feasible solutions satisfying the additional local branching constraint:

$$\sum_{j \in N: x_j^*=0} x_j + \sum_{j \in N: x_j^*=1} (1 - x_j) \leq \xi \tag{7.44}$$

where ξ is a positive integer parameter. The local branching constraints has been extended to all the binary variables (i.e. I_k^T, I_k^V and I_k^P) in order to push the solver to switch their values either from 1 to 0 or from 0 to 1, respectively, with respect to x^*.

$$
\left\{
\begin{array}{ll}
\underset{\substack{I_k^T, I_k^P, \zeta_k, q_r \\ q_k^+, q_k^-, H_i, H_k^{T+} \\ H_k^{T-}, H_k^{p+}, H_k^{P-}}}{\text{maximize}} & NPV = \sum_{k=1}^{l}(-C_k^T\ - C_k^V\ - C_k^P) + \sum_{y=1}^{Y} \frac{(E_y^{p,T} - E_y^{s,P} + W_y^s)}{(1+r)^y} \\
 & -tol_i^Q \leq \sum_{k=1}^{K_i}(q_k^+ - q_k^-)^{in} - \sum_{k=1}^{K_i}(q_k^+ - q_k^-)^{out} + \\
 & -f_i\ p_i^\beta - q_i^d \leq tol_i^Q \\
 & -tol_k^H \leq H_i - H_j - r_k L_k - (H_k^{T+} - H_k^{T-}) - (H_k^{V+} - H_k^{V-}) \\
 & +(H_k^{P+} - H_k^{P-}) \leq tol_k^H \\
 & C_k^T \geq c_P\ P_{max}^T\ + (c_z + c_{inst})\ I_k^T \\
 & C_k^T \leq ((c_P\ \gamma\ H_{k_{max}}\ Q_{max}\ \eta^T)\ + c_z + c_{inst})\ I_k^T \\
 & C_k^V \geq (c_z + c_{inst})\ I_k^V \\
 & C_k^P \geq c_P\ P_{max}^P + (c_z + c_{inst})\ I_k^P \\
 & C_k^P \leq ((c_P\ \frac{\gamma\ H_{k_{max}}^P\ Q_{max}}{\eta_P}) + c_z + c_{inst})\ I_k^P \\
 & E_y^{p,T} \leq c_e\ \sum_{k=1}^{l} 365\ \sum_{\theta=1}^{n_d} P_k^T(\theta)\ \eta^T\ \Delta t_d(\theta) \\
 & E_y^{p,T} \leq c_e\ \sum_{k=1}^{l} 365\ \sum_{\theta=1}^{n_d}(\gamma\ H_{k_{max}}\ Q_{max}\ \eta^T)\ I_k^T\ \Delta t_d(\theta) \\
 & E_y^{s,P} \geq c_e\ \sum_{k=1}^{l} 365\ \sum_{\theta=1}^{n_d} \frac{P_k^P(\theta)}{\eta^P}\ \Delta t_d(\theta) \\
 & E_y^{s,P} \leq c_e\ \sum_{k=1}^{l} 365\ \sum_{\theta=1}^{n_d}(\frac{\gamma\ H_{k_{max}}^P\ Q_{max}}{\eta^P})\ I_k^P\ \Delta t_d(\theta) \\
\text{subject to} & W_y^s \leq c_w \left(\sum_{\theta=1}^{n_d} Q_l^0(\theta)\ \Delta t_d(\theta) - \sum_{\theta=1}^{n_d} Q_l^S(\theta)\ \Delta t_d(\theta)\right) \\
 & P_{max}^T >= \overline{P_{min}}\ I_k^T \\
 & P_k^T >= \overline{P_{min}}\ I_k^T \\
 & P_{max}^T <= (\gamma\ H_{k_{max}}\ Q_{max}\ \eta^T)\ I_k^T \\
 & P_{max}^P <= (\frac{\gamma\ H_{k_{max}}^P\ Q_{max}}{\eta^P})\ I_k^P \\
 & \overline{P_k^T}\ \eta^T \geq \overline{P_{min}} I_k^T \\
 & P_k^T = \gamma\ (H_k^{T+}(\theta) + H_k^{T-}(\theta))\ (q_k^+(\theta) + q_k^-(\theta)) \\
 & P_k^P = \gamma\ (H_k^{P+}(\theta) + H_k^{P-}(\theta))\ (q_k^+(\theta) + q_k^-(\theta)) \\
 & P_k^T\ (\theta) <= (\gamma\ H_{k_{max}}\ Q_{max})\ I_k^T \\
 & P_k^P\ (\theta) <= (\gamma\ H_{k_{max}}^P\ Q_{max})\ I_k^P \\
 & I_k^T + I_k^V + I_k^P \leq 1 + \zeta_k(\theta_1) - \zeta_k(\theta_2) \\
 & I_k^T + I_k^V + I_k^P \leq 1 - \zeta_k(\theta_1) + \zeta_k(\theta_2) \\
 & I_k^T + I_k^V + I_k^P \leq 1 \\
 & \qquad \qquad \ldots
\end{array}
\right. \tag{7.45}
$$

$$
\begin{cases}
\qquad \qquad \qquad \qquad \dots \\
\text{subject to} \quad \frac{p_{min}}{\gamma} \le H_i(t) - z_i \le \frac{p_{max}}{\gamma} \\
\qquad 0 \le H_k^{T+}(\theta) \le H_{k_{max}} \ \zeta_k(\theta) \\
\qquad 0 \le H_k^{T-}(\theta) \le H_{k_{max}} \ (1 - \zeta_k(\theta)) \\
\qquad 0 \le H_k^{P+}(\theta) \le H^P_{k_{max}} \ \zeta_k(\theta) \\
\qquad 0 \le H_k^{P-}(\theta) \le H^P_{k_{max}} \ (1 - \zeta_k(\theta)) \\
\qquad 0 \le H_k^{V+}(\theta) \le H_{k_{max}} \ \zeta_k(\theta) \\
\qquad 0 \le H_k^{V-}(\theta) \le H_{k_{max}} \ (1 - \zeta_k(\theta)) \\
\qquad H_k^{T+}(\theta) + H_k^{T-}(\theta) \le H_{k_{max}} \ I_k^T \\
\qquad H_k^{V+}(\theta) + H_k^{V-}(\theta) \le H_{k_{max}} \ I_k^V \\
\qquad H_k^{P+}(\theta) + H_k^{P-}(\theta) \le H^P_{k_{max}} \ I_k^P \\
\qquad \overline{(H_k^{T+}(\theta) + H_k^{T-}(\theta)} \ge \overline{H_{kmin}} \ I_k^T \\
\qquad \overline{(H_k^{V+}(\theta) + H_k^{V-}(\theta)} \ge \overline{H_{kmin}} \ I_k^V \\
\qquad Q_{min} \ \zeta_k(\theta) \le q_k^+(\theta) \le Q_{max} \ \zeta_k(\theta) \\
\qquad Q_{min} \ (1 - \zeta_k(\theta)) \le q_k^-(\theta) \le Q_{max} \ (1 - \zeta_k(\theta)) \\
\qquad 0 \le I_k^T \le 1 \\
\qquad 0 \le I_k^P \le 1 \\
\qquad 0 \le \zeta_k \le 1 \\
\qquad (I_k^T, I_k^V, I_k^P, \zeta_k) \in \mathbb{Z}, \quad (P_k^T, P_k^P) \in \mathbb{R} \\
\qquad (H_k^{T+}, H_k^{T-}, H_k^{V+}, H_k^{V-}, H_k^{P+}, H_k^{P-}) \in \mathbb{R} \\
\qquad (C_k^T, C_k^V, C_k^P, E_y^{p,T}, E_y^{s,P}, W_y^s, P^T_{max}, P^P_{max}) \in \mathbb{R} \\
\qquad (q_k^-, q_k^-) \in \mathbb{R}, \quad H_i \in \mathbb{R} \\
\qquad \forall i,j = 1 \dots n, \quad \forall k = 1 \dots l, \quad \forall \theta = 1 \dots n_d, \\
\qquad \forall \theta_1, \theta_2 = 1 \dots n_d : \theta_1 < \theta_2
\end{cases}
$$

The solver SCIP [122] has been used to perform the optimization and several heuristics have been implemented to accelerate primal solution findings.
Compared with the previous version of the mathematical model (in Equation (7.45)), the new formulation of the objective function and constraints has been determinant in increasing the convergence of the optimization and finding good solutions in both average and variable demand conditions.

7.4.1 Daily average condition

In Table 7.6, the solution of the optimization of PATs, PRVs and pumps within the real water network is presented and compared with the results previously achieved by the optimization of only PATs and pumps on the same network.

Table 7.6 Main figures of turbines, valves and pumps optimization in average demand condition.

	NPV [€]	N of PATs [−]	N of PRVs [−]	N of Ps [−]	Av. produced/spent power [kW]	Investment cost [€]	Water saving [m^3/day]
Optimization PAT+PRV+P	148218	4	7	3	9.72/1.90	43857	165
Optimization PAT+P	139404	8	−	8	10.33/2.38	49996	160

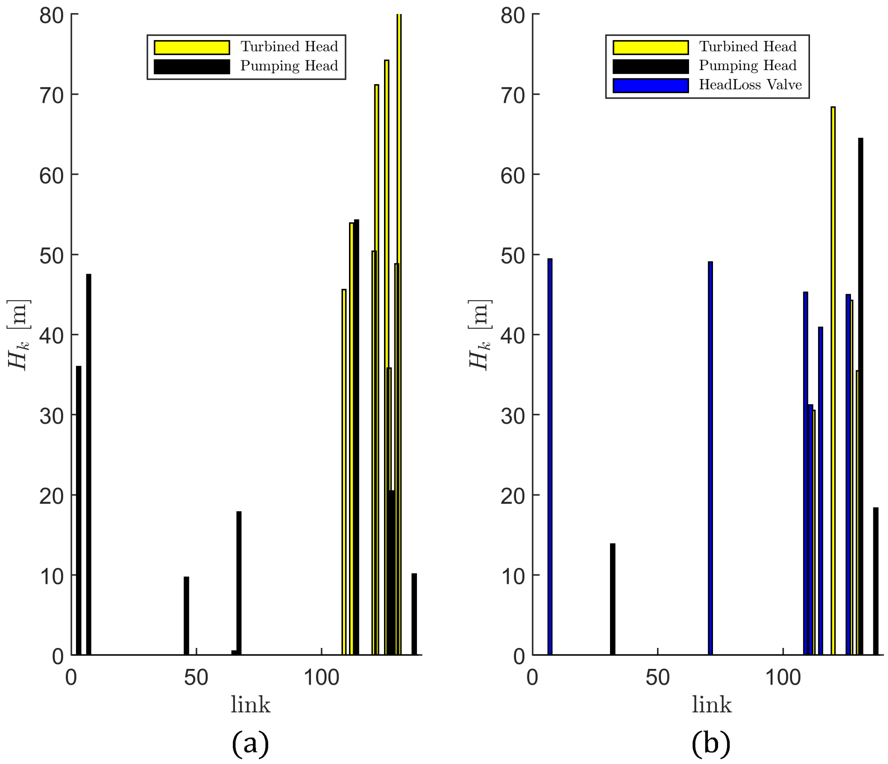

Fig. 7.12 Comparison between the optimal location of turbines and pumps (a) and turbines, valves and pumps (b) in terms of head-loss and pumping head within the hydraulic devices, in daily average demand condition.

With reference to Table (7.6), the new solution ensures a NPV equal to 148218 €, which is higher than the NPV resulting from the installation of only PATs and pumps (i.e. 139404 €). The total number of installed devices is equal to 14 (i.e. 4 PATs, 7 PRVs and 3 pumps) whereas the previous optimization of only turbines and pumps found 16 locations (i.e. 8 PATs and 8 pumps). The new installation cost is therefore slightly smaller (43857 € against 49996 €). According to the new found solution, the total power produced and absorbed by the machines amounts to 9.72 kW and 1.90 kW, whereas by installing only turbines and pumps such power is equal to 10.33 kW and 2.38 kW, respectively. The resulting net powers are therefore comparable, being equal to 7.82 kW and 7.95 kW, respectively. Finally, the water saving resulting from the new solution is 165 m^3 per day, which is slightly larger than the saving ensured by only PATs and pumps. According to the results, the installation of valves increases the number of dissipation points and reduces the number of installed pumps. Indeed, in presence of only turbines and pumps, the dissipation points were located only if determined 500 W of minimum produced power, thus high head-losses and consequent higher need of pumping towards the most disadvantage nodes. According to the comparison shown in Figure 7.12, when valves are installed within the network (b), the head-losses within the devices are smaller on the whole and smaller is also the need of pumping systems. The location of the devices within the network is shown in Figure 7.13.

The contour plot of pressure within the network in daily average demand condition is presented in Figure 7.14.

According to Figure 7.14, despite the pressure being significantly reduced with respect to the values before the installation of any device (see Figure 7.8), the pressure values are still quite high and only in a few nodes such pressure is reduced by up to the minimum requirement (i.e. 25 m). To investigate whether the same result is achieved when water saving has a higher priority than energy production, the simulation has been also performed by maximizing the only leakage reduction. The comparison between the two solutions obtained by optimizing the NPV and water savings (i.e. W_y^s) alternatively is presented in Table 7.7.
With reference to Table 7.7, if the objective function is limited to the maximization of only water savings (see OF:W_y^s) without accounting for neither the cost of device installation nor the power generation, the number of installed devices is higher (i.e. 22 against 14) as expected, and the net power can be accounted as 1.5 kW, which is significantly smaller than 7.82 kW achieved by the maximization of the NPV (see OF:NPV). Due to the increased number of installed devices, the maximization of water

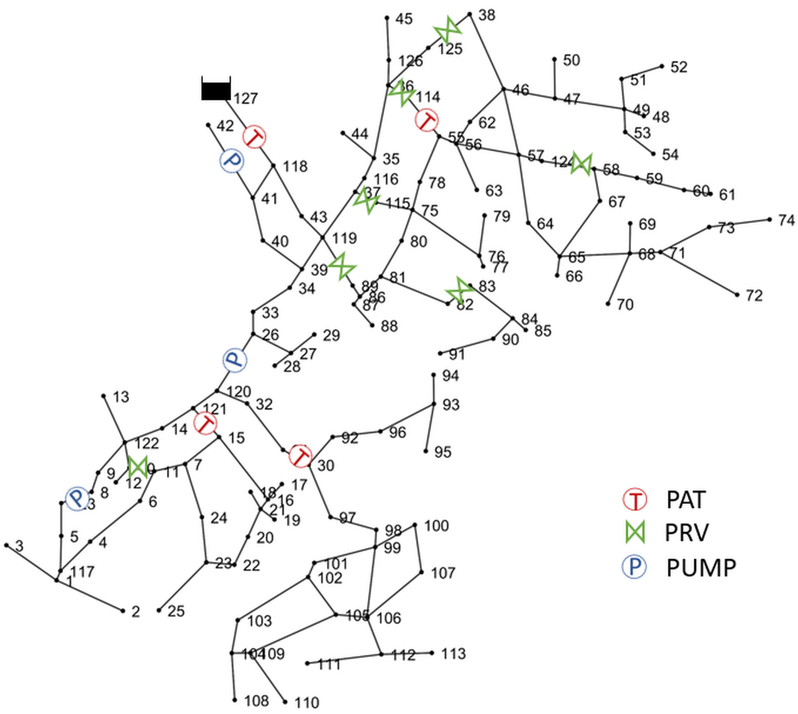

Fig. 7.13 Location of the installed turbines, valves and pumps within the case study network in daily average demand condition.

Table 7.7 Comparison between objective functions in daily average condition.

	N of PATs [−]	N of PRVs [−]	N of Ps [−]	Av. produced/spent power [kW]	Water saving [m^3/day]
OF: NPV	4	7	3	9.72/1.90	165
OF: W^S	3	13	6	8/6.50	184

savings clearly results in larger amount of saved water, which has been accounted as 184 m^3 per day, that is, 19 m^3 per day more than the saving obtained by considering the NPV as objective function. However, it is interesting to note that such an increase of dissipation points and, thus, of saved water does not implicate significant pressure reduction and the pressure values are still reduced by up to the minimum requirement only in a few nodes, as shown in Figure 7.15.

However, the leaked water, which amounted to 20% before the installation of the devices, is reduced to 11% and 9.7% when, respectively, NPV and water saving is assumed

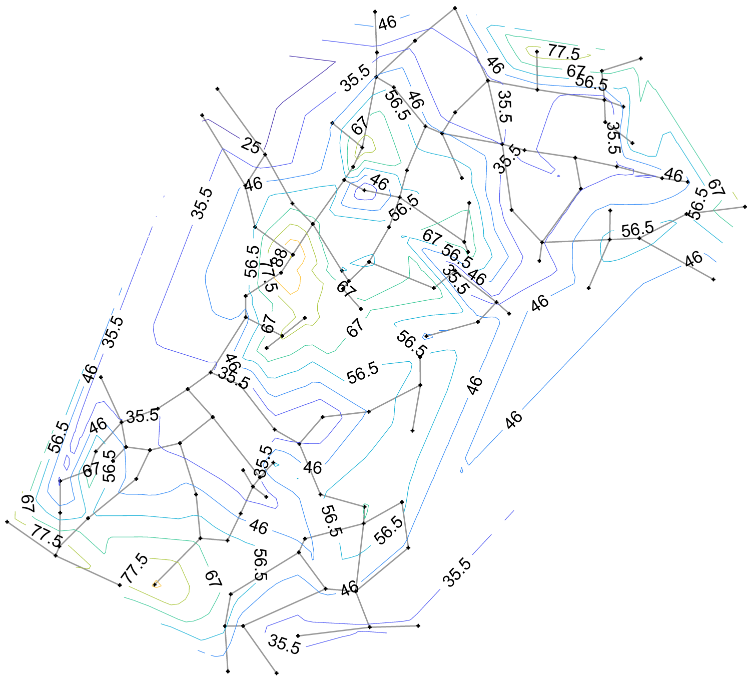

Fig. 7.14 Pressure contour plot in average demand condition after the installation of pumps, valves and turbines.

as objective function of the optimization procedure. To sum up, the maximization of leakage reduction results in a slight increase of the water saving (i.e. 1.3%) but in a significantly larger number of installed devices and very small net power. According to the results, the employment of the NPV as objective function of the optimization procedure ensures more viable solutions and gives the same priority to both savings and costs.

7.4.2 Daily pattern

The solution found in daily pattern condition is presented in Table 7.8 and compared with the results previously obtained by installing only turbines and pumps. According to Table 7.8, the solution obtained by the optimization of turbines, valves and pumps result slightly better in terms of NPV (i.e. 121072 € against 115075 €). The new solution consists of 5 PATs producing an average power of 8.33 kW, 7 pumps consuming an average power of 2.4 kW, with a resulting net average power of 5.93 kW. Amounting to 6 the number of installed valves, the total number of devices is 18 and the corresponding investment cost is accounted as 56547 €, whereas the water saving is equal to 162 m^3

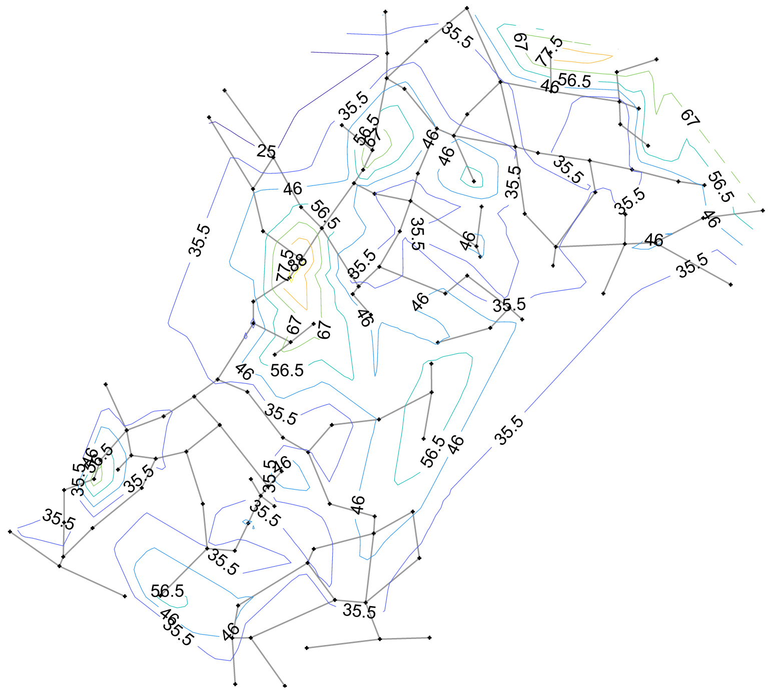

Fig. 7.15 Pressure contour plot in average demand condition when maximizing water savings.

Table 7.8 Comparison of the optimization results in daily pattern condition.

	NPV [€]	N of PATs [−]	N of PRVs [−]	N of Ps [−]	Av. produced/spent power [kW]	Investment cost [€]	Water saving [m^3/day]
Optimization PAT+PRV+P	121072	5	6	7	8.33/2.4	56547	162
Optimization PAT+P	115075	6	–	12	9.46/3.82	57355	159

per day. According to the comparison, the two solution are very similar in terms of total number of installed devices and savings. Nevertheless, the reduction of installed turbines and pumps, as well as the increase of installed valves result in lower maintenance costs and higher resilience of the system.

The daily trend of turbined heads, pumping heads and head-loss within the valves are presented in Figure 7.16. Compared to the values previously presented in Figure 7.11, the new values of both turbined and pumping head are sightly smaller. Indeed, as already mentioned in daily average condition, when PATs are the only dissipation points, such devices are positioned where the producible power, and thus head-loss,

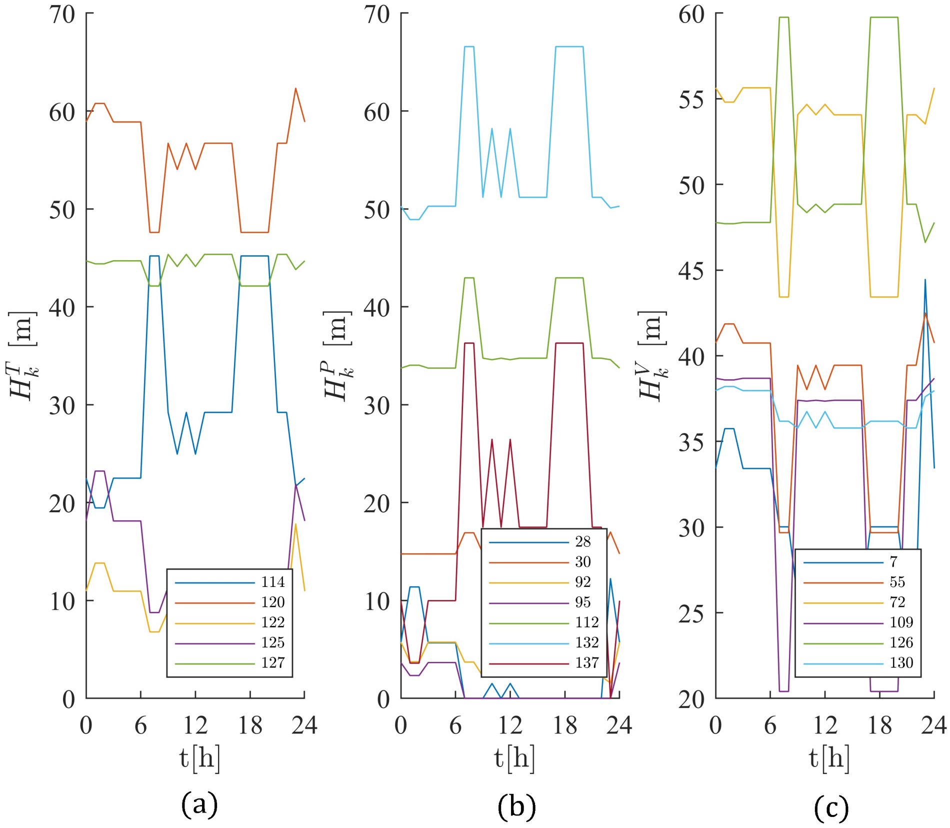

Fig. 7.16 Daily trend of turbined heads (a), pumping heads (b) and head-loss within the valves (c), according to the found solution in daily pattern condition.

was large, with consequent higher pumping requirements. The location of the devices within the network is instead shown in Figure 7.17.

7.5 Optimization by new feasibility tolerances

So far the optimization has been carried out by the use of feasibility tolerances within momentum balance and continuity equation (i.e. tol_i^Q and tol_k^H), which have been crucial to enhance the convergence of the solver. It is worth highlighting that on the one hand increased values of feasibility tolerance result in reduced computational time, but on the other the error in the hydraulic modelling of the network increases according to them. With the previous formulation of the mathematical model in Equation (7.17), any attempt to decrease such tolerances resulted to fail, as the computational effort increased accordingly. Nevertheless, the high robustness of the new mathematical model

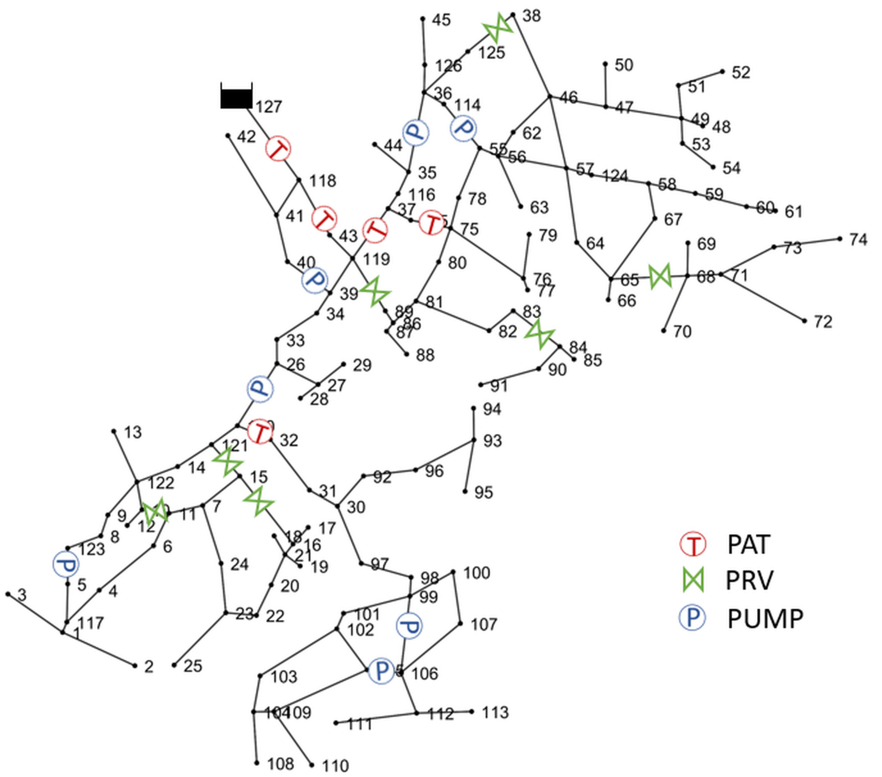

Fig. 7.17 Location of the installed turbines, valves and pumps within the case study network in daily pattern condition.

in Equation (7.45) could allow to assign the feasibility tolerances to more reasonable values. With reference to the tolerance affecting the momentum balance equation, that is tol_k^H, it has been formulated so far as a percentage (ϵ_H) of H_{kmax} (see Equation (4.23)). It is worth noting that even with small percentage of ϵ_H as 1%, the resulting tolerance may be not reasonable with regard to the links characterized by very small values of the head-loss (i.e. large diameters and roughness coefficients or small lengths of the links), since the tolerance is likely to be greater than the head-loss itself. To let the feasibility tolerance (tol_k^H) account for the magnitude of the head-loss term, it may be more reasonable to express such tolerance as a function of the parameters determining the resistance term (i.e. D_k, C_k, L_k). As a result, all the uncertainties related to the characteristics of the network (i.e. D_k, C_k, L_k) can be now expressed within one single tolerance. Let τ_k be the following quantity:

$$\tau_k = \frac{10.67\ L_k}{C_k^{1.852}\ D_k^{4.8704}} \tag{7.46}$$

Thus, the head-loss within the branch k ($k = 1 \dots l$) can be expressed as:

$$r_k\ L_k = \tau_k\ ((q_k^+)^{1.852} - (q_k^-)^{1.852}) \tag{7.47}$$

The feasibility tolerance tol_k^H has been defined as:

$$tol_k^H = \epsilon_H\ \tau_k\ \frac{(tol_i^Q + tol_k^Q)}{2} \tag{7.48}$$

where tol^Q is still the feasibility tolerance within the continuity equation, and the superscripts i and j refer to the initial and final node, respectively, of the k-th link. With reference to tol_Q, it has been kept equal to the formulation presented in Equation (4.22), accounting for the uncertainties related to the evaluation of the demand at the nodes. In this application, ϵ_Q has been set as 0.01 and ϵ_H as 100. As a result, the feasibility tolerance within the momentum balance equation has been expressed by a more reasonable formulation and, in addition, has been significantly decreased. Indeed, the reduction of tol_k^H ranges between a maximum value of 99 % and a minimum of 32 %. Despite the optimization with such small values of tolerances being really challenging, the new - more robust - formulation of the mathematical model has made the optimization possible in both average and daily pattern condition.
In the next section, the results obtained in both the demand conditions will be presented and compared with the values achieved with the previous formulation of the feasibility tolerances.

7.5.1 Results

The results obtained by the use of the new feasibility tolerances in average condition are presented in Table 7.9.

With reference to Table 7.9, the solution obtained by the use of new feasibility tolerances consists of the installation of 4 turbines, 7 valves and 6 pumps, whose investment cost amounts to 52670 €. The location of the installed devices is shown in Figure 7.19. According to the comparison, despite the water saving being almost the same, the new solution ensures a net average power of 7.41 kW against 7.82 kW obtained by

Table 7.9 Comparison of the found solutions for different values of feasibility tolerance in average demand condition.

	NPV [€]	N of PATs [−]	N of PRVs [−]	N of Ps [−]	Av. produced/ spent power [kW]	Investment cost [€]	Water saving [m^3/day]
Optimization New tolerances	140560	4	7	6	9.43/2.02	52670	169
Optimization Old tolerances	148218	4	7	3	9.72/1.90	43857	165

the previous solution. Such a little difference in power, together with a slightly larger investment cost, results in lower net present value (i.e. 140560 € against 148218 €). Despite the new solution being apparently less promising than the solution previously obtained, it is definitely more meaningful from a mathematical point of view due to the reduced values of feasibility tolerances.
The values of produced and consumed power by turbines and pumps, respectively, as well as the head-loss and pumping head within the installed devices are presented in Figure 7.18. With reference to daily pattern condition, the results of the optimization are shown in Table 7.10.

Table 7.10 Comparison of the found solutions for different values of feasibility tolerance in daily pattern condition.

	NPV [€]	N of PATs [−]	N of PRVs [−]	N of Ps [−]	Av. produced/spent power [kW]	Investment cost [€]	Water saving [m^3/day]
Optimization New Tolerances	112275	4	7	6	7.90/3.20	53673	159
Optimization Old Tolerances	121072	5	6	7	8.33/2.4	56547	162

According to Table 7.10, the solution obtained by the use of new feasibility tolerances consists of the installation of 17 devices (i.e. 4 turbines, 7 valves and 6 pumps), determining a net average power of 4.7 kW and a water saving equal to 159 m^3 per day. As previously highlighted, despite the energy and water savings being smaller than the solution achieved with higher tolerances, thus the solution apparently being less valuable, the new results are definitely more reasonable and meaningful. The new location of the installed devices is shown in Figure 7.20.

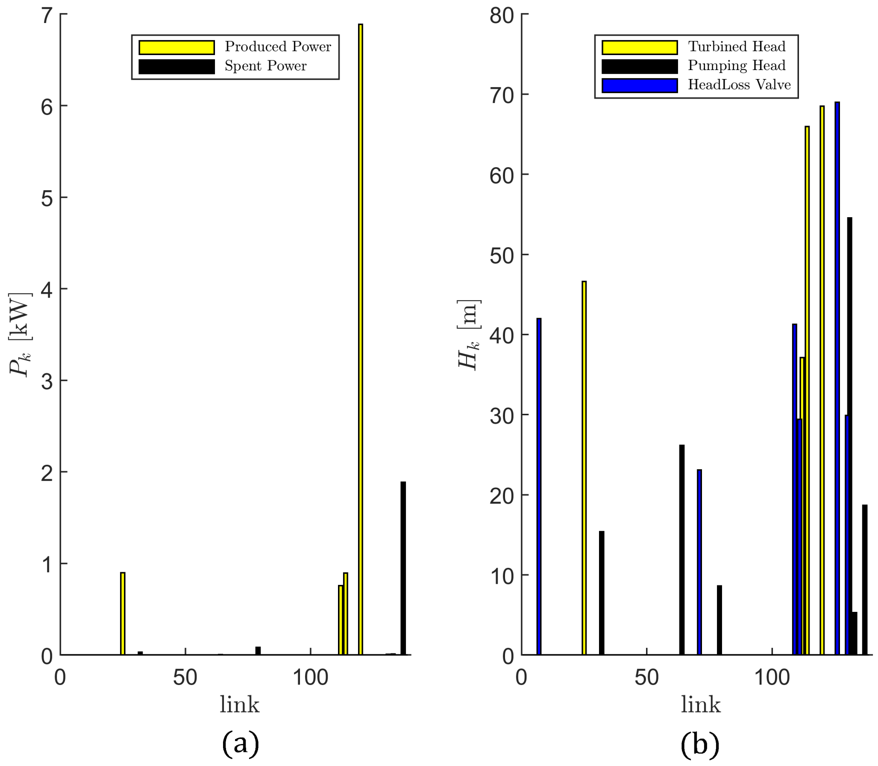

Fig. 7.18 Produced/consumed power (a) and head-loss/pumping head (b) according to the optimization of turbines, valves and pumps with new values of feasibility tolerance in daily average condition.

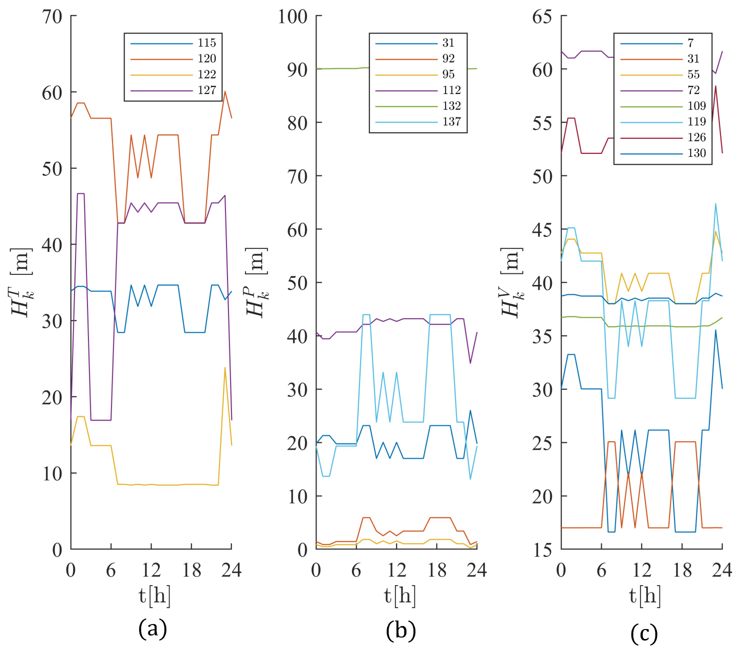

Fig. 7.21 Daily trend of turbined heads (a), pumping heads (b) and head-loss within the valves (c) according to the new feasibility tolerances in daily pattern condition.

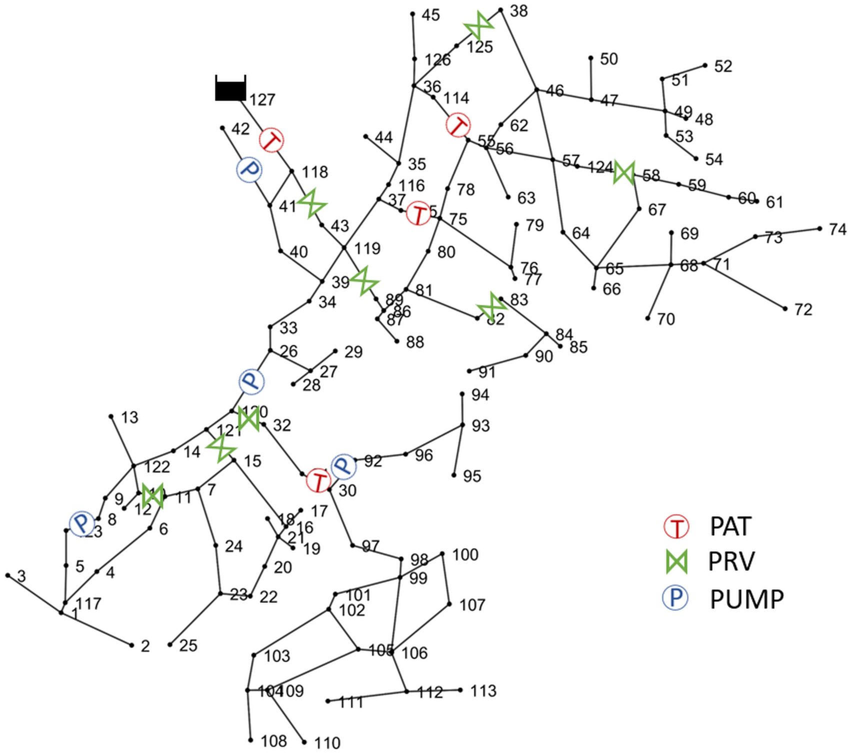

Fig. 7.19 Location of the installed turbines, valves and pumps within the case study network according to the optimization performed by new values of feasibility tolerances in daily average condition.

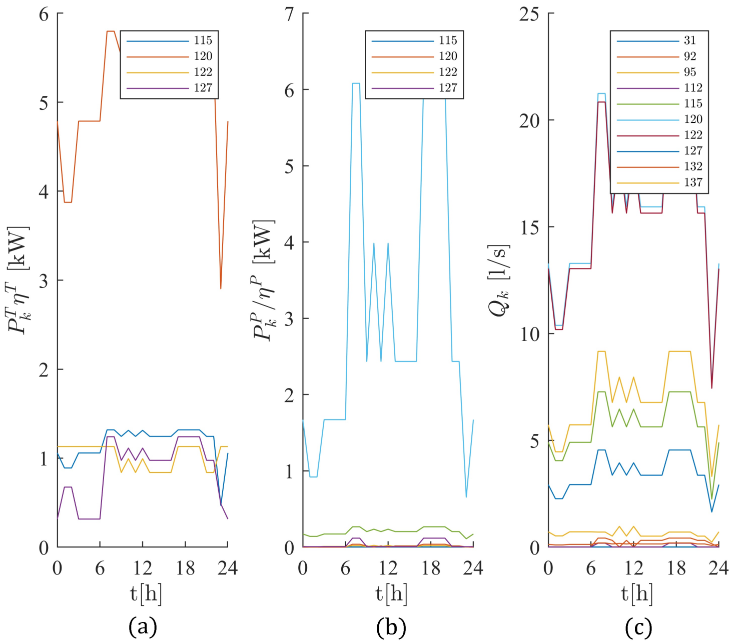

Fig. 7.22 Daily trend of produced power (a), consumed power (b) and discharge (c) according to the new feasibility tolerances in daily pattern condition.

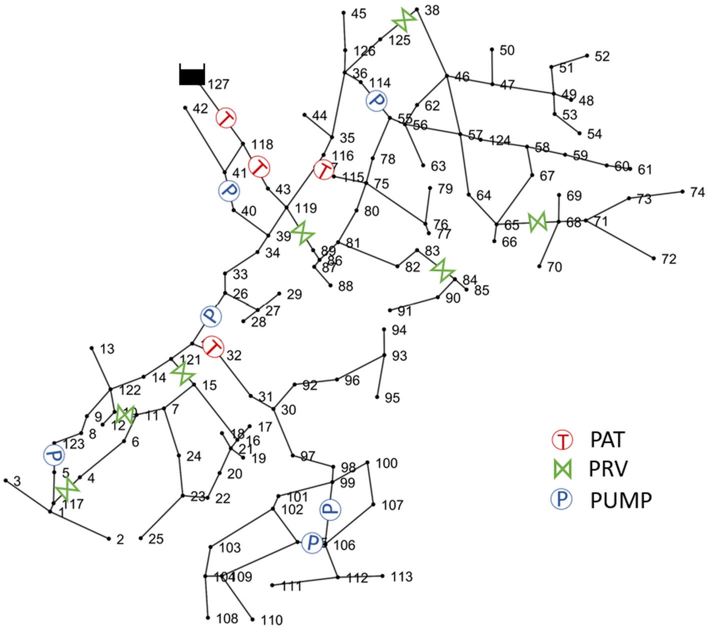

Fig. 7.20 Location of the installed turbines, valves and pumps within the case study network according to the optimization performed by new values of feasibility tolerances in daily pattern condition.

Finally the daily trend of the solution found in daily pattern condition is presented in Figure 7.21 and 7.22.

7.6 Comparison between cost models

As in the previous chapters, a comparison with different cost models has been carried out. In particular, the cost model presented by Novara et al. (2019) [97, 57] (see Equation (5.25)) is employed to assess the total cost of PATs and pumps, while the model obtained by Garcia et al. (2019) (see Figure 6.7) [57] has been used to evaluate the total costs of the PRVs.

The comparison between cost models in daily average condition is shown in Table 7.11, where cost model 1 refers to the cost model employed so far, while cost model 2 refers to the more recent cost models in literature [97, 57]. With reference to the results in Table 7.11, despite the total number of installed devices being smaller (i.e. 14 against 17), the use of more recent cost models [97, 57] leads to higher investment cost. The comparison in terms of device installation is presented in Figure 7.23. According to Figure 7.23, installing turbines where the pressure is high and pumping where the energy required is contained do not seem to reward the higher costs of both turbines

Table 7.11 Comparison of the found solutions for different cost models in daily average condition.

	NPV [€]	N of PATs [−]	N of PRVs [−]	N of Ps [−]	Av. produced/ spent power [kW]	Investment cost [€]	Water saving [m^3/day]
cost model 1	140560	4	7	6	9.43/2.02	52670	169
cost model 2	106629	2	8	4	7.80/2.55	66705	163

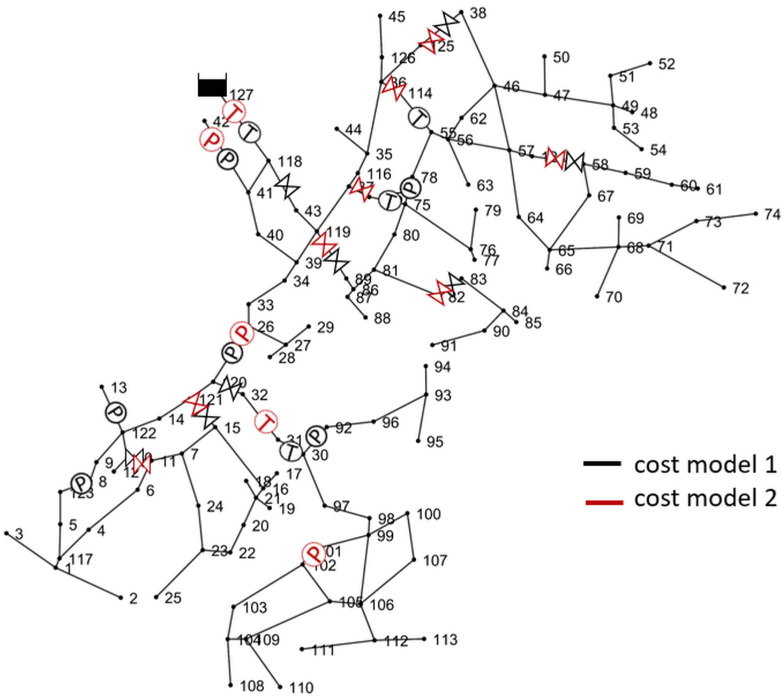

Fig. 7.23 Installation of the devices according to cost model 1 (in black) and cost model 2 (in red), in daily average condition.

and pumps in cost model 2. Indeed, the number of installed turbines and pumps is significantly reduced and limited to the links where the installation of such devices is really worth it. Nevertheless, despite such a different number of installed devices, the locations are quite similar between the two cost models, as shown in Figure 7.23. However, with reference to Table 7.11, the water saving is approximately the same, while the produced power according to the cost model 2 is smaller due to the smaller number of installed turbines.

The same comparison in daily pattern condition is presented in Table 7.12.

Table 7.12 Comparison of the found solutions for different cost models in daily pattern condition.

	NPV [€]	N of PATs [−]	N of PRVs [−]	N of Ps [−]	Av. produced/ spent power [kW]	Investment cost [€]	Water saving [m^3/day]
cost model 1	112275	4	7	6	7.90/3.20	53673	159
cost model 2	72063	3	9	6	6.70/3.08	90705	159

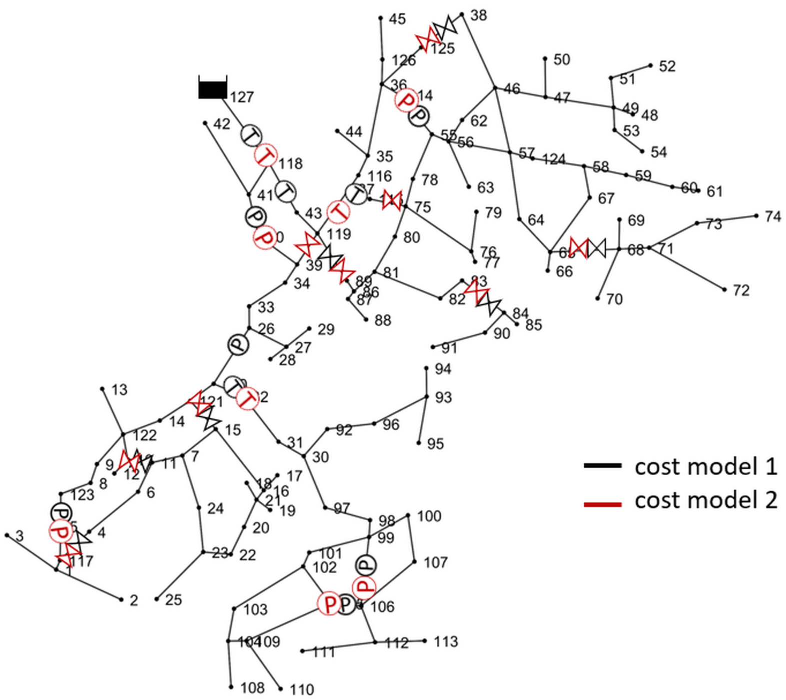

Fig. 7.24 Devices installation according to cost model 1 (in black) and cost model 2 (in red), in daily pattern condition.

With reference to Table 7.12, despite the number of installed devices being the same according to both the cost models, the cost model 2 determine a far larger investment cost. The water saving and the spent power is equal in both the cost models (i.e, 159 m^3 per day and around 3 kW, respectively), whereas the produced power is slightly smaller in cost model 2 (i.e, 6.70 kW against 7.90 kW) owing to the installation of one turbine less. On the whole, according to Figure 7.24, the position of the installed devices is approximately the same.

7.7 Final remarks

In this chapter the optimal installation of hydraulic devices within a real water distribution network has been progressively investigated. The model developed in the chapter 6 for the optimal installation of turbines and valves has been initially adapted for the search of turbines and pumps within a larger water network in both daily average and variable demand condition. Then, as soon as the introduction of pressure reducing valves within the same mathematical model has been attempted, the optimization solver failed to find any solution, due to the hard computational complexity affecting the problem. New mathematical formulations of the objective function and constraints have been therefore proposed in order to develop a more robust mathematical model enhancing the convergence of the optimization problem. According to the results, the installation of valves allows to achieve promising savings with a lower requirement of turbines and pumps, hence reducing the need of maintenance works and ensuring a more resilient hydraulic system. However, the pressure values are far above the minimum requirements and this result has been also proven by maximizing the only saving due to the reduction of water leakages. In addition, the newly proposed mathematical model has been improved so much in terms of both computational effort and practical convergence, that it has made possible to implement the optimization procedure also with more reasonable values of feasibility tolerance, reducing the error in the hydraulic modelling of the network. Finally, the solutions obtained by using different cost models in literature have been compared, showing high difference in terms of investment cost, thus of NPV, but quite comparable savings and total number of installed devices. Nevertheless, it is worth considering that, in order to be suitable for a sustainable urban water management, such an optimal solution should also account for further multiple aspects, such as the real price of energy, repair and maintenance works, which are not taken into account in this study.

It is also worth pointing out that the aim of this part of work is not to assess the improvement in terms of energy efficiency with respect to the water network in the reality, but rather the employment of an increased size network to test the robustness of the developed optimization procedure. As a matter of fact, it is not straightforward to make a comparison with the actual configuration of the network due to several reasons. First of all, the real network consists of around 4 PRVs, as well as a high number of water tank (around 11) about whose operation there is not detailed information available. Therefore, the water tanks have not been modeled in this study, but rather the installation of turbines has been introduced in order to exploit the excess pressure

with the aim to save water and also produce energy. Moreover, as already explained in the first part of this chapter, the real amount of water that is leaked within the whole network is not known and in this study the water leakage has been assessed calibrating both the emitter coefficients and pressure exponent in order to account the total leaked volume as the 20% of the daily volume supplied by the reservoir, in the scenario without any installed devices. For this reason, it has not been possible to compare the reduction of water leakage with respect to the amount of water leaked in the reality, but rather the effectiveness of the found installation has been evaluated comparing the leaked water after the pressure control strategy with the 20% leakage of the starting scenario and the reduction has been assessed as 11%.
Beyond the development of a new robust mathematical model for the location of general devices within any water distribution network, the strength of this work also results from new formulation of mathematical constraints requiring less computational effort, which could find application also in more general hydraulic problems.

List of Symbols

β	Exponent in the relation between leakage and pressure
γ	Specific weight of water
$\delta(t)$	Demand coefficient
$\hat{\delta}$	Average demand coefficient
Δt_d	Duration of the time steps with the same demand coefficient
ϵ_H	Coefficient in the evaluation of tol_k^H
ϵ_Q	Coefficient in the evaluation of tol_i^Q
ζ_k	Binary variable modeling the versus of the flow within the k-th pipe
η^P	Efficiency of pump
η^T	Efficiency of turbine
θ	Index for demand step
ς	Number of reservoirs
c	Coefficient for the evaluation of f_i
c_e	Energy unit selling price
c_{inst}	Installation cost of turbine
c_k^P	Total cost of pump
c_k^P	Dependent variable total cost of pump
c_k^T	Total cost of turbine
C_k^T	Dependent variable total cost of turbine
c_k^V	Total cost of valve

C_k^V	Dependent variable total cost of valve
c_P,c_Z	Coefficients for the evaluation of the turbine and valve total cost
c_w	Cost of water
C_k	Roughness coefficient of the k-th pipe
C_y^{in}	Cash inflow at the y-th year
C_y^{out}	Cash outflow at the y-th year
D_k	Diameter of the k-th pipe
$E_y^{p,T}$	Energy production during the y-th year
$E_y^{p,P}$	Energy consumption during the y-th year
f_i	Leakage coefficient
H_i	Head at the i-th node
H_i^0	Head at the i-th node without pressure control
H_k^P	Pumping head in the k-th pipe
$\overline{H_k^P}$	Daily average pumping head in the k-th pipe
$H_{k\ max}^P$	Maximum pumping head in the k-th pipe
$\overline{H_k^P}_{min}$	Minimum average pumping head within the pump in the k-th pipe
$\overline{H_{kmin}}$	Minimum average head-loss within the device in the k-th pipe
H_k^{P+}	Positive component of the pumping head in the k-th pipe
H_k^{P-}	Negative component of the pumping head in the k-th pipe
$\overline{(H_k^{P+} + H_k^{P-})}$	Daily average total pumping head in the k-th pipe
H_k^T	Head-loss within the turbine in the k-th pipe
H_k^{T+}	Positive component of the head-loss within the turbine in the k-th pipe
H_k^{T-}	Negative component of the head-loss within the turbine in the k-th pipe
H_k^V	Head-loss within the valve in the k-th pipe
H_k^{V+}	Positive component of the head-loss within the valve in the k-th pipe
H_k^{V-}	Negative component of the head-loss within the valve in the k-th pipe

H_{kmax}	Upper bound of H_k^T and H_k^V
i, j	Indices for nodes
I_k^P	Binary variable representing the presence of a pump within the k-th pipe
I_k^T	Binary variable representing the presence of a turbine within the k-th pipe
I_k^V	Binary variable representing the presence of a valve within the k-th pipe
k	Index for pipes
K_i	Number of pipes approaching the i-th node
l	Number of pipes of the network
K	Positive integer parameter
$L_{i,j}$	Length of pipe connecting the i-th and j-th nodes
n	Number of nodes of the network
n_d	Number of ranges in the daily pattern of demand coefficients
NPV	Net present value
p_{max}	Maximum allowable pressure
p_{min}	Minimum allowable pressure
P_k^P	Hydraulic power of the pump in the k-th pipe
P_k^T	Hydraulic power of the turbine in the k-th pipe
P_{max}^P	Maximum power spent by the pump in the k-th pipe
P_{max}^T	Maximum power produced by turbine in the k-th pipe
$\overline{P_k^T}$	Daily average hydraulic power produced by the turbine in the k-th pipe
$\overline{P_{min}}$	Minimum allowable power producible by the turbine
q_k^+	Positive component of the discharge flowing in the k-th pipe
q_k^-	Negative component of the discharge flowing in the k-th pipe
$(q_k^+ + q_k^-)^{in}$	Total discharge flowing through the k-th pipe into the i-th node
$(q_k^+ + q_k^-)^{out}$	Total discharge flowing through the k-th pipe into the i-th node
$q_i^d(t)$	End-user demand at the i-th node

$\overline{q_i^d}$	Average end-user demand at the i-th node
q_r	Discharge flowing into or out of the reservoir
Q_{max}	Upper bound of total discharge Q_k
Q_l^0	Total leaked discharge without pressure control
Q_l^S	Total leaked discharge with pressure control strategy
r	Discount rate
r_k	Resistance term of the k-th pipe calculated by Hazen-Williams formula
t	Time
tol_i^Q	Feasibility tolerance within continuity equation
tol_k^H	Feasibility tolerance within momentum balance equation
y	Index for years
Y	Number of years
W_y^s	Water saving during the y-th year
z_i	Elevation of the i-th node

Chapter 8

Newly proposed supply solutions

8.1 Introduction

The quantification of the energy embedded in water streams is crucial for the assessment of the efficiency of pressurized systems [9] and the evaluation of the potential of energy savings [43]. Gómez et al. (2015) [63] and Cabrera et al. (2015) [14] defined some energy performance indicators providing an assessment of the whole energy efficiency, with reference to two scenarios of supplying a water distribution network. The first scenario consisted of an indirect pumping towards an upstream reservoir which supplied a downstream water distribution network with a constant head, whereas the second scenario presented a direct supply of the water network by an upstream pumping system. The authors [14, 63] demonstrated that direct pumping is, by far, more convenient from both energetic and economic points of view. Nevertheless, the authors [14, 63] did not consider any energy recovery in the indirect pumping scheme, where a hydropower production plant could increase the energy efficiency of the whole system by converting the excess pressure in energy, instead of dissipating this by a pressure reducing valve. Moreover, on one hand an indirect pumping towards an upstream reservoir can be considered a more resilient solution, guaranteeing the supply of the downstream network even in case of power failure. On the other hand, an upstream reservoir could have a significant environmental impact depending on its location and its size.

This chapter is a presentation of the study made by Morani et al. (2018), entitled "A Comparison of Energy Recovery by PATs against Direct Variable Speed Pumping in Water Distribution Networks" [89]. In this work, a real network has been assesses as case study. This network is supplied by an upstream reservoir, and a part of the excess head should be dissipated within a valve, to reduce the pressure level within the network and contain leakage. Two different solutions to increase the energy efficiency of the network will be investigated. In the first solution, a PAT will be located in place of a pressure reducing valve in order to both reduce pressure and recover energy. In the second supply scheme, the downstream network will be supplied by a pumping directly from the source, bypassing the reservoir as in [14, 63], with smaller pumping head. The two scenarios will be compared in terms of required energy. Furthermore, the boundary condition of the network, that is, the source location and elevation, will be varied in order to compare the feasibility and the benefit of each of the two scenarios under differing design and operating conditions. The assessment of the energy efficiency of the two different technical solution will be performed by a new energy index and two literature efficiency indices [14, 63].

8.2 Methodology

8.2.1 Study Area

The case study is the water supply network of a small village in Ireland, located in County Laois, about 100 km from the capital city (Dublin). A reservoir is located at 147 m a.s.l. and supplied by a source placed at 99 m a.s.l. The layout of the network is showed in Figure 8.1. The studied network consists of 55 nodes and 58 links. For each link, information about roughness, diameter, and length was available. Each node was characterized by an elevation and a demand coefficient, namely the ratio between the demand of the node and the demand of the whole network. Hourly values of flow rate for the year 2016, recorded at the link 8–10 (8.1) were available. The time series of the year-averaged hourly values of discharge ($Q(t)$) were calculated, resulting in the pattern in Figure 8.2. The average daily value of discharge $\bar{Q}$ resulted as 4.35 l/s. According to Figure 8.2, the minimum value of discharge occurs during the night and is higher than 3 l/s, that is, about the 70% of the average discharge. As a result, a significant amount of water is leaked at nigh-time, thus a pressure control strategy is required to increase the efficiency of the whole system. In this study, a renovation of the pipeline, which may be effective to further decrease the amount of leakage, is not investigated, but rather the only strategy considered consists in the containment of water pressure.

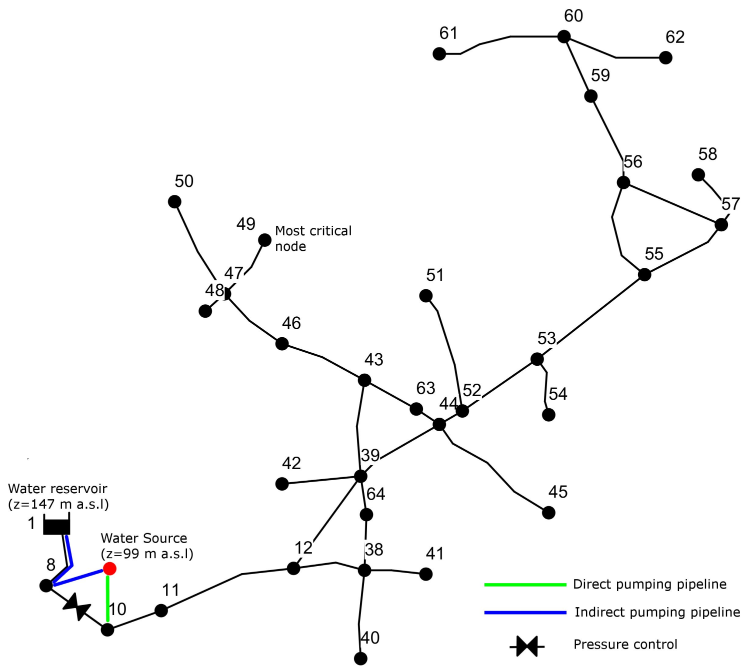

Fig. 8.1 Layout of the hydraulic network in the studied area

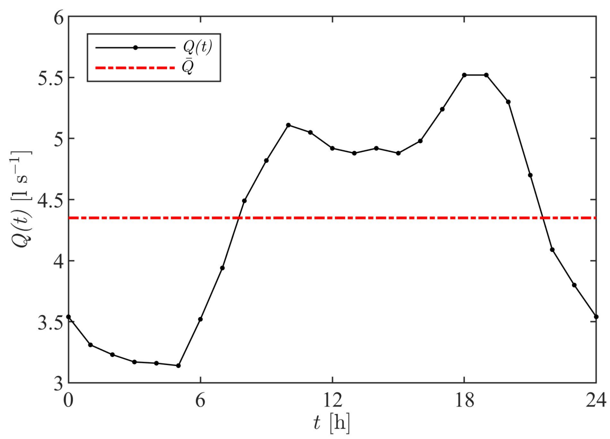

Fig. 8.2 Average hourly values of discharge of the year 2016 at the link 8–10.

8.2.2 Direct and Indirect Pumping

The indirect pumping scheme is presented in Figure 8.3 and consisted of a hydraulic configuration characterized by a pump supplying a reservoir. The supplied population is located in the downstream area and supplied by a network branching from the reservoir.

In the indirect pumping scenario, a surplus of head is available due to changes in

elevation. This surplus head can be either dissipated within a valve or exploited to produce energy by the employment of any energy production device (EPD) located downstream of the reservoir. In this study, a PAT has been chosen as EPD for the reasons highlighted in section 2.3.1.
With reference to Figure 8.3, ΔH_{ind} and ΔH_{PAT} represent the pumping head in indirect supply scenario and the head-loss within the PAT, respectively.

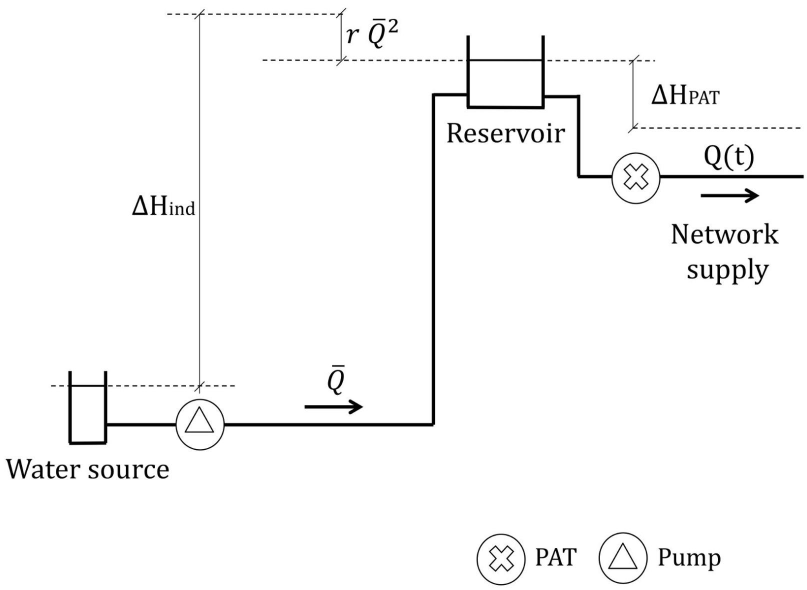

Fig. 8.3 Scheme of indirect pumping with energy recovery.

Figure 8.4 represents direct pumping scheme characterized by a pumping performed directly from the source to the distribution network, bypassing the upper reservoir and benefiting from a smaller pressure head. The pump in Figure 8.4 will be designed to obtain the best possible efficiency and continuously regulated according to the request of the network. In Figure 8.4 ΔH_{dir} represents the pumping head of direct supply scenario.
The energy efficiency of the two cases will be assessed in the following sections, the boundary conditions of the network, that is, the location and elevation of the source,

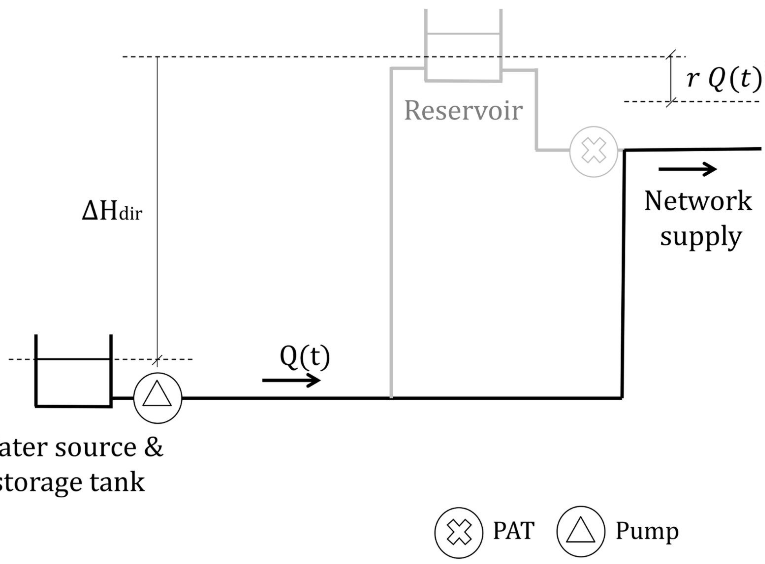

Fig. 8.4 Scheme of pumping supplying a water distribution network directly from a water source.

will be arbitrarily changed to analyze different conditions and compare the feasibility and the benefit of each of the two scenarios in different cases.

8.2.3 The Variable Operating Strategy (VOS) in HR mode

Variable Operating Strategy (VOS) is a method that allows for the geometry selection of an EPD for given flow-head distribution pattern and network backpressure, ensuring quite high efficiency values. Such a procedure consists of the following steps:

1. A measured pattern of flow rate and pressure head is assigned and available head is defined according to the required back-pressure (BP);
2. A PAT type is considered (e.g., centrifugal, axial);
3. A wide set of PAT characteristic curves is considered in the PAT operating region, by changing the number of stages and impeller diameter;

4. For each PAT, the overall plant efficiency (η_P) is calculated as follows:

$$\eta_P = \frac{\sum_{i=1}^{n_p} \Delta H_i^{PAT}\ Q_i^{PAT}\ \eta_i^{PAT}\ \Delta t_i}{\Delta H_i\ Q_i\ \Delta t_i} \tag{8.1}$$

   where n_p are the PAT operating points, ΔH_i^{PAT} and Q_i^{PAT} represent the head drop and the discharge delivered by the PAT, respectively. Moreover, η_i^{PAT} is the PAT efficiency, ΔH_i and Q_i are the available head drop and discharge. Finally, Δt_i is the time-interval discretization of discharge-head drop pattern. According to the formulation in Equation (8.1), the overall efficiency represents the fraction of the energy producible by the power plant.

5. The PAT having the largest overall efficiency η_P can be considered the optimal design solution;

6. The near-optimal machine is selected from the market and its efficiency is further verified.

8.2.4 Pressure management and energy recovery

With reference to Figure 8.1, the network is provided with an upstream valve located along the pipe 8-10 in order to contain the pressure within the network. Instead of performing a pressure control strategy by a traditional regulation valve [20, 19], a PAT has been employed in order to convert the head drop in energy, increasing the efficiency and the sustainability of the whole system. The hydropower plant consists of a series-parallel hydraulic circuit, as shown in Figure 8.5.

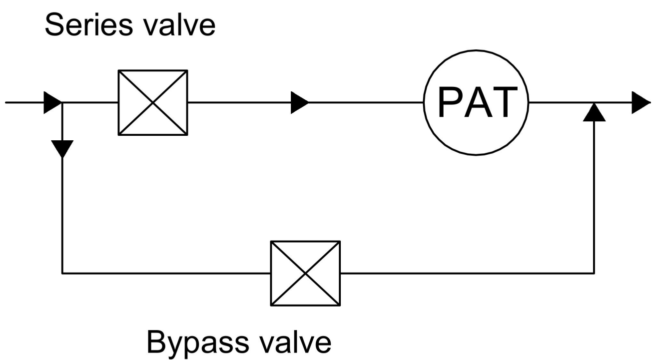

Fig. 8.5 Scheme of the series-parallel hydraulic circuit [20, 19].

With regard to the regulation of the PAT, the hydraulic regulation (HR mode) has been preferred over the electrical regulation (ER mode), which instead consists of an inverter that modifies the frequency of the device, thus the rotational speed. The HR mode has been selected for its better efficiency, as well as a lower cost of equipment and a shorter payback period [20, 19].
As shown in Figure 8.5, the hydraulic circuit consists of two parallel branches with a PAT and two valves. An illustration of PAT operating condition is presented in Figure 8.6.

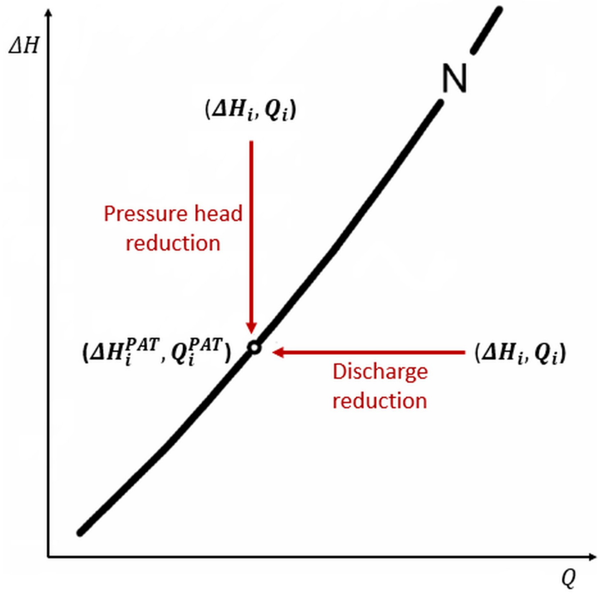

Fig. 8.6 PAT operating condition for hydraulic regulation (HR) mode [20, 19].

When the head is higher than the head-drop deliverable by the machine, the excess of pressure is dissipated by a series pressure reducing valve (PRV). Instead, when the discharge is larger, a bypass is opened to reduce the discharge flowing in the PAT, so that the PAT produces a head-drop equal to the available head.

8.3 Experimental investigation

8.3.1 Pump under variable speed

In water distribution networks, the water demand is time-dependent; thus, pumping in a direct scheme should be performed by a machine working under variable speed. As reference machine, a centrifugal multistage end-section pump HMU50-2/2 (Caprari

S.p.A., Modena, Italy) has been chosen and tested in the Hydro Energy Laboratory (HELab) of the University of Naples "Federico II". HELab was specifically realized to perform the test included in the new standard EN16480/2016, according to the specification of ISO 9906. An asynchronous motor has been coupled to the pump and powered by a variable frequency driver to convert the 50 Hz input frequency to the desired value, f, in order to set the rotational speed of the pump. Two pressure transducers (0–10 bar and 1–1.6 bar, respectively; ±0.1% accuracy) were used to measure the head, ΔH, for each discharge value, Q, which has been measured by a magnetic flow meter (0–15 L/s, ±0.1 % accuracy). The input power, P, has been measured by a wattmeter (0–60 kW, ±0.3 % accuracy) whereas the optical speedometer (0–380 rad/s ± 0.1 % accuracy) has been used to measure the rotational speed of the pump, N.

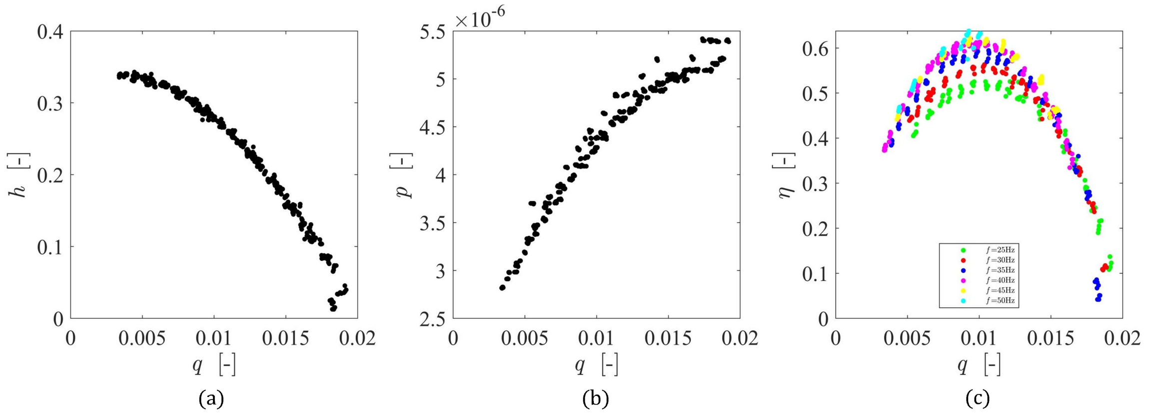

Fig. 8.7 Average hourly values of discharge of the year 2016 at the link 8–10.

Figure 8.7 shows the dimensionless head (h), power (p), and efficiency (η) curve of the pump, as being:

$$q = \frac{Q}{ND^3},\ h = \frac{g\Delta H}{N^2D^2},\ p = \frac{P}{\rho N^3 D^5} \tag{8.2}$$

where g is the gravity acceleration, equal to 9.806 m/s^2; ρ the density of the water, about 1000 kg/m^3; and D the diameter of the pump. Finally, the efficiency of the whole pumping system (i.e. pump with motor), η, can be calculated as:

$$\eta = \frac{qh}{p} \tag{8.3}$$

With reference to Figure 8.7, unlike the dimensionless head curve $h = h(q)$, a larger dispersion occurs for the power experimental points ($p = p(q)$). In fact, the efficiency curve, $\eta = \eta(q)$, is different for each frequency value (f), as shown in Figure 8.7 (c). For each frequency f, the value of efficiency at the best efficiency point (BEP), η_{BEP}, has been found.
Figure 8.8 shows the trend of η_{BEP} against the frequency f. A best-fit polynomial approximation of second degree has been used to model the curve $\eta_{BEP}(f)$, as following:

$$\eta_{BEP} = af^2 + bf + c \tag{8.4}$$

where the values of a, b and c are presented in Figure 8.8.

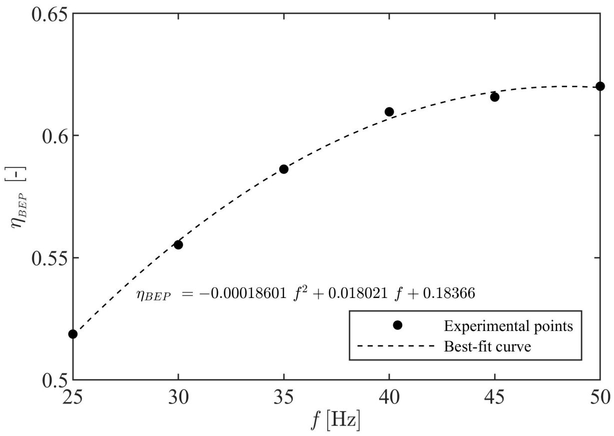

Fig. 8.8 Best-fit polynomial curve of frequency against best efficiency point (f vs η_{BEP}).

Since $\eta(q, f)$ is a function of both dimensionless discharge (q) and frequency (f) whereas η_{BEP} depends on the only frequency (f), the ratio between $\eta(q, f)$ and η_{BEP}, namely e, will be independent on the frequency, as shown in Figure 8.9. Furthermore, for an asynchronous motor, the rotating speed, N, can be expressed as:

$$N = \frac{2\pi f}{pp} \tag{8.5}$$

being pp the number of pole pairs for each phase.
Thus, once the impeller diameter (D) and the frequency (f) are known, for each value of discharge (Q) it is possible to calculate the dimensionless value (q) by Equation (8.2). Then, the dimensionless head (h) can be obtained by the polynomial best fit curve

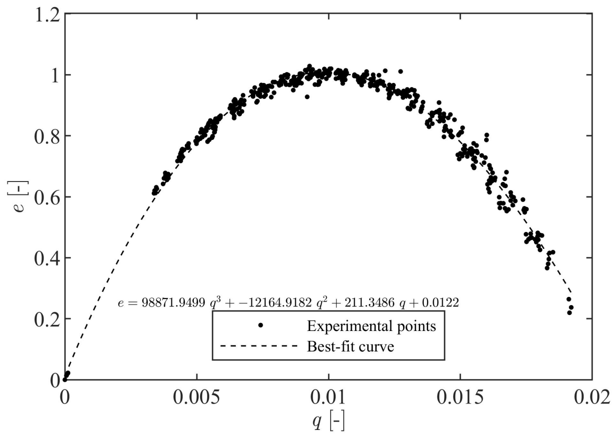

Fig. 8.9 Experimental measurements and best fit line of e against the dimensionless discharge q.

approximating the plot of h against q in Figure 8.2 (a), thus ΔH can be calculated by Equation (8.2). Then, e, η_{BEP} and η can be obtained by Equations (8.3) and (8.4). Therefore, the absorbed power can be calculated as:

$$P = \frac{P_{hydr}}{\eta(q, f)} \tag{8.6}$$

being P_{hydr} the hydraulic power, expressed in Equation (8.7).

$$P_{hydr} = \gamma\ \Delta H\ Q \tag{8.7}$$

and γ the specific weight of water, equal to 9806 N/m^3.

For the tested pump, with a D = 170 mm impeller, at the maximum frequency f = 50 Hz, the discharge, head, and efficiency at the BEP resulted in: Q_{BEP}= 14 l/s, ΔH_{BEP} = 81.9 m, and η_{BEP} = 0.63. If the methodology described in EN16480/2016 is applied, then a minimum efficiency index (MEI) equal to 0.6 can be assigned to the pump.

The same machine was tested in turbine mode (i.e. with reversed flow), in the laboratory of Caprari SPA, Modena (IT). The machine was tested without the generator, and the mechanical power was measured at the PAT shaft by a torque meter (0–1000 Nm, 0–380 rad/s, ±0.2 % accuracy). Discharge and pressure were measured by similar flow meter and pressure transducers.

In Figure 8.10, the resulting head and produced power are plotted against the discharge in terms of dimensionless parameters.

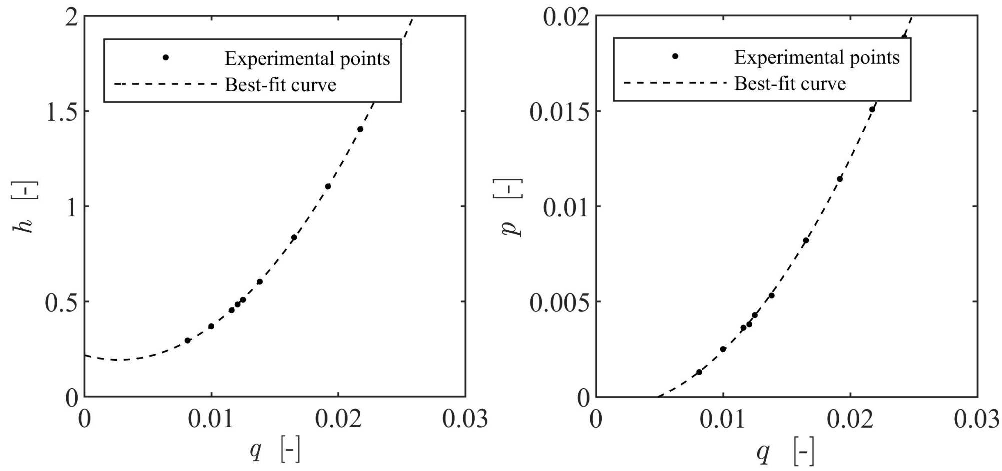

Fig. 8.10 Dimensionless discharge (q) against dimensionless head (h) and power (p) of pump HMU50-2/2 in reverse mode.

8.4 Application to the case study network

8.4.1 Indirect Pumping

The indirect pumping scenario refers to a pump supplying a reservoir from a water source. The pipe linking the source and the reservoir is 1069 m long with a 200 mm diameter and a 0.26 mm roughness. The pumping head, namely ΔH_{ind}, is the sum of the difference in elevation between the reservoir and the source and the head-loss within the pipe. The discharge at BEP (Q_{BEP}) is set equal to the annual daily average discharge, i.e. $\bar{Q}$.

A Darcy–Weisbach formula was used to calculate the head-loss within the pipe, which is expected to be very low, as the approaching pipe results to be oversized.

As reference pump, an end suction own bearing (ESOB) pump with a rotational speed of 2900 rpm has been chosen.

In order to obtain the value of η_{BEP}, the minimum efficiency of the standard pumps, suggested by EN 16480/2016 and presented in Equation (8.8), has been referred to.

$$\begin{aligned}\eta_{BEP} = &- 11.48(\ln{(n_S)})^2 - 0,85(\ln{(n_S)})^2 - 0,38\ln{(n_S)}\ln{(Q_{BEP})} + \\ &+ 88,59\ln{(n_S)} + 13,46\ln{(Q_{BEP})} - C\end{aligned} \tag{8.8}$$

Q_{BEP} being the flow at the BEP condition expressed in m^3/h; C a constant depending both on the minimum efficiency index (MEI) and the model of pump. If the MEI is fixed equal to 0.6, as the one of the tested pump (HMU50-2/2), for the chosen ESOB pump C results as 128.12. Finally, n_S (expressed in $\min^1$) is following presented:

$$n_S = N\,\frac{\sqrt{Q_{BEP}}}{H_{BEP}^{0.75}} \tag{8.9}$$

wherein N is the rotational speed of the pump and H_{BEP} is the pumping head at the BEP condition, set equal to ΔH_{ind}. Then, the absorbed energy E_{ind} can be expressed by Equation .

$$E_{ind} = \frac{E_{hydr,ind}}{\eta_{BEP}\;\eta_{MOT}} = T\frac{\gamma\;\Delta H_{ind}\;Q}{\eta_{BEP}\;\eta_{MOT}} \tag{8.10}$$

where T is the reference time period, that is, one year. In Equation (8.10), η_{MOT} is the efficiency of the motor belonging to the IE3 efficiency class, suggested by EC Regulation 640/2009.

Such procedure has been also implemented by varying the number of stages between one and fifteen. The chosen number of stages is the one allowing the maximum efficiency, which results as 7. The resulting required energy E_{ind} has been accounted as 32420 kWh/year.

8.4.2 Pressure management

With reference to Figure 8.1, the head downstream of the valve, H_{req}, and thus drop within the valve, was set for each hour in order to guarantee a minimum value of 10 m in the most critical downstream node (i.e. node 49) and reducing the pressure in the whole network. The hydraulic simulator EPANET has been used to estimate available head versus flow variation during the day. Then, the valve was replaced with a PAT to convert the drop in energy. The resulting time series (in hours) of the flow (Q(t)) and the head-loss within the PAT system in link 8–10 (ΔH_{PAT}) for the average day are presented in Figure 8.11, along with the $(\Delta H, Q(t))$ pattern. Thus, the variable

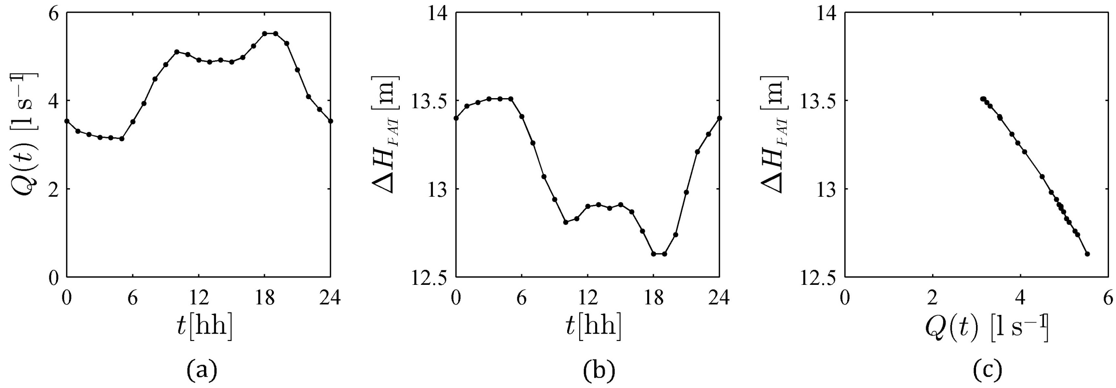

Fig. 8.11 Time series of flow (a) and head-loss (b) through the PAT system; pattern $(\Delta H, Q(t))$ (c).

operating strategy [20, 19] was performed in order to find the optimal PAT, in terms of impeller diameter and rotational speed, maximizing the produced energy E_{PAT} (Equation (8.11).

$$E_{PAT} = \int_T \gamma \; Q \; \Delta H_{PAT} \; \eta \; dt \tag{8.11}$$

To simulate similar machines having different diameter and rotational speed, the affinity laws were used and the experimental curves in Figure 8.10 have been used as reference curves.
The MATLAB optimization toolbox [83] was used to perform this optimization [13, 12]. In particular, the diameter was varied between 80 mm and 500 mm, whereas the values of rotational speed considered were 1025 rpm (three couples of poles), 1550 rpm (two couples of poles), and 3100 rpm (one couple of poles).
According to the result of the optimization, the rotational speed and the diameter of the optimal machine resulted in 155 mm and 1025 rpm, respectively. Then, for each hour, the power produced by the PAT was obtained and this energy was further multiplied by the efficiency of the generator (EI3 class), as suggested by EC Regulation 640/2009. With reference to the chosen PAT, the produced energy has been accounted as 2234 kWh/year.

8.4.3 Direct Pumping

In the direct pumping scenario, the upper reservoir is bypassed and the water is directly pumped from the source to the network (node 10 of Figure 8.1).

The length of the approaching pipe is equal to 710 m and the diameter is 200 mm. The roughness of the pipe has been set as 0.26 mm, comparable to the values of the whole network. A Darcy–Weisbach formula has been used to calculate the head-loss within the pipe. The required head was set equal to the head downstream of the valve in the indirect pumping scenario, that is, H_{req}. Thus, a minimum 10 m pressure in the most critical node of the whole network is guaranteed also in this scenario. The pumping discharge in the direct scenario is variable according to Figure 8.2. The pumping head (ΔH_{dir}) results to be variable during the day as well, depending on the required head and the head-loss. Given the variable pattern of pumping discharge and head, the pump should be equipped with a variable frequency driver to modify the rotational speed according to the network requests. The design of the pump has been performed by an optimization routine [13, 12] in order to find the values of the number of stages (varied between one and fifteen, as in the indirect pumping scenario), the diameter and the hourly rotational speed, both minimizing the daily energy usage and ensuring the required pressure head for each hour. The affinity law has been applied to the characteristic curves of the reference pump in Figure 8.7. Then, the objective function of the optimization is the energy absorbed by the pump, evaluated as:

$$E_{dir} = \int_T \frac{\gamma\ Q\ \Delta H_{dir}}{\eta} dt \tag{8.12}$$

According to the optimization for the analyzed case study, the optimal diameter has been accounted as 116 mm, the rotational speed varying during the day from 2679 rpm to 3000 rpm, and the number of stages as 2. The total amount of energy has been resulted in 22327 kWh/year.

8.5 Results

To analyze the results and to compare the different scenarios, the following two indices have been introduced:

$$EI_1 = \frac{E_{ind} - E_{PAT} - E_{dir}}{E_{ind}} = \frac{\Delta E}{E_{ind}} \tag{8.13}$$

$$EI_2 = \frac{E_{ind} - E_{dir}}{E_{ind}} = \frac{\Delta E}{E_{ind}} \tag{8.14}$$

where $(E_{ind} - E_{PAT})$ represents the energy consumption of the indirect pumping scenario with energy recovery; E_{dir} represents the energy required in the direct pumping scenario; and E_{ind} is the energy consumption of the indirect pumping scenario if no energy recovery is performed. Thus, ΔE represents the difference in energy spent in both the scenarios. The index EI_1 measures the convenience of the direct pumping scenario when compared to the scenario with indirect pumping and energy recovery. Thus, if the index is positive, then the energy required to pump water directly to the network is lower than the energy required by the indirect scenario. The index EI_2 measures the convenience of a direct pumping over the indirect pumping scenario when the energy is not recovered by any EPD. It is worth underlining that in both the indices EI_1 and EI_2, the water saving due to the reduction of leakage is not taken into account, even though it can be a considerable value. However, since the pressure distribution along the network is equal for both scenarios, thus the contribution of water saving is equal both for indirect and direct pumping.
For the analyzed case study, EI_1 is equal to 0.24 and EI_2 is 0.31. This means that for the case study network, if water is directly pumped to the network, the amount of recovered energy is up to 31%. Thus, the direct pumping scenario is definitely more convenient than indirect pumping scenario, since the amount of energy that can be saved by a PAT is lower than the saving achieved by direct pumping. In fact, in the direct pumping scenario, the required daily energy is equal to 61 kWh/day, while the indirect pumping daily energy is equal to 89 kWh/day and 6 kWh/day can be recovered by the PAT. Moreover, the energy losses due to the efficiency of the two machines (indirect pump and PAT) also contribute to make the direct pumping scenario more convenient. In Table 8.1, the main figures of the two scenarios are reported.

Table 8.1 Main figures of the indirect and direct pumping scenarios for the analyzed case study.

Scenario	Pumping Head [m]	Energy [kWh/year]	Efficiency Index EI$_1$	Efficiency Index EI$_2$	Recovered Energy [kWh/year]
Indirect	48.14	32420	0.24	0.31	2234
Direct	34.88	22327			–

The analyzed conditions do not cover all the design solutions. Indeed, indirect pumping could be operated only during the night when the energy cost is cheaper. During the day, when the flow demand and the price of the energy are higher, water could be provided from the reservoir. The most convenient solution depends on multiple factors, such as the real price of energy, civil works, and the selling price of renewables. A deeper analysis should include a life cycle assessment [56] in order to also consider the environmental sustainability.

8.5.1 Energy Indices under Differing Boundary Conditions

For the sake of generality, some differing boundary conditions have been studied, by varying the pumping head of both scenarios, corresponding to different distances and elevations of the source from the network. For the indirect pumping scenario, different values of pumping head were assigned, namely $\Delta H_{ind} = 25$ m, $\Delta H_{ind} = 50$ m, and $\Delta H_{ind} = 100$ m.
Then, i_1 has been set between 0.5 and 1.5, i_1 being:

$$i_1 = \frac{\overline{\Delta H_{dir}}}{\Delta H_{ind}} \tag{8.15}$$

Indeed, even though the required head at the end of the pipeline in direct pumping is lower, $\overline{\Delta H_{dir}}$ can be larger than ΔH_{ind} due to the head-losses, that is, due to a smaller diameter pipe or a longer path. Thus, for each value of ΔH_{ind} and i_1, several values of the average pressure head in direct pumping scenario $\overline{\Delta H_{dir}}$ have been considered. Then, for each value of ΔH_{ind} and i_1, several values of head-loss in the approaching pipe in the direct pumping scenario have been considered, setting i_2 to 25%, 50%, and 75%, where i_2 is defined according to Equation (8.16). Thus, i_2 is the ratio between the head-loss produced by the average daily discharge, $\overline{Q}$, calculated by the Hazen–Williams formula, and ΔH_{ind}.

$$i_2 = \frac{J Ł}{\Delta H_{ind}} = \frac{\frac{10.67\ \overline{Q}^{1.852}\ L}{K^{1.852}\ D^{4.8704}}}{\Delta H_{ind}} = \frac{r\ \overline{Q}^{1.852}}{\Delta H_{ind}} \tag{8.16}$$

With reference to Equation (8.16), L and D represent the length and the diameter of the pipe linking the water source and the network, respectively; K is the roughness coefficient corresponding to a different material of the aforementioned pipe; and $\overline{Q}$ is the average daily demand of the network, equal to 4.35 l/s. The terms L, D, and K

were assembled in only one term, namely r. For each combination of ΔH_{ind}, i_1 and i_2, the amount of required energy in both scenarios has been evaluated and the two indices, EI_1 and EI_2, have been calculated.
Figure 8.12 shows the values of EI_1 and EI_2 when ΔH_{ind} is set to 25 m.
For each value of i_1, the small variability occuring for both indices depends on i_2. This means that the head-loss affects the energy efficiency of the system very slightly. Furthermore, where i_1 is equal to 1, that is, when $\overline{\Delta H_{dir}}$ is equal to ΔH_{ind}, EI_1 is negative, thus indirect pumping with energy recovery is more convenient and this saving amounts to about 5%. Instead, in the condition of no energy recovery, the most convenient scenario is direct pumping and the benefit amounts to around 8%. Furthermore, in the absence of energy recovery, direct pumping is the most convenient scenario until a value of $\overline{\Delta H_{dir}} = 1.09\ \Delta H_{ind}$. Instead, the convenience of pumping water directly to the network decreases if the energy recovery strategy is performed, being direct pumping the favorite scenario until a value of pressure head of approximately $\overline{\Delta H_{dir}} = 0.94\ \Delta H_{ind}$ is reached. Obviously, both indices increase as i_1 decreases; that is, the convenience of direct pumping increases as the direct pumping head $\overline{\Delta H_{dir}}$ decreases.

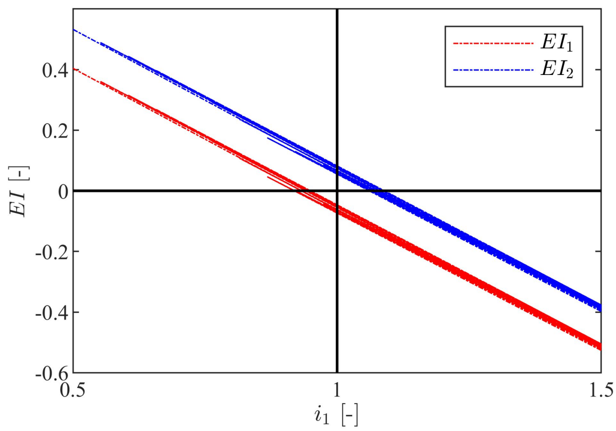

Fig. 8.12 Trend of efficiency indices for $\Delta H_{ind} = 25$ m with i_2 equal to 25%, 50%, and 75%, respectively.

Figure 8.13 shows that by increasing ΔH_{ind} to 50 m and 100 m, for i_1 equal to 1, the convenience of indirect pumping with energy recovery reduces to 2% for $\Delta H_{ind} = 50$ m and 0.5% for $\Delta H_{ind} = 100$ m. This reduction happens because the amount of energy that can be recovered by the PAT decreases with respect to the total energy required for the pumping. In the absence of energy recovery, direct pumping is still the most convenient scenario, even though such a convenience decreases to around

5% for $\Delta H_{ind} = 50$ m and 3% for $\Delta H_{ind} = 100$ m. In absence of energy recovery, the convenience of direct pumping scenario occurs up to $i_1 =$ 1.04 ($\Delta H_{ind} = 50$ m) and 1.02 ($\Delta H_{ind} = 100$ m). When energy recovery strategy is performed by a PAT, the indirect pumping is convenient for i_1 greater than 0.98 if $\Delta H_{ind} = 50$ m and greater than 0.99 when $\Delta H_{ind} = 100$ m. Such a behavior probably occurs because E_{PAT} is constant among the different conditions and its relevance decreases as ΔH_{ind} (and thus $\overline{\Delta H_{dir}}$, E_{ind}, and E_{dir}) increases. The convenience of direct pumping increases as i_1 decreases.

In Table 8.2, "saving" represents the percentage of energy saved by indirect pumping (if energy recovery is performed) and by direct pumping (in the absence of energy recovery) for i_1 equal to 1. Moreover, "direct scenario cutoff" represents the value of $\overline{\Delta H_{dir}}$ until which direct pumping is the most convenient scenario.

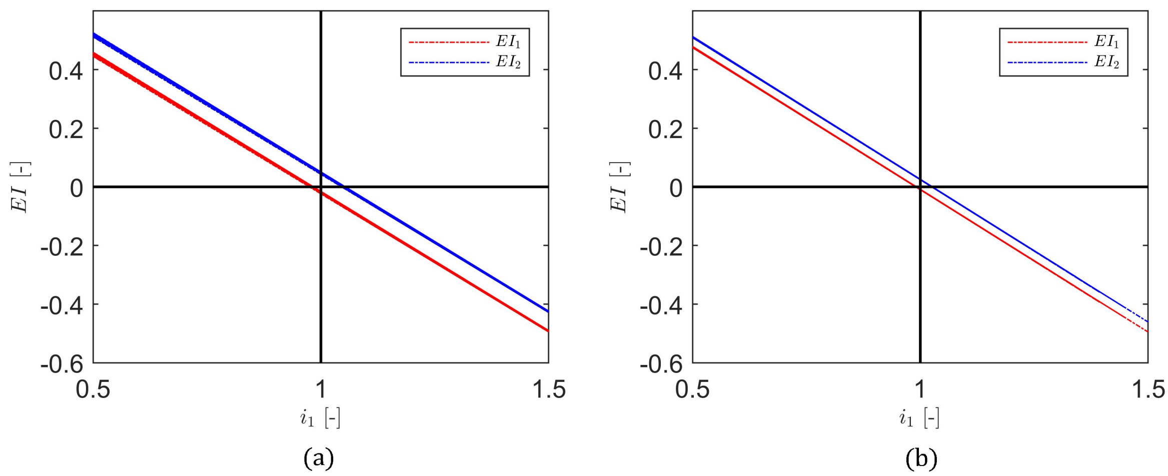

Fig. 8.13 Trend of efficiency indices for $\Delta H_{ind} = 50$ m (a) and $\Delta H_{ind} = 100$ m (b) with i_2 equal to 25%, 50%, and 75%, respectively.

Table 8.2 Main figures of the indirect and direct pumping scenarios.

	Energy Recovery		No Energy Recovery	
ΔH_{ind} $[m]$	Saving [%]	Direct Scenario Cutoff	Saving [%]	Direct Scenario Cutoff
25	5	0.94 ΔH_{ind}	8	1.09 ΔH_{ind}
50	2	0.98 ΔH_{ind}	5	1.04 ΔH_{ind}
100	0.5	0.99 ΔH_{ind}	3	1.02 ΔH_{ind}

8.5.2 Literature Energy Indices for Different Boundary Conditions

Gómez et al.(2015) [63] and Cabrera et al. (2015) [14] defined some efficiency indices of ideal (η_{ai}) and real (η_{ar}) systems. These indices are presented in Equations (8.17)-(8.18).

$$\eta_{ai} = \frac{E_{uo}}{E_{si}} = \frac{E_{uo}}{E_{uo} + E_{ti} + E_{ei}} \tag{8.17}$$

$$\eta_{ar} = \frac{E_{uo}}{E_{sr}} = \frac{E_{uo}}{E_{uo} + E_{tr} + E_{er} + E_{rg}} = \frac{E_{uo}}{E_{sr,n} + E_{sr,p}} \tag{8.18}$$

With reference to Equations (8.17)-(8.18), E_{uo} is the minimum required energy by users (no matter whether the system is ideal or real) and is related to the topography of the network, E_{ti} is the topographic energy required by an ideal system, and E_{ei} is the supplied excess energy for an ideal system. Moreover, real system efficiency is characterized by an additional term, E_{rg}, representing reducible global energy. Furthermore, regarding $E_{sr,n}$ and $E_{sr,p}$, these are the natural and shaft energy supplied to the system, respectively. The former depends on the location and the elevation of the source, whereas the latter is the energy spent by pumping. The energy recovered by the PAT is subtracted to $E_{sr,p}$ for the calculation of η_{ar}. The authors [63, 14] defined these indices to give an overview of the energy efficiency of the supply system and the whole distribution. Applying these to the current case study, for the indirect pumping scenario, η_{ai} is equal to 0.37, whereas η_{ar} is equal to 0.24 with energy recovery ($\eta_{ar,1.1}$) and 0.22 otherwise ($\eta_{ar,1.2}$). In the direct pumping scenario, η_{ai} and η_{ar} (i.e. $\eta_{ar,2}$) can be evaluated as 0.46 and 0.30, respectively. The higher efficiency of the direct pumping scenario highlights its convenience for this case study. In Table 8.3, the main figures of the two scenarios are reported. Furthermore, the literature efficiency indices have been calculated for different conditions of sourcing, that is, different values of i_1 and i_2. Figure 8.14 shows trends of the η_{ar} efficiency index against i_1 for different values of ΔH_{ind} and i_2.

As shown in Figure 8.14, for a given value of i_1, the efficiency reduces with increasing i_2, thus with increasing the proportion of head-loss on the total pumping head. This leads to higher elevation of the source, thus higher values of natural energy $E_{sr,n}$, which means smaller values of η_{ar}, according to Equation (8.18). Furthermore, the comparison between the values of $\eta_{ar,1.1}$ and $\eta_{ar,2}$ gives information about the convenience of each of the two scenarios. As demonstrated above, the convenience of direct pumping

Table 8.3 Main figures of the indirect and direct pumping scenarios: efficiency index of ideal system (η_{ai}), efficiency index of real indirect pumping system with energy recovery ($\eta_{ar,1.1}$) and otherwise ($\eta_{ar,1.2}$), efficiency index of real direct pumping system ($\eta_{ar,2}$).

Scenario	η_{ai}	$\eta_{ar,1.1}$	$\eta_{ar,1.2}$	$\eta_{ar,2}$
Indirect	0.37	0.24	0.22	–
Direct	0.46	–	–	0.30

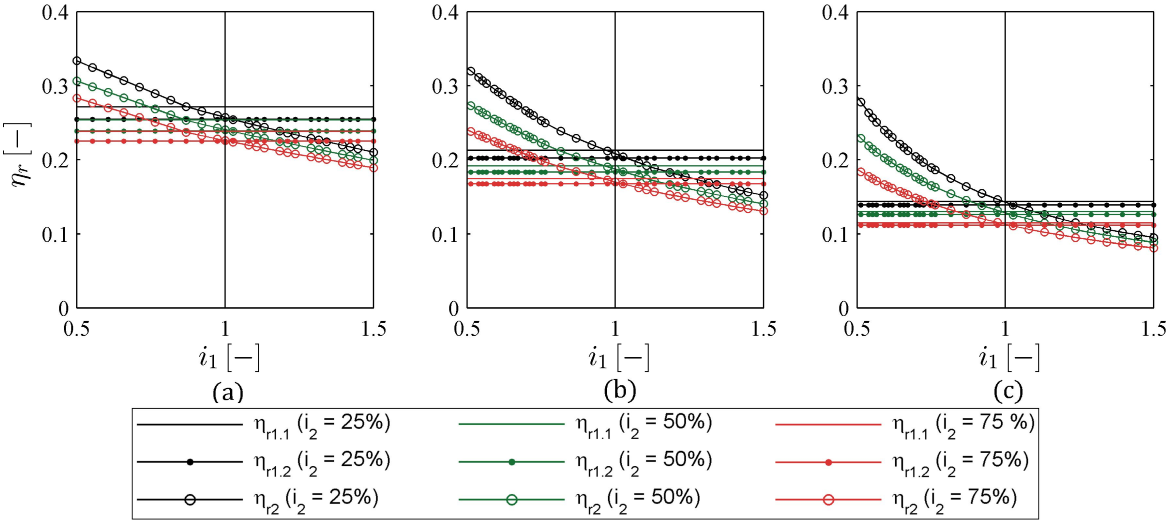

Fig. 8.14 Trend of literature efficiency indices [63, 14] for $\Delta H_{ind} = 25$ m (a) ; $\Delta H_{ind} = 50$ m (b) ; and $\Delta H_{ind} = 199$ m (c).

increases for decreasing i_1. Thus, direct pumping can be considered more convenient if a certain amount of the pumping head can be saved bypassing the storage reservoir upstream of the network. As Figures 8.12-8.13, the plot of Figure 8.14 shows that, despite the energy recovery, if the reduction of pumping head is significant, that is, i_1 is lower than a certain value, then direct pumping is the more convenient strategy. Nevertheless, for $H_{ind} = 25$ m, the η_{ar} efficiency of direct pumping is higher for values of i_1 lower than 0.88, whereas the plot of EI_1 shows that the cutoff occurs for i_1 equal to 0.94. Also for for $H_{ind} = 50$ m and for $H_{ind} = 100$ m, the analysis of the values of η_{ar} could lead to results slightly different from the values of Figures 8.12-8.13. Finally, even if the calculation of η_{ar} gives an overview of the mutual convenience of the two practices, it does not give detailed information about the amount of energy that can be saved in either of the two scenarios.

8.6 Conclusions

In this study, the energy audit of the supply system of a case study water distribution network has been analyzed. The supply network serves the area of Ballacolla (IE) with an average discharge of 4.35 l/s, and it is representative of many situations that occur in water supply systems, where the water is pumped to an elevated tank or reservoir and then distributed to the network after a pressure reduction to control the water leakage. Two different solutions to increase the energy efficiency of a supply system have been investigated: (i) pumping up to a reservoir and converting the excess pressure in energy by a PAT; (ii) pumping directly to a downstream water distribution network, bypassing the reservoir and benefiting of lower pressure head. In the first case, the energy requirement has been assessed as 32420 kWh/year whereas the amount of produced energy ensured by the PAT has been accounted as 2234 kWh/year. In the second case, the variable speed pump has required 22327 kWh/year, with a saving of 10090 kWh/year. Thus, for the analyzed case study, direct pumping with lower pressure head has been proved to be a more efficient strategy when compared to the indirect pumping scenario, even though an energy recovery strategy is performed. This does not occur if other supply conditions are simulated, corresponding to different combinations of source location, source elevation, head-loss in direct pumping, and head-loss in indirect pumping. To assess the benefit of either of the two scenarios for differing boundary conditions, two energy indices have been introduced. If the energy recovery strategy is not performed, the direct pumping scenario is more convenient, unless high value of pressure head are required due to high head-loss in the approaching pipe. On the other hand, if the system is equipped with a PAT, when the values of pumping head both in the direct and indirect scenarios are equal, indirect pumping with energy recovery is up to 5% more convenient than direct pumping. The convenience of direct pumping increases as the pressure head can be reduced up to 6%. A similar behavior is proved by the analysis of the efficiency indices proposed by Gómez et al. [63] and Cabrera et al. [14], even though such literature indices do not allow for the evaluation of the amount of energy recoverable in either of the two scenarios.

Despite direct pumping supply being a strategy avoiding the high environmental impact of a reservoir, it is not a robust approach since it cannot guarantee the supply of the network in case of power or pump failure. Therefore, indirect pumping to an elevated tank or reservoir could be preferred, if the system is provided with a PAT for energy recovery, as the presence of a reservoir increases the resilience of the water system. However, it is worth considering that, in case the PAT or grid fails, no power or savings

would be produced in indirect pumping scheme, but water supply might be guaranteed via a bypass.
To sum up, the optimal solution must be studied case by case, depending on the hydraulic conditions of the system and on the real costs and benefits of each possible design solution.

List of Symbols

γ	Specific weight
ΔE	Net energy of the indirect supply scenario
ΔH	Head
ΔH_{BEP}	Pumping head at the best efficiency point
ΔH_{dir}	Pumping head of the direct supply scenario
$\overline{\Delta H_{dir}}$	Average pumping head of the direct supply scenario
ΔH_{ind}	Pumping head in the indirect supply scenario
ΔH_{PAT}	Head-loss within the PAT
Δt_i	Time interval
η_{ai}	Efficiency index of an ideal system
η_{ar}	Efficiency index of a real system
$\eta_{ar,1.1}$	Efficiency index of real indirect pumping system with energy recovery
$\eta_{ar,1.2}$	Efficiency index of real indirect pumping system without energy recovery
$\eta_{ar,2}$	Efficiency index of real direct pumping system
η^{BEP}	Efficiency at the best efficiency point
η^{MOT}	Efficiency of the motor
η^{P}	Overall plant efficiency
η	Device efficiency
a, b, c	Coefficients best-fit polynomial approximation
ρ	Density

C	Constant within the formula to evaluate the efficiency at the best efficiency point
D	Diamater
e	Ratio between the efficiency at a general working condition and the efficiency at the B
E_{dir}	Absorbed energy in the direct supply scenario
$E_{hydr,ind}$	Hydraulic energy in the indirect supply scenario
E_{ind}	Absorbed energy in the indirect supply scenario
E_{PAT}	Energy produced by the PAT
E_{ei}	Supplied excess energy for an ideal system
E_{rg}	Reducible global energy
E_{si}	Energy supplied to an ideal system
E_{sr}	Energy supplied to a real system
$E_{sr,n}$	Natural energy supplied to the system
$E_{sr,p}$	Shaft energy supplied to the system
E_{ti}	Topographic energy required by an ideal system
E_{uo}	Minimum required energy
EI_1	New energy efficiency related to the indirect supply scenario
EI_2	New energy efficiency related to the direct supply scenario
f	Frequency
g	Gravity acceleration
h	Dimensionless head
H_{req}	Drop within the valve in link 8-10
i	Index of PAT operating points
K	Roughness coefficient
L	Length of the pipe linking source and network
n_P	PAT operating points
n_S	Specific rotational speed

N	Rotating speed
q	Dimensionless discharge
p	Dimensionless power
pp	Number of pole pairs
P	Power
P_{hydr}	Hydraulic power
Q	Discharge
$\overline{Q}$	Average discharge
Q^{BEP}	Discharge at the best efficiency point
Q^{PAT}	Discharge through the PAT
r	Term accounting for length, diameter and roughness of the pipe
t	Time

Chapter 9

A newly proposed device to save energy in urban water management

9.1 Introduction

An innovative strategy increasing the sustainability of supply systems is recently represented by turbo-pumps [17], namely, systems consisting of a turbine and a pump which are directly coupled and mounted on the same shaft. In such a system, neither a generator nor a motor are needed, as the turbine does not produce electrical power, but rather converts the hydraulic power in mechanical power and transfers the torque to the pump.

Turbo-pumps can be adopted whenever a pumping system is required within a storage tank to supply an upper part of the network. The excess pressure upstream of the tank can be exploited by the turbine to produce power and feed the pump, instead of being dissipated by a pressure valve. Such a strategy may therefore increase the energy efficiency of the whole system, ensuring both the energy recovery and the reduction of pumping energy consumption. Furthermore, in order to reduce equipment costs, a pump as turbine (PAT) [22] could be employed instead of a classic turbine, obtaining a PAT–pump turbocharger (P&P). Other possible applications may occur in the process industry, where the excess pressure of a process can be used to pump liquids for other purposes.

This chapter is a presentation of the study made by Morani et al. (2020), entitled "Energy transfer from the freshwater to the wastewater network using a PAT-equipped turbopump" [90]. The aim of this study consists of analyzing a new strategy to recover energy in a water system. A PAT–pump turbocharger (P&P) has been adopted to convey wastewater into a treatment plant from a lower topographical level. The wastewater is pumped in a co-located drinking water network, where the pressure is kept low by a PAT due to the need of supplying water from a higher elevation to this low topographical location. As PAT and pump operate with clean and wastewater, respectively, the resulting system would be a mixed PAT–pump turbocharger (MP&P). Such a system could be adopted in low ground level areas, where pumping stations are required to carry wastewater to a treatment plant. In particular, this plant arises whenever the wastewater pumping station is required in the same location as an excess clean-water pressure is available. Despite being not so common, this situation can happen in towns having a large variability in elevation. In these cases, the highest pressure in the freshwater network occurs where the ground elevation is the lowest, and there, a pressure control is generally required to minimize the leakage. In the same areas, due to the need to treat the wastewater, the sewage system is usually equipped with pumping stations, to pump toward the treatment plants. Furthermore, if the energy recoverable by the PAT is small, a conversion to electricity through a PAT/generator would not be convenient, due to the installation costs and the need for connecting the generator to the grid. Thus, a direct transfer of the available mechanical power from the PAT to the pump can be a more convenient solution. Another advantage of the MP&P is the simplification of the mechanic of the plant. Two separate plants operating independently (a hydropower recovery plant with its own generator and a pumping plant with its own motor) apparently exhibit a higher resilience than a coupled system, where a failure of one device also affects the operation of the one coupled to it. Nevertheless, the absence of electric devices simplifies the mechanic of the plant and could reduce the failure rate as well as the maintenance costs. In the next sections, the main features of the MP&P plant are explained and a new method to perform a preliminary design of the plant is also presented. Moreover, a new mathematical model describing the plant operation is defined for different boundary conditions. Then, an economic comparison with a conventional wastewater pumping system working in ON/OFF mode is also performed. The limitations of the plant are finally investigated.

9.2 Mixed Pump-PAT Turbocharger operation

In a mixed PAT–pump turbocharger plant, a PAT is adopted to convert an excess pressure in mechanical energy. On the same shaft as the PAT, a pump is located and rotates as the same rotational speed of the PAT ($N_P = N_{PAT} = N$). The pump is not supplied by any external electrical motor, but rather exploits the mechanical energy produced by the PAT ($P_P = P_{PAT} = P$) to carry sewage to a water treatment plant. In the mixed PAT–pump turbocharger, the pump and PAT can achieve any rotational speed, which result from the combination of the performance curves of the two devices with the network characteristics. Compared to P&P in freshwater systems [17], the MP&P is characterized by a reduced overall efficiency, as the pumps for wastewater (e.g. channel pumps, vortex pumps) present a lower performance. A simplified scheme of a MP&P plant is presented in Figure 9.1.

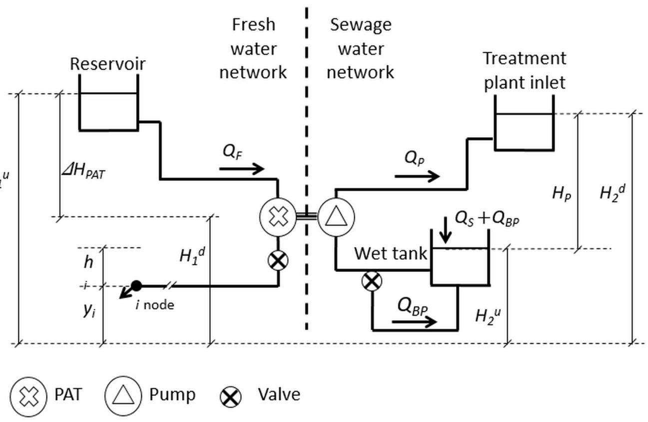

Fig. 9.1 Hydraulic scheme of mixed pump as turbine–pump (MPP).

According to Figure 9.1, H_1^u and H_1^d are the head available at the hydropower plant inlet and outlet, respectively; Q_F is the freshwater discharge; ΔH_{PAT} is the head-loss within the PAT; Q_S and Q_P are, respectively, the wastewater discharge reaching the wet tank and the discharge pumped to the treatment plant with a hydraulic head equal to H_2^d. In addition, Q_{BP} represents a bypassed discharge. The bypass is adopted in order to avoid the emptying of the wet tank, so that when the pumped discharge is too high, a part of the flow is recirculated to the wet tank. In this way, the damages due to the suction of the air is prevented, and the sedimentation of solid material is also avoided. Finally, H_P is the pumping head computed with respect to the water level in the tank, namely, H_2^u. In this study, head-loss within sewage pumping pipelines have been neglected, since these pipes generally present very short length in order to avoid system blockage. In addition, due to the shortness of the branch, head-loss have been also considered negligible from the freshwater storage tank to the hydropower plant. Carravetta et al. (2017) [17] deeply investigated the relationship between turbined and pumped discharge, as well as, the relationship between pumping head and head-loss exploited by the PAT. Different number of stages of both the devices were considered by the authors [17] in order to vary the operating condition of the plant. If the number of PAT stages is fixed to one, the range of flow rate ratio Q_P/Q_F decreases while the head ratio $H_P/\Delta H_{PAT}$ increases. Regarding the efficiency, for a number of PAT stages equal to 1, the lowest plant efficiency is attained for a single-stage pump, whereas it significantly increases (from less than 0.35 up to more than 0.45) by increasing the number of pump stages, with a maximum of 0.45 for a three-stage pump.

9.3 Study Area

As case study, the real water network employed in chapter 8 has been investigated. As already mentioned, the network is provided with an upstream valve located along the pipe connecting nodes 8 and 10 (see Figure 8.1), to perform a pressure control strategy within the network. In Figure 9.2, the daily trend of fresh water Q_F (a) and head-loss ΔH_v (b) within the valve in link 8-10, as well as the available power P_{av} (c) upstream of the valve is presented. According to Figure 9.2, the daily average values

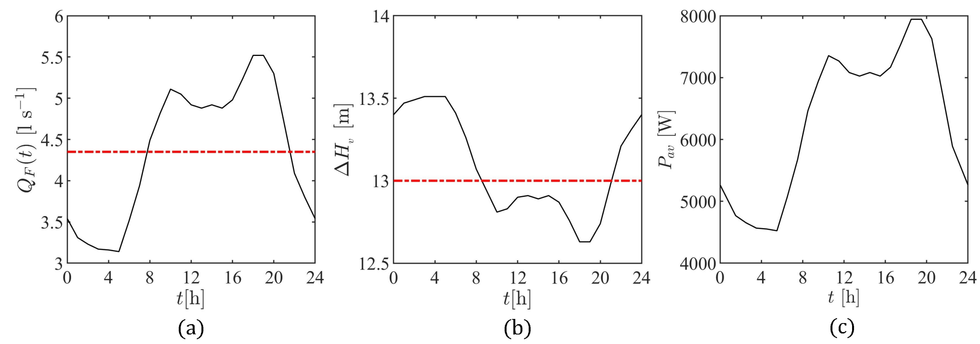

Fig. 9.2 Daily pattern of flow (a) and head-loss (b) though the valve located in links 8–10, available power (c) upstream of the valve.

of the discharge ($\overline{Q_F}$) and head-loss within the valve ($\overline{\Delta H_v}$) are 4.35 l/s and 13 m, respectively.

With reference to the study presented in chapter 8, the valve was replaced with a hydropower plant, whose regulation has been performed by a series-parallel hydraulic circuit (Figure 8.5) in order to guarantee a minimum pressure head in all the nodes of the network and, in particular, a pressure of 10 m in the most critical node of the network (i.e. node 49). The minimum head downstream of the valve to ensure a pressure of 10 m in the most critical node is 134 m.

9.4 Drainage discharge pattern

A drainage network has been supposed covering a part of the water supply area and carrying the wastewater to a point close to the hydropower plant. According to the topography of the village, the wastewater flow direction has been predicted and a hypothetical drainage network has been overlaid on to the drinking water network, as shown in Figure 9.3.

The evaluation of a sewage discharge pattern is required to investigate the behavior

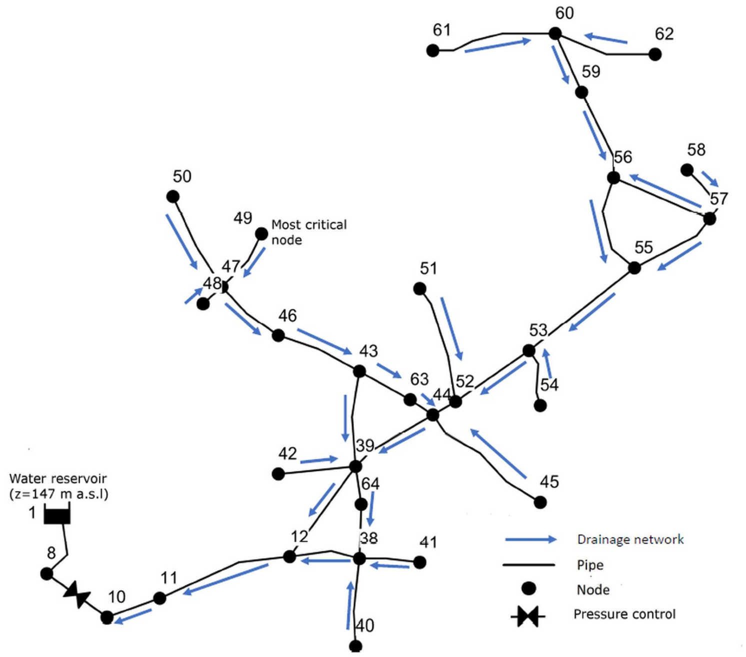

Fig. 9.3 Layout of the drainage network.

of the MP&P. For such purpose, a response function needs to be formulated, since freshwater input and the wastewater hydrograph are non-linearly convoluted. In this study, the Clark's model [28] has been chosen as a reference inflow–outflow model for simulating this kind of flow transformation. According to Clark's model, the hydrologic response can be considered a combination of two different functions, such as a translation and an attenuation function. In particular, the former function is reproduced by a linear channel, whereas the latter is represented by a single reservoir.

Clarks Instantaneous Unit Hydrograph (CIUH) is shown in Equation (9.1).

$$\begin{cases} u(t) = \frac{1}{t_c}[1 - e^{-t/K}] & if\ t < t_c \\ u(t) = \frac{1}{t_c}[e^{\frac{-t}{K}}(e^{-t_c/k} - 1)] & if\ t > t_c \end{cases} \tag{9.1}$$

t_c being the time of concentration, namely, the time required by the head drop of the flow at the hydraulically most remote point of the catchment to reach the storage tank; K is the storage coefficient accounting for the time delay between freshwater flow and the wastewater hydrograph. To evaluate K the formula proposed by [42] has been used:

$$K = t_c\ c \tag{9.2}$$

where c is a coefficient accounting for the phenomenon of peak attenuation. In this study, c has been set equal to 0.25, 0.5, and 0.75, thus around the value of 0.6, which is often used in literature [85].

The sewage water hydrograph has been obtained by performing a convolution between the available fresh flow data and Clark Instantaneous Unit Hydrograph [42], as shown following:

$$Q_S(t) = \int_0^t \phi\ Q_F(\tau)\ u(t-\tau)\ d\tau \tag{9.3}$$

Q_S being the sewage discharge at a general time instant t; $d\tau$ is the convolution interval time, set as one minute; and ϕ the runoff coefficient, which does not take into account the rainfall though.

For the sake of generality, several wastewater hydrographs have also been obtained by combining different values of t_c, c, and ϕ. Varying ϕ means considering different sizes of flooding areas. In particular, ϕ has been varied in a range between 0.1 and 0.8. According to Figure 9.4, ϕ_1, ϕ_2 and ϕ_3 are three general runoff coefficient values in ascending order, which correspond to three increasing flooding areas. The time of concentration (t_c) has been estimated by the literature formula [86] presented in Equation (9.4).

$$t_c = 1.7\ L_m^{0.6}\ S_m^{-0.3} \tag{9.4}$$

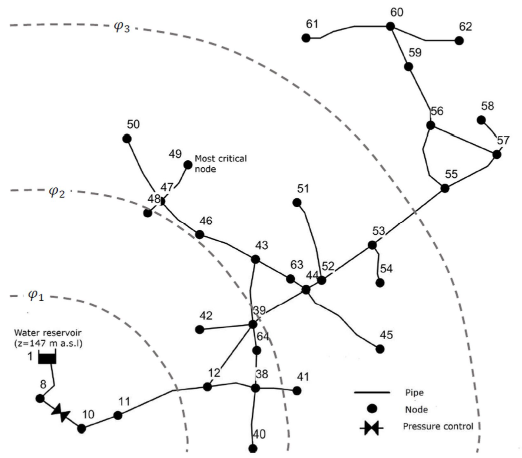

Fig. 9.4 Different flooding areas withing the network.

where L_m and S_m are the hydraulic length (expressed in mile) and the slope (expressed in feat/mile), both referring to the longest channel of the network. According to Equation (9.4), t_c resulted in around 1.5 h, thus, for the sake of generality, this parameter has been varied between 1 and 2 h.

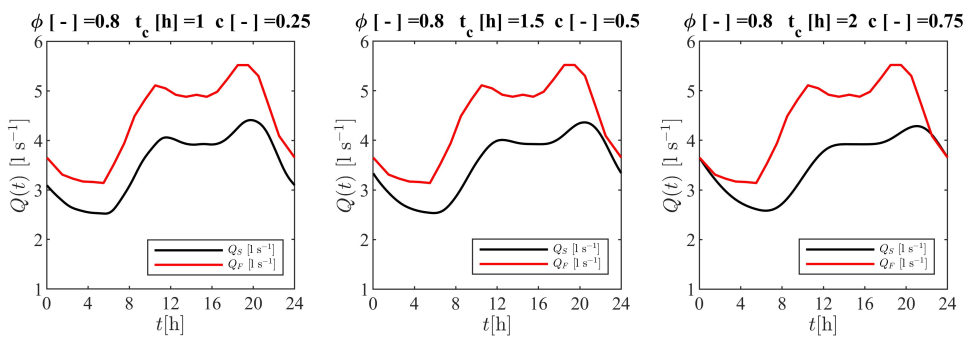

Fig. 9.5 Average fresh flow pattern, and wastewater hydrographs for ϕ= 0.8 and different values of t_c and c.

As shown in Figure 9.5, assuming a constant value of ϕ equal to 0.8 and increasing t_c and c, the wastewater hydrograph diverges from the average fresh flow pattern. The confluence of the drainage system into a point close to the hydropower plant (i.e. links 8–10) allows for the possibility of aligning a pump and a PAT on a same shaft, where the freshwater and wastewater networks may be co-located. Compared to the turbo pumps used for water supply [17], the main difference here is represented by the time lag between fresh flow pattern and wastewater hydrograph: the peaks of the incoming discharge of the sewage systems are shifted with respect to the discharge pattern in the drinking water distribution system. As a result, the peaks of the available power for turbining and the required power for pumping do not match. Thus, when the maximum discharge is flowing through the sewage pipe, the available power may be not enough to pump the required flow rate. A storage tank is therefore required in order to compensate for this difference.

9.5 PAT and Pump selection strategy

A new strategy has been defined in order to select both the pump and PAT of which the MP&P consists. This strategy is based on the maximum daily average fresh discharge ($\overline{Q_{F,max}}$) and the maximum daily average sewage discharge ($\overline{Q_{S,max}}$). With regard to the preliminary selection of the PAT, this can be done based on the maximum values of ΔH_v in section 9.3. The selection of the PAT can be not unique, because the rotational speed is not fixed. Once a PAT has been selected, its mechanical power ($P = P_{PAT} = P_P$) can be known from the performance curves of the machine. Thus, based on the values of discharge ($\overline{Q_{S,max}}$) and power (P), a pump can be selected from the pump manufacturer catalogues. Again, since the rotational speed is not known a-priori, the choice of the pump is not unique, since different machines can exhibit similar performances at different rotational speeds. The real hydraulic characteristics of the system, as well as the rotational speed, depend on the mutual behavior of the two machines. Thus, the choice of the two machines should be validated, as explained hereafter. In this research, a large database of PAT curves was available, since this study is part of the REDAWN project (project EAPA 198/2016) of the European Union, which collected a large number of data on the reverse behavior of pumps. The selection involved three different PATs and five different pumps, and the coupling was validated for each of the possible combinations. In fact, only two different preliminary pump and PAT models have been chosen for the case study in question: one centrifugal-multistage open-shaft sewage pump and one multistage centrifugal pump have been chosen. Then, the PAT performance has been modified by varying the number of stages ($n_{st,PAT}$) from one to three, while for the pumps, five different impellers, differing by the diameter (D_P) ranging between 150 and 260 mm, have been tested hereafter. Finally, for each possible coupling of a pump and PAT, the following equations have been solved:

$$
\begin{cases}
\left[a_{PAT}^{N}\left(\frac{\overline{Q_{F,max}}}{N}\right)^2 + b_{PAT}^{N}\left(\frac{\overline{Q_{F,max}}}{N}\right) + c_{PAT}^{N}\right] N^2 \; n_{st,PAT} + \\
- \; \overline{\Delta H_{PAT,max}} = 0 \\
\left[a_{P}^{N}\left(\frac{\overline{Q_{S,max}}}{N}\right)^2 + b_{P}^{N}\left(\frac{\overline{Q_{S,max}}}{N}\right) + c_{P}^{N}\right] N^2 - \overline{H_{P,max}} = 0 \\
\alpha_{P}^{N}\left(\frac{\overline{Q_{S,max}}}{N}\right)^3 + \beta_{P}^{N}\left(\frac{\overline{Q_{S,max}}}{N}\right)^2 + \gamma_{P}^{N}\left(\frac{\overline{Q_{S,max}}}{N}\right) + \delta_{P}^{N} = \\
\left[\alpha_{P}^{N}\left(\frac{\overline{Q_{F,max}}}{N}\right)^3 + \beta_{P}^{N}\left(\frac{\overline{Q_{F,max}}}{N}\right)^2 + \gamma_{P}^{N}\left(\frac{\overline{Q_{F,max}}}{N}\right) + \delta_{P}^{N}\right] n_{st,PAT}
\end{cases}
\tag{9.5}
$$

In equation (9.5), the three unknown variables N, $\overline{\Delta H_{PAT,max}}$, and $\overline{H_{P,max}}$ represent the rotational speed of both the pump and PAT, the daily average head dissipated by the PAT, and the daily average pressure head of the pump, respectively. The other parameters are: a_{PAT}^N, b_{PAT}^N, c_{PAT}^N, α_{PAT}^N, β_{PAT}^N, γ_{PAT}^N, δ_{PAT}^N, a_P^N, b_P^N, c_P^N, α_P^N, β_P^N, γ_P^N, and δ_P^N, which represent the experimental regression coefficients of the head and the power curves of the PAT and pump. The experimental curves of the PAT for $N =$ 1520 rpm and for the three stages are presented in Figure 9.6, whereas the catalogue curves of the pump for different impeller diameters and $N = 875$ rpm, are shown in Figure 9.7.

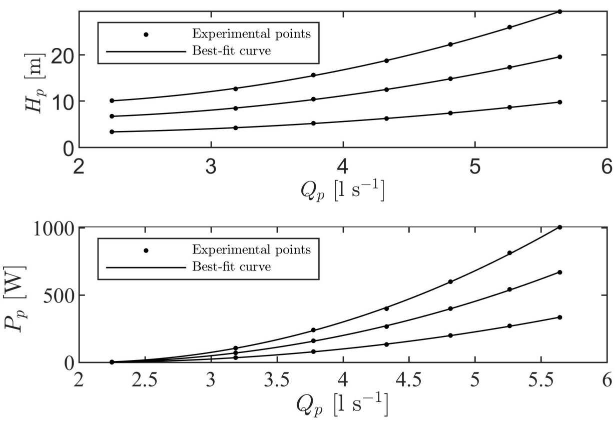

Fig. 9.6 Experimental curve of the pump as turbine (PAT) for $N = 1520$ rpm.

With reference to Equation (9.5), $\overline{Q_{S,max}}$ is the maximum daily average sewage discharge, set equal to $\phi\ \overline{Q_{F,max}}$, where $\overline{Q_{F,max}}$ is the maximum daily average fresh discharge, equal to 5.5 l/s. Furthermore, the runoff coefficient ϕ has been varied in a range between 0.1 and 0.8.

Figure 9.8 shows an example of the system's behavior when $n_{st,PAT} = 1$, $D_P = 260$ mm, and $\phi = 0.2$. The top plot shows the power versus the rotational speed when the discharge is assigned. In particular, the blue line represents the power produced by the

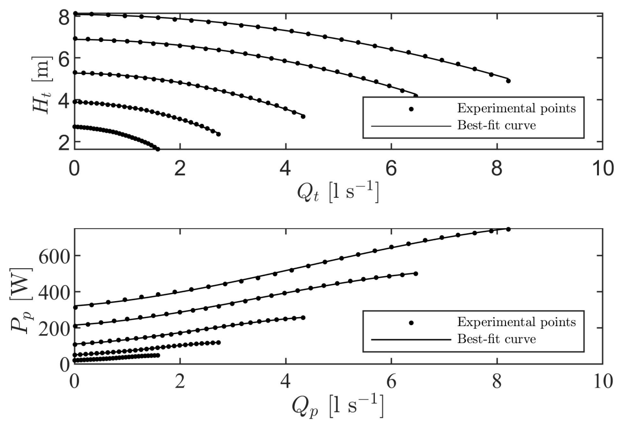

Fig. 9.7 Catalogue curve of the pump for $N = 875$ rpm.

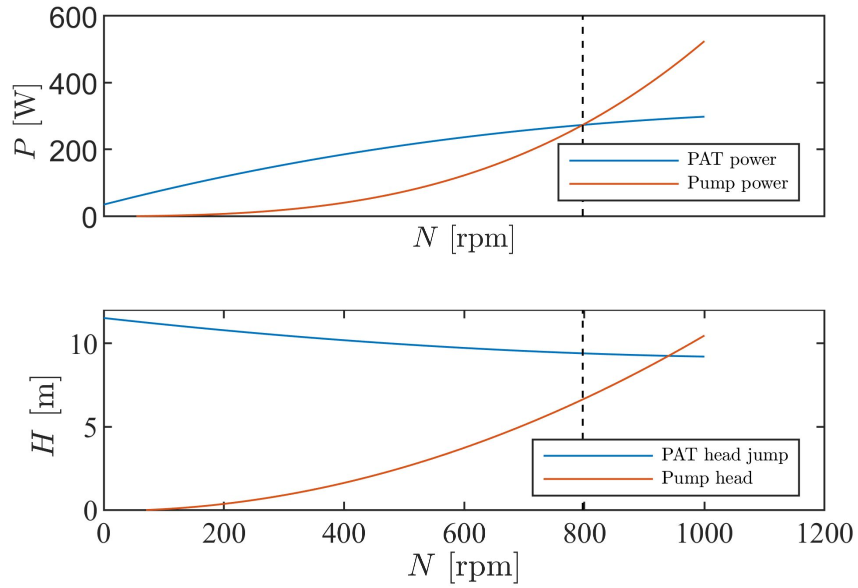

Fig. 9.8 Power and head curve versus rotational speed for the PAT and the pump, when $n_{st,PAT} = 1$, $D_P = 260$ mm, and $\phi = 0.2$.

PAT when the turbined discharge is $\overline{Q_{F,max}} = 5.5$ l/s (i.e. the left-hand side of the third equation of the set (9.5)), while the red line shows the power absorbed by the pump when the pumped flow rate is $\overline{Q_{F,max}} = \phi\ \overline{Q_{F,max}}$ (i.e. the left-hand side of the third equation of the set (9.5)). The intersection point of the two curves represents the operating rotational speed of the turbocharger. The bottom plot of Figure 9.8 shows the head jump in the PAT, (i.e. $\overline{\Delta H_{PAT,max}}$), and the head of the pump, (i.e. $\overline{H_{P,max}}$) versus the rotational speed. For the operating speed, the head jump of the turbine is lower than the maximum allowed value (13.5 m), while the pumping head is equal to 6.69 m. Figure 9.9 shows the complete behavior of the turbocharger for the same conditions of Figure 9.8. The four curves have been calculated for $N = 797$ rpm, as resulted from the calculation. The head of the PAT is showed in the left-bottom plot. For the sake of illustration, let the turbined discharge be 5.5 l/s: the operating point lies below the red line, which represents the maximum allowed head jump. The output power of the PAT and the input power of the pump are equal to 273 W, while the pumped discharge is equal to 1.1 l/s. The pumping head is instead shown in the right-bottom plot.

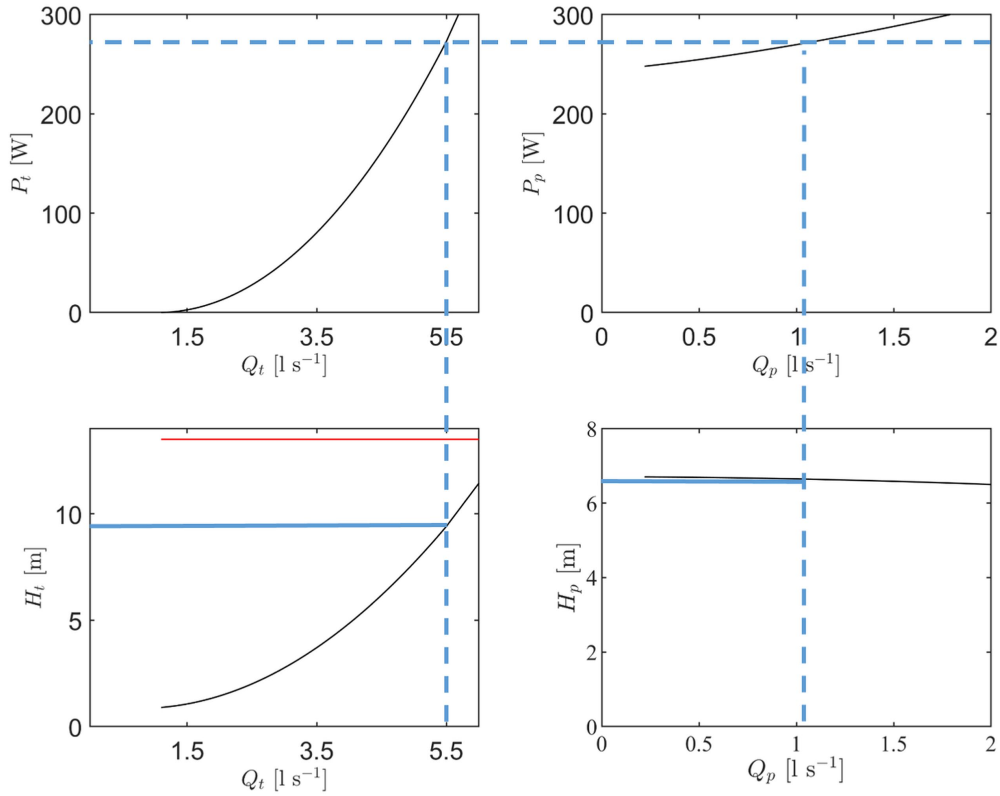

Fig. 9.9 Operation of the plant for N = 797 rpm, $n_{st,PAT}$ = 1, D_P = 260 mm, and ϕ = 0.2. (The red line is the maximum allowed head jump within the PAT, which is 13.5 m, according to Figure 9.2).

For each possible coupling of PAT-pump ($n_{st,PAT}$, D_P), several operating conditions have been obtained. All the values ($\overline{\Delta H_{PAT,max}}$ and $\overline{H_{P,max}}$) resulting from the resolution of the system (9.5) will be evaluated to select the most advantageous combination of pump and PAT for the MP&P plant, as further will be explained.
For the sake of illustration, Table 9.1 shows the results obtained for ϕ equal to 0.2.

According to Table 9.1, the number of stages of the PAT equal to two and three will not

Table 9.1 Main figures of preliminary design for ϕ= 0.2.

$n_{st,PAT}$ [−]	D_P [m]	$\overline{H_{P,max}}$ [m]	$\overline{\Delta H_{PAT,max}}$ [m]
1	0.15	3.79	9.24
1	0.18	5.21	9.28
1	0.21	5.47	9.38
1	0.24	6.15	9.44
1	0.26	6.69	9.48
2	0.15	6.32	18.64
2	0.18	8.86	18.50
2	0.21	9.46	18.46
2	0.24	10.70	18.48
2	0.26	11.65	18.51
3	0.15	8.28	28.64
3	0.18	11.73	28.18
3	0.21	12.70	27.80
3	0.24	14.42	27.72
3	0.26	15.74	27.69

be considered any longer, since the corresponding values of $\overline{\Delta H_{PAT,max}}$ exceed 13.5 m, that is, the maximum value of head that can be dissipated by the PAT, according to Figure 9.2. Thus, only the one-stage PAT will be further considered. Moreover, among all the pump diameters, D_P as 0.26 m has been chosen, being the one ensuring greater values of both pressure $\overline{H_{P,max}}$ and dissipated head $\overline{\Delta H_{PAT,max}}$ for an assigned number of stages, according to Table 9.1. Since values of ($\overline{H_{P,max}}$ and $\overline{\Delta H_{PAT,max}}$ in Table 9.1 referred to the maximum daily average discharge in the network, the operation of both pump and PAT will be further verified in the next section, considering the instantaneous values of discharge during the day. Nevertheless, this selection strategy has been useful to perform a preliminary geometric selection of both the pump and PAT constituting the turbo pump. The behavior of the MP&P should be otherwise simulated as many times as the number of all possible machines, which may suit the operating conditions.

9.6 Simulation of MP&P behavior

Before proceeding to the simulation of the mixed PAT–pump turbocharger behavior, some variables (previously presented in Section 9.2) should be set. In particular:

- Q_F and Q_S have been set according to Figure 9.2(a) and Figure 9.5, respectively;
- H_1^u is equal to the hydraulic head in the node upstream of the power plant inlet, which has been estimated by the hydraulic simulator Epanet [104];
- H_2^d is the required head to pump the water from the wet tank to the inlet of the treatment plant. It depends on the water level within the wet tank, as well as the topographical level of the treatment plant, and the head-losses in the pipeline. It is a design parameter, and the machine selection procedure should enable the accomplishment of this. In this case, since no real-world information is available about the sewage system, it has been chosen as a function of the pump head resulting from the selection procedure, while the head-losses in the pipeline have been neglected. Therefore, H_2^d has been calculated as:

$$H_2^d = \frac{W_1}{\Sigma} + \overline{H_{p,min}} \tag{9.6}$$

W_1 and Σ being the volume and cross-sectional area of the water tank, set equal to 1.5 m^3 and 1 m^2, respectively. Then, in order to simulate the MP&P behavior, a mathematical system consisting of five equations has been solved by applying the Newton Raphson method [54]:

$$\begin{cases} \alpha_P^N\left(\frac{Q_P}{N\ D_P^3}\right)^3 + \beta_P^N\left(\frac{Q_P}{N\ D_P^3}\right)^2 + \gamma_P^N\left(\frac{Q_P}{N\ D_P^3}\right) + \delta_P^N = \\ \alpha_{PAT}^N\left(\frac{Q_F}{N\ D_{PAT}^3}\right)^3 + \beta_{PAT}^N\left(\frac{Q_F}{N\ D_{PAT}^3}\right)^2 + \gamma_{PAT}^N\left(\frac{Q_F}{N\ D_{PAT}^3}\right) + \delta_{PAT}^N \\ H_1^u - H_1^d - \left[a_{PAT}^N\left(\frac{Q_F}{N\ D_{PAT}^3}\right)^2 + b_{PAT}^N\left(\frac{Q_F}{N\ D_{PAT}^3}\right) + \right. \\ \left. + c_{PAT}^N\right] N^2 D_{PAT}^2 = 0 \\ H_2^d - H_2^u - \left[a_P^N\left(\frac{Q_P}{N\ D_P^3}\right)^2 + b_P^N\left(\frac{Q_P}{N\ D_P^3}\right) + c_P^N\right] N^2 D_P^2 = 0 \\ Q_S - Q_P - \Sigma\frac{dH_2^u}{dt} + \frac{Q_P}{(H_2^u+1)^{20}} = 0 \end{cases} \tag{9.7}$$

where the unknown variables are N, Q_P, H_2^u and H_1^d, and affinity laws have been used to simulate the behavior of the machines under variable speed [18]. According to the system (9.7), the first equation states that the power at the shaft is the same for both the PAT and pump; the second equation expresses the negative head drop in the PAT (namely, ΔH_{PAT} in Figure 9.1) as the difference between the head available at the power plant inlet and outlet; the third equation states the positive head drop in the pump as the difference between the hydraulic head at the pumping station outlet and inlet; finally, the latter is the continuity equation of the wet tank, whose cross-sectional area is Σ. In particular, in the latter equation, the last term represents the bypass discharge (Q_{BP}). With regard to the differential equation in the fourth equation of the set (9.7), it was solved using the finite differences method with a first-order backward numerical scheme. In addition, a time step equal to one minute has been assumed, and a six-day simulation was performed. Hereafter, the results will refer to the last 24 h of the whole simulation, so that any dependency on the initial level in the wet tank from the results could be omitted. For the sake of generality, results following presented correspond to only one configuration, i.e. ϕ= 0.7, t_c = 1 h, and c = 0.25. For this configuration, the pattern of fresh and sewage discharge is shown in Figure 9.10.
Figure 9.11 shows the daily pattern of the unknown variables. According to Figure 9.11, the water level in the tank (H_2^u) and pumped wastewater discharge (Q_P) are strictly related: a reduction of the water level is due to an increase in pumped discharge, and vice versa. It is worth underlining that the zero values of H_2^u correspond to the minimum level in order to avoid cavitation in the pumping system. The cavitation problem is indeed overcome by the employment of the bypass, which avoids the emptying of the tank that may occur when the pumped flow is too high.

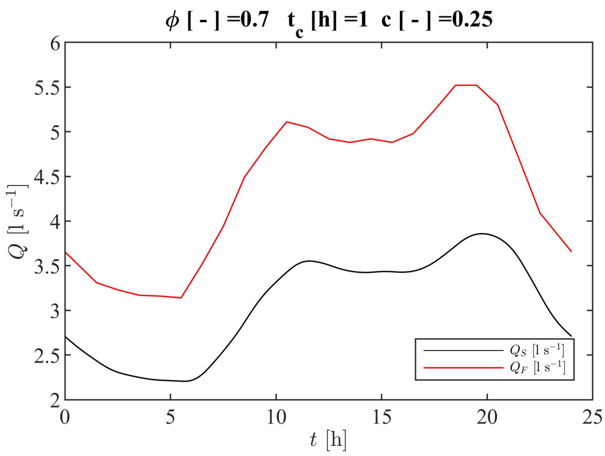

Fig. 9.10 Time series of fresh and sewage discharge, for ϕ= 0.7, t_c = 1 h, and c = 0.25.

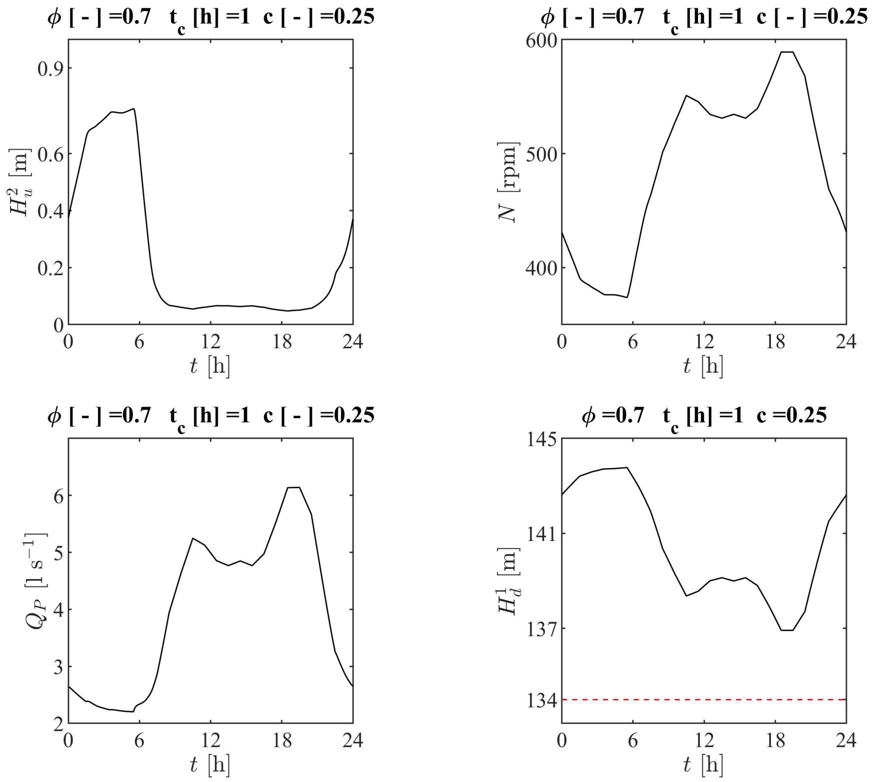

Fig. 9.11 Daily pattern of the unknown variables of system (9.7)

Note that the head downstream of the hydropower plant, namely, H_1^d has been ensured to be always greater than the minimum allowed value, i.e. 134 m. Thus, in a MP&P plant only a part of the available head is used to pump the wastewater to the treatment plant, whereas all of the available head (and thus the available power) is used when a PAT and a generator are installed in a traditional hydropower plant to produce electricity. Finally, according to Figure 9.11 the trend of rotational speed (N) follows the trend of pumped wastewater discharge (Q_P).

9.7 Economic comparison

In order to assess the economic benefit of the mixed PAT–pump turbocharger, an economic comparison has been performed with a conventional wastewater pumping system, working in ON/OFF mode. The net present value (NPV) of the investment has been assessed in both scenarios, for each configuration (t_c, c, ϕ). Since the number of valves and bypass is the same in both the scenarios, the corresponding costs will be neglected in the economic computation, as well as the cost of the hydraulic pump and PAT. As regards the MPP scenario, the NPV can be expressed as:

$$NPV_1 = \sum_{y=0}^{Y} \frac{C_{1,y}^{in} - C_{1,y}^{out}}{(1+r)^y} = -C_{1,y=0}^{out} = -C_{1,w}^{tank} \tag{9.8}$$

In Equation (9.8), Y is the number of y years, C_y^{in} and C_y^{out} are the cash inflow and outflow, respectively, at the y-th year, and r represents the discount rate, which is set equal to 5%. Moreover, $C_{1,y}^{in}$ is equal to zero since the energy recovered by the PAT does not represent a gain, but rather it is totally employed to supply the pump. Concerning the cash outflow in the mixed PAT–pump turbocharger scenario, namely $C_{1,y}^{out}$, it is due to the purchasing cost faced at the first year, consisting of only the cost of the water tank ($C_{1,W}^{tank}$). With regard to the construction cost of the holding tank, this has not been accounted in the cash outflow, since it has been assumed that such a tank already existed previously, in order to contain the hydrovalve for the pressure control.

In order to evaluate $C_{1,W}^{tank}$, a price list (Price List of Public Works. Reg. Campania 2016) has been employed. In particular, since the tank is characterized by a volume of 1.5 m^3 and a cross-sectional area equal to 1 m^2, the cost of a prefabricated tank having a dimension of (150 cm × 150 cm × 90 cm) has been adopted. To sum up, due to the neglected terms, the NPV_1 is represented by the investment cost of the water tank, which is equal to approximately 300 . As regards the conventional system, the NPV has been calculated as:

$$NPV_2 = \sum_{y=0}^{Y} \frac{C_{2,y}^{in} - C_{2,y}^{out}}{(1+r)^y} = -C_{2,y=0}^{out} + \sum_{y=1}^{Y} \frac{C_{2,y}^{E,PAT} - C_{2,y}^{E,pump}}{(1+r)^y} \tag{9.9}$$

According to Equation (9.9), $C_{2,y}^{E,PAT}$ is the cost related to the recovered energy, whereas $C_{2,y}^{E,pump}$ is the cost associated to the energy spent to pump the wastewater discharge. Finally, $C_{2,y=0}^{out}$ represents the purchasing cost faced at the first year, accounted as:

$$C_{2,y=0}^{out} = C_{2,MOT} + C_{2,GEN} + C_{2,W}^{tank} \tag{9.10}$$

Unlike the mixed PAT–pump turbocharger scenario, Equation (9.10) accounts for the costs of the motor ($C_{2,MOT}$) and generator ($C_{2,GEN}$). Finally, $C_{2,W}^{tank}$ is the cost of the water tank. In order to evaluate $C_{2,MOT}$, a commercial catalogue (Caprari, S.P.A.

Modena) has been used, and a cost function has been obtained as polynomial best fit curve, as shown in Figure 9.12. With regard to the PAT, a centrifugal multistage

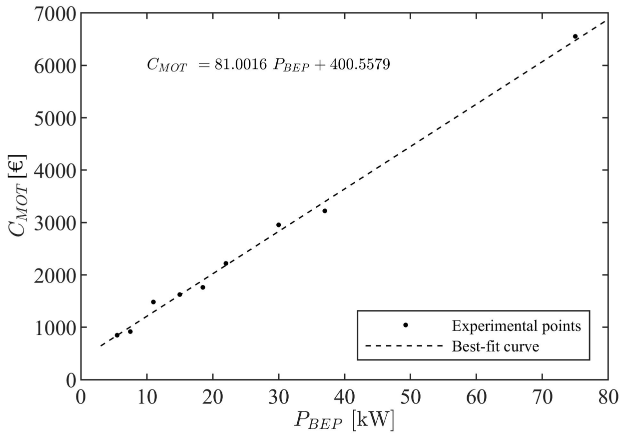

Fig. 9.12 Commercial costs and polynomial best fit curve.

end-suction pump HMU50-2/2 (Caprari, S.P.A. Modena) has been chosen as the reference machine, since it has been already designed in chapter 8 in order to maximize the energy produced in the same network. Therefore, in order to evaluate $C_{2,GEN}$, the following literature generator cost function [97] has been employed:

$$C_{gen}[€] = 60.19\ P[kW] + 163.15 \tag{9.11}$$

P being the power produced at the best efficiency point (BEP), expressed in kW. Equation (9.11) refers to a generator characterized by three pairs of poles [97], since the optimal configuration investigated in chapter 8 is characterized by a PAT working at a rotating speed equal to 1025 rpm. Furthermore, in order to evaluate the water tank cost, $C_{2,w}^{tank}$, the computation of the preliminary tank volume is required. Such a volume has been computed as:

$$W_2 = \max_{c,t_c,\phi} \left(900 \frac{Q_{max}}{n_{av}} \right) \tag{9.12}$$

where n_{av} is the number of pump starts per hour, set equal to eight according to the technical catalogue, and Q_{max} is the maximum discharge, which has been calculated as:

$$Q_{max} = \alpha\ Q_{s,max}^{c,t_c,\phi} \tag{9.13}$$

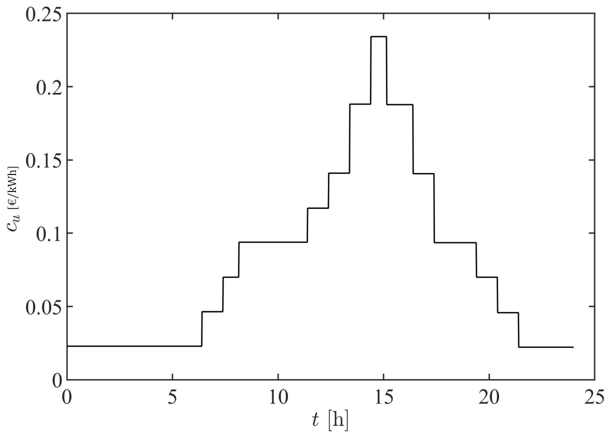

Fig. 9.13 Energy cost distribution over the time.

where $Q^{c,t_c,\phi}_{s,max}$ is the maximum wastewater discharge for an established combination (c, t_c, ϕ) and α is a safety factor, set equal to two and accounting for the random variation around the daily average peak value $Q^{c,t_c,\phi}_{s,max}$. The volume W_2 resulted in 0.5 m^3 and the corresponding price, $C^{tank}_{2,W}$, has been obtained from commercial price lists (Price List of Public Works. Reg. Campania 2016.), as in the MP&P scenario.

According to Equation (9.9), conversely to the mixed PAT–pump turbocharger, in which the whole energy produced by the PAT is employed to pump the wastewater, in the conventional scheme, both the costs associated to recovered and spent energy have been taken into account in the NPV. For each configuration (c, t_c, ϕ), the cost of the spent energy has been calculated as:

$$C_2^{E,pump} = \int_{day} \frac{\gamma \; Q_S \; \overline{H_P} \; c_u}{\eta_{2,M} \; \eta_{2,P}} dt \tag{9.14}$$

where dt is equal to one minute, and $\overline{H_P}$ represents the daily average pumping head, calculated as:

$$\overline{H_P} = H_2^d - \overline{H_2^u} \tag{9.15}$$

$\overline{H_2^u}$ being the daily average water level in the tank.

With reference to Equation (9.14), $\eta_{2,M}$ is the motor efficiency, which has been set equal to 0.8, and c_u is the energy cost distribution presented in Figure 9.13.

Finally, $\eta_{2,P}$ is the hydraulic pump efficiency at the best efficiency point (BEP) condition, equal to 0.6. Thus, for each configuration (c, t_c, ϕ), a different pump is assumed, having the same efficiency as the BEP condition of the pump employed in MP&P. Finally:

$$C_2^{E,PAT} = \int_{day} P_{2,PAT}\ c_u\ \eta_{2,GEN}\ dt \tag{9.16}$$

$P_{2,PAT}$ being the power produced by the PAT and $\eta_{2,GEN}$ the efficiency of the generator. Both the quantities have been already computed in chapter 8.

9.8 Discussion

The NPV has been calculated for different time periods (i.e. 5, 10, and 20 years). The main figures of the comparison are shown in Table 9.2, in which the difference between NPV_1 and NPV_2 at time periods of 5, 10, and 20 years has been divided for the average pumped power $\overline{P_{hyd}}$, resulting in ΔNPV_5, ΔNPV_{10}, and ΔNPV_{20}, respectively. This amount represents the economic convenience of the mixed PAT–pump turbocharger over the conventional system. Firstly, it is worth highlighting that the figures in Table 9.2 are small due to the small size of the case study network (indeed, the mean flow rate from the reservoir is only 4.35 l/s). Nevertheless, the obtained results are meaningful to investigate the performance of the MP&P plant. Furthermore, according to Table 9.2, MP&P is shown to be the most economically advantageous scenario, since the values of ΔNPV are all positive. Moreover, this advantage over the conventional approach reduces with the increasing time periods, since, in the conventional system, the production of energy amortizes the investment costs over time. As shown in Table 9.2 by increasing ϕ the advantage of MP&P increases, since in the conventional scheme, the increase of pumped wastewater is not compensated by the reduction of pressure head. This result is further shown in Figure 9.14.

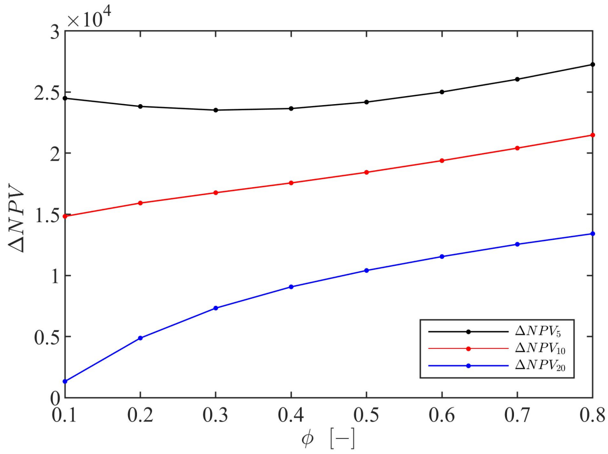

Fig. 9.14 Difference of net present value (NPV) between MP&P plant and conventional scheme, against the runoff coefficient (ϕ), for different time periods (5, 10, and 20 years).

As shown in Figure 9.15, by increasing ϕ from 0.2 to 0.5, and thus increasing the sewage water (Q_S) by 150%, the pressure head reduces by only 24%; thus, $C_2^{E,pump}$ increases. As a result, the MP&P results become more economically attractive than the conventional scheme. By increasing ϕ from 0.2 to 0.8, such convenience amounts to 14% after a time period of five years. Furthermore, the convenience of MP&P increases to 34% and 175% up to time periods equal to 10 and 20 years, respectively. On the other hand, according to Table 9.2, the NPV seems to be not very sensitive to the variation of c and t_c.

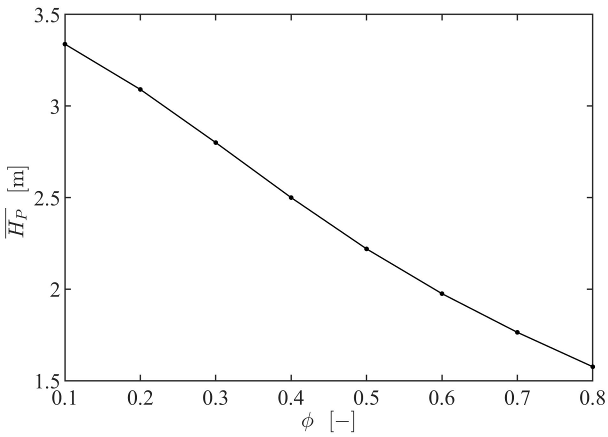

Fig. 9.15 Daily averaged pressure head ($\overline{H_P}$) against runoff coefficient (ϕ).

Definitively, the MP&P system can be certainly preferred over the conventional system

Table 9.2 Main figures of preliminary design for ϕ= 0.2.

t$_c$ [h]	c [$-$]	ϕ [$-$]	$\overline{H_p}$ [m]	$\overline{P_{hyd}}$ [W]	ΔNPV_5 [€/kW]	ΔNPV_{10} [€/kW]	ΔNPV_{20} [€/kW]
1.00	0.25	0.20	2.17	67.84	23825	15922	4878
1.00	0.25	0.50	1.63	73.01	24180	18435	10407
1.00	0.25	0.80	1.07	66.44	27257	21484	13417
1.00	0.50	0.20	2.17	67.86	23809	15900	4846
1.00	0.50	0.50	1.63	73.00	24160	18397	$10,345$
1.00	0.50	0.80	1.07	66.37	27248	21438	13319
1.00	0.75	0.20	2.17	67.88	23789	15873	4811
1.00	0.75	0.50	1.63	73.00	24138	18356	10276
1.00	0.75	0.80	1.05	66.29	27239	21388	13211
1.50	0.25	0.20	2.17	67.86	23802	15889	4831
1.50	0.25	0.50	1.63	73.00	24150	18379	10314
1.50	0.25	0.80	1.06	66.33	27244	21414	13267
1.50	0.50	0.20	2.16	67.90	23770	15848	4777
1.50	0.50	0.50	1.62	72.99	24116	18314	10206
1.50	0.50	0.80	1.04	66.20	27230	21336	13100
1.50	0.75	0.20	2.16	67.96	23731	15801	4718
1.50	0.75	0.50	1.60	72.97	24078	18242	10088
1.50	0.75	0.80	0.99	66.09	27208	21251	12927
2.00	0.25	0.20	2.16	67.90	23772	15849	4778
2.00	0.25	0.50	1.63	72.99	24117	18316	10208
2.00	0.25	0.80	1.04	66.19	27232	21337	13100
2.00	0.50	0.20	2.16	67.97	23721	15787	4701
2.00	0.50	0.50	1.60	72.97	24067	18221	10051
2.00	0.50	0.80	0.97	66.04	27204	21224	12868
2.00	0.75	0.20	2.16	68.05	23665	15720	4616
2.00	0.75	0.50	1.56	72.95	24013	18119	9883
2.00	0.75	0.80	0.91	65.93	27162	21103	12635

up to a time period of 20 years, i.e. the useful life of the plant, beyond which the cash inflow due to the production of energy overcomes the initial cash outflow.
In the MP&P plant, the absence of electric devices significantly reduces the need for maintenance and repair works. Nevertheless, as the maintenance costs are not easily evaluable due to the scarcity of data in the literature, in the evaluation of ΔNPV, such costs have been considered the same in both the plants, in order to avoid pushing the comparison in favor of the MP&P plant.

9.9 Conclusions and limitations

In this chapter, a new strategy to increase the energy efficiency of a water system is analyzed. This strategy is a plant consisting of a pump and PAT mounted on the same shaft: the PAT exploits the excess pressure within a fresh water network to produce energy and supply a pump conveying a wastewater stream into a treatment plant. This configuration arises whenever it is possible to co-locate a point of excess pressure dissipation with a wastewater pumping station. Therefore, the feasibility of the plant is strictly dependent on the topography of the network. A preliminary method to select the machines employed in the plant has been developed, based on the maximum daily averaged values of fresh and wastewater discharge. Such a method allows for the selection of the pump and of the PAT, once the discharge and the head jump of the two flows are given. According to the results of this strategy, a centrifugal pump with a diameter equal to 260 mm has been selected, whereas the resulting PAT has been the one stage centrifugal pump, with a diameter equal to 142 mm. Hereafter, the behavior of the mixed PAT–pump turbocharger has been simulated by means of a mathematical system consisting of four equations. The resolution of this system has allowed for the determination of the values of the shaft rotational speed, as well as the wastewater pumped discharge, the water level in the wet tank, and the value of pressure downstream of the MP&P plant, at 1-min intervals. Moreover, for the sake of generality, the behavior of the plant has been investigated for several wastewater hydrographs. Furthermore, in order to assess the benefits of the plant, an economic comparison with a conventional wastewater pumping system working in ON/OFF mode has been carried out. The comparison relies on the evaluation of the net present value of the investment in both scenarios, which was calculated for different time periods and for several wastewater hydrographs. The comparison has shown the advantages of the MP&P plant, whose investment consists of only the purchase of hydraulic machines, pipes, valves, a wet tank, and a holding tank. Unlike MP&P plant, the conventional scheme working in ON/OFF mode is characterized by additional costs related to the motor and the generator, as well as to the energy spent for pumping. According to the comparison, the mixed PAT–pump turbocharger represents the most economically viable configuration, at least until the useful life of the plant is reached. Despite the promising results, the plant presents some limitations. First of all, it may be possible that the point of pressure dissipation is not close enough to the pumping station, thus, the PAT and pump could not be practically coupled on the same shaft. However, beyond the feasibility within freshwater and wastewater networks, such plant could find application wherever it is needed for pressure reduction and pumping in two streams of different nature, e.g. deep mining. Furthermore, due to the small available power, this plant may be not employed in a mixed storm–wastewater sewage, unless an auxiliary pump is chosen. In this research, storm water has not been taken into account. Nevertheless, the plant may be employed to empty a wet retention basin in a storm water sewage. Moreover, despite several wastewater hydrographs having been considered in this study by combining different values of t_c, c, and ϕ, it is worth underlining that not all networks follow the patterns presented in Figure 9.5, especially in cities with commercial and industrial demands of a different nature. In those cases, the need for pumping wastewater can be significantly different from the working condition of the analyzed network, as well as very variable according to the seasons. A further limitation may be consequent to the lack of PAT performance curves: therefore, mathematical systems (9.5) and (9.7) may not be solvable. Finally, this plant should require sanitary measures in order to avoid the contamination of freshwater by the sewage.

List of Symbols

α	Safety factor
ΔH_{PAT}	Head-loss within the PAT
$\overline{\Delta H_{PAT,max}}$	Average head-loss within the PAT for the maximum daily average freshw
ΔH_v	Head-loss within the valve
$\overline{\Delta H_v}$	Daily average head-loss within the valve
η_M	Efficiency of the motor
η_P	Efficiency of the hydraulic pump
Σ	Cross-sectional area of the water tank
ϕ	Runoff coefficient
a^N_{PAT}, b^N_{PAT}, c^N_{PAT}	Experimental regression coefficient of the head curve of the PAT
α^N_{PAT}, β^N_{PAT}, γ^N_{PAT}, δ^N_{PAT}	Experimental regression coefficient of the power curve of the PAT
a^N_P, b^N_P, c^N_P	Experimental regression coefficient of the head curve of the pump
α^N_P, β^N_P, γ^N_P, and δ^N_P	Experimental regression coefficient of the power curve of the pump
c	Coefficient of peak attenuation
c_u	Energy cost
C_{GEN}	Cost of the generator
C_{MOT}	Cost of the motor
C^{tank}_W	Cost of the water tank
C^{in}_y	Cash inflow
$C^{E,PAT}_y$	Cost associated to the recovered energy

$C_y^{E,pump}$	Cost associated to the consumed energy
C_y^{out}	Cash outflow
D_P	Diameter of the pump
d_τ	Convolution interval time
H_1^u	Head available at the hydropower plant inlet
H_1^d	Head available at the hydropower plant outlet
H_2^d	Hydraulic head of the treatment plant inlet
H_2^u	Water level of the wet tank
$\overline{H_2^u}$	Daily average water level of the wet tank
H_P	Pumping head
$\overline{H_P}$	Daily average pressure head
$\overline{H_{P,max}}$	Daily average pressure head for the maximum daily average wastewater
K	Storage coefficient
L_m	Hydraulic length of the longest channel of the network
n_{av}	Number of pump starts per hour
$n_{st,PAT}$	Number of stages of the PAT
N	Rotational speed
N_P	Rotational speed of the pump
N_{PAT}	Rotational speed of the PAT
NPV	Net Present Value
P	Power
P_{av}	Available power upstream of the valve
P_P	Power spent by the pump
P_{PAT}	Power produced by the PAT
Q_{BP}	Bypassed discharge
$\overline{Q_F}$	Daily average freshwater discharge

Q_F	Freshwater discharge
Q_{max}	Maximum discharge
$Q_{s,max}^{c,t_c,\phi}$	Maximum discharge for the combination (c, t_c, ϕ)
$\overline{Q_F}$	Daily average freshwater discharge
$\overline{Q_{F,max}}$	Maximum daily average freshwater discharge
Q_S	Wastewater discharge reaching the wet tank
$\overline{Q_{S,max}}$	Maximum daily average wastewater discharge
Q_P	Discharge pumped to the treatment plant
r	Discount rate
S_m	Slope of the longest channel of the network
t_c	Time of concentration
u	Clark Instantaneous Unit Hydrograph
W	Volume of the water tank
Y	Number of the years
1	Subscript referred to MPP scenario
2	Subscript referred to conventional scenario

Chapter 10

Research conclusions and future developments

10.1 Summary of the proposed research

In this research work, several strategies to increase the energy efficiency of water systems have been proposed and organized in three lines of research.
The first line of research is based on the optimal location of hydraulic devices within a water distribution network. As a result of many trials and progressive findings, a robust mixed-integer non-linear programming model has been developed allowing for the placement of hydraulic devices, such as turbines, valves and pumps, within a water distribution network in order to maximize the recovered energy, as well minimize the amount of water that is leaked due to the high values of pressure. As a case study, a literature synthetic hydraulic network has been initially considered and a comparison with results previously achieved by other studies in literature have been presented in order to highlight the achieved improvements. Then the optimization has been extended to a real water distribution network. Most of the computations have been performed by a global optimization solver, which potentially finds the global optimum in both convex and non-convex problems. Nevertheless, due to the strong technical complexities affecting the hydraulic problem in question, the search of the exact solution may require an infinite time. Due to the limited computer memory, the solver has been used with the intention of finding good quality local optima. In all the performed optimization, the results have been assessed according to a cost model used by previous authors in literature, in order to easily make the comparison. However,

more recent cost models available in literature have been also employed to achieve more reasonable values of the results. According to the comparison between results obtained by different cost models, despite the employment of more recent models leading to significantly larger installation cost of the devices, the solutions are quite similar in terms of both number and location of installed devices, and the water and energy savings are quite comparable as well. Among all the devices, the optimization of PAT and PRV location has clearly shown that the use of more recent cost models seems to affect more PRV than PAT location, due to the strong dependency of the valve costs on the pipe diameter. However, it is worth highlighting that the optimal solutions progressively found in this research study do not take into account some multiple aspects (e.g. the real price of energy, maintenance and repair works) which are determinant in the management of water distribution networks.
The value of the proposed research study results from not only the promising results achieved, but also from the development of a new, robust and comprehensive mathematical model suitable for the global optimization of hydraulic device location (GOHyDeL). Moreover, the proposed research study have provided new formulation of mathematical constraints requiring less computational effort, which could find application also in more general hydraulic problems.
In the second line of research, two different modalities to supply a water distribution network have been investigated. The first solution consists of a pumping system transferring the drinkable water from the source up to a reservoir, and a PAT converting the excess pressure in energy. The second solution relies on pumping directly to a downstream water distribution network and benefiting of lower pressure head. New energy efficiency indices have been defined and used to both asses and compare the energy requirements of the two supply solutions. The investigation has been performed with reference to the system supplying the area of Ballacolla (IE), for which the direct pumping solution has resulted to be the most efficient strategy. Moreover, different operating conditions have been investigated, corresponding to different combinations of distance and elevation of the source from the distribution. The results have shown that, when the values of pumping head in both the direct and indirect scenarios are equal, indirect pumping with energy recovery is up to 5% more convenient that pumping directly to the distribution network, as well as increases the resilience of the supply system (e.g., in the case of power failure). On the contrary, direct pumping strategy has resulted to be convenient if the pumping head could be reduced up to 6%. According to this study, it is not possible to define which supply strategy is more efficient, but rather the convenience of a supply solutions over the other one basically depends on

the hydraulic conditions and should be investigated case by case.
The third line of research is instead based on the design of a mixed PAT–pump turbocharger, that is a PAT-Equipped turbopump exploiting the excess pressure within a fresh water network to produce energy and convey a wastewater stream into a treatment plant. This plant does not rely on any electrical devices (e.g., generators and motors), since the excess pressure is converted by the hydraulic turbine in a mechanical torque, which is in turn transferred to a pump located on the same shaft. Such a kind of plant could be realized provided that it is possible to co-locate the point of excess pressure dissipation and a wastewater pumping station. As a case study, the water distribution network of Ballacolla (IE) has been assessed, being suitable for this kind of plant configuration. Moreover, the selection of the employed machine has been performed by a new preliminary method, based on the maximum daily averaged values of fresh and wastewater discharge. Then, the behavior of the plant has been simulated by means of a mathematical system and several wastewater hydrograph have been investigated. The benefits of the new plant have been finally highlighted by the comparison with a conventional wastewater pumping system working in ON/OFF mode. The comparison has been made in terms of net present value of the investment and has shown the advantages of the MP&P plant, whose investment consists of only the cost related to the purchase of hydraulic machines, pipes, valves, a wet tank, and a holding tank, whereas a conventional scheme is subject to the additional costs related to the motor and the generator, as well as to the energy spent for pumping.

10.2 Research dissemination

This research has been disseminated in both journal and conference papers, including:

- Morani, M. C., Carravetta, A., D'Ambrosio, C., and Fecarotta, O. (2020a). A New Preliminary Model to Optimize PATs Location in a Water Distribution Network.Environmental Sciences Proceedings, 2(1):57;
- Morani, M. C., Carravetta, A., D'Ambrosio, C., and Fecarotta, O. (2021). A new mixed integer non-linear programming model for optimal PAT and PRV location in water distribution networks. Urban Water Journal;

- Morani, M. C., Carravetta, A., Del Giudice, G., McNabola, A., and Fecarotta, O.(2018). A Comparison of Energy Recovery by PATs against Direct Variable Speed Pumping in Water Distribution Networks. Fluids, 3(2);
- Morani, M. C., Carravetta, A., Fecarotta, O., and McNabola, A. (2020b). Energy transfer from the freshwater to the wastewater network using a PAT-equipped turbopump. Water (Switzerland);

Other related journal papers are the following:

- Fecarotta, O., Carravetta, A., Morani, M. C., and Padulano, R. (2018). Optimal Pump Scheduling for Urban Drainage under Variable Flow Conditions.Resources,7(4);
- Fecarotta, O., Martino, R., and Morani, M. C. (2019). Wastewater pump control under mechanical wear. Water (Switzerland).

10.3 Future developments

Future researches will mainly regard the first line of research, that is, the optimal location of hydraulic devices within a water distribution network. Indeed, despite the considerable achievements obtained, future developments are necessary to further reduce the computational effort affecting this kind of optimization problems. As mentioned several times, despite the newly proposed formulation of the mathematical model having enhanced the practical convergence, the solver still struggles to reduce the upper bound of the problem, whose evaluation is a key factor to assess the effectiveness of any found solution. As a result, even a good quality solution could be far from the upper bound of the problem, and could be therefore misinterpreted as a low quality solution. New relaxation and decomposition techniques could be employed in future works to further improve the performance of the optimization solver in terms of bound tightening. Moreover, in future works real machines should be considered and properly designed in terms of diameter and rotational speed. The integration of the affinity laws within the mathematical model will be necessary to model and better simulate the behavior of the installed devices, as well as of operation of HR, depending on the working conditions, in order to better evaluate the effective power produced by the turbines, which has been merely overestimated in this study.

References

[1] a.a. Williams (1996). Pumps as turbines for low cost micro hydro power. *Renewable Energy*, 9(1-4):1227–1234.

[2] Ali, M. E. (2015). Knowledge-based optimization model for control valve locations in water distribution networks. *Journal of Water Resources Planning and Management*.

[3] Araujo, L. S. (2005). *Controlo de perdas na gestao sustenavel dos sistemas de abastecimento de agua*. PhD thesis.

[4] Araujo, L. S., Ramos, H. M., and Coelho, S. T. (2006). Pressure Control for Leakage Minimisation inWater Distribution Systems Management. *Water Resources Management*, 20(1):133–149.

[5] Bagirov, A., Karmitsa, N., Mäkelä, M. M., Bagirov, A., Karmitsa, N., and Mäkelä, M. M. (2014). Subgradient Methods. In *Introduction to Nonsmooth Optimization*, pages 295–297. Springer, Cham, Switzerland.

[6] Belotti, P., Kirches, C., Leyffer, S., Linderoth, J., Luedtke, J., and Mahajan, A. (2013). Mixed-integer nonlinear optimization. *Acta Numerica*, 22:1–131.

[7] Belotti, P., Lee, J., Liberti, L., Margot, F., and Wächter, A. (2009). Branching and bounds tighteningtechniques for non-convex MINLP. *Optimization Methods and Software*.

[8] Binama, M., Su, W. T., Li, X. B., Li, F. C., Wei, X. Z., and An, S. (2017). Investigation on pump as turbine (PAT) technical aspects for micro hydropower schemes: A state-of-the-art review.

[9] Bolognesi, A., Bragalli, C., Lenzi, C., and Artina, S. (2014). Energy efficiency optimization in water distribution systems. In *Procedia Engineering*, volume 70.

[10] Bonami, P., Biegler, L. T., Conn, A. R., Cornuéjols, G., Grossmann, I. E., Laird, C. D., Lee, J., Lodi, A., Margot, F., Sawaya, N., and Wächter, A. (2008). An algorithmic framework for convex mixed integer nonlinear programs. *Discrete Optimization*, 5(2):186–204.

[11] Brook, A., Kendrick, D., and Meeraus, A. (1988). GAMS, a user's guide. *ACM SIGNUM Newsletter*.

[12] Byrd, R. H., Gilbert, J. C., and Nocedal, J. (2000). A trust region method based on interior point techniques for nonlinear programming. *Mathematical Programming, Series B*, 89(1):149–185.

[13] Byrd, R. H., Hribar, M. E., and Nocedal, J. (1999). An Interior Point Algorithm for Large-Scale Nonlinear Programming. *SIAM Journal on Optimization*, 9(4):877–900.

[14] Cabrera, E., Gomez, E., Cabrera Jr., E., Soriano, J., and Espert, V. (2015). Energy Assessment of Pressurized Water Systems. *Journal of Water Resources Planning and Management*, 141(8):1–12.

[15] Cabrera, E., Pardo, M. a., Cobacho, R., and Cabrera, E. J. (2010). Energy Audit of Water Networks. *Journal of Water Resources Planning and Management*, 136(December):669–677.

[16] Capelo, B., Pérez-Sánchez, M., Fernandes, J. F., Ramos, H. M., López-Jiménez, P. A., and Branco, P. J. (2017). Electrical behaviour of the pump working as turbine in off grid operation. *Applied Energy*.

[17] Carravetta, A., Antipodi, L., Golia, U., and Fecarotta, O. (2017). Energy saving in a water supply network by coupling a pump and a Pump As Turbine (PAT) in a turbopump. *Water (Switzerland)*, 9(1).

[18] Carravetta, A., Conte, M. C., Fecarotta, O., and Ramos, H. M. (2014a). Evaluation of PAT performances by modified affinity law. In *Procedia Engineering*, volume 89, pages 581–587.

[19] Carravetta, A., Del Giudice, G., Fecarotta, O., and Ramos, H. (2013). PAT Design Strategy for Energy Recovery in Water Distribution Networks by Electrical Regulation. *Energies*, 6(1):411–424.

[20] Carravetta, A., Del Giudice, G., Fecarotta, O., and Ramos, H. M. (2012). Energy Production in Water Distribution Networks: A PAT Design Strategy. *Water Resources Management*, 26(13):3947–3959.

[21] Carravetta, A., Derakhshan, S., and Ramos, H. M. (2018a). Pumps as Turbines: Fundamentals and applications. pages 97–116. Springer, Cham, Switzerland.

[22] Carravetta, A., Derakhshan Houreh, S., and Ramos, H. M. (2018b). PAT selection. In *Pumps as Turbines: Fundamentals and applications*, pages 77–96. Springer, Cham, Switzerland.

[23] Carravetta, A., Fecarotta, O., Martino, R., and Antipodi, L. (2014b). PAT efficiency variation with design parameters. In *Procedia Engineering*, volume 70, pages 285–291.

[24] Carravetta, A., Fecarotta, O., and Ramos, H. (2018c). A new low-cost installation scheme of PATs for pico-hydropower to recover energy in residential areas. *Renewable Energy*, 125:1003–1014.

[25] Carravetta, A., Fecarotta, O., Sinagra, M., and Tucciarelli, T. (2014c). Cost-Benefit Analysis for Hydropower Production in Water Distribution Networks by a Pump as Turbine. *Journal of Water Resources Planning and Management*, 140(6):4014002.

[26] Castro-Gama, M., Pan, Q., Lanfranchi, E. A., Jonoski, A., and Solomatine, D. P. (2017). Pump scheduling for a large water distribution network. Milan, Italy. pages 436–443. Elsevier.

[27] Chabal, L. and Stanko, S. (2015). Sewerage Pumping Station Optimization Under Real Conditions. *GeoScience Engineering*, 60(4):19–28.

[28] Clark, C. O. (1943). Storage and the Unit Hydrograph. *ASCE*, 110:1419–1446.

[29] Coelho, B. and Andrade-Campos, A. (2014). Efficiency achievement in water supply systems - A review.

[30] Colombo, A. F. and Karney, B. W. (2002). Energy and Costs of Leaky Pipes: Toward Comprehensive Picture. *Journal of Water Resources Planning and Management*, 128(6):441–450.

[31] Corcoran, L., Mcnabola, A., and Coughlan, P. (2015). Optimization of Water Distribution Networks for Combined Hydropower Energy Recovery and Leakage Reduction. *Journal of Water Resources Planning and Management*, 142(2):1–8.

[32] Covelli, C., Cozzolino, L., Cimorelli, L., Della Morte, R., and Pianese, D. (2016). Optimal Location and Setting of PRVs in WDS for Leakage Minimization. *Water Resources Management*.

[33] Creaco, E., Alvisi, S., and Franchini, M. (2016). Multistep Approach for Optimizing Design and Operation of the C-Town Pipe Network Model. *Journal of Water Resources Planning and Management*.

[34] Creaco, E., Franchini, M., and Alvisi, S. (2010). Optimal Placement of Isolation Valves in Water Distribution Systems Based on Valve Cost and Weighted Average Demand Shortfall. *Water Resources Management*.

[35] Creaco, E. and Pezzinga, G. (2015a). Embedding linear programming in multi objective genetic algorithms for reducing the size of the search space with application to leakage minimization in water distribution networks. *Environmental Modelling and Software*.

[36] Creaco, E. and Pezzinga, G. (2015b). Multiobjective Optimization of Pipe Replacements and Control Valve Installations for Leakage Attenuation in Water Distribution Networks. *Journal of Water Resources Planning and Management*.

[37] Dai, P. D. and Li, P. (2014). Optimal Localization of Pressure Reducing Valves in Water Distribution Systems by a Reformulation Approach. *Water Resources Management*.

[38] Dai, P. D. and Li, P. (2016). Optimal Pressure Regulation in Water Distribution Systems Based on an Extended Model for Pressure Reducing Valves. *Water Resources Management*.

[39] D'Ambrosio, C. and Lodi, A. (2013). Mixed integer nonlinear programming tools: An updated practical overview. *Annals of Operations Research*.

[40] D'Ambrosio, C., Lodi, A., Wiese, S., and Bragalli, C. (2015). Mathematical programming techniques in water network optimization.

[41] De Paola, F., Fontana, N., Giugni, M., Marini, G., and Pugliese, F. (2017). Optimal solving of the pump scheduling problem by using a Harmony Search optimization algorithm. *Hydroinformatics*, 19(6):879–889.

[42] Del Giudice, G. and Padulano, R. (2016). Sensitivity Analysis and Calibration of a Rainfall-Runoff Model with the Combined Use of EPA-SWMM and Genetic Algorithm. *Acta Geophysica*, 64(5):1755–1778.

[43] Emec, S., Bilge, P., and Seliger, G. (2015). Design of production systems with hybrid energy and water generation for sustainable value creation. *Clean Technologies and Environmental Policy*, 17(7):1807–1829.

[44] Fecarotta, O., Aricò, C., Carravetta, A., Martino, R., and Ramos, H. M. (2015). Hydropower Potential in Water Distribution Networks: Pressure Control by PATs. *Water Resources Management*, 29(3):699–714.

[45] Fecarotta, O., Carravetta, A., Morani, M. C., and Padulano, R. (2018). Optimal Pump Scheduling for Urban Drainage under Variable Flow Conditions. *Resources*, 7(4).

[46] Fecarotta, O., Carravetta, A., Ramos, H. M., and Martino, R. (2016). An improved affinity model to enhance variable operating strategy for pumps used as turbines. *Journal of Hydraulic Research*, 1686(February):1–10.

[47] Fecarotta, O., Martino, R., and Morani, M. C. (2019). Wastewater pump control under mechanical wear. *Water (Switzerland)*.

[48] Fecarotta, O. and McNabola, A. (2017). Optimal Location of Pump as Turbines (PATs) in Water Distribution Networks to Recover Energy and Reduce Leakage. *Water Resources Management*, (15).

[49] Fischetti, M. and Lodi, A. (2003). Local branching. In *Mathematical Programming*.

[50] Fontana, N., Giugni, M., Glielmo, L., and Marini, G. (2016). Real Time Control of a Prototype for Pressure Regulation and Energy Production in Water Distribution Networks. *Journal of Water Resources Planning and Management*, 142(7):4016015.

[51] Fontana, N., Giugni, M., and Portolano, D. (2012). Losses Reduction and Energy Production in Water-Distribution Networks. *Journal of Water Resources Planning and Management*, 138(3):237–244.

[52] Fontanella, S., Fecarotta, O., Molino, B., Cozzolino, L., and Morte, R. D. (2020). A performance prediction model for pumps as turbines (PATs). *Water (Switzerland)*.

[53] Fourer, R., Gay, D. M., and Kernighan, B. W. (1990). A Modeling Language for Mathematical Programming. *Management Science*.

[54] Galántai, A. (2000). The theory of Newton's method. *Journal of Computational and Applied Mathematics*, 124(1-2):25–44.

[55] Gallagher, J., Styles, D., McNabola, A., and Williams, A. P. (2015a). Making green technology greener: Achieving a balance between carbon and resource savings through ecodesign in hydropower systems. *Resources, Conservation and Recycling*, 105:11–17.

[56] Gallagher, J., Styles, D., McNabola, A., and Williams, A. P. P. (2015b). Life cycle environmental balance and greenhouse gas mitigation potential of micro-hydropower energy recovery in the water industry. *Journal of Cleaner Production*, 99:152–159.

[57] García, J. M., Salcedo, C., and Saldarriaga, J. (2019). Minimization of water losses in WDS through the optimal location of valves and turbines: A comparison between methodologies. In *World Environmental and Water Resources Congress 2019: Hydraulics, Waterways, and Water Distribution Systems Analysis - Selected Papers from the World Environmental and Water Resources Congress 2019*, Pittsburgh, Pennsylvania.

[58] Germanopoulos, G. and Jowitt, P. W. (1989). Leakage reduction by excess pressure minimization in a water supply network. *Proceedings - Institution of Civil Engineers. Part 2. Research and theory.*

[59] Ghaddar, B., Claeys, M., Mevissen, M., and Eck, B. J. (2017). Polynomial optimization for water networks: Global solutions for the valve setting problem. *European Journal of Operational Research.*

[60] Giacomello, C., Kapelan, Z. S., and Nicolini, M. (2013). Fast Hybrid Optimization Method for Effective Pump Scheduling. *Water Resources Planning and Management*, 139(2):175–183.

[61] Giugni, M., Fontana, N., and Ranucci, A. (2014). Optimal Location of PRVs and Turbines in Water Distribution Systems. *Journal of Water Resources Planning and Management*, 140(9):6014004.

[62] Giustolisi, O. and Savic, D. (2010). Identification of segments and optimal isolation valve system design in water distribution networks. *Urban Water Journal.*

[63] Gómez, E., Cabrera, E., Balaguer, M., and Soriano, J. (2015). Direct and indirect water supply: An energy assessment. In *Procedia Engineering*, volume 119, pages 1088–1097.

[64] Greyvenstein, B. and van Zyl, J. E. (2007). An experimental investigation into the pressure - leakage relationship of some failed water pipes. *Journal of Water Supply: Research and Technology - Aqua*, 56(2):117–124.

[65] Grunow, M. and Günther, H. O. (1995). AMPL. *OR Spektrum.*

[66] Gupta, A., Bokde, N., Kulat, K., and Yaseen, Z. M. (2020). Nodal matrix analysis for optimal pressure-reducing valve localization in a water distribution system. *Energies.*

[67] Gupta, A., Bokde, N., and Kulat, K. D. (2018). Hybrid Leakage Management for Water Network Using PSF Algorithm and Soft Computing Techniques. *Water Resources Management*.

[68] Gupta, O. K. and Ravindran, A. (1985). Branch and Bound Experiments in Convex Nonlinear Integer Programming. *Management Science*, 31(12):1533–1546.

[69] Gurobi, O. (2018). Gurobi Optimizer Reference Manual, Version 5.0. *Www.Gurobi.Com*.

[70] Hanson, M. A. (1999). Invexity and the Kuhn-Tucker theorem. *Journal of Mathematical Analysis and Applications*.

[71] Jafari, R., Khanjani, M. J., and Esmaeilian, H. R. (2015). Pressure management and electric power production using pumps as turbines.

[72] Jawahar, C. P. and Michael, P. A. (2017). A review on turbines for micro hydro power plant.

[73] Jowitt, P. W. and Xu, C. (1990). Optimal Valve Control in Water Distribution Networks. *Journal of Water Resources Planning and Management*, 116(4):455–472.

[74] Kawajir, Y., Laird, C. D., and Waechter, A. (2010). Introduction to IPOPT: A tutorial for downloading, installing, and using IPOPT . *Most*.

[75] Khosravanian, R., Mansouri, V., Wood, D. A., and Alipour, M. R. (2018). A comparative study of several metaheuristic algorithms for optimizing complex 3-D well-path designs. *Journal of Petroleum Exploration and Production Technology*.

[76] Kronqvist, J., Bernal, D. E., Lundell, A., and Grossmann, I. E. (2018). A review and comparison of solvers for convex MINLP. *Optimization and Engineering*.

[77] Lee, K. S. and Geem, Z. W. (2005). A new meta-heuristic algorithm for continuous engineering optimization: Harmony search theory and practice. *Computer Methods in Applied Mechanics and Engineering*.

[78] Liberatore, S. and Sechi, G. M. (2009). Location and calibration of valves in water distribution networks using a scatter-search meta-heuristic approach. *Water Resources Management*, 23(8):1479–1495.

[79] Liberti, L. (2006). Writing Global Optimization Software. In *Global Optimization*.

[80] Lima, G. M., Luvizotto Junior, E., and Brentan, B. M. (2017). Selection and location of Pumps as Turbines substituting pressure reducing valves. *Renewable Energy*, 109:392–405.

[81] Lin, M. H., Tsai, J. F., and Yu, C. S. (2012). A review of deterministic optimization methods in engineering and management.

[82] Martello, S. (2014). *Ricerca Operativa*. Esculapio, Bologna, Italy.

[83] Mathworks (2016). MATLAB Global Optimization Toolbox.

[84] McCormick, G. P. (1976). Computability of global solutions to factorable nonconvex programs: Part I - Convex underestimating problems. *Mathematical Programming.*

[85] McCuen, R. (1982). *A guide to hydrologic analysis using SCS methods.* Prentice-Hall, Inc., New Jersey.

[86] McCuen, R. H., Wong, S. L., and Rawls, W. J. (1984). Estimating urban time of concentration. *Journal of Hydraulic Engineering*, 110(7):887–904.

[87] Morani, M. C., Carravetta, A., D'Ambrosio, C., and Fecarotta, O. (2020a). A New Preliminary Model to Optimize PATs Location in a Water Distribution Network. *Environmental Sciences Proceedings*, 2(1):57.

[88] Morani, M. C., Carravetta, A., D'Ambrosio, C., and Fecarotta, O. (2021). A new mixed integer non-linear programming model for optimal PAT and PRV location in water distribution networks. *Urban Water Journal.*

[89] Morani, M. C., Carravetta, A., Del Giudice, G., McNabola, A., and Fecarotta, O. (2018). A Comparison of Energy Recovery by PATs against Direct Variable Speed Pumping in Water Distribution Networks. *Fluids*, 3(2).

[90] Morani, M. C., Carravetta, A., Fecarotta, O., and McNabola, A. (2020b). Energy transfer from the freshwater to the wastewater network using a PAT-equipped turbopump. *Water (Switzerland).*

[91] Motwani, K. H., Jain, S. V., and Patel, R. N. (2013). Cost analysis of pump as turbine for pico hydropower plants - A case Study. In *Procedia Engineering*, volume 51.

[92] Muhammetoglu, A., Karadirek, I. E., Ozen, O., and Muhammetoglu, H. (2017). Full-Scale PAT Application for Energy Production and Pressure Reduction in a Water Distribution Network. *Journal of Water Resources Planning and Management*, 143(8):4017040.

[93] Mushtaq, S., Maraseni, T. N., Reardon-Smith, K., Bundschuh, J., and Jackson, T. (2015). Integrated assessment of water-energy-GHG emissions tradeoffs in an irrigated lucerne production system in eastern Australia. *Journal of Cleaner Production*, 103:491–498.

[94] Nautiyal, H., Varun, and Kumar, A. (2010). Reverse running pumps analytical, experimental and computational study: A review. *Renewable and Sustainable Energy Reviews*, 14(7):2059–2067.

[95] Nguyen, K. D., Dai, P. D., Vu, D. Q., Cuong, B. M., Tuyen, V. P., and Li, P. (2020). A MINLP model for optimal localization of pumps as turbines in water distribution systems considering power generation constraints. *Water (Switzerland).*

[96] Nicolini, M. and Zovatto, L. (2009). Optimal Location and Control of Pressure Reducing Valves in Water Networks. *Journal of Water Resources Planning and Management*, 135(3):178–187.

[97] Novara, D., Carravetta, A., McNabola, A., and Ramos, H. M. (2019). Cost Model for Pumps as Turbines in Run-of-River and In-Pipe Microhydropower Applications. *Water Resources Planning and Management*, 145(5):04019012.

[98] Ostojin, S., Mounce, S., and Boxall, J. B. (2011). An artificial intelligence approach for optimizing pumping in sewer systems. *Journal of Hydroinformatics*, 13(3):295–306.

[99] Paish, O. (2002). Small hydro power: Technology and current status. *Renewable and Sustainable Energy Reviews*, 6(6):537–556.

[100] Pecci, F., Abraham, E., and Stoianov, I. (2019a). Global optimality bounds for the placement of control valves in water supply networks. *Optimization and Engineering*.

[101] Pecci, F., Abraham, E., and Stoianov, I. (2019b). Model Reduction and Outer Approximation for Optimizing the Placement of Control Valves in Complex Water Networks. *Journal of Water Resources Planning and Management*.

[102] Ramos, H. M., Mello, M., and De, P. K. (2010). Clean power in water supply systems as a sustainable solution: from planning to practical implementation. *Water Science & Technology: Water Supply*, 10(1):39.

[103] Reis, L. F. R., Porto, R. M., and Chaudhry, F. H. (1997). Optimal Location of Control Valves in Pipe Networks by Genetic Algorithm. *Journal of Water Resources Planning and Management*, 123(6):317–326.

[104] Rossman, L. A. (2000). Epanet 2 User 's Manual.

[105] Sahinidis, N. V. (1996). BARON: A general purpose global optimization software package. *Journal of Global Optimization*.

[106] Sammartano, V., Sinagra, M., Filianoti, P., and Tucciarelli, T. (2017). A Banki–Michell turbine for in-line water supply systems. *Journal of Hydraulic Research*, 55(5):686–694.

[107] Samora, I., Franca, M. J., Schleiss, A. J., and Ramos, H. M. (2016a). Simulated Annealing in Optimization of Energy Production in a Water Supply Network. *Water Resources Management*, 30(4):1533–1547.

[108] Samora, I., Manso, P., Franca, M., Schleiss, A., and Ramos, H. (2016b). Energy Recovery Using Micro-Hydropower Technology in Water Supply Systems: The Case Study of the City of Fribourg. *Water*, 8(8):344.

[109] Savić, D. A. and Walters, G. A. (1996). Integration of a model for hydraulic analysis of water distribution networks with an evolution program for pressure regulation. *Computer-Aided Civil and Infrastructure Engineering*.

[110] Simpson, A. R. and Marchi, A. (2013). Evaluating the Approximation of the Affinity Laws and Improving the Efficiency Estimate for Variable Speed Pumps. *Journal of Hydraulic Engineering*, 139(12):1314–1317.

[111] Sinagra, M., Sammartano, V., Morreale, G., and Tucciarelli, T. (2017). A New Device for Pressure Control and Energy Recovery in Water Distribution Networks. *Water*, 9(5):309.

[112] Smith, E. M. and Pantelides, C. C. (1999). A symbolic reformulation/spatial branch-and-bound algorithm for the global optimisation of nonconvex MINLPs. In *Computers and Chemical Engineering*.

[113] Sperlich, A., Pfeiffer, D., Burgschweiger, J., Campbell, E., Beck, M., Gnirss, R., and Ernst, M. (2018). Energy efficient operation of variable speed submersible pumps: simulation of a ground water well field. *Water*, 10(9).

[114] Stefanizzi, M., Capurso, T., Balacco, G., Torresi, M., Binetti, M., Piccinni, A. F., Fortunato, B., and Camporeale, S. M. (2019). Preliminary assessment of a pump used as turbine in a water distribution network for the recovery of throttling energy. In *13th European Turbomachinery Conference on Turbomachinery Fluid Dynamics and Thermodynamics, ETC 2019*, Lausanne, Switzerland.

[115] Sterling, M. J. and Bargiela, A. (1984). Leakage reduction by optimised control of valves in water networks. *TRANS. INST. MEAS. & CONTROL*.

[116] Stokes, J. R., Horvath, A., and Sturm, R. (2013). Water loss control using pressure management: Life-cycle energy and air emission effects. *Environmental Science and Technology*, 47(19):10771–10780.

[117] Swamee, P. K. and Sharma, A. K. (2008). *Design of Water Supply Pipe Networks*.

[118] Tahani, M., Yousefi, H., Noorollahi, Y., and Fahimi, R. (2019). Application of nature inspired optimization algorithms in optimum positioning of pump-as-turbines in water distribution networks. *Neural Computing and Applications*.

[119] Tricarico, C., Morley, M. S., Gargano, R., Kapelan, Z., Savić, D., Santopietro, S., Granata, F., and de Marinis, G. (2018). Optimal energy recovery by means of pumps as turbines (PATs) for improved WDS management. *Water Science and Technology: Water Supply*, 18(4):1365–1374.

[120] Vairavamoorthy, K. and Lumbers, J. (1998). Leakage Reduction in Water Distribution Systems: Optimal Valve Control. *Journal of Hydraulic Engineering*, 124(11):1146–1154.

[121] Vicente, D. J., Garrote, L., Sánchez, R., Santillán, D., Garrote, . L., Sánchez, . R., and Santillán, D. (2016). Pressure Management in Water Distribution Systems: Current Status, Proposals, and Future Trends. *Journal of Water Resources Planning and Management*, 142(2):4015061.

[122] Vigerske, S. and Gleixner, A. (2018). SCIP: global optimization of mixed-integer nonlinear programs in a branch-and-cut framework. *Optimization Methods and Software*.

[123] Wächter, A. and Biegler, L. T. (2006). On the Implementation of an Interior Point Filter Line-Search Algorithm for Large-Scale Nonlinear Programming. *Mathematical Programming*, 106(1):25–57.

[124] Waltz, R. A., Morales, J. L., Nocedal, J., and Orban, D. (2006). An interior algorithm for nonlinear optimization that combines line search and trust region steps. *Mathematical Programming*.

[125] Wood, D. J. and Charles, C. O. (1972). HYDRAULIC NETWORK ANALYSIS USING LINEAR THEORY. *ASCE J Hydraul Div*.

[126] Wylie, E. B. and Streeter, V. L. (1993). *Fluid Transient in Systems*. Prentice Hall, Englewood Cliffs, NJ 7632.

[127] Xu, Q., Chen, Q., Ma, J., and Blanckaert, K. (2013). Optimal pipe replacement strategy based on break rate prediction through genetic programming for water distribution network. *Journal of Hydro-Environment Research*, 7(2):134–140.

[128] Xue, X., Hawkins, T., Schoen, M., Garland, J., and Ashbolt, N. (2016). Comparing the Life Cycle Energy Consumption, Global Warming and Eutrophication Potentials of Several Water and Waste Service Options. *Water*, 8(4):154.

Appendix A

Table A.1 Characteristics of the nodes of the synthetic network.

i [-]	q_i^d [l/s]	H_i [m]	z_i [m]	f_i [l/(s m$^\beta$)]
1	5	–	18	0.0127
2	10	–	18	0.0354
3	0	–	14	0.0338
4	5	–	12	0.0059
5	30	–	14	0.0193
6	10	–	15	0.0202
7	0	–	14.5	0.0056
8	20	–	14	0.0198
9	0	–	14	0.0037
10	5	–	15	0.0209
11	10	–	12	0.0066
12	0	–	15	0.0257
13	0	–	23	0.0177
14	5	–	20	0.0205
15	20	–	8	0.0304
16	0	–	10	0.0142
17	0	–	7	0.0115
18	5	–	8	0.0056
19	5	–	10	0.0097
20	0	–	7	0.0114
21	0	–	10	0.0212
22	20	–	15	0.0368
23	–	56	50	0.0053
24	–	56	50	0.0419
25	–	56	50	0.007

Table A.2 Characteristics of the links of the synthetic network.

k [-]	i [-]	j [-]	C_k [-]	L_k [m]	D_k [mm]
1	1	2	110	1930	457
2	1	23	110	606	457
3	2	3	10	5150	305
4	3	4	100	326	152
5	3	6	100	1274	152
6	4	5	110	844	229
7	5	6	90	1115	229
8	5	7	110	500	381
9	5	22	100	1408	152
10	6	7	110	615	381
11	6	8	110	743	381
12	6	9	90	300	229
13	8	9	90	443	229
14	8	10	105	249	305
15	8	12	110	1600	457
16	8	22	125	931	229
17	10	11	90	542	229
18	10	24	100	3382	305
19	11	12	90	777	229
20	12	13	110	762	457
21	12	15	95	1996	229
22	13	14	135	1014	381
23	13	24	110	1767	475
24	14	24	105	2782	229
25	14	25	135	304	381
26	15	16	125	914	229
27	15	21	90	832	152
28	15	22	100	2334	229
29	16	17	140	822	305
30	16	25	6	1097	381
31	17	18	100	411	152
32	17	19	135	1072	229
33	18	20	110	701	229
34	19	20	90	864	152
35	20	21	90	711	152
36	21	22	100	2689	152
37	23	24	110	454	457

Table A.3 Characteristics of the nodes of the network supplying Blackstairs area (IE).

i [-]	q_i^d [l/s]	H_i [m]	z_i [m]	f_i [l/(s m$^\beta$)]	i [-]	q_i^d [l/s]	H_i [m]	z_i [m]	f_i [l/(s m$^\beta$)]
1	0.12	–	62	0.001402	66	0.12	–	112	0.0001805
2	0.12	–	68	0.0007195	67	0.12	–	101	0.0010035
3	0.12	–	59	0.0006075	68	0.12	–	75	0.001876
4	0.12	–	90	0.0011915	69	0.12	–	86	0.0003055
5	0.12	–	94	0.000767	70	0.12	–	82	0.000542
6	0.12	–	116	0.000979	71	0.12	–	74	0.0017345
7	0.12	–	134	0.001358	72	0.12	–	96	0.0008815
8	0.12	–	135	0.00048	73	0.12	–	77	0.0011245
9	0.12	–	142	0.000619	74	0.12	–	53	0.0005875
10	0.12	–	163	0.000814	75	0.12	–	117	0.00185
11	0.12	–	121	0.000872	76	0.12	–	90	0.0012985
12	0.12	–	152	0.000186	77	0.12	–	93	0.0001145
13	0.12	–	184	0.000563	78	0.12	–	104	0.0007805
14	0.12	–	172	0.0008185	79	0.12	–	101	0.0004015
15	0.12	–	140	0.0015955	80	0.12	–	107	0.000747
16	0.12	–	136	0.0011035	81	0.12	–	113	0.00146
17	0.12	–	113	0.0002085	82	0.12	–	93	0.001025
18	0.12	–	145	0.000197	83	0.12	–	93	0.0007915
19	0.12	–	138	0.0001625	84	0.12	–	84	0.0009775
20	0.12	–	125	0.0006175	85	0.12	–	73	0.000176
21	0.12	–	145	0.0007775	86	0.12	–	103	0.000518
22	0.12	–	107	0.0005825	87	0.12	–	98	0.000374
23	0.12	–	100	0.0013935	88	0.12	–	97	0.000272
24	0.12	–	115	0.001034	89	0.12	–	111	0.0006635
25	0.12	–	74	0.0006745	90	0.12	–	67	0.0008215
26	0.12	–	157	0.001288	91	0.12	–	73	0.000542
27	0.12	–	118	0.000887	92	0.12	–	135	0.0009285
28	0.12	–	122	0.000196	93	0.12	–	90	0.0013525
29	0.12	–	116	0.000291	94	0.12	–	98	0.0002785
30	0.12	–	126	0.0012475	95	0.12	–	91	0.0004705
31	0.12	–	134	0.0008785	96	0.12	–	111	0.00115
32	0.12	–	138	0.0008965	97	0.12	–	104	0.0010545
33	0.12	–	150	0.00066	98	0.12	–	91	0.0006425
34	0.12	–	111	0.0006475	99	0.12	–	91	0.0019165
35	0.12	–	127	0.0012995	100	0.12	–	95	0.0009045
36	0.12	–	163	0.0018095	101	0.12	–	114	0.000763
37	0.12	–	156	0.0009015	102	0.12	–	105	0.0015055
38	0.12	–	123	0.0013335	103	0.12	–	93	0.0011715
39	0.12	–	112	0.001067	104	0.12	–	96	0.00097
40	0.12	–	157	0.0009075	105	0.12	–	108	0.0017625
41	0.12	–	167	0.001522	106	0.12	–	113	0.0020885
42	0.12	–	204	0.000817	107	0.12	–	113	0.0011605
43	0.12	–	148	0.0008325	108	0.12	–	117	0.0004645
44	0.12	–	165	0.0003905	109	0.12	–	117	0.001713
45	0.12	–	155	0.000391	110	0.12	–	111	0.0005805
46	0.12	–	132	0.0024135	111	0.12	–	126	0.000733
47	0.12	–	126	0.0015665	112	0.12	–	122	0.00162
48	0.12	–	120	0.0002155	113	0.12	–	122	0.0004915
49	0.12	–	136	0.0014075	114	0.12	–	150	0.0007
50	0.12	–	80	0.0003775	115	0.12	–	145	0.0006
51	0.12	–	95	0.000719	116	0.12	–	133	0.00038
52	0.12	–	93	0.000428	117	0.12	–	62	0.0010335
53	0.12	–	141	0.000569	118	0	–	190	0.0016405
54	0.12	–	100	0.0003495	119	0	–	143	0.0017275
55	0.12	–	122	0.001172	120	0	–	175	0.001242
56	0.12	–	122	0.001562	121	0	–	179	0.001019
57	0.12	–	132	0.0021835	122	0	–	173	0.001799
58	0.12	–	108	0.001306	123	0	–	110	0.0005985
59	0.12	–	102	0.000917	124	0	–	129	0.0007525
60	0.12	–	99	0.0007365	125	0	–	178	0.001079
61	0.12	–	90	0.000259	126	0	–	177	0.000742
62	0.12	–	142	0.0006985	127	291	288	288	0.0007945
63	0.12	–	105	0.0005045					
64	0.12	–	121	0.001115					
65	0.12	–	102	0.0020005					

Table A.4 Characteristics of the links of the network supplying Blackstairs area (IE).

k [-]	i [-]	j [-]	C_k [-]	L_k [m]	D_k [mm]	k [-]	i [-]	j [-]	C_k [-]	L_k [m]	D_k [mm]
1	3	1	150	1215	50	70	84	85	150	352	50
2	2	1	150	1439	50	71	82	83	150	539	100
3	6	4	150	1336	50	72	83	84	150	1044	100
4	8	9	150	427	100	73	81	86	150	564	100
5	6	11	150	622	50	74	86	87	150	204	50
6	11	7	150	646	50	75	87	88	150	544	50
7	10	11	150	476	50	76	86	89	150	268	100
8	10	12	150	372	50	77	84	90	150	559	50
9	7	15	150	900	50	78	90	91	150	1084	50
10	15	16	150	1564	100	79	30	92	150	764	50
11	16	17	150	417	50	80	92	96	150	1093	50
12	18	21	150	394	25	81	96	93	150	1207	50
13	16	21	150	226	50	82	93	94	150	557	50
14	21	19	150	325	25	83	93	95	150	941	50
15	21	20	150	610	50	84	30	97	150	1160	100
16	20	22	150	625	50	85	97	98	150	949	100
17	22	23	150	540	50	86	98	99	150	336	100
18	24	23	150	898	50	87	99	100	150	899	100
19	24	7	150	1170	50	88	99	101	150	1234	100
20	23	25	150	1349	50	89	101	102	150	292	100
21	26	27	150	800	50	90	102	103	150	1701	100
22	27	28	150	392	50	91	103	104	150	642	50
23	27	29	150	582	50	92	105	106	150	611	50
24	32	31	150	1186	100	93	106	107	150	1411	50
25	31	30	150	571	100	94	107	100	150	910	50
26	26	33	150	454	100	95	99	106	150	1364	100
27	33	34	150	866	100	96	102	105	150	1018	50
28	35	36	150	1438	150	97	104	109	150	369	50
29	34	39	150	429	100	98	109	105	150	1896	50
30	39	40	150	994	100	99	106	112	150	791	100
31	40	41	150	821	100	100	112	113	150	983	50
32	41	42	150	1634	100	101	112	111	150	1466	50
33	44	35	150	781	50	102	109	110	150	1161	50
34	38	46	150	1588	150	103	104	108	150	929	50
35	46	47	150	1015	150	104	49	51	150	582	50
36	47	49	150	1363	150	105	51	52	150	856	50
37	49	48	150	431	50	106	36	126	150	702	50
38	47	50	150	755	50	107	45	126	150	782	50
39	49	53	150	439	50	108	36	125	150	1079	150
40	53	54	150	699	50	109	38	125	150	1079	150
41	55	56	150	369	100	110	57	124	150	454	100
42	56	57	150	1254	100	111	58	124	150	1051	100
43	58	59	150	879	75	112	55	114	150	1000	100
44	59	60	150	955	75	113	114	36	150	400	100
45	60	61	150	518	75	114	75	115	150	900	100
46	56	62	150	492	50	115	37	115	150	300	100
47	62	46	150	905	50	116	35	116	150	380	150
48	57	46	150	1319	50	117	116	37	150	380	150
49	56	63	150	1009	50	118	5	117	150	870	100
50	57	64	150	1340	50	119	4	117	150	1047	50
51	64	65	150	890	50	120	127	118	150	1589	150
52	65	66	150	361	50	121	118	41	150	589	100
53	67	65	150	1325	75	122	118	43	150	1103	150
54	58	67	150	682	75	123	43	119	150	562	150
55	65	68	150	1425	75	124	39	119	150	711	150
56	68	71	150	632	75	125	37	119	150	1123	150
57	71	73	150	1074	75	126	119	89	150	1059	100
58	73	74	150	1175	50	127	32	120	150	607	100
59	71	72	150	1763	50	128	121	120	150	555	100
60	68	69	150	611	50	129	14	121	150	756	100
61	68	70	150	1084	50	130	121	15	150	727	100
62	75	76	150	1565	50	131	8	123	150	533	100
63	76	77	150	229	50	132	5	123	150	664	100
64	75	78	150	586	100	133	13	122	150	1126	50
65	78	55	150	975	100	134	9	122	150	811	100
66	76	79	150	803	50	135	122	10	150	780	75
67	75	80	150	649	100	136	14	122	150	881	100
68	80	81	150	845	100	137	26	120	150	1322	100
69	81	82	150	1511	100	138	117	1	150	150	100